Inaugural dissertation

for

obtaining the doctoral degree

of the

Combined Faculty of Mathematics, Engineering and Natural Sciences

of the

Ruprecht - Karls - University

Heidelberg

Presented by

M.Sc. Elisa Damo

Born in: Aprilia, Italy

Oral examination: 27.06.2023

Activation of beta2-adrenergic receptors alleviates neuropathic pain hypersensitivity in mice: focus on spinal glial cells

Referees:

Prof. Dr. Daniela Mauceri

Prof. Dr. Rohini Kuner

Prof. Dr. Christoph Schuster

PD Dr. Georg Köhr

To my brother and my parents.

Table of contents

Summary

Chronic pain affects roughly one-fifth of the world's population, and many patients do not respond to current therapies or conventional analgesics. Thus, studying the molecular mechanisms underlying neuropathic pain is crucial in identifying novel molecular targets that can be used to develop effective pain relief therapies. Previous studies have thus far focused on α2-adrenergic receptors (α2-ARs) and neuronal excitability, among others. However, recent research suggests that astrocytes and microglia, which express adrenergic receptors, contribute significantly to neuropathic pain. In particular, microglia have been found to express elevated levels of Gs-coupled β2-AR and they are responsive to norepinephrine application. Additionally, systemic administration of β2-AR agonists, such as Formoterol, has anti-inflammatory and anti-nociceptive properties in neuropathic pain, but the underlying processes are poorly understood. Therefore, this thesis work focuses on investigating glial noradrenergic signaling via β2-AR, specifically on microglia and its contribution to the modulation of neuropathic pain in mice.

In the present study, activation of the β2-ARs through Formoterol induced a decrease of anti-inflammatory cytokine levels in primary isolated microglia and reversed nerve injury-induced morphological alterations in spinal dorsal horn microglia. Systemic administration of Formoterol inhibited evoked behaviors as well as aversive components related to neuropathic pain and reduced chronically-established neuropathic pain. The analgesic effects of Formoterol were mainly mediated by microglia, as demonstrated by employing the conditional knock-out mouse line lacking the β2-AR specifically in microglia. Remarkably, the effect of Formoterol on neuropathic pain-related behavior and microgliosis was lost in mice with the microglia-specific deletion of β2-ARs. In addition, microglia phenotype showed a sex-dependency in the late phase of neuropathic pain, which was not observed in response to β2-AR stimulation. Notably, Formoterol also reduced astrogliosis in the late stage of neuropathic pain independently of β2-AR signaling in microglia.

Collectively, this work highlights the impact of microglial β2-AR stimulation in mediating the inhibition of pro-inflammatory signaling in the spinal cord during the initial phase of neuropathic pain. These results emphasize the importance of exploring microglial β2-AR agonists in alleviating neuropathic pain and elucidating the underlying mechanisms.

Zusammenfassung

Etwa ein Fünftel der Weltbevölkerung leidet unter chronischen Schmerzen, und viele Patienten sprechen nicht auf aktuelle Therapien oder konventionelle Analgetika an. Es ist daher notwendig, die molekularen Mechanismen neuropathischer Schmerzen zu untersuchen, um neue molekulare Targets zu identifizieren, die zur Entwicklung wirksamer Schmerzlinderungstherapien verwendet werden können. Bisherige Forschungen konzentrierten sich unter anderem auf α2-adrenerge Rezeptoren (α2-ARs) und neuronale Erregbarkeit. Neuere Studien legen jedoch nahe, dass auch Astrozyten und Mikroglia, die adrenerge Rezeptoren exprimieren, signifikant zur neuropathischen Schmerzentstehung beitragen. Insbesondere wurde festgestellt, dass Mikroglia erhöhte Mengen an Gs-gekoppelten β2-AR exprimieren und auf die Anwendung von Norepinephrin reagieren. Die systemische Verabreichung von β2-AR-Agonisten wie Formoterol hat entzündungshemmende und antinozizeptive Eigenschaften bei neuropathischen Schmerzen, aber die zugrunde liegenden Mechanismen sind wenig verstanden. Daher konzentriert sich die vorliegende Doktorarbeit auf die Untersuchung glialer noradrenerger Signalgebung über β2-AR, insbesondere auf Mikroglia, und ihren Beitrag zur Modulation neuropathischer Schmerzen bei Mäusen.

Formoterol induzierte anti-inflammatorische molekulare Veränderungen in primär isolierten Mikroglia und kehrte nervenverletzungs-induzierte morphologische Veränderungen in nativen Populationen von Mikroglia im spinalen Rückenmark um. Die systemische Verabreichung von Formoterol hemmte evozierte Verhaltensweisen sowie aversive Komponenten, die mit neuropathischem Schmerz zusammenhängen, und reduzierte chronisch neuropathische Schmerzen. Die analgetischen Wirkungen von Formoterol wurden hauptsächlich durch Mikroglia vermittelt, wie durch den Einsatz kondizioneller Gen-Knockout-Technologie zur mikroglia-spezifischen Deletion von β2-ARs gezeigt wurde. Bemerkenswerterweise waren die Wirkungen von Formoterol auf neuropathische Schmerzverhaltensweisen und Mikrogliose bei Mäusen, denen β2-ARs spezifisch in Mikroglia fehlten, verloren. Zusätzlich zeigte der Mikroglia-Phänotyp eine geschlechtsabhängige Komponente in der späten Phase des neuropathischen Schmerzes, die bei der β2-AR-Stimulation nicht beobachtet wurde. Interessanterweise reduzierte Formoterol auch die Astrogliose in der späteren Phase des neuropathischen Schmerzes unabhängig von der β2-AR-Signalgebung in Mikroglia.

Zusammenfassend ist diese Arbeit eine der ersten, die Beweise für die Rolle der mikroglialen β2-AR-Aktivierung bei der Blockierung pro-inflammatorischer Signale im Rückenmark während der Anfangsphase des Auftretens neuropathischer Schmerzen liefert. Diese Ergebnisse betonen den Wert der Erforschung von β2-AR-Agonisten für Mikrogliazellen zur

Linderung von neuropathischen Schmerzen und zur Klärung der zugrunde liegenden Mechanismen.

List of Abbreviations

5-HT 5-hydroxytryptamine

ACC anterior cingulate cortex

aCSF Artificial Cerebrospinal Fluid

AR adrenergic receptor

AUC area under the curve

BBB blood-brain barrier

BDNF brain-derived neurotrophic factor

BLA basolateral amygdala

cAMP cyclic 3',5'-adenosine monophosphate

Cav voltage-gated calcium channels

CCI chronic constriction injury

CCR2 C-C Motif Chemokine Receptor 2

CGPR calcitonin-gene-related peptide

CYP2D6: cytochrome P-450 2D6

FDA Food and Drug Administration

GABA γ-aminobutyric acid

GFAP glial fibrillary acidic protein

GPCR guanine nucleotide-binding G protein-coupled receptor

GRK G-coupled receptor kinase

Hes5 Hes Family BHLH Transcription Factor 5

IB4 isolectin-B4

CNS central nervous system

COPD chronic obstructive pulmonary disease

CPP conditioned place preference

CSF-1 colony-stimulating factor 1

CX3CR1 fractalkine receptor

CXCL1 keratinocyte-derived chemokines ligand 1

CXCR2 CXC motif chemokine receptor 2

DβH dopamine beta-hydroxylase

DOP δ-opioid receptors

DPN diabetic neuropathic pain

DRG dorsal root ganglia

EMA European Medicines Agency

ERK extracellular signal-regulated protein kinase

Iba1 ionized calcium-binding adapter molecule 1

IκB inhibitor of κB

IKBKB IκB by IκB kinase

IL-1β interleukin1β

INF-γ, interferon-gamma

i.p. intraperitoneal

JNK c-Jun N-terminal kinases

KOR κ-opioid receptors

LABA long-acting β2-AR agonist

LC locus coeruleus

LPS lipopolysaccharide

LTD long-term depression

MACS magnetic-assisted cell sorting

MAPK mitogen-activated protein kinases

MOR μ-opioid receptors

NE noradrenaline, norepinephrine

NET noradrenaline transporter

NF-Kb nuclear factor kappa-light-chain-enhancer of activated B cells

NMDA *N*-methyl-D-aspartate

P2X4 P2X purinoceptor 4

PAG periaqueductal gray

PenStrep Penicillin/Streptomycin

PFC prefrontal cortex

PI3K phosphoinositide 3-kinase

PINP paclitaxel-induced neuropathic pain

PKA protein kinase A

PLGA poly lactic-co-glycolic acid

PNS peripheral nervous system

PSNL sciatic nerve ligation

RMg magnus raphe nucleus

RVM rostral ventromedial medulla

SCI spinal cord injury

SDH spinal dorsal horn

SEM standard error of the mean

SGC satellite glial cell

SNI spared nerve injury

SNL spinal nerve ligation

SNRI serotonin-norepinephrine reuptake inhibitor

sNRI selective norepinephrine reuptake inhibitor

TCA tricyclic antidepressant

tDCS transcranial direct current stimulation

TGF-β transforming growth factor beta

TNF-α tumor necrosis factor alpha

TrkB tropomyosin receptor kinase B

TRPV1 transient receptor potential cation channel subfamily V member 1

List of Tables

List of Figures

1. Introduction

1.1 Neuropathic pain

Divinum est opus sedare dolorem (Hippocrates).

Pain can serve a protective function as it alerts the body to potential or actual tissue damage and prompts the individual to take action to prevent further harm. However, experiencing deleterious pain is recognized as a debilitating condition. The International Association for the Study of Pain describes pain as “an unpleasant sensory and emotional experience associated with or reminiscent of that associated with, actual or potential tissue damage” (Raja et al., 2020). When the damage results in a lesion or disease of the somatosensory nervous system, which includes peripheral nerve fibers (Aβ, Aδ, and C fibers) and central neurons, it is referred to as neuropathic pain (Colloca et al., 2017). The prominent clinical manifestations of neuropathic pain include spontaneous (continuous or episodic) or evoked pain, which can be a painful response to a typically innocuous stimulus (allodynia), or an exaggerated response to a painful stimulus (hyperalgesia) (Finnerup et al., 2021).

Neuropathic pain affects 7–10% of the European population (Hebert et al., 2021) and impact significantly on the quality of life of the patient, leading to problems, including anxiety, depression, disturbed sleep, and impaired cognition (Colloca et al., 2017). Effective treatment necessitates a multimodal approach with a specific pharmacological component (Baron et al., 2010; Finnerup et al., 2015). The financial burden of chronic pain is considerable and varies per country, ranging from 9,305 € in Italy to 14,446 € in Germany (Liedgens et al., 2016).

1.1.1 Current Treatments

Generally, neuropathic pain management involves a combination of pharmacological and non-pharmacological interventions. Pharmacological options include the use of antidepressants, anticonvulsants, local anesthetics, and opioids (Finnerup et al., 2021). Interventional procedures including intrathecal drug delivery, nerve blocks, and spinal cord stimulation (de Geus et al., 2023; Nguyen et al., 2011), as well as non-invasive methods, such as transcranial direct current stimulation (tDCS) and repetitive transcranial magnetic stimulation (rTMS), may be employed to alleviate neuropathic pain (Ferreira et al., 2019; Lefaucheur et al., 2008). Physical rehabilitation and complementary alternative therapies, including acupuncture, chiropractic, and massage, may be integrated with other treatments (Liampas et al., 2020; Skelly et al., 2022). Psychological therapies, such as cognitive-behavioral and mindfulness-based therapies, can help improve mood and minimize the psychological burden of chronic pain (Skelly et al., 2022).

1.1.1.1 Pharmacological treatments

Pharmacological interventions for neuropathic pain involve using medication to alleviate pain symptoms. The analgesic drugs for neuropathic pain are enlisted in Table 1.

Table 1. Analgesics agents for neuropathic pain.
Modified from (Finnerup, 2019).

Drug	Indication	Side effects and Risks #	Other Information
Amitriptyline £	Neuropathic pain (first-line therapy), fibromyalgia, prevention of tension-type headache or migraine	Somnolence, tremors, dizziness, headache, drowsiness, tachycardia, orthostatic hypotension, dry mouth, constipation, nausea, micturition disorder, weight gain, hyperhidrosis, decreased libido, increased risk of suicidal thoughts	Patients with poor metabolism of CYP2D6 require lower doses; contraindicated in patients with recent myocardial infarction or cardiac rhythm disorders; avoid abrupt discontinuation; caution if used with other serotonergic agents
Duloxetine	Neuropathic pain (first-line therapy), chronic musculoskeletal pain, fibromyalgia	Somnolence, dizziness, headache, nausea, increased blood pressure, increased risk of suicidal thoughts	Avoid abrupt discontinuation; caution if used with other serotonergic agents
Gabapentin	Neuropathic pain (first-line therapy)	Somnolence, dizziness, peripheral edema, fever, infection, nausea, lack of coordination, blurred vision, increased risk of suicidal thoughts	Dose adjustment for renal impairment; misuse, abuse, and addiction have been reported
Pregabalin	Neuropathic pain (first-line therapy), fibromyalgia	Somnolence, dizziness, headache, peripheral edema, nausea, weight gain, disorientation, blurred vision, increased risk of suicidal thoughts	Dose adjustment for renal impairment; misuse, abuse, and addiction have been reported
Tramadol	Neuropathic pain (second-line therapy	Dizziness, fatigue, constipation, nausea, somnolence, dry mouth, itch	Dose adjustment for renal impairment; seizure disorder, allow 4 weeks for an adequate trial
Strong opioids	Neuropathic pain (third-line therapy	Dizziness, fatigue, constipation, nausea, somnolence, dry mouth, itch, abuse	Monitor patients with hepatic and renal disorders and with a history of mental disorders
Lidocaine, 1.8% or 5% patch	Postherpetic neuralgia, peripheral neuropathic pain	Application-site pain, pruritus, erythema, and skin irritation	Approved by FDA and EMA for postherpetic neuralgia only
Capsaicin 8% patch	Peripheral neuropathic pain	Application-site pain and erythema, transient increase in blood pressure, risk of reduced sensation	Applied by a health care professional wearing nitrile gloves

The medications mentioned are commonly prescribed for neuropathic pain, but this list is not exhaustive and other analgesics may be used for other types of pain. CYP2D6: cytochrome P-450 2D6; EMA: European Medicines Agency; FDA: Food and Drug Administration.
[#] For a comprehensive list of potential side effects, risks, contraindications, and warnings associated with each drug, it is necessary to consult the product information.
[£] Additional tricyclic antidepressants such as imipramine, desipramine, and nortriptyline have not been studied as extensively for pain management but may offer more tolerable side-effect profiles.

Antidepressants, including tricyclic antidepressants (TCAs) and serotonin-norepinephrine reuptake inhibitors (SNRIs), are adopted to treat neuropathic pain by reducing pain sensitivity and improving sleep. The mechanisms behind their analgesic effects are not yet completely understood but may involve presynaptic inhibition of serotonin (or 5-hydroxytryptamine, 5-HT) and norepinephrine (or noradrenaline, NE) reuptake in pain inhibitory pathways, activation of descending monoaminergic pathways in spinal or supraspinal sites, and peripheral mechanisms involving the interaction between adrenergic receptors and the opioid system (Kremer, Salvat, et al., 2016; Kremer et al., 2018). Anticonvulsants, such as gabapentin and pregabalin, are designed as gamma amino butyric acid (GABA) analogs but inhibit voltage-gated calcium channels (Cav) α2δ subunit, thereby reducing activity-dependent calcium signaling, excitatory transmitter release, and neuronal hyperexcitability (Patel & Dickenson, 2016).

Opioids are broadly used for pain management and work by inhibiting nociceptive transmission through the action of μ-opioid receptors (MOR) in both presynaptic and post-synaptic neurons. Tramadol, a weak MOR agonist acting also as an inhibitor of serotonin and norepinephrine reuptake, and strong opioids, including morphine and oxycodone, are recommended as second- and third-line treatments, respectively, due to their potential to induce hyperalgesia, abuse, diversion, misuse, overdose and lack of effectiveness (Cavalli et al., 2019; Frieden, 2016; Wilson et al., 2021).

Lidocaine-medicated patches block voltage-gated sodium channels, resulting in nerve membrane stabilization and ectopic discharge inhibition (Devor et al., 1992). Capsaicin, found in chili peppers, binds to transient receptor potential cation channel subfamily V member 1 (TRPV1) causing a reversible decrease in intraepidermal nerve fiber density and the desensitization of nociceptors upon repeated or high-concentration application (Anand & Bley, 2011; Anand et al., 2022).

These drugs may bind their targets at peripheral, spinal, and supraspinal levels, and their actions may involve different cell types, not only belonging to the central nervous system (CNS) (Damo, 2022; Fornasari, 2017; Harris et al., 2013; Kremer, Salvat, et al., 2016). The choice of treatment depends on various factors, including the type, severity, and duration of pain, along with individual characteristics like age, health status, and other medications. Combinational therapy is commonly employed when a single drug is not entirely effective. In refractory cases,

neuromodulation or spinal drug administration may be an option, although further randomized controlled trials are needed (Cruccu et al., 2007; Finnerup, 2019).

Therefore, it is necessary to investigate the molecular mechanisms underlying neuropathic pain to identify new molecular targets that can be utilized for the development of novel pain-relieving therapies.

1.1.2 Spared nerve injury as a murine model of neuropathic pain

Experimental animal models of nerve injury have been developed to tease out the mechanisms associated with neuropathic pain: partial or complete peripheral nerve transections (Bennett & Xie, 1988; Seltzer et al., 1990; Woolf & Salter, 2000), spinal cord injuries (Hao et al., 2000) and toxic and inflammatory neuritis models (Courteix et al., 1993; Eliav et al., 1999; Polomano et al., 2001). All these conditions lead to increase nociception such as allodynia and hyperalgesia, which are similar to those experienced by patients with neuropathic pain (Jensen et al., 2001).

Spared nerve injury (SNI) enables the investigation of chronic treatments that can resemble clinical situations (Urban et al., 2011). SNI involves sparing the sural nerve when two other terminal branches of the sciatic nerve, the common peroneal and tibial nerves, are injured (Decosterd & Woolf, 2000). It results in marked hypersensitivity in the cutaneous lateral paw territory innervated by the spared sural nerve. The non-operated side serves as a control, and the SNI model exhibits pronounced mechanical and cold allodynia as early as the day after surgery, which persists for several weeks, up to one year (Bourquin et al., 2006; Costigan et al., 2009). This model does not affect daily activities, such as food intake, drinking, locomotion, or circadian patterns (Tappe-Theodor & Kuner, 2014; Urban et al., 2011). Autotomy is not observed in C57BL/6 mice, unlike other models including sciatic nerve transection models (Koplovitch et al., 2012). Nonetheless, SNI produces a low local inflammation that is also present in spinal nerve ligation (SNL), partial sciatic nerve ligation (PSNL), and chronic constriction injury (CCI) models (Cichon et al., 2018). Sciatic nerve injuries in humans are uncommon due to their deep anatomical location within the lower extremity (Guida et al., 2020). However, this model has been extensively utilized due to the reproducible and consistent reproducible pain hypersensitivity in the spared sural nerve territory that the rodent exhibits.

1.2 Nociceptive pathways from the periphery to the brain

Pain circuitry involves the activation of peripheral sensory neurons located in the dorsal root ganglia (DRGs) and trigeminal ganglia. They transduce and transmit information about innocuous and noxious stimuli to the spinal dorsal horn (SDH) and brainstem, where the

nociceptive information is received, processed, transmitted to the brain centers, and modulated by descending control (Sandkuhler, 2009).

The SDH area is divided into five layers (Laminae I–V) (Rexed, 1952). Laminae I and II receive predominantly high-threshold unmyelinated C-type nociceptor and thinly myelinated Aδ-type nociceptor fibers. The superficial laminae I and II can be delineated by the afferent-specific markers calcitonin-gene-related peptide (CGRP) and Isolectin-B4 (IB4), respectively (Todd, 2017). Laminae III to V receive the low-threshold Aδ or Aβ afferents, that transmit innocuous touch signals (Arcourt & Lechner, 2015; Solorzano et al., 2015; Todd, 2010). Once activated, the primary afferent nociceptors, also known as first-order neurons, release neuropeptides and/or neurotransmitters, including CGRP, substance P, somatostatin, glutamate, or aspartic acid, that activate the second-order pain-transmission neurons located in the SDH. The synaptic transmission between the first- and second-order neuron is modulated by neighborhood interneurons by releasing GABA (Todd, 2022). The axons of the second-order neurons cross the midline of the spinal cord and project to the thalamus and brainstem through the spinothalamic and spinoreticulothalamic tracts, respectively. Moreover, neurons from the lamina I send their axons through the spinoparabrachial tract to the parabrachial region of the dorsolateral pons. From this area, information is relayed to the amygdala, a region thought to be responsible for processing information related to the unpleasant aspects of the pain experience (Andrew, 2009). Information travels from the brainstem and thalamic loci to the cortical structures where painful stimuli are integrated and consciously evaluated (Kuner & Flor, 2016).

There is no single brain area that is critical for pain (Apkarian et al., 2005). Instead, pain arises from the activation of a network of brain structures, some of which are more associated with the sensory-discriminative aspects of pain (such as location, intensity, and quality), including the somatosensory cortex. The anterior cingulate gyrus (ACC), insular cortex, and prefrontal cortex (PFC) are other structures related to the affective/emotional component of pain (Figure 1). Brain imaging studies in patients suffering from chronic back pain have reported activation and plasticity of prefrontal cortical areas, as well as regions not generally linked to pain processing, such as the basal ganglia (Baliki et al., 2012).

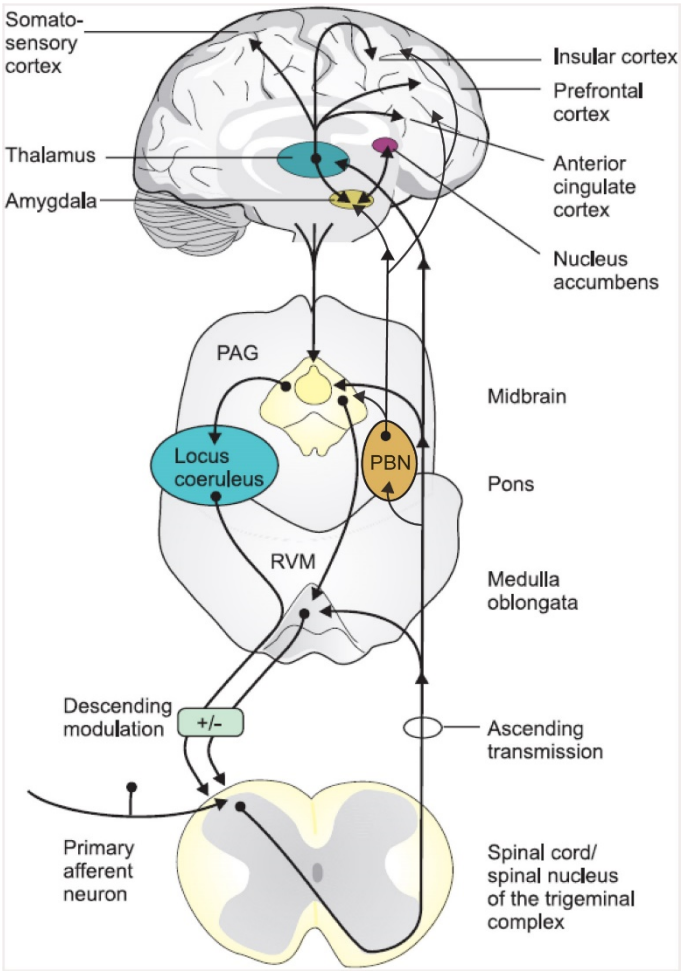

Figure 1. The neural pathways and brain regions involved in pain signal transmission and regulation.

Pain transmission implicates primary afferent neurons whose cell bodies are located in either the dorsal root ganglia (DRGs) or trigeminal ganglion. These neuronal cells synapse with second-order neurons located in the SDH or the spinal nucleus of the trigeminal complex. Their axons cross over to the contralateral side of the spinal cord and project to several targets, including the rostral ventromedial medulla (RVM), periaqueductal gray (PAG), parabrachial nucleus (PBN) and thalamus. From the PBN and thalamus, third-order neurons send projection to limbic cortical areas, such as the anterior cingulate gyrus, prefrontal and insular cortex. Moreover, thalamic relays send their axons to cortical areas, such as the somatosensory cortex. The amygdala receives projection mainly from the PBN, but also the thalamus, and interacts with the nucleus accumbens. These brain regions transmit to the PAG, which in turn sends descending pain modulatory signals back to the first synapses in the afferent pathways through the locus coeruleus and raphe nuclei in the RVM. Modified from (Brodin, 2016).

Whereas the ascending pathways convey the pain transmission to the brain, the descending pathways modulate the pain signal from the brain to the spinal cord and the ascending pathways. Descending pathways can either be facilitatory or inhibitory, enhancing or suppressing pain perception, respectively (Basbaum et al., 2009; Porreca et al., 2002).

1.3 Descending inputs

The SDH comprises molecularly and morphologically heterogeneous populations of non-neuronal and neuronal cells that receive, process, and transmit sensory input from the periphery to the brain but also integrate descending excitatory and inhibitory projections coming from the brain (Dogrul et al., 2009; Kato et al., 2006; Lu & Perl, 2007).

Signals from the frontal cortex, amygdala, and hypothalamus reach the periaqueductal gray (PAG) in the midbrain, which project to the spinal cord through the rostral ventromedial medulla (RVM) and the locus coeruleus (LC) (Heinricher et al., 2009; Li & Sheets, 2018). Serotonin and NE are released from the magnus raphe nucleus (RMg) of the RVM and the LC (A5–A7 nuclei), respectively (Fields et al., 1983; Howorth et al., 2009; Sluka & Westlund, 1992; Zhuo & Gebhart, 1990). Serotoninergic and noradrenergic axons terminate diffusely throughout the SDH, and although some form synapses, a significant proportion of their action is mediated by volume transmission, where the neuromodulators bind their receptors across the synaptic cleft (Heinricher et al., 2009; Zoli et al., 1999). Additionally, GABAergic axons from the RVM arise and arborize extensively in the SDH (Antal et al., 1996) and synapse with lamina II interneurons (Kato et al., 2006).

Depending on the pathological state, the brain nuclei, and the types of neurons that are activated, the descending pathways have dual conflicting actions. The 5-HT1A/B and 5-HT7 serotonin receptors are expressed in the laminae I and II of the spinal cord (Doly et al., 2005; Perrin et al., 2011). These receptors generally have an inhibitory effect on pain transmission and perception, whereas 5-HT2A and 5-HT3 spinal receptors activation in lamina II has the opposite effect (Alba-Delgado et al., 2018; Dogrul et al., 2009; Rahman et al., 2011; Viisanen & Pertovaara, 2010). However, recent studies report that RMg projecting 5-HT neurons activate local spinal inhibitory interneurons via 5-HT2- or 5-HT3-mediated mechanism, which can diminish the excitability of SDH neurons blocking nociceptive inputs (Aby et al., 2022). The LC sends descending projections to the SDH, which have been shown to exert inhibitory actions on nociception (Pertovaara, 2006; Tavares et al., 2021). However, the LC can also facilitate pain through its projections to several pain-control modulatory system brain areas, including the PFC and the dorsal reticular nucleus (Hirschberg et al., 2017; Martins et al., 2015; Martins & Tavares, 2017). The LC has widespread projections to cortical regions, hippocampus, ventral tegmental area, basolateral amygdala (BLA), and spinal cord, all of which are important structures in the context of pain (Loughlin et al., 1986; Plummer et al., 2020; Sara & Bouret, 2012). Adrenergic receptors, which mediate the effect of NE, are broadly expressed in the CNS and peripheral nervous systems (PNS).

1.3.1 Adrenergic receptors

The adrenergic receptors (or adrenoceptors, ARs) belong to the guanine nucleotide-binding G protein-coupled receptor (GPCR) superfamily (Graham, 1990). ARs are classified into two major categories, α and β which can be further divided into α1, α2, β1, β2, and β3 subtypes, several of which are widely expressed throughout the peripheral tissues and CNS (Ahlquist, 1948; Bylund et al., 1994). The distribution, physiological roles, and pharmacological mediators of ARs are summarized in Table 2.

Table 2. Classification of ARs and therapeutic drugs.
Modified from (Scanzano & Cosentino, 2015).

Subtype	**Main transduction mechanisms**	**Human tissue distribution**	**Physiological functions**	**Therapeutic drugs (indications)**
α1A	$G_{q/11}$ (phospholipase C stimulation, calcium channel)	Cerebral cortex, cerebellum, heart, liver, predominant subtype in prostate and urethra, lymphocytes	Contraction of urethral smooth muscle, skeletal muscle resistance arteries, subcutaneous arteries, control of cerebral blood flow, roles in neurotransmission and cognition	Agonists: methoxamine, methylnoradrenaline, oxymetazoline, midodrine, metaraminol, phenylephrine (vasoconstriction and mydriasis, used as vasopressors, nasal decongestants, and eye exams) Antagonists: alfuzosin, doxazosin, prazosin, phenoxybenzamine, phentolamine, terazosin, tamsulosin, trazodone (hypertension, benign prostatic hyperplasia)
α1B		Spleen, kidney, somatic arteries and veins, endothelial cells, lymphocytes, osteoblasts	Contraction of arteries and veins, osteoblast proliferation, control of cerebral blood flow	
α1D		Cerebral cortex, aorta, lymphocytes, blood vessels of prostate, bladder	Contraction of arteries, ureteral contraction, control of cerebral blood flow	
α2A	G_i/G_o (adenylate cyclase inhibition, potassium channel, calcium channel, phospholipase A2 stimulation)	Brain, spleen, kidney, aorta, lung, skeletal muscle, heart, liver	Presynaptic inhibition of noradrenaline release, hypotension, sedation, analgesia, hypothermia	Agonists: xylazine, dexmedetomidine, medetomidine, clonidine, romifidine, brimonidine, detomidine, lofexidine, tizanidine, guanfacine, amitraz (sedatives, antihypertensives, treatment of opiate dependence and alcohol withdrawal symptoms)
α2B		Kidney, liver, brain, lung, heart, skeletal muscle (also reported in the aorta and spleen)	Vasoconstriction	

α2C		Brain, kidney (also reported in spleen, aorta, heart, liver, lung, skeletal muscle)	Presynaptic inhibition of noradrenaline release	Antagonists: phentolamine, idazoxan, yohimbine, atipamezole, trazodone, mianserin, mirtazapine (reversal of α2-AR agonist-induced sedation, antidepressants, aphrodisiac)
β1	G_s (adenylate cyclase stimulation)	Brain, lung, spleen, heart, kidney, liver, muscle	Increase of cardiac output (heart rate, contractility, automaticity, conduction), renin release from juxtaglomerular cells, lipolysis in adipose tissue	Agonists: dobutamine, isoprenaline, (heart failure, bradycardia, cardiogenic shock) Antagonists: metoprolol, atenolol, propranolol, bisoprolol, timolol, nebivolol (glaucoma, cardiac arrhythmia, congestive heart failure, myocardial infarction, migraine prophylaxis)
β2		Brain, lung, lymphocytes, skin, liver, heart	Smooth muscle relaxation, striated muscle tremor, glycogenolysis, increased mass and contraction speed, increase of cardiac output, increase of aqueous humor production in eye, dilatation of arteries, glycogenolysis and gluconeogenesis in liver, insulin secretion, bronchodilation	Agonists: (short-acting) salbutamol, ritodrine, levosalbutamol terbutaline, pirbuterol, procaterol, fenoterol, metaproterenol, bitolterol mesylate, isoprenaline, (long-acting) salmeterol, formoterol, bambuterol, clenbuterol, (ultra-long-acting) indacaterol (asthma, other effects: vasodilation in muscle and liver, relaxation of uterine muscle, and release of insulin) Antagonists: butoxamine, timolol, propranolol (glaucoma, heart attacks, hypertension, migraine headache)

β3		Adipose tissue, gall bladder, small intestine, stomach, prostate, left atrium, bladder, endothelium of coronary microarteries	Lipolysis, thermogenesis, relaxation of miometrium and colonic smooth muscle cells, vasodilatation of coronary arteries, negative cardiac inotropic effect	Agonists: amibegron (investigational: antidepressant, anxiolytic), solabegron (overactive bladder, irritable bowel syndrome) Antagonists: SR 59230A

1.3.1.1 β2-adrenergic receptors

The gene encoding β2-AR, which is intron-less, is located on chromosome 5 (5q31) and encodes a 46 kDa, 413 amino acid polypeptide (Kobilka et al., 1987). The receptor was the first GPCR to be cloned (Dixon et al., 1986) and the first GPCR structure to be solved (Cherezov et al., 2007). Human β2-ARs are expressed not only in airway smooth muscles, but also in a wide variety of cells such as epithelial cells, endothelial cells, brain cells, and immune cells (Barnes, 1993). The receptor can activate canonical or noncanonical signal transduction pathways. In the first pathway, the typical activation and dissociation of the Gα-subunit trigger effector proteins, starting the second messenger cyclic 3',5'-adenosine monophosphate (cAMP) and protein kinase A (PKA)-mediated intracellular signaling pathway. The second pathway is G-protein independent and involves G-coupled receptor kinases (GRKs) and β-arrestins (Barisione et al., 2010; Shukla et al., 2011). During non-canonical signaling, β-arrestin2 couples β2-AR to mitogen-activated protein kinases (MAPK) signaling pathway, allowing nuclear translocation of transcriptional factors (Azzi et al., 2003). The diversity of the β2-AR activation leads to the complexity of signaling mechanisms and multiple functions.

1.3.1.2 β2-adrenergic receptor agonists in neuroprotection

The available agonists and antagonists for diverse AR subtypes show limited selectivity between the closely related α1- and α2-AR subtypes, resulting in conflicting outcomes (Perez, 2020). However, long-acting β2-AR agonists (LABAs), such as Salmeterol and Formoterol, present high selectivity for the β2-AR (a 1,000-fold selectivity over the β1-AR subtype). These agonists bind to the lipophilic transmembrane domains which prolong their duration of action. This propriety makes them clinically useful and approved by the FDA as bronchodilators for chronic obstructive pulmonary disease (COPD) and asthma treatments (Baker et al., 2015; Linden et al., 1996; Tashkin & Cooper, 2004).

Moreover, β2-AR agonists are suggested to have neuroprotective functions against degeneration and also have anti-inflammatory effects (Abdelmotilib & West, 2017; Chai et al., 2016; Dang et al., 2014; Qian et al., 2011). Formoterol (commercial name Symbicort) may also have potential as an analgesic agent (Yalcin et al., 2010). The clinical efficacy of β2-AR

agonists has been examined in various neurological disorders and a few of them are summarized in Table 3.

Table 3. Clinical trials using β2-agonists in neurological conditions.
Modified from (Sharma & Flood, 2019).

Disease	Design	Dose	Drug	Reference
Neuropathic pain	Controlled, double-blinded	5 mg twice/day for 28 days	Terbutaline	(Salvat et al., 2015)
Spinal cord injury	Randomized controlled	4 mg twice/day for 1st week then 8 mg twice/day for 15 weeks	Albuterol	(Schilero et al., 2018)
Alzheimer´s disease	Randomized controlled	20 mg/2 ml for 12 months	Formoterol	(Phillips et al., 2016)
Memory and cognition	Randomized controlled	4 mg, single oral administration	Salbutamol	(de Quervain et al., 2017)
Multiple sclerosis	Blinded controlled	4 mg/day	Albuterol	(Khoury et al., 2010)
Amyotrophic Lateral Sclerosis (ALS)	Uncontrolled	60 mg/day for 6 months	Clenbuterol	(Soraru et al., 2006)
Spinal muscular atrophy (SMA)	Uncontrolled	3-8 mg/day for 6 months	Albuterol	(Kinali et al., 2002)
Spinal and bulbar muscular atrophy (SBMA)	Uncontrolled	20 µg/day for 2 days, then 40 µg/day	Clenbuterol	(Querin et al., 2013)

Further research is required to decouple Formoterol analgesic effect from adverse effects, such as cardiac dysrhythmias and muscle spasms. Furthermore, long-term LABA use can lead to tolerance, hypotension, headaches, and hypokalemia (Abosamak & Shahin, 2022; Cazzola et al., 1998). These drugs should be utilized with caution in patients with diabetes due to the risk of ketoacidosis (Benfante et al., 2016).

1.3.2 Noradrenergic pain modulation

At supraspinal levels, the pain modulatory effect of NE depends on several factors, including the supraspinal site, AR type, pain duration and pathophysiological condition. The noradrenergic system contributes to the top-down control of pain, such as modulating the behavioral state (Pertovaara, 2006).

1.3.2.1 Central noradrenergic modulation

The LC descending pathways send signals to the spinal cord to suppress pain through a variety of mechanisms. The release of NE in the SDH suppresses pain by (1) presynaptic inhibition via α2A-AR action on central terminals of primary afferent nociceptors which prevent neuropeptides and/or neurotransmitter release (Bahari & Meftahi, 2019); (2) postsynaptic hyperpolarization through direct α2-AR action on pain-relay neurons, inhibiting voltage-gated calcium (Ca^{2+}) channels and opening inwardly rectifying potassium (K^{+}) channels (Basbaum et al., 2009; Heinricher et al., 2009; Pan et al., 2008); (3) mediating pain suppression by α1-AR-mediated activation of inhibitory interneurons to promote GABA or glycine release to inhibit secondary neurons (Braga et al., 2004); (4) controlling α2C-AR on axon terminals of excitatory interneurons (Olave & Maxwell, 2003); and (5) promoting the spinal release of enkephalins, which activate opioid receptors and impede pain transmission (Bohn et al., 2000).

Chronic pain conditions result also from an imbalance between descending pain inhibition and facilitation, leading to an enhanced abnormal pain sensation. This is due to plastic changes that occur in the central noradrenergic system which affect its anti-nociceptive efficacy (Pertovaara, 2006). These changes include an increase in spinal α2C-ARs (Stone et al., 1999), an intensification in the coupling efficiency between α2A-ARs and $G\alpha_i$ subunits (Bantel et al., 2005), and an augmented activity of pre- and postsynaptic α2-ARs that mitigate glutamatergic transmission in the SDH (Chen et al., 2011). Moreover, animal studies have shown that at the initial stage of neuropathic pain following peripheral nerve injury, descending noradrenergic pathways mediate the increase in brain-derived neurotrophic factor (BDNF) levels which, through tropomyosin receptor kinase B (TrkB) receptors, changes the coupling of the α2-ARs expressed in the SDH cholinergic interneurons from inhibitory $G\alpha_i$ to excitatory $G\alpha_S$ (Hayashida & Eisenach, 2010). These adaptive changes in the CNS indicate that the inhibitory tone of the descending noradrenergic may be compromised after nerve injury. Notably, the enhanced α2-AR efficacy may be advantageous for the action of NE reuptake inhibitors, that increase the synaptic concentration of NE.

1.3.2.2 Peripheral noradrenergic modulation

Locally, sympathetic nerve fibers release NE, which interacts with diverse receptors to modulate peripheral nociception (Pertovaara, 2006). Expression of new ARs, sprouting of sympathetic nerve fibers, and alterations in ionic channel properties of primary afferent nociceptors mediate pro-nociceptive effects, whereas interactions with the peripheral immune system contribute to the anti-nociceptive effects (Bravo et al., 2019). In chronic pain, peripheral α-AR stimulation enhances pain sensation. This excitability is partially associated with neuroplastic changes, which may be influenced by variations in the ARs expression, as

suggested by an increased α2- and α1B-AR mRNA in primary afferent neurons (Donello et al., 2011; Martin et al., 2019; Raja et al., 1991). Indeed, topical α2-AR agonist application results in analgesia, a phenomenon inhibited by pretreatment of α2-AR antagonists (Bravo et al., 2019).

Moreover, a study has reported that peripheral terminals and cell bodies of primary afferent nociceptors respond to β-AR stimulation (Khasar et al., 1999); however, another group has shown the restriction of *Adrb2* expression solely in satellite glial cells (SGCs) that surround DRG neurons and not in the DRG neurons themselves (Bohren et al., 2013). More recently, the latter hypothesis is endorsed by another study in which fluorescence in situ hybridization limits the *Adrb2* expression in SGCs (Shen et al., 2022). Still, it has not been studied if *Adrb2* mRNA is expressed in DRGs microglia-like cells (macrophages).

Studies have demonstrated that β2-AR activation suppresses mechanical hypersensitivity in part by inhibiting the peripheral release of tumor necrosis factor-α (TNF-α) from SGCs of nerve-injured mice (Bohren et al., 2013; Kremer et al., 2018). Conversely, acute dermal administration of a β2-AR agonist produces pro-nociceptive effects (Li et al., 2013). As a result, it is unclear whether the activation of these receptors is pro- or anti-nociceptive.

Overall, these studies indicate that β2-AR agonists can act on numerous cell types to produce anti-nociceptive or pro-nociceptive effects, and the efficacy of β2-mimetics as analgesic may vary depending on the pain state and site of action.

1.3.2.3 Adrenergic regulation of immune cell function

NE is secreted by the adrenal gland and local sympathetic neurons and regulates both local and systemic immune responses through AR activation, particularly the β2-ARs (Sharma & Farrar, 2020). Even though the α-ARs expression in immune cells may be low, there are indications that the α1-AR may enhance cytokine secretion in innate immune cells, predominantly macrophages, indicating opposing roles for α and β receptors in the regulation of pro-inflammatory cytokines (Staedtke et al., 2018).

Macrophages are classified into yolk sac-derived embryonic macrophages and bone marrow-derived monocytes based on the high expression of classical markers, including fractalkine receptor (CX3CR1) and C-C motif chemokine receptor 2 (CCR2), respectively (Geissmann et al., 2003; Stremmel et al., 2018). CX3CR1 is predominantly expressed in tissue-resident macrophages (yolk sack-derived), which are considered a long-lived subset that patrols the blood. In contrast, $CCR2^{+}$ monocytes are short-lived and actively recruited into inflamed tissue (Auffray et al., 2007; Yona et al., 2013). NE stimulates phagocytic activities in macrophages through both α- and β-ARs, whereas chemotactic function is regulated by α-ARs (Garcia et al., 2003a, 2003b). β2-ARs activation may dampen pro-inflammatory macrophage polarization (Bacou et al., 2017) and promote anti-inflammatory or regulatory macrophage induction

(Grailer et al., 2014; Mai et al., 2022). Signaling via β2-ARs inhibits the release of inflammatory cytokines from dendritic cells and macrophages responding to lipopolysaccharide (LPS) (Donnelly et al., 2010; Grailer et al., 2014; Spengler et al., 1994), along with T cells activation (Estrada et al., 2016). Due to the complexity of β2-AR signaling mechanisms and duality of function, β2-AR activation can result in immunomodulatory actions with diverse effects on immune cell function (Lorton & Bellinger, 2015; Shenoy et al., 2006).

1.4 Glial cells

The important role of glial cells in the regulation of nociception and pain pathways has been extensively studied and documented (Donnelly et al., 2020; Old et al., 2015), highlighting their crucial involvement in the development and maintenance of chronic pain (Taves et al., 2013). ARs are expressed by both cortical and spinal astrocytes and microglia and are responsive to NE (Gyoneva & Traynelis, 2013; Morioka et al., 2009; Oe et al., 2020; Zorec et al., 2018). Activation of ARs on glial cells maintains homeostasis in the brain through anti-inflammatory actions, and inhibition of neuroinflammation, thereby limiting the degeneration of neurons (Feinstein et al., 2016). However, while adrenergic signaling in neurons has received considerable attention, the potential role of glial adrenergic signaling in neuropathic pain remains substantially unexplored.

1.4.1 Astrocytes

Astrocytes are the most abundant and heterogeneous glial cells in the CNS (Freeman, 2010). Mature astrocytes are involved in essential processes for maintaining CNS homeostasis, including synaptogenesis and synaptic transmission modulation, neurotransmitter recycling, regulation of pH and ionic balance, and maintenance of blood-brain barrier (BBB). Each astrocyte interfaces with the microvasculature and contacts several neurons and hundreds to thousands of synapses. They dynamically regulate synaptic transmission as they are elements of the tripartite synapses (Abbott et al., 2006; Alvarez et al., 2013; Volterra & Meldolesi, 2005). A unique feature of astrocytes is the formation of cellular networks with each other through gap-junction protein complexes, which allow neighboring astrocytes to freely exchange small cytosolic proteins and ions (Iadecola & Nedergaard, 2007). Astroglia cells also participate in the immune response to CNS injury and disease by releasing cytokines and growth factors, promoting neuroprotection and regeneration (Lee et al., 2022). Dysregulation of astrocytes function has been implicated in a variety of neurological and psychiatric disorders, including Parkinson's disease, Alzheimer's disease, and schizophrenia, making these cells a promising target for therapeutic interventions (Lee et al., 2022).

1.4.1.1 Astrocytes in pain

Astrocytes are involved in synaptic transmission regulation and plasticity in pain pathways by modulating neurotransmitter release, uptake and metabolism, as well as by affecting the strength of synapses between neurons. This can influence the activity of pain pathways and contribute to the development and maintenance of chronic pain (Donnelly et al., 2020). Recent studies demonstrated that Hes Family BHLH Transcription Factor 5 (Hes5)-expressing astrocytes, a population of astrocytes, that is confined to the superficial laminae of the SDH, control mechanosensory behavior by gating descending noradrenergic commands (Kohro et al., 2020). Furthermore, dorsal horn astrocytes regulate peripheral nociceptive signals. A study reported that Aβ-fibers activation led to calcium elevation in SDH astrocytes, which then triggered long-term depression (LTD) in neurokinin-1 receptor-positive projection neurons, ultimately inhibiting pain (Xu et al., 2021).

Astrocyte hypertrophy occurs several days post nerve injury and lasts for several months (Li et al., 2020). The reactive state of cells is distinguished by alterations in morphology, molecular composition, and functionality. Reactive astrocytes are recognized by hypertrophy and glial fibrillary acidic protein (GFAP) upregulation, including in ventrolateral PAG in diabetic neuropathic pain (DNP) rats (X. Liu et al., 2022), BLA and SDH following SNI (De Luca et al., 2022; L. Liu et al., 2022), SDH post after peripheral nerve injury (Qian et al., 2018), SNL (Chen, Luo, et al., 2018; Guo et al., 2022), CCI (Garrison et al., 1991; Ono et al., 2020; Xue et al., 2017), and spinal cord injury (SCI) (Allahyari et al., 2022; Faulkner et al., 2004). The activated astrocytes release diverse pro-inflammatory factors and chemokines (Ji et al., 2019).

Astroglia regulate neuropathic pain through several mechanisms, among others, reactive astrocytes potentiate *N*-methyl-D-aspartate (NMDA) receptor function on spinal neurons by enhancing D-serine secretion, ultimately endorsing central sensitization (Ji et al., 2016; Moehring et al., 2018). In the SNL model, the expression of keratinocyte-derived chemokines ligand 1 (CXCL1) and its receptors CXC motif chemokine receptor 2 (CXCR2) is increased in the injured spinal cord astrocytes and neurons, respectively (Ni et al., 2019). In neuropathic pain conditions, an elevated TNF-α level stimulates c-Jun N-terminal kinases (JNK) phosphorylation in astrocytes, leading to CXCL1 upregulation, among other cytokines (Chen et al., 2014; Zhang et al., 2013). Released CXCL1 can directly act on CXCR2 in peripheral neurons, leading to calcium influx and primary neuron sensitization (Silva et al., 2017). Astroglial activation can also affect the bioenergetic state of SDH neurons, resulting in further aberrant activity along spinal circuits (Marty-Lombardi et al., 2022).

Astrocytes primarily express α1-, α2-, β1- and β2-ARs, and their activation modulates astrocytic functions (Hertz et al., 2010; Jensen et al., 2016). NE can increase intracellular

Ca^{2+} of spinal astrocytes through α1A-ARs (Ding et al., 2013) and intrathecal administration of NE induces mechanical hypersensitivity via α1A-ARs activation present on spinal Hes5-expressing astrocytes in a peripheral nerve injury mouse model (Kohro et al., 2020). Conversely, the endogenous NE released by activation of LC-spinal cord noradrenergic pathway neurons suppresses astrocyte activation in the SDH (Li et al., 2022). Various *in vivo* studies also reported neuroprotective roles of long-acting β2-AR agonists by reducing astrocyte activation in neuropathic pain models (Chen et al., 2021; Zhang et al., 2016). However, optogenetic activation of ACC astrocytic β2-ARs contributes to pain-related aversive memory in rats (Iqbal et al., 2023). In addition, hippocampal astrocytic β2-AR activation leads to fear memory consolidation via lactate release (Gao et al., 2016) and β-arrestin-1 plays a role in regulating lactate metabolism, which in turn contributes to β2-AR-mediated memory formation (Dong et al., 2017). Thus, inappropriate regulation of β2-AR activity can disrupt normal glucose metabolism and leads to accelerate neuronal disease development (Dong et al., 2012).

Overall, the diverse effects of NE on astrocytes suggest a complex modulation of astrocyte function via ARs. The findings highlight the significance of studying the specific subtypes of adrenergic receptors in astrocytes to better comprehend their role in pain processing and modulation.

1.4.2 Microglia

Microglia are the resident immune cells of the CNS and are responsible for maintaining a healthy neural environment by constantly monitoring the CNS for any signs of damage, infection, or abnormality (Prinz et al., 2019). In a healthy brain, microglia are involved in the regulation of neurogenesis, synaptic pruning and plasticity, and they contribute to the maintenance of the BBB. Upon sensing threat or injury signals, microglia become activated, undergo morphological and functional changes, and release a variety of pro- and anti-inflammatory chemokines, cytokines, and reactive oxygen species. Activated microglia can phagocytose damaged or dead cells, pathogens, debris, and produce trophic and growth factors that promote tissue repair and regeneration. However, excessive or chronic microglia activation can contribute to the development and progression of neurodegenerative diseases, including Parkinson's disease, Alzheimer's disease, and multiple sclerosis, by producing neurotoxic factors and promoting neuroinflammation and neuronal damage (Muzio et al., 2021). Microglia can be manipulated to produce some beneficial effects in the context of new therapeutic interventions.

1.4.2.1 Microglia in pain

Microglia are a type of cell in the CNS that play a key role in immune defense and tissue repair. Peripheral nerve injury induces microgliosis in the SDH, as evidenced by microglia proliferation, morphological changes, and the production of microglial inflammatory mediators, which can sensitize nearby neurons and contribute to the development of pain hypersensitivity. Indeed, microglia have been implicated in neuropathic pain pathogenesis and maintenance, and their activation is dependent on neuronal cues (Chen, Zhang, et al., 2018). Stimulation of C-fibers is sufficient to trigger spinal reactive microglial activation (Hathway et al., 2009), and large A-fiber activation is important for maintaining microglial activation (Suter et al., 2009).

Microglia promptly respond to the nociceptive stimulus and proliferate, and this phenomenon reaches a maximum in the first week following nerve injury contributing to the development of neuropathic pain (Inoue & Tsuda, 2018; Peng et al., 2016). Minocycline, a microglial inhibitor, prevents or delays neuropathic pain (Ledeboer et al., 2005; Raghavendra et al., 2003), and blocking microgliosis attenuates pain behaviors (Guan et al., 2016; Sorge et al., 2015). Preclinical studies of neuropathic pain models, have shown that activated spinal microglia become hypertrophied, secrete pro-inflammatory mediators (interleukin-1β (IL-1β), interleukin-6 (IL-6), TNF-α, BDNF), and lead to phosphorylation of the MAPKs, including p38, extracellular signal-regulated protein kinase (ERK), and JNK (Caraci et al., 2019; Inoue & Tsuda, 2018; Obata & Noguchi, 2004; Wang et al., 2014). These glial cell-derived inflammatory mediators promote the onset, development, maintenance, and transition of neuropathic pain (Peng et al., 2016). Moreover, nerve injury upregulates the ATP receptors P2X purinoceptor 4 (P2X4) and P2Y receptor (P2Y12R), and the chemokine receptor CX3CR1 specifically in spinal microglia. The inhibition of these receptors leads to the alleviation of neuropathic pain (Kobayashi et al., 2008; Tsuda et al., 2003; Verge et al., 2004; Zhuang et al., 2007). Alternatively, anti-inflammatory microglia significantly contribute to the resolution of inflammation and promote tissue repair. Neuroprotective microglia antagonize central sensitization and pain chronicity via phagocytic activity and the release of anti-inflammatory cytokines, including IL-4, IL-10, and transforming growth factor beta 1 (TGF-β1) (Kohno et al., 2022; Sideris-Lampretsas & Malcangio, 2022)

Recent studies suggest that there are sex differences in pain processing throughout the neuroaxis (Mogil, 2020). Animal models have shown a sexually dimorphic microglial function in the development of neuropathic pain and pain relief (Sorge et al., 2015; Taves et al., 2016). However, inconsistencies in the literature have been reported regarding the existence of sex-based differences within the microglial response after nerve injury (Lopes et al., 2017; Peng et al., 2016). Therefore, further investigations are required.

The selective activation of the LC noradrenergic pathway towards the spinal cord alleviates neuropathic nociception in mice by augmenting the NE release and reducing neuroinflammation in SDH (Li et al., 2022). It is known that microglia express α1-, α2-, β1- and β2-ARs (Gyoneva & Traynelis, 2013), and in the SDH, NE may act on microglia which relieves neuropathic pain by reducing neuroinflammation (Caraci et al., 2019; Li et al., 2022). Moreover, administration of the α2-AR agonist Clonidine diminishes hypersensitivity post L5–L6 SNL, which is facilitated by the sprouting of noradrenergic fibers in the spinal cord and increased α2-ARs expression on cholinergic neurons (Hayashida & Eisenach, 2010). This phenomenon necessitates the presence of BDNF that is released from microglia (Coull et al., 2005), indicating that microglia can modulate in different ways the descending noradrenergic pathways in chronic pain-mediated analgesia.

In vitro studies have demonstrated that NE application suppresses microglia activation and proinflammatory cytokine expression (Dello Russo et al., 2004; Gyoneva & Traynelis, 2013; Hertz et al., 2010; Ishii et al., 2015; Morioka et al., 2009; Zhang et al., 2014). Microglia are known to particularly express significantly higher levels of β2-AR compared to the other CNS cell types (O'Donnell et al., 2012), and NE may exert its anti-inflammatory actions on glial cells mainly through microglia. Moreover β1- and β2-ARs appear to be the only significantly functional ARs in microglia (Heneka et al., 2010; Steininger et al., 2011). However, it is unclear whether NE can act directly on β2-ARs expressed by microglia in the SDH *in vivo*.

In summary, microglial function modulation by the descending noradrenergic pathway via β2-ARs presents a promising target for pain management.

1.5 Open Questions

Less than 50 % of current analgesics provide 50 % pain relief (Finnerup et al., 2010). NE is notorious for exerting strong anti-inflammatory activity in the CNS, and its endogenous neuroprotective role in chronic pain is possibly linked to this action. Microglia, which play an important role in the development and maintenance of neuropathic pain, express ARs, and they have been demonstrated to modulate microglial function in diverse contexts.

The precise mechanisms by which β2-ARs regulate microglia in the neuropathic pain framework remain ambiguous and research is required to determine whether targeting ARs could be a viable therapeutic strategy for treating this debilitating condition. Particularly, whether β2-ARs activation on microglia modulates pain in a sex-dependent manner is unclear. Furthermore, whether and how β2-ARs activation on microglia impacts the interactions between microglial and astroglial activation and signaling in the spinal cord in the context of neuropathic pain is not known.

Additionally, neuropathic pain prompts adaptive alterations in response to the compromised descending noradrenergic inhibitory tone and it is currently unclear if other ARs are modulated

in these maladaptive changes during neuropathic pain. This may be attributed to the challenges in obtaining reliable antibodies for ARs and the limitations of genetic models commonly used to study this issue. AR expression patterns are still a subject of discussion and are being gradually elucidated.

Further understanding of the potential analgesic effect of the microglia β2-ARs in neuropathic pain will guide the search for novel therapeutic options.

2. Aims of the study

The role of glial β2-AR represents an untapped therapeutic target in chronic pain treatment. It is unclear whether microglial β2-AR activation can lead to adequate analgesia, particularly in therapy-resistant neuropathic conditions.
The general aim of this project is to comprehend if β2-AR activation on microglia contributes to analgesia in a murine model of neuropathic pain.

This study was designed with the intent to:

- Analyze AR modulation post-nerve injury specifically in the glial cell population found in the spinal cord.

- Investigate the impact of Formoterol on functional changes in pure culture of primary spinal microglia without modulation by other spinal cell types and in *ex vivo* spinal cord acute slices to explore the morphology modifications that Formoterol induces in spinal microglia.

- Study the effect of diverse regimens of the β2-AR agonist in wild type (WT) mice in the SNI neuropathic pain model to determine the timeline of efficacy from early time points post nerve injury, assessing both the sensory and emotional components of pain.

- Examine how Formoterol administration influences spinal microglia and astrocytes throughout the diverse regimens and whether it modulates nerve injury-induced gliosis.

- Assess whether and how the specific deletion of β2-ARs on microglia via genetic manipulations affects the analgesic effect of Formoterol.

- Scrutinize potential sexual dimorphism at the behavioral and cellular level in the SNI model and post-β2-AR agonist application.

Overall, the goal is to elucidate whether targeting β2-AR in neuropathic pain may have therapeutic potential and to provide valuable scientific insights into the neurobiological mechanisms of neuropathic pain.

3. Materials and Methods

3.1 Reagents

Reagents are listed in Table 4.

Table 4. Reagents

Reagent	**Manufacturer**	**Catalog # (Cat #)**
Albumin Fraktion V	Carl Roth GmbH & Co. KG	T844.1
B-27 supplement (50X)	Gibco/Thermo Fischer Scientific	17504044
Biozym LE Agarose	Biozym Scientific GmbH	840001
Bromophenol blue	Carl Roth GmbH & Co. KG	T116.1
Cholesterol	Sigma-Aldrich/Merck	C3045
Collagenase	Sigma-Aldrich/Merck	C-01330
Colony stimulating factor-1 (CSF-1)	Peprotech	300-25
D(+)-Glucose	Carl Roth GmbH & Co. KG	X997.1
Deoxynucleotide Set (100 mM)	Sigma-Aldrich/Merck	DNTP100A-1KT
Deoxyribonuclease I Amplification Grade	Sigma-Aldrich/Merck	18068-015
DirectPCR Lysis Reagent (Ear)	Viagen Biotech Inc.	401-E
DMEM high glucose, pyruvate	Gibco/Thermo Fisher Scientific	11995
Ethylenediaminetetraacetic acid (EDTA)	AppliChem GmbH	A2937
Ethanol	Sigma-Aldrich/Merck	100983
Fetal bovine serum	Gibco/Thermo Fisher Scientific	26140
Formoterol	Tocris	1448
G-5 supplement (100X)	Gibco/Thermo Fisher Scientific	17503012
GelRed® Nucleic Acid Gel Stain	Biotium Inc.	41003
Glycine	AppliChem	A1067
Hoechst 33342, Trihydrochloride	Gibco/Thermo Fisher Scientific	H3570
Interleukin-34 (IL-34)	Peprotech	200-34

L-Glutamine (200 mM)	Gibco/Thermo Fisher Scientific	11539876
Mineral oil	Sigma-Aldrich/Merck	8042-47-5
Mowiol-488	Carl Roth GmbH & Co. KG	0713.1
N2 supplement	Gibco/Thermo Fischer Scientific	11520536
NEB Smart Ladder	Eurogentec	MW-1700-100
Normal horse serum	Gibco/Thermo Fisher Scientific	31874
Oligo(dT)20 primers	Sigma-Aldrich/Merck	18418020
Orange G	Sigma-Aldrich/Merck	1936-15-8
Paraformaldehyde	Sigma-Aldrich/Merck	30525-89-4
Penicillin/Streptomycin (PenStrep)	Gibco/Thermo Fisher Scientific	15140-122
Phosphate buffered saline (PBS)	Gibco/Thermo Fisher Scientific	J61196.AP
Poly-D-Lysine	Sigma-Aldrich/Merck	P6407-5MG
Proteinase K	Sigma-Aldrich/Merck	p6556
qPCRBIO SyGreen mix separate-Rox	PCRBIOSYSTEMS	PB20.14-51
Random hexamer	Sigma-Aldrich/Merck	N8080127
RPMI 1640	Gibco/Thermo Fisher Scientific	11875093
SmartLadder™	Eurogentec	MW-1700-10
Sucrose	Carl Roth GmbH & Co. KG	57-50-1
Sunflower/corn oil	Sigma-Aldrich/Merck	S-5007
SuperScript III Reverse Transcriptase	Sigma-Aldrich/Merck	18080044
Tamoxifen	Sigma-Aldrich/Merck	T-5648-1G
Tissue Freezing Medium	Leica Microsystems CMS GmbH	14020108926
Transforming growth factor-beta 2 (TGF-β2)	Peprotech	100-35B
Trypsin	Sigma-Aldrich/Merck	T-1005
Tris-HCl	Carl Roth GmbH & Co. KG	9090.3
Triton X-100	Sigma-Aldrich/Merck	9036-19-5

TRIzol	Thermo Fisher Scientific	15596018
Tween 20	Carl Roth GmbH & Co. KG	9005-64-5
Xylene cyanol FF	Sigma-Aldrich/Merck	335940

3.2 Antibodies

First and secondary antibodies are listed in Table 5 and Table 6, respectively.

Table 5. First antibodies.

Antigen	**Species**	**Type**	**Manufacturer**	**Cat #**	**Dilution**
Iba1	Rabbit	Polyclonal	Wako	019-19741	1:500
Iba1	Chicken	Monoclonal	Synaptic System	234 009	1:500
p-p38	Rabbit	Polyclonal	Cell Signaling Technology	9212	1:300
p-JNK	Rabbit	Polyclonal	Cell Signaling Technology	4668	1:100
GFAP	Guinea pig	Polyclonal	Synaptic System	173 004	1:1000
β-tubulin III	Rabbit	Polyclonal	Abcam	Ab18207	1:2000
F4/80	Rat	Monoclonal	Biolegend	123102	1:200
CD11b	Rat	Monoclonal	Abcam	Ab8878	1:200

Table 6. Secondary antibodies.

Antigen	**Species**	**Type**	**Manufacturer**	**Cat #**	**Dilution**
Chicken IgG	Donkey	Alexa Fluor-488	Thermo Fisher Scientific, Invitrogen	A-78948	1:1000
Rat IgG	Donkey	Alexa Fluor-488	Thermo Fisher Scientific, Invitrogen	A-21208	1:1000
Rabbit IgG	Donkey	Alexa Fluor-594	Thermo Fisher Scientific, Invitrogen	A-21207	1:1000
Guinea pig IgG	Goat	Alexa Fluor-647	Thermo Fisher Scientific, Invitrogen	A-11076	1:1000

3.3 Buffers and Solutions

Buffers and solutions are listed in Table 7.

Table 7: Buffers and solutions.

Name	Component	Concentration	Comments
10x Buffer for PCR	Tris KCl	200 mM 500 mM	pH = 8.4
Agarose Sample Loading buffer	Glycerol H_2O Bromophenol blue Orange G Xylene cyanol FF	60% 40% Spatula tip Spatula tip Spatula tip	
Antigen retrieval buffer (immunohistochemistry)	PBS Sodium citrate Tween-20	1X 10 mM 0.05%	pH 6.0
Artificial cerebrospinal fluid (aCSF)	NaCl KCl CaCl2 MgCl2 NaH2PO4 NaHCO3 Myo-inositol Sodium Pyruvate Ascorbic Acid	124 mM 2.4 mM 2 mM 1 mM 1 mM 25 mM 3 mM 2 mM 0.4 mM	315 mOsm/L
Blocking buffer (immunohistochemistry)	PBS Normal horse serum	1X 10%	
Blocking buffer for phosphorylated antibodies (immunohistochemistry)	PBS Horse serum NaF BGC NaO4	1X 10% 1:50 1:100 1:100	
Enzymatic solution for DRG dissociation	RPMI 1640 Trypsin Collagenase PenStrep	1X 1.5 mg/ml 2 mg/ml 2%	
Loading buffer (DNA electrophoresis)	Glycerol Bromophenol blue	20% 0.025%	
Lysis buffer for DNA extraction	DirectPCR Lysis Reagent (Ear) Proteinase K	1X 2.5%	
Mowiol	Glycerol Mowiol 4-88 Tris pH 8.5	12% 4.3 M 0.1 M	

N-methyl-D-glucamine (NMDG) based cutting solution	NMDG KCl KH2PO4 MgCl2 CaCl2 choline bicarbonate Dextrose	135 mM 1 mM 1.2 mM 1.5 mM 0.5 mM 20 mM 12.95 mM	310 mOsm/l pH 7.4
Paraformaldehyde (PFA) 4%	PBS PFA NaOH	1X 4% drops	pH 7.2
PBST (1X)	PBS Triton-X100	1x 10 M	
TAE buffer (1X)	Acetic acid EDTA Tris-HCl	20 mM 2 mM 40 mM	pH 8.0

3.4 Machines

Instruments and machines are listed in Table 8.

Table 8. Instruments and machines.

Instrument	**Manufacturer**
Biometra BioDoc Analyze Ti5 Transilluminator	Analytik Jena GmbH
Biometra P25 Standard Power Pack	Analytik Jena GmbH
Biometra T advanced Thermal cycler	Analytik Jena GmbH
Two Photon Microscope – Bergamo II (custom-made)	Thorlabs Inc.
20X water-immersion Objective	Olympus
Confocal laser scanning microscope (Leica TCS SP8 AOBS + 20x/40x object)	Leica Microsystems CMS GmbH
Epifluorescence microscope Y-TV55 + 40x object	Nikon
Hot/Cold Plate 35100	Ugo Basile Inc.
Leica CM1950 Cryostat	Leica Microsystems CMS GmbH
LightCycler 96 Real-Time PCR System	Roche
MACS Dissociator	Miltenyi Biotec
Milli-Q®	Merck
NanoDrop 2000	Thermo Fisher Scientific
Vibratome VT1200 S	Leica

3.5 Animals

In this study, 8 weeks old (adult) C57BL/6J mice of both sexes (Janvier Labs, France), also named wild type (WT) were utilized for qPCR, behavioral, and immunofluorescence experiments. For microglia primary cell culture 5 weeks old C57BL/6J mice were employed. For acute spinal cord slices adult, 8–12 weeks old *Cx3cr1*-eGFP mice were used (provided by Prof. Dr. Frank Kirchhoff, University of Saarland). Mice lacking the β2-AR specifically in *Cx3cr1*-expressing cells were generated by crossing mice with a conditional allele for the *Adrb2* (*Adrb2*$^{fl/fl}$) gene (made available by Prof. Dr. Gerald Karsenty, Columbia University) with mice presenting the inducible *Cx3cr1*-CreERT2 gene (provided by Prof. Dr. Steffen Jung, Weizmann Institute of Science, and Prof. Dr. Frank Kirchhoff, University of Saarland). These mice express the tamoxifen-inducible Cre under the control of *Cx3cr1* macrophages and microglia-specific promoter. To induce the recombination Cre-mediated of the *Adrb2* floxed allele, 5-week-old *Cx3cr1*-CreERT2; *Adrb2*$^{fl/f}$ mice were intraperitoneally (i.p.) injected with 50 mg/kg of tamoxifen (10 mg/ml) once daily for 5 consecutive days. A waiting period of more than three weeks was observed to ensure the complete loss of β2-AR in microglial cells. Behavioral and immunohistochemistry experiments were conducted using 8–9 weeks old *Cx3cr1*-CreERT2; *Adrb2*$^{-/-}$ mice.

All mice employed in this study had the C57BL/6 as genetic background. Mice were housed in a controlled environment (22 ± 2 °C temperature, 50–60% humidity, along with 12 h light / dark cycle) with food and water provided *ad libitum*, and caged in groups of 2–4 in conformity with ARRIVE guidelines. All experimental procedures were approved by the local governing body (Regierungspräsidium Karlsruhe, Germany, Ref. 35-9185.81/G-177/17 and 35-9185.81/G-274/19) and abided by German Law that regulates animal welfare and the protection of animals used for the scientific purpose (TierSchG, TierSchVersV).

3.5.1 Genotyping verification

To obtain DNA for mouse genotyping, mice ear punches were taken and added to 100-200 µL of lysis buffer. The tubes were incubated in a hybridization oven at 55 °C overnight at 700 RPM. The next day, the tubes were incubated at 85 °C for 45 minutes (min). The crude lysate was then centrifuged and stored at -20 °C.

The following PCR primer sets were used in mouse genotyping: *Cx3cr1*-forward (5´-TCAGTTTTCTCCCGCTTGC-3´; cat # 5927), *Cx3cr1*-forward R2F (5´-ATCAACGTTTTGTTTTCGGA-3´) and *Cx3cr1*-reverse (5´-CCTTCGGGTTCTCGTAGTGAC-3´; cat # 5828) for *Cx3cr1*-CreERT2. The sizes of the PCR products are 600 base pairs (bp) for the CreERT2 knock-in and 400 bp for the WT mice. For A*drb2*$^{fl/fl}$ mice, B2 fl F (5´-

CCAAAGTTGTTGCACGTCAC-3) and B2 fl R (5´-GCACACGCCAAGGAGATTAT-3´) were utilized. For knock-in animals, the PCR product size is approximately 570 bp, and for WT mice is 520 bp. For *Cx3cr1*-eGFP mice, *Cx3cr1*-forward WT (5´-GTCTTCACGTTCGGTCTGGT-3´), *Cx3cr1*-forward mutant (5´-CTCCCCCTGAACCTGAAAC-3´) and *Cx3cr1*-reverse common (5´-CCCAGACACTCGTTGTCCTT-3´) were used. The expected bands are long 500 bp for the knock-in and 410 for the WT mice.

All primers are purchased by Sigma-Aldrich. Amplification of purified DNA was conducted by polymerase chain reaction (PCR). The PCR mixture was prepared as follows: 2.5 µl 10X PCR buffer, 0.2 µl T37, 0.6 µl $MgCl_2$, 0.5 µl dNTPs, 1.2 µl each primer used (10 µmol/l), 1 µl DNA, H_2O up to 24 µl. The PCR mixtures were run under the conditions listed in Table 9, Table 10 and Table 11.

Table 9. Thermocycler program for *Cx3cr1*-CreERT2.

Step	**Temperature (°C)**	**Time (min)**	**Number of cycles**
1. Initial denaturation	94	3:00	
2. Denaturation	94	0:30	
3. Annealing	52	0:30	
4. Extension	72	1:00	31x from step 2
5. Final extension	72	10:00	
6. Store	4	∞	

Table 10. Thermocycler program for *Adrb2*$^{fl/fl}$.

Step	**Temperature (°C)**	**Time (min)**	**Number of cycles**
1. Initial denaturation	95	5:00	
2. Denaturation	95	1:00	
3. Annealing	58	1:00	
4. Extension	72	1:00	40x from step 2
5. Final extension	72	5:00	
6. Store	4	∞	

Table 11. Thermocycler program for *Cx3cr1*-eGFP.

Step	**Temperature (°C)**	**Time (min)**	**Number of cycles**
1. Initial denaturation	95	5:00	
2. Denaturation	95	0:30	

3. Annealing	60	0:30	
4. Extension	72	0:30	30x from step 2
5. Final extension	72	5:00	
6. Store	4	∞	

3.5.2 DNA-agarose gel electrophoresis

DNA sequences of *Cx3cr1*-CreERT2, *Cx3cr1*-eGFP, and *Adrb2*$^{fl/fl}$ were run on a 1.5, 2.0, and 2.5% agarose gel, respectively. Agarose gel was prepared in 1X TAE buffer and Gelred nucleic acid gel stain (5 µl / 100 ml) was added while the mixture was on a magnetic stirrer. DNA samples were mixed with a 4X loading buffer and subjected to electrophoresis at 130 V. Afterward, the gel was exposed to UV light and the resulting image of DNA bands was captured using a Biometra Ti5 acquisition system and BioDocAnalyze software.

3.6 Spared nerve injury surgery

The spared nerve injury (SNI) surgery was performed according to an earlier protocol (Decosterd & Woolf, 2000) with minor modifications. Briefly, 8-week-old mice were anesthetized utilizing a mixture of 2% isoflurane, nitrous oxide, and oxygen. The tibial and common peroneal nerves were uncovered through an incision in the lateral thigh skin, tightly ligated, and cut distally. A 1 mm piece of nerve was removed below the suture, leaving the sural nerve intact. The sham surgery followed the same procedure without causing any nerve damage. The muscle layer was then gently closed and the skin was stitched with Marlin 4-0 absorbable suture.

3.7 Drug administration

Mice were given an i.p. injection of 5, 50, or 500 µg/kg Formoterol (Yalcin et al., 2010) or its solvent, 0.9% NaCl, one hour before perfusion for subsequent immunofluorescence or behavioral experiments.

3.8 Microglia and astrocytes isolation from the spinal cord

Isolated microglia for cell culture were taken from the entire spinal cord of 5-week-old mice. Microglia and astrocytes for RNA extraction and analysis were extracted from the spinal segments L3–L5 of three 8-week-old mice that were pooled together. Three pooled mice were counted as n = 1. Microglia and astrocytes were isolated using the gentle magnetic-assisted cell sorting (MACS) Dissociator (Miltenyi Biotec) by homogenizing the spinal cord tissue with the Adult Brain Dissociation Kit (cat # 130-107-677, Miltenyi Biotec) and employing the gentleMACS program 37C_ABDK_02. When used for RNA extraction, the resulting cell

suspension was treated with Myelin Removal Beads II (cat # 130-096-731, Miltenyi Biotec) to remove myelin, adapting the volume of the buffer and beads to the initial tissue quantity. This passage was skipped when dealing with cell culture. The cells mixture was then incubated with CD11b Microbeads (1:10, cat # 130-049-601, Miltenyi Biotec) when microglia were the goal of the separation, or astrocyte cell surface antigen-2 (ACSA-2) Microbeads (1:10, cat # 130-097-678, Miltenyi Biotec) when astrocytes were isolated. Microglia and astrocytes were isolated using a magnetic MACS separator. The purified cell types were collected for further cell culture or snap-frozen on dry ice and kept at -80 °C for RNA extraction.

3.9 RNA extraction, reverse transcription and quantitative PCR

Mice were perfused trans-cardially with cold PBS and the SDH segments L3–L5 were rapidly collected, snap-frozen on dry ice, and store at -80 °C. RNA extraction was also applied to microglia and astrocytes from the L3–L5 SDH isolated as described in 3.8. Total RNA was extracted using the TRIzol method and purified with Deoxyribonuclease I Amplification Grade according to the company's instructions. First-strand cDNA was synthesized from 1 µg of total RNA, random hexamers, oligo(dT)20 primers, and SuperScript III Reverse Transcriptase as instructed by the manufacturer. The reverse transcriptase was omitted as control for each reaction.

Quantitative PCRs (qPCRs) were run utilizing qPCRBIO SyGreen mix with separate Rox and specific primers (Table 12, Table 13) on a LightCycler 96 Real-Time PCR System. The data were processed with the related software and normalized by the expression of glyceraldehyde-3-phosphate dehydrogenase (*Gapdh)* mRNA (housekeeping gene). The relative gene expression levels were determined by employing the comparative ΔΔCt method. The purity of the isolated microglia was examined by qPCR using specific gene markers for astrocytes (Aquaporin-4, *Aqp4*), microglia (*Cx3cr1)* oligodendrocytes (Myelin basic protein, *Mbp*), and neurons (Synaptotagmin-1, *Syt1*) (see Table 12).

Table 12. Primers employed for qPCR analysis to assess the purity of microglia and astrocyte purification, as well as for primary microglia cell culture.

Primer	**Sequence 5' → 3' Forward**	**Sequence 5' → 3' Reverse**	**Efficiency**
Aqp4	TGGAGGATTGGGAGTCACC	TGAACACCAACTGGAAAGTGA	1.98
Cx3cr1	CGTGAGACTGGGTGAGTGAC	GGACATGGTGAGGTCCTGAG	1.96
Mbp	ATTGGGTCGCCATGGGAAAC	CCAGCCTCTCCTCGGTGAAT	2.07
Syt1	CTCAACTGGCATTTGTTAGTCAA	AGACTGCGGATGTTGGTTGT	2.01

Table 13. Primers utilized for qPCR to study spinal cord and microglial expression of ARs.

Primer	Sequence 5' → 3' Forward	Sequence 5' → 3' Reverse	Efficiency
Adra1a	CTGAAGGTCCGCTTCTCCT	CCTGGAGCTTCGTTTATCTGA	2.04
Adra1b	GCCTAAGACGTTGGGCATTGT	GTTGAAGTAGCCCAGCCAGA	1.94
Adra1d	GTCTTCGTCCTGTGCTGGTT	CTTGAAGACGCCCTCTGATG	2.02
Adra2a	TAGAACTGACTTTTCTTCCGTTCTC	AACATACACGCTCTTCTTCAAGC	1.98
Adra2b	AGCACCTGTGGTTCTCCTTG	CAGCAACCAGCCACTAGACCA	2.05
Adra2c	CTTCAGGCAATGACCCTCTG	AGAGCTGTCCAGGACGTCAG	2.04
Adrb1	CGTGCCCCTGTGCATCA	GTCGATCTTCTTTACCTGTTTTTGG	2.01
Adrb2	GCATGGAAGGCTTTGTGAAC	CTTGGGAGTCAACGCTAAGG	1.96
Gapdh	AGAAGGTGGTGAAGCAGGCATC	CGAAGGTGGAAGAGTGGGAGTTG	1.98

3.10 Primary microglia cell culture

The purified microglia obtain as aforementioned in section 3.8, were resuspended in cell culture medium, which consisted of DMEM medium supplemented with PenStrep (1%), G-5 supplement (1:100), IL-34 (100 ng/mL), TGF-β2 (2 ng/mL), and cholesterol (1.5 g/mL) (Bohlen et al., 2017). Then they were plated on poly-D-Lysine coated glass coverslips in a 24-well plate. The cells were grown at 37 °C under 5% CO_2 in an incubator. To enhance cell proliferation and survival during the initial five days of culture, CSF-1 (10 ng/mL) was added to the culture medium. Subsequently, the primary cultures were maintained for an additional five days in culture medium with CSF-1 to imitate a neuropathic state (reactive microglia).

3.11 Dot blot

Primary reactive microglia obtained as described in section 3.10 were treated with Formoterol (10 ng/ml) or vehicle for 1 h before the supernatant collection. The supernatant was collected and stored at -80 °C. The Mouse Inflammation Antibody Array, Membrane 40 Targets (cat # ab133999, Abcam) was utilized to determine levels of released inflammatory mediators, as per the manufacturer's instructions.

3.12 Acute preparation of spinal cord slices

After cervical dislocation, spinal cord L1–L6 were extracted, and transversal sections were cut at 300 µm thickness in ice-cold NMDG-based cutting solution (adapted from (Rieder et al., 2022)). Spinal cord slices were incubated in aCSF for 30 min at 37 °C, then another 30 min at RT, and the same condition remained during two-photon microscopy recording. Solutions and slices were continuously purged by carbogen.

3.13 Two-Photon microscopy imaging of spinal cord slices

To perform *ex vivo* spinal cord slices imaging, a custom-made two-photon laser-scanning microscope (2P-LSM), with a 20X water-immersion objective (1.0NA, XLUMPLFLN, Olympus), 8 kHz galvo/resonance scanner, piezo drive for fast z-scanning, and two GaAsP PMT detectors were employed. Two-photon excitation for eGFP at a single wavelength was achieved using a mode-locked Ti:sapphire pulsed laser (Chameleon Ultra II, Coherent) adjusted at 940 nm and the power was tuned from 30 to 40 mW, according to the imaging depth. Areas of the spinal dorsal horn were recorded as field of view with 1024 × 1024 pixels per image, at 1.9 frame rate, and averaging 4 times each frame. Each imaging session consisted of a 7-10 min recording. The *ex vivo* spinal cord slices were subjected to 2P-LSM while being continuously perfused with carbogenated aCSF. Videos were captured with the ThorImage®LS (Thorlabs) software.

For each spinal cord slice, three videos were recorded: baseline, incubation with Formoterol (10 µg/ml), and washout (incubation with carbogenated aCSF). Between the baseline recording and Formoterol recording, slices were incubated for 15 min in carbogenated aCSF with Formoterol (10 µg/ml). Between Formoterol recording and washout, slices were incubated for 10 min in carbogen aCSF. As a control, three videos with the same experimental timeline without the Formoterol application were recorded.

3.13.1 Video analysis

The sequences of images obtained from the 2P-LSM recording were analyzed utilizing Fiji-Image J software (version 1.52p, National Institutes of Health, USA). Hyperstacks from the sequence of images were created with z-slices and t-frames. 2D maximum-intensity z-projection files were generated to obtain a 2D maximum-intensity projection two-photon microscopy time series.

3.13.1.1 MotiQ analysis

To analyze the aforementioned file, MotiQ software was employed. It is an open-source ImageJ plugin approved for the quantification of the cell morphology and dynamics of microglia (Hansen et al., 2022). The MotiQ software consists of several functions that are beneficial for analyzing single-cell images of microglia and extracting them as regions of interest (ROIs) from image stacks and time series. The cropper function enables the definition of a single-cell image of microglia and extracts them as regions of interest (ROIs) from image stacks and time series. The threshold function allows for automated image segmentation of MotiQ cropper-obtained images. The 2D analyzer function can automatically process background-depleted or binary images that have been generated by the MotiQ thresholder. This facilitates the analysis of 5–

6 single-cell microglia per slice. The MotiQ 2D analyzer can process 2D images in time series. The data I obtained are 2D maximum-intensity projection 2P microscopy time series (*ex vivo*) and for those types of files the authors suggested that for the pre-processing step, the scale-down reference image for calculation – factor should be "1" and "not convert input and reference images into 8-bit before processing". For the threshold determination, I adopted "MinError" as threshold algorithm and for the stack handling, I selected "apply threshold determined in the stack histogram".

3.13.1.2 Python Script

The data obtained from the MotiQ analyzer were processed through a custom-written Python script (kindly written by Ph.D. student Antonio Albanese, University Carlos III of Madrid, Leganés, Spain; Anaconda Software Distribution. Computer software. Vers. 2-2.4.0. Anaconda, Nov. 2016. Web. https://anaconda.com). The data were combined to have a single table of values for each single-cell image containing the values of the baseline, Formoterol, and washout recordings. Data are normalized on the first frame value of the same parameter chosen. Values are then plotted as the average between the single cells belonging to the same mouse over time. The area under the curve (AUC) calculation for each mouse was performed and plotted as control spinal cord slices, which were incubated only with aCSF, and treated spinal cord slices, which receive Formoterol treatment.

3.14 Behavioral tests

All behavioral tests were conducted with double-blinding to adhere to the guidelines of the IASP. The experimenter was blinded to the treatment group allocations. All behavioral assessments were conducted on awake, unrestrained, age- and sex-matched adult mice.

3.14.1. Experimental design

Baseline measurements for mechanical hypersensitivity and thermal allodynia were performed twice, once per day, two days before the SNI or sham surgery utilizing von Frey filaments and cold plate tests. The cold plate test was conducted in series to the von Frey filament test. The behavioral responses were assessed according to three distinct experimental paradigms:

i) In the first plan, mechanical hypersensitivity and cold allodynia were assessed on day 3 post-surgery, 1 h after administering an i.p. injection of either Formoterol or vehicle.

ii) In the second strategy, the behavioral response was tested on days 6 and 21 post-surgery, each day 1 h post-Formoterol or vehicle i.p. injection.

iii) In the third administration paradigm, behavioral parameters were assessed solely on day 21 post-surgery, 1 h after post-i.p. injection of Formoterol or vehicle.

To examine the effect of Formoterol injection on mechanical and cold response over time, von Frey filaments measurements were obtained at 1, 6, 12, and 24 h after drug administration. However, due to the two-hour duration of the mechanical experiment, there was a delay in conducting the thermal tests, resulting in each group being evaluated for cold allodynia at 3, 8, 14, and 26 h after injection. To ensure that no potential early analgesic effects were missed and to minimize the time interval between different recordings, the missing time points for each test were evaluated (i.e., 3 h for the mechanical test and 1 h for the cold test). These time points were examined separately in graphs since a different cohort of mice was used to minimize stress to the animals. The conditioned place preference (CPP) experiment was conducted starting from days 4 or 32 after the SNI or sham surgery as described in section 3.14.4.

3.14.2. Mechanical sensitivity

Prior to mechanical sensitivity testing, mice were habituated to the experimental setup (Large Framed Perforated Metal Sheet, cat # 37450-005, Ugo Basile Inc.), which included an elevated grid equipped with von Frey filaments (Semmes-Weinstein, cat # 37450-27, Ugo Basile Inc.). The habituation counted for a total of 1 h in three separate sessions within the week preceding the testing as well as 20–30 min before each testing session. A series of von Frey filaments with increasing forces (ranging from 0.008 to 1.0 g) was applied to the ipsilateral and contralateral hind paws using the up-down method defined by Dixon (Dixon, 1980). The withdrawal frequency was determined from five solicitations per filament, with a minimum pause of 5 min between filaments. A positive nociceptive reaction induced by the filaments is defined as paw withdrawal, flinching, and/or paw licking. To determine the 50% withdrawal threshold, response rate versus von Frey force curves were plotted and fitted with a Boltzmann sigmoid equation. The lower and upper constraints of the equation were set to 0 and 100, respectively (Nees et al., 2023). The area under the curve (AUC) was calculated as the integral of the response frequency-von Frey force intensity curves, which filaments ranging from 0.008 to 0.1 g. This information was used to assess mice hypersensitivity to mechanical stimuli.

3.14.3. Thermal sensitivity

Cold plate test was employed to assess the mice sensitivity to cold stimuli. Mice were placed on a 4 °C cold metal surface surrounded by a Perspex cylinder (Hot/Cold Plate) and observed for nociceptive responses such as paw lifting, shaking, licking, or jumping. The latency of the first nociceptive response was recorded and a minimum of three measurements were

conducted during each testing session. To prevent potential injury to the paws, a 30-second cut-off was used.

3.14.4. Conditioned place preference test

To evaluate whether Formoterol provides pain relief from spontaneous pain, the conditioned place preference (CPP) test was employed, as described in Huang et al. (Huang et al., 2003). During the CPP experiment, mice were conditioned to associate one of the two chambers with Formoterol (pain relief). Behavioral testing was conducted between 9:00 a.m. and 4:00 p.m. and each session lasted 30 min. The mice preferences were determined before the conditioning (baseline preference) allowing them to freely move between compartments. Mice with a preference superior to 70% for one chamber were excluded. The conditioning began one day after the baseline preference was determined. For three consecutive days, the mice were first injected with saline and 10 min later placed in one of the chambers. After a minimum of 4 h from the saline injection, mice received β2-AR i.p. injection and then placed in the other compartment after 50 min. The following day, the mice were again placed in the setup and allowed to freely move between the chambers. The CPP sessions were recorded on video and the time spent in each chamber was calculated using ANY-maze software (Stoelting Europe, Churchtown, Dublin, Ireland, ANY-maze 7.1). The change in time spent in the Formoterol-associated chamber was scored as the difference in time spent in that chamber on the baseline and test days.

3.15 Peripheral macrophage isolation

Mice were anesthetized by isoflurane and killed by cervical dislocation before the following procedures.

3.15.1 Isolation of macrophages from the peritoneal cavity

The inner skin lining the peritoneal cavity was exposed and 3 mL of ice-cold PBS with 5% PenStrep were injected. After injection, I gently massaged the peritoneum and collected the fluid. The collected fluid was spinned at 450 RPM for 10 min. The supernatant was discarded and resuspended in 90 µL of MACS buffer and 10 µL F4/80 beads (1:10, cat # 130-110-443, Miltenyi Biotec). Magnetic sorting continued as described previously in paragraph 3.8. Sorted macrophages F4/80^{+} were plated in glass coverslip in a 24-well plate in 500 µL of RPMI 1640, 10% FBS, and 10% PenStrep. The morning after macrophages adhered to the coverslip. The coverslips were washed one time with RPMI, once with PBS, and finally with 400 µL of Trizol for successive RNA extraction or 500 µL of 4% PFA for immunofluorescence staining to check macrophage purity. The procedure for the RNA extraction continued as aforementioned in paragraph 3.9. The immunostaining protocol is described in section 3.16.3.

3.15.2 Isolation of macrophages for DRG

35 - 40 DRGs were collected from *Cx3cr1-Adrb2*$^{-/-}$ and *Adrb2*$^{fl/fl}$ mice and incubated in 1 mL of enzymatic solution at maximum velocity for 30 min at 37°C. After digestion, the DRGs were mechanically dissociated with coated glass pipettes and minced through 40 µm cell strainers. To stop cell digestion, 100 µL of FBS was added. The cell suspension was centrifuged at 1000 RPM for 3 min at RT. The supernatant was removed and cells were resuspended in 2 mL of RPMI 1640 and 10% FBS. Again, the suspension was centrifuged for 3 min at 1000 RPM, the supernatant was discarded and cells were resuspended in 90 µL of MACS buffer and 10 µL CD11b beads (1:10). Procedure continued as described in the previous paragraph 3.15.1.

3.16 Immunohistochemistry

3.16.1 Mouse spinal cord tissue preparation

On days 3, 6, and 21 post-surgery, and 1 h after i.p. injection of Formoterol or vehicle mice were perfused trans-cardially with cold PBS followed by 4% PFA. The spinal columns were collected and post-fixed overnight in 4% PFA at 4 °C. The next day, spinal segments L3–L4 were extracted and cryopreserved in 30% sucrose overnight. Subsequently, they were cryosectioned into 20 µm thick sections and stored at -20 °C.

3.16.2 Immunofluorescence procedure for spinal cord slices

Immunostaining on spinal cord sections was performed according to standard protocols (Damo et al., 2023). Briefly, sections were washed in PBS and in 50 mM glycine for 15 min. After, they were incubated for 1 h in blocking solution. The primary antibodies listed in Table 5 were incubated overnight at 4 °C in blocking solution. The next day, slices were washed in blocking solution, then in PBST for 15 min. Successively, sections were incubated in the secondary antibodies listed in Table 6 for 1h, followed by three 10-min washes in blocking solution. Slices were treated with Hoechst 33342 diluted 1:10'000 in PBS for 15 min, and rinsed twice in PBST. Lastly, the spinal cord slices were washed in 10 mM TRIS/HCl for 10 min before mounting them on glass slides with Mowiol and stored at 4 °C.

For p-JNK detection, sections were first pretreated in an antigen retrieval buffer in a water bath at 80 °C for 20 min and then allowed to cool down to RT for 30 min. The standard protocol was then followed.

3.16.3 Immunofluorescence procedure for macrophages on coverslips

Immunostaining of macrophages on glass coverslips derived from cell culture was conducted according to the protocol described in section 3.15.2 with minor modifications. Briefly, coverslips were washed three times with PBS and then blocked for 1 h in blocking solution.

The primary antibodies listed in Table 5 were incubated for 2 h at RT. Slices were then washed three times in blocking solution for 15 min and PBS for 10 min. The secondary antibodies listed in Table 6 were incubated for 1 h at RT. Hoechst 33342 diluted 1:10´000 in PBS was kept for only 2 min on the coverslips before the slides were rinsed twice with PBS and once with 10 mM TRIS/HCl for 10 min. Then they were mounted on glass slides with Mowiol and stored at 4 °C.

3.16.4 Image acquisition

Labeled slices were imaged using a confocal laser-scanning microscope (20x, 40x objectives) employing identical illumination exposure parameters for all groups. The acquisition of a montage of confocal image stacks was conducted via sequential line scans over a z-stacks of 12 µm. Images for microglia morphology analysis were taken using an epifluorescence microscope (40x objective). The Fiji-Image J software was employed to analyze the maximum z-projection of spinal cord images.

3.16.5 Image analysis

I used the FIJI-Image J cell counter plug-in to count the number of ionized calcium-binding adapter molecule 1 (Iba1)-positive cells and double-positive p-p38/Iba1, p-JNK/Iba1, and p-JNK/GFAP. For each mouse, I took 3–6 images of the region of interest, which is the ipsilateral and contralateral SDH laminae I–III. In these regions, the fluorescence intensity detection of GFAP was calculated as the mean grey value. The cell density and fluorescence intensity density resulted from the ratio of the ipsilateral and contralateral side results and the ROI area. Data are represented as the ratio between the ipsi and contralateral sides of the SDH. For morphological analysis, I analyzed 15–20 microglia per mouse, assessing the microglial soma perimeter and the process length via the FIJI-image J measurements feature.

3.17 Statistical analysis

Statistical analysis was performed using Prism 9 (GraphPad Software). When two groups of data were compared two-tailed, unpaired Student's t-test was employed. When comparing multiple groups and two variables, two-way ANOVA was utilized followed by post-hoc Tukey's test for multiple comparisons conducted to define statistically significant differences. When multiple groups and three variables were compared, three-way ANOVA was performed followed by post-hoc Bonferroni´s test for multiple comparisons. A p-value of < 0.05 was considered significant. Sample number (n) and p-values are indicated in the figure legends. Actual p-values and interactions are indicated in Appendix Table 14. Data are represented as mean ± standard error of the mean (SEM).

4. Results

4.1 Analysis of the adrenergic receptor expression in SNI-operated mice

Nerve injury causes plastic changes to occur in the central noradrenergic system which influences its anti-nociceptive efficacy (Pertovaara, 2006). To investigate the ARs modulation early on after neuropathic pain was induced, the segments L3–L5 of the SDHs were collected three days post-SNI or sham surgery. The three-day time point was selected due to the prevailing understanding that microglia become activated within a few days following injury. As demonstrated in Figure 2A, qPCR investigation indicated that A*drb2* mRNA had a trend towards increment in SNI mice compared to sham mice. Due to these initial results, I addressed whether nerve injury affected *Adrb2* mRNA expression in spinal glial cells, precisely microglia and astrocytes. Therefore, microglia were isolated via magnetic-activated cell sorting (MACS) from segments L3–L5 of the SDH of SNI or sham mice 3 days post-surgery. The purity of isolated microglia was asserted through qPCR analysis and it showed the unique expression of the specific microglial marker *Cx3cr1* and the absence of genes specifically expressed in neuronal cells (*Syt*1), astroglia cells (*Aqp4*), and oligodendrocytes (*Mbp*) (Figure 2B). Three days post-surgery, *Adrb2* mRNA expression in spinal microglia presented a significant upregulation in SNI compared to sham mice (Figure 2C). Since astrocytes also present β2-ARs, spinal astrocytes deriving from segments L3–L5 of SDH from operated mice were isolated and investigated for *Adrb2 mRNA* expression (Figure 2D, E). Analysis of astrocytes from SNI mice did not demonstrate a significant difference in *Adrb2* mRNA expression compared to sham mice three days post-nerve injury (Figure 2E). Thus, nerve injury specifically upregulates *Adrb2* expression in spinal microglia.

4.2 Effects of Formoterol in microglia culture and *ex-vivo* preparations

4.2.1 β2-ARs stimulation diminished the release of inflammatory mediators from reactive primary microglia in culture

Due to the preliminary results indicating that *Adrb2* mRNA expression in microglia was modulated in neuropathic conditions, I aimed to discern the impact of β2-AR stimulation on microglia from the other cell populations. Primary spinal microglia were isolated from WT mice via MACS sorting and plated. After one day of plating, microglial cells were treated with CSF-1 for 5 days (Guan et al., 2016) to mimic activation following nerve injury. Then the cells were incubated with the β2-AR agonist Formoterol (10 ng/mL) or the control solution for 1 h (Figure 3).

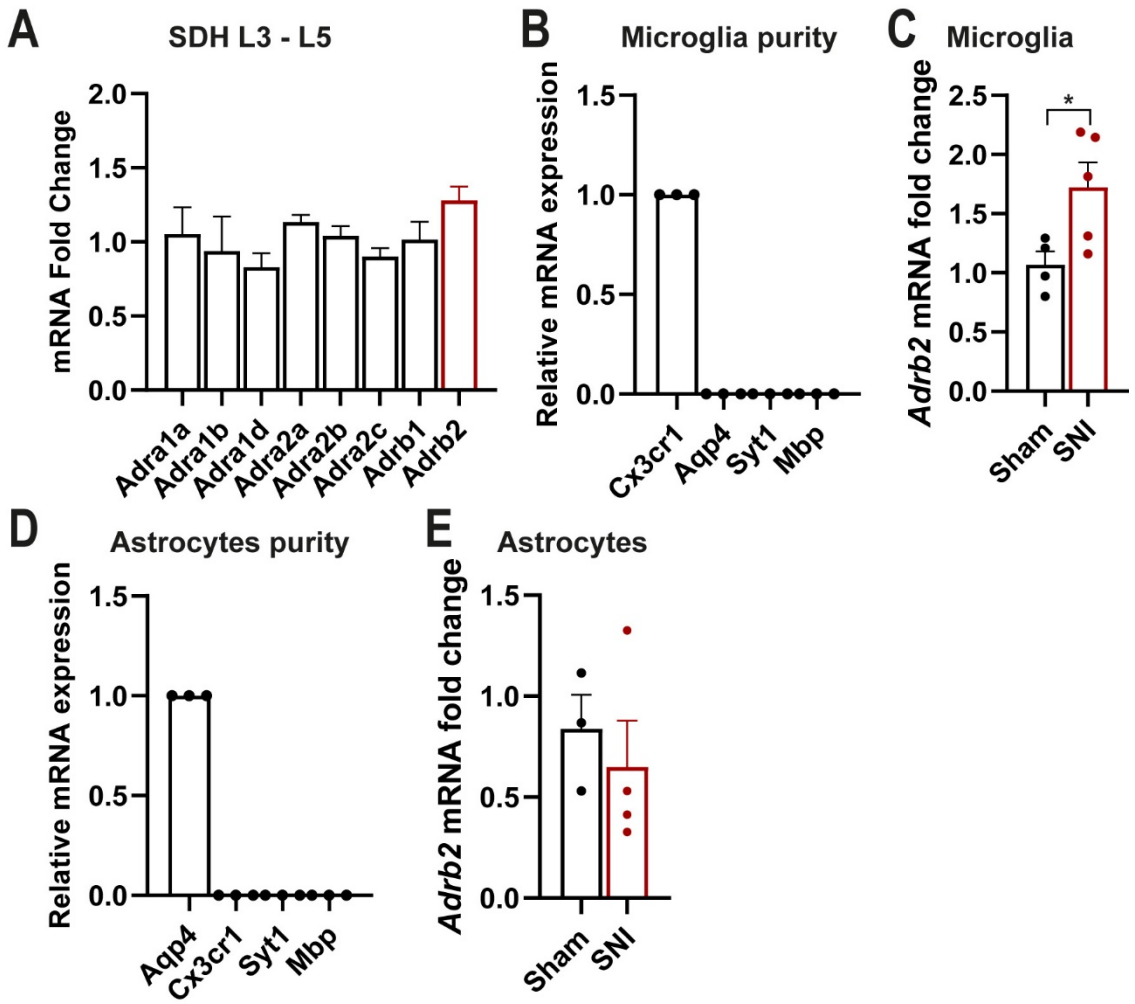

Figure 2. AR expression changed in spinal glial populations of the spinal cord early on after neuropathic pain.

(A) Analysis of qPCR expression of ARs mRNA from the segments L3–L5 of SDH of mice, three days post-surgery, is depicted as fold change compared to sham mice. n = 3/group. (B) Purity assessment of MACS-sorted microglia segments L3–L5 of SDH on markers specific for microglia (*Cx3cr1*), astroglia (*Aqp4*), neuronal cells (*Syt1*), and oligodendrocytes (*Mbp*). n = 3/group. (C) *Adrb2* mRNA was significantly increased in microglia isolated from the SDH of SNI compared to sham mice on day three post-surgery. n = 4–5/group; Mann-Whitney test was conducted; * $p < 0.05$ as compared to sham group. (D) MACS-sorted astrocytes from segments L3–L5 of SDH were analyzed for purity via qPCR. n = 3/group. (E) Relative expression of *Adrb2* mRNA in astrocytes from the SDH of neuropathic and uninjured mice on day three post-surgery. n = 3–4/group. Data are represented as mean ± SEM.

A

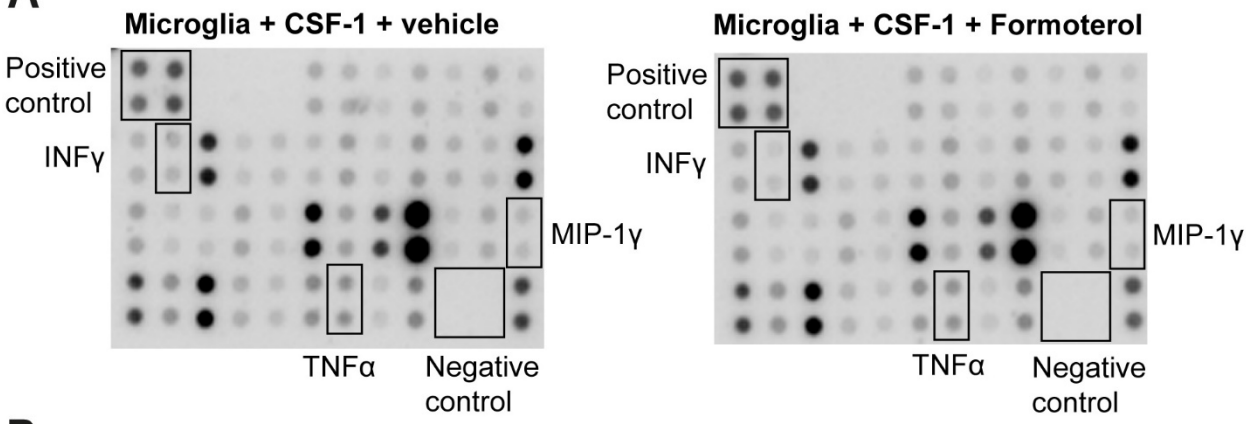

B

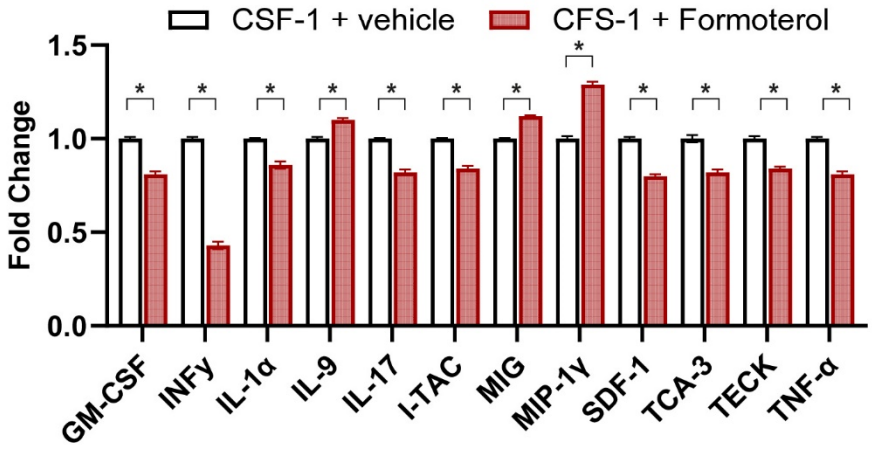

C

	CSF-1 + vehicle	CSF-1 + Formoterol
GM-CSF	1 ± 0.02	0.81 ± 0.03
INFγ	1 ± 0.02	0.43 ± 0.04
IL-1α	1 ± 0.01	0.86 ± 0.04
IL-9	1 ± 0.02	1.10 ± 0.02
IL-17	1 ± 0.01	0.82 ± 0.03
I-TAC	1 ± 0.01	0.84 ± 0.03
MIG	1 ± 0.01	1.12 ± 0.01
MIP-1γ	1 ± 0.03	1.29 ± 0.03
SDF-1	1 ± 0.02	0.80 ± 0.02
TCA-3	1 ±0.04	0.82 ± 0.03
TECK	1 ± 0.03	0.84 ± 0.02
TNF-α	1 ± 0.02	0.81 ± 0.03

Figure 3. Formoterol stimulation diminished the release of inflammatory mediators from reactive primary microglia *in vitro*.

(A) Images of inflammatory cytokine dot blots which were utilized. (B) CSF-1-stimulated microglia secreted less inflammatory mediators post-Formoterol treatment compared to vehicle incubation. (C) The values of cytokines significantly changed in Formoterol-treated primary microglial cultures compared to untreated. n = 4/group; Mann-Whitney test was conducted; * $p < 0.05$ as compared to

vehicle-treated group. Data are represented as mean ± SEM. Experiments and analysis were done by Dr. Manuela Simonetti (Institute of Pharmacology, Heidelberg University).

Formoterol-treated microglia showed a significantly reduced release of pro-inflammatory substances triggered by incubation with CSF-1, including IL-1α, IL-17, interferon-gamma (INF-γ) and TNF-α compared to the control. Furthermore, Formoterol incubation significantly decreased the secretion of cytokines and chemokines that typically stimulate immune cells to proliferate and/or migrate towards the injury site, including T cell activation gene-3/CC-chemokine ligand 1 (TCA-3/CCL1), interferon-inducible T cell alpha chemoattractant (I-TAC), thymus-expressed chemokine/CC-chemokine ligand 25 (TECK/CCL25), granulocyte-macrophage colony-stimulating factor (GM-CSF), and stromal cell-derived factor 1 (SDF-1). Conversely, the release of anti-inflammatory cytokines, such as IL-9, and other chemotactic cytokines for migrating immune cells, including macrophage inflammatory protein-1 gamma/CC-chemokine ligand 9 (MIP-1γ/CCL9) and monokine induced by interferon-gamma (MIG), significantly increased after Formoterol compared to untreated cultures (Figure 3B, C). These results suggest that β2-AR stimulation in cultured activated microglia attenuates the secretion of pro-inflammatory mediators and promoted the release of anti-inflammatory molecules.

4.2.2 Effect of Formoterol on spinal microglia morphology in *ex vivo* spinal cord preparations

Microglia morphology is crucial for their cellular functions and interactions within the CNS. Modifications in microglial morphology serve as strong indicators of the inflammatory condition of the CNS. Reactive amoeboid microglia exhibit larger cell bodies and shorter processes than resting microglia, characterized by a ramified morphology.

Ex vivo preparations of spinal cord slices from *Cx3cr1*-eGFP mice were employed for the investigation of microglia morphology. The excessive manipulation required for spinal cord extraction and acute slice preparation caused changes in microglia morphology resulting in a more amoeboid and reactive appearance (Rieder et al., 2022). Formoterol was applied to decipher if the β2-AR activation could restore microglial homeostatic morphology. Microglia from spinal cord slices were recorded using two-photon laser scanning microscope (2P-LSM) before, during and post-Formoterol incubation. As control for the potential phototoxicity that could perturb microglia morphology, slices were incubated only with artificial cerebrospinal fluid (aCSF) and recorded with the same protocol (Figure 4A, B).

Microglia structure was investigated via morphological and dynamic parameters. Microglia morphology is predominantly characterized by their ramification, which refers to the complexity of the branch structure of their processes. There are two main approaches for measuring

microglial ramification. The first is to analyze microglial cell skeleton, which involves examining the structure of the microglial process tree (Leyh et al., 2021; Nimmerjahn et al., 2005). This approach provides more detailed information about the subcomponents of the microglial process tree and their spatial arrangement. The second method is the ramification index, which is determined by analyzing the relationship between the cell surface and cell volume. This approach provides an overall measure of the complexity of the microglial cell (Orr et al., 2009; Paris et al., 2018). Formoterol incubation induced a significant increase in the tree length and augmented the ramification index of single microglial cells, compared to the control cells (Figure 4C, D). Thus, Formoterol changed the spatial arrangement and complexity of microglial cells.

Dynamic changes in microglial cells and their process tree were also studied. As parameters for cell shape alteration, the shape dynamics (the sum of the total extended and retracted area in 2D) and the number of extensions and retractions (> 1 px; 1/sec) were considered (Hansen et al., 2022). Formoterol incubation led to a trend towards increased overall area of microglia compared to control (Figure 5A). Furthermore, the number of extensions was significantly augmented in Formoterol-incubated slices, which also demonstrated an increase in the number of retractions (Figure 5B, C).

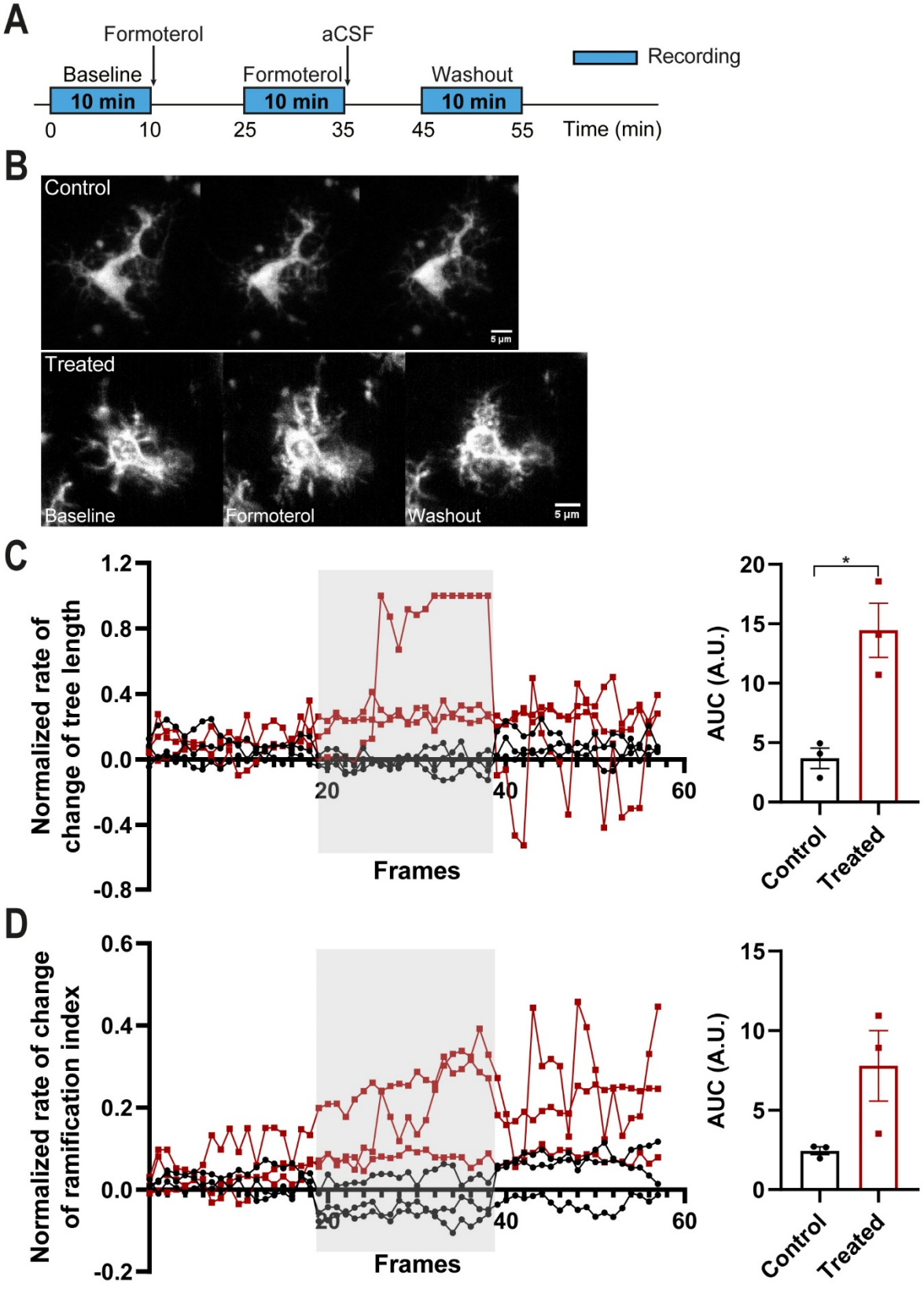

Figure 4. β2-AR stimulation modified microglia morphology in *ex vivo* spinal cord slices.

(A) Two-photon recordings strategy of *ex vivo* spinal cord slices from *Cx3cr1*-eGFP mice. (B) Representative images of microglial cells from control and treated slices in the three experimental phases. Scale bar = 5 µm. (C) The tree length parameter of microglia increased after Formoterol

incubation. (D) Formoterol treatment augmented the ramification index in microglia. Grey area = Formoterol incubation. A.U. = arbitrary unit. n = 3 mice/group; Mann-Whitney test was conducted; * $p < 0.05$ as compared to vehicle-treated group. Data are represented as mean ± SEM.

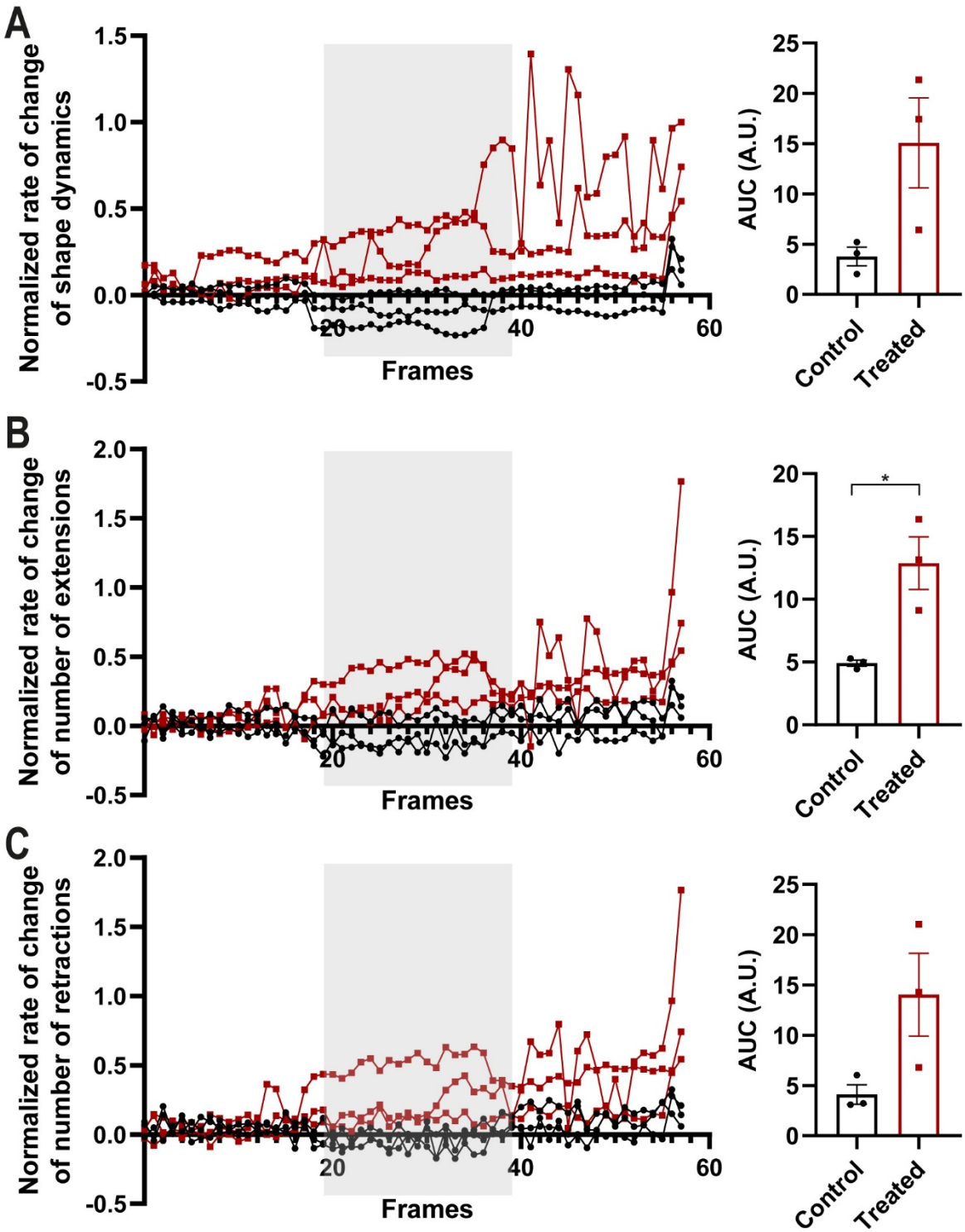

Figure 5. Formoterol modulated microglia dynamic parameters in *ex vivo* spinal cord slices. (A) The shape dynamic parameter studied as the sum of the total extended and retracted area in 2D, of treated microglia, increased after Formoterol incubation. (B) β2-AR agonist treatment significantly augmented the number of process extensions in treated microglia. (C) Formoterol treatment increased

the number of process retractions in treated microglia. Grey area = Formoterol incubation. n = 3 mice/group; Mann-Whitney test was conducted; * $p < 0.05$ as compared to vehicle-treated group. Data are represented as mean ± SEM.

4.3 Impact of β2-AR agonist in diverse regimens

4.3.1 Dose and time course analysis of Formoterol treatment on mechanical and cold allodynia

Previous studies have reported that Formoterol can alleviate hypersensitivity in a neuropathic pain model after some weeks of nerve injury (Yalcin et al., 2010); however, the underlying mechanism was not yet elucidated. In this study, Formoterol was administered intraperitoneally in SNI mice to test therapeutic relevance. A detailed dose and time course analysis were conducted with three different Formoterol concentrations on mechanical and cold stimuli-induced behavioral responses post-SNI surgery. Mechanical allodynia was investigated using the 0.07 g von Frey force, which typically does not elicit responses under basal conditions but leads to an exaggerated response frequency post-SNI. Findings indicated that Formoterol injections of 50 and 500 µg/kg reduced mechanical hypersensitivity within 1 h after administration (Figure 6A) and peak inhibition of cold allodynia occurred at 3 h compared to saline and the lowest concentration of Formoterol injected (5 µg/kg) (Figure 6B).

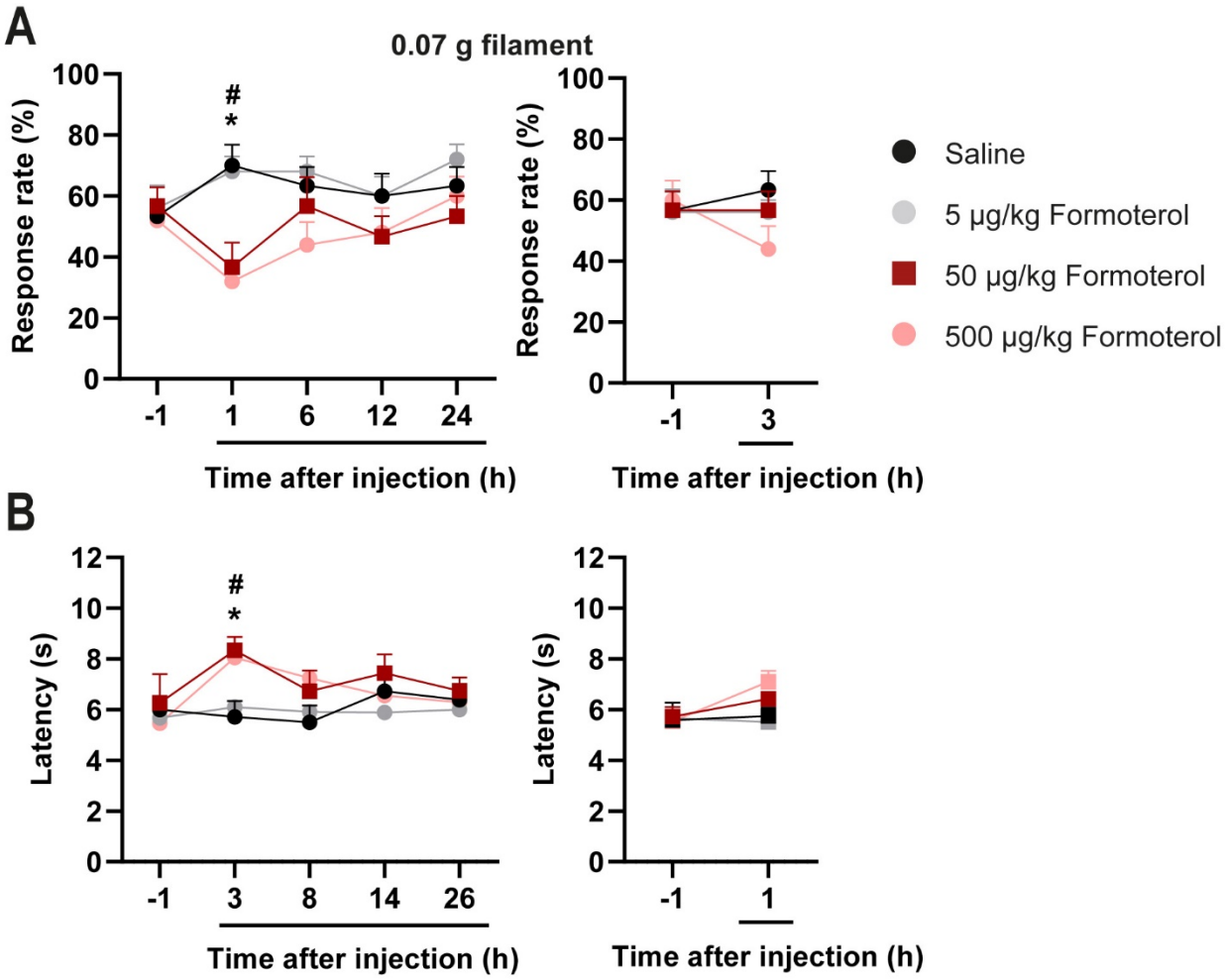

Figure 6. Analysis of the optimal dose and time of Formoterol treatment in SNI mice.

(A) Three different Formoterol doses (5, 50, and 500 µg/kg) were examined compared to saline application in SNI mice. The application of 0.07 g von Frey filament on SNI mice was analyzed 1, 6, 12, and 24 h post-injection, and for a different group of mice, the mechanical allodynic response was measured 3 h post-injection. (B) Cold plate test was performed 3, 8, 14, and 26 h post-injection, and after 1 hour for a separate group. n = 5–6/group; repeated measures ANOVA was conducted followed by post-hoc Tukey's test; * $p < 0.05$, as compared among saline- and 50 µg/kg Formoterol-injected mice at the same time point; # $p < 0.05$, as compared between saline- and 500 µg/kg Formoterol-injected mice at the same time point.

4.3.2 Impact of systemic Formoterol administration on mechanical hypersensitivity and cold allodynia on day three post-surgery

SNI prompts mechanical hypersensitivity and cold allodynia compared to sham mice (Decosterd & Woolf, 2000), as was reiterated by the results displayed in Figure 7. Thus, it was tested whether formoterol could exert its analgesic effect in the early phase after nerve injury and whether there were differences based on the sex of the mice. When compared to saline-treated SNI mice, Formoterol application significantly alleviated mechanical hypersensitivity demonstrated as threshold and area under the curve (AUC) equally in both sexes (Figure 7A, B). Moreover, Formoterol decreased thermal allodynia, shown as latency of paw withdrawal after cold stimuli in both male and female mice (Figure 7C). Overall, these results indicate that Formoterol systemic administration can alleviate mechanical hypersensitivity and cold allodynia three days post-nerve injury.

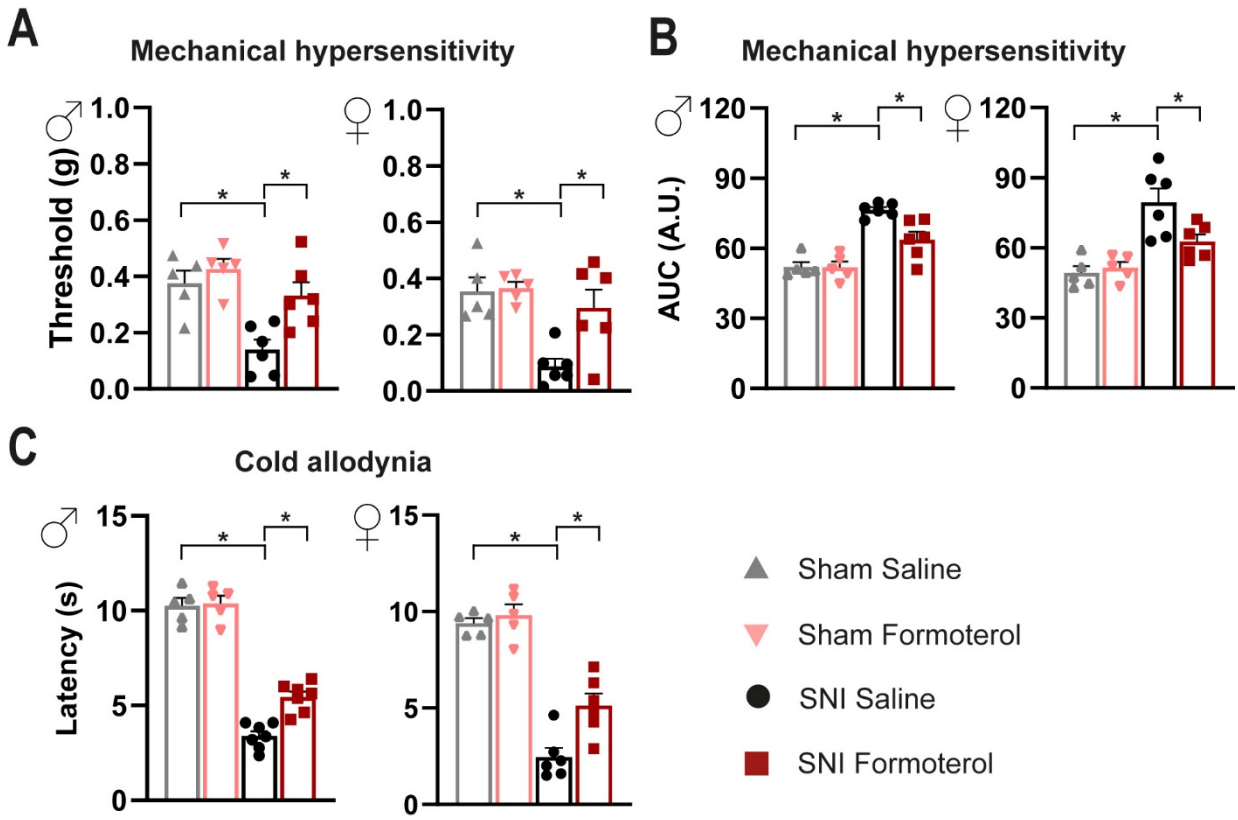

Figure 7. β2-AR agonist systemic delivery alleviated sensitization in SNI mice three days post-surgery.

(A, B) Formoterol intraperitoneal administration relieved mechanical hypersensitivity when measured 1 h after injection, demonstrated as threshold (A) and integral of response frequency–von Frey force intensity (from 0.008 to 0.1 g) curves (AUC) (B), in male (left) and female (right) SNI or sham mice. A.U. = arbitrary unit. (C) Cold allodynia was measured after Formoterol injection using operated mice of both

sexes (male, left; female, right). n = 5–7/group; two-way ANOVA test was conducted followed by post-hoc Tukey's test; * $p < 0.05$. Data are represented as mean ± SEM.

4.3.3 The β2-AR agonist reversed evoked nociceptive hypersensitivity in SNI mice on days 6 and 21 post-surgery

The results obtained on day 3 post-SNI revealed that Formoterol could impede the onset of nociceptive hypersensitivity towards mechanical and cold inputs (Figure 7). Thus, it was examined the effectiveness of Formoterol in reversing established hypersensitivity that had developed over a period of several days to weeks (Figure 8A). Compared to vehicle administration, β2-AR agonist application on days 6 and 21 post-SNI resulted in a significant reduction in mechanical hypersensitivity in mice of both sexes (Figure 8B, C). There was no significant decrease in the response rate to the 0.07 g filament for the female SNI group that received Formoterol on day 6 (Figure 8B), but they showed a tendency towards mechanical allodynia alleviation. Furthermore, Formoterol significantly attenuated the thermal allodynia induced by cold stimuli in both male and female mice 6 days post-SNI (Figure 8D). On day 21 post-SNI, mice of both sexes that received the β2-AR agonist exhibited a tendency of augmented latency of paw withdrawal (Figure 8D). These findings revealed the analgesic effects of Formoterol when administered systemically at early and late time points after surgery for mechanical allodynia, as well as at an early stage easing cold allodynia.

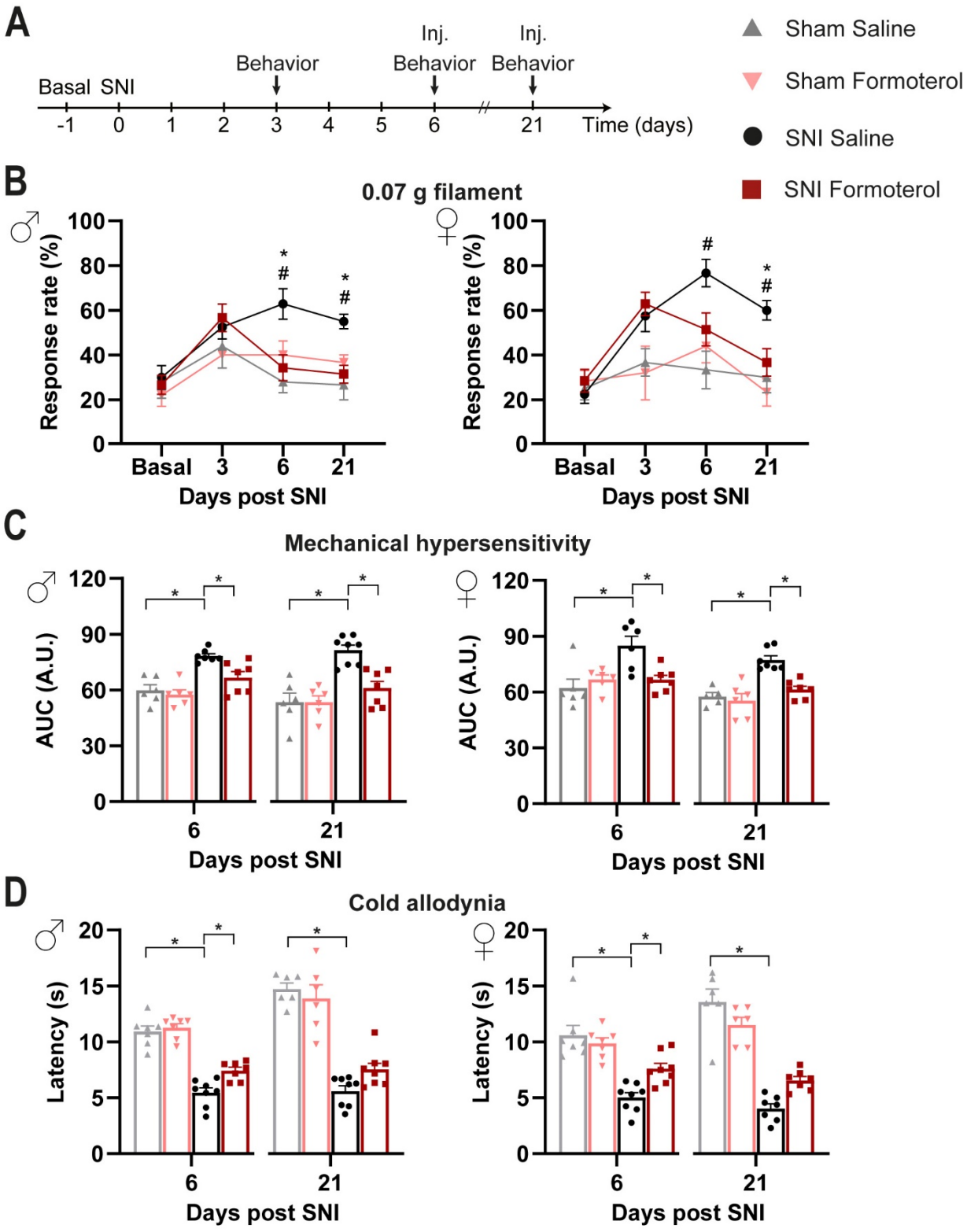

Figure 8. Impact of Formoterol treatment on nociceptive behaviors on days 6 and 21 post-surgery.

(A) Strategy utilized for mechanical and cold nociception tests. Inj. = injection. (B) Mechanical allodynia was exhibited as the response rate to the 0.07 g von Frey filament in mice of both sexes (male, left; female, right) pre-surgery (basal), 3 days afterward to check allodynia development, 6 and 21 days, and

1 h post-Formoterol i.p. injection. n = 6–7/group; repeated measures two-way ANOVA was conducted followed by post-hoc Tukey's test; * p < 0.05, as compared to SNI Saline and SNI Formoterol; # p < 0.05 as compared to SNI Saline and Sham Saline for the same time point. (C) Mechanical hypersensitivity was attenuated post-Formoterol i.p. injection in mice of both sexes (male, left; female, right) compared to saline-treated mice. A.U. = arbitrary unit. (D) Formoterol attenuated cold allodynia in male (left) and female (right) SNI mice. n = 6–8/group; two-way ANOVA test was conducted followed by post-hoc Tukey's test; * $p < 0.05$. Data are represented as mean ± SEM.

4.3.4 Effect of a single Formoterol injection 21 days post-surgery on evoked nociception

In the aforementioned analysis, the possibility, that the analgesic effect of the β2-AR agonist seen at 21 days post-surgery was influenced by its administration at 6 days post-nerve injury, could not be ruled out. Therefore, an additional experiment was conducted where Formoterol was administered only once on day 21 post-SNI (Figure 9A). Surprisingly, a single Formoterol injection significantly decreased mechanical hypersensitivity in mice of both sexes (Figure 9B). The magnitude of this reduction was comparable to that observed in the experiments described in section 4.3.3, where Formoterol was administered on days 6 and 21 post-surgery. Moreover, the single late injection of Formoterol significantly alleviated cold allodynia in both sexes (Figure 9C). These findings indicate that the first β2-AR agonist injection does not influence the effects of the second one at late stages following neuropathic pain.

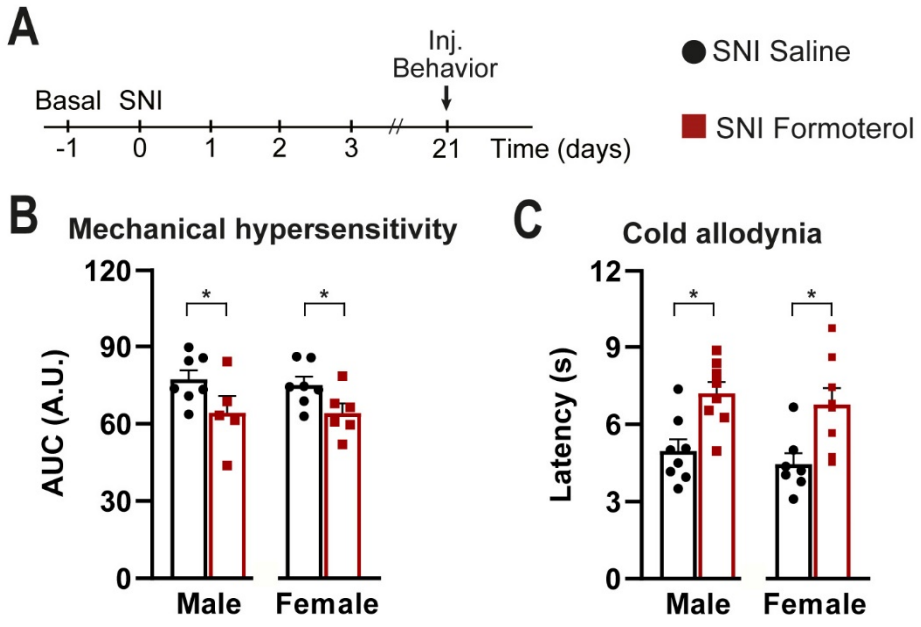

Figure 9. Behavioral analysis of a single Formoterol injection 21 days post-surgery.
(A) Experimental scheme for mechanical hypersensitivity and cold allodynia assessments. Inj. = injection. (B, C) A single Formoterol injection decreased mechanical hypersensitivity (B) and cold

allodynia (C) in male and female mice when given on day 21 post-SNI. A.U. = arbitrary unit. n = 5–8/group, Mann-Whitney test was conducted; * $p < 0.05$ as compared to saline group. Data are represented as mean ± SEM.

4.3.5 Formoterol modulated spontaneous pain in SNI mice

A prominent feature of neuropathic pain in patients is the occurrence of spontaneous pain (Finnerup et al., 2021). In mice, the conditioned place preference test (CPP) is a well-established method for assessing ongoing pain in the SNI model (Pitzer et al., 2016). Typically, in the CPP test, mice are conditioned to an analgesic treatment in a compartment with specific contextual cues. In this case, each of the two compartments had two contextual cues: odor and a visual pattern. Preference for the compartment on the day of testing, without the drug utilized during the conditioning phase, is used as an indicator of persistent pain (King et al., 2009). This experiment aimed to explore whether Formoterol modulates spontaneous pain in mice with nerve injury. In order to accurately establish the link between pain relief and a single compartment in which the mouse is placed after drug administration, the time window of the analgesic effect of the drug must be restricted to the duration of the mouse's stay in the conditioned chamber. In previous experiments, the duration of the analgesic action of Formoterol was less than 6 h after a single application, meeting this requirement (Figure 6).

The CPP test was conducted early after the nerve injury, in accordance with the earliest paradigm used for testing mechanical hypersensitivity and thermal allodynia (Figure 10A). Figure 10B depicted that on day 8 post-surgery, male neuropathic - but not sham - mice showed conditioned place preference for the chamber paired with the β2-AR agonist. Conversely, female SNI mice only presented a tendency towards the Formoterol-paired compartment (Figure 10C). To further investigate the relevance of these results from a clinical point of view, CPP was verified to Formoterol on day 36 post-surgery (Figure 11A). Male neuropathic mice preserved a preference for the compartment paired with the β2-AR agonist compared to sham mice (Figure 11B). Notably, female SNI mice also developed significant CPP phenotypes compared to the sham mice (Figure 11C). These findings suggest that at early stages post-nerve injury, β2-AR agonist reduces spontaneous pain only in male mice, whereas at late phase post-SNI, Formoterol can improve spontaneous pain in male and female mice.

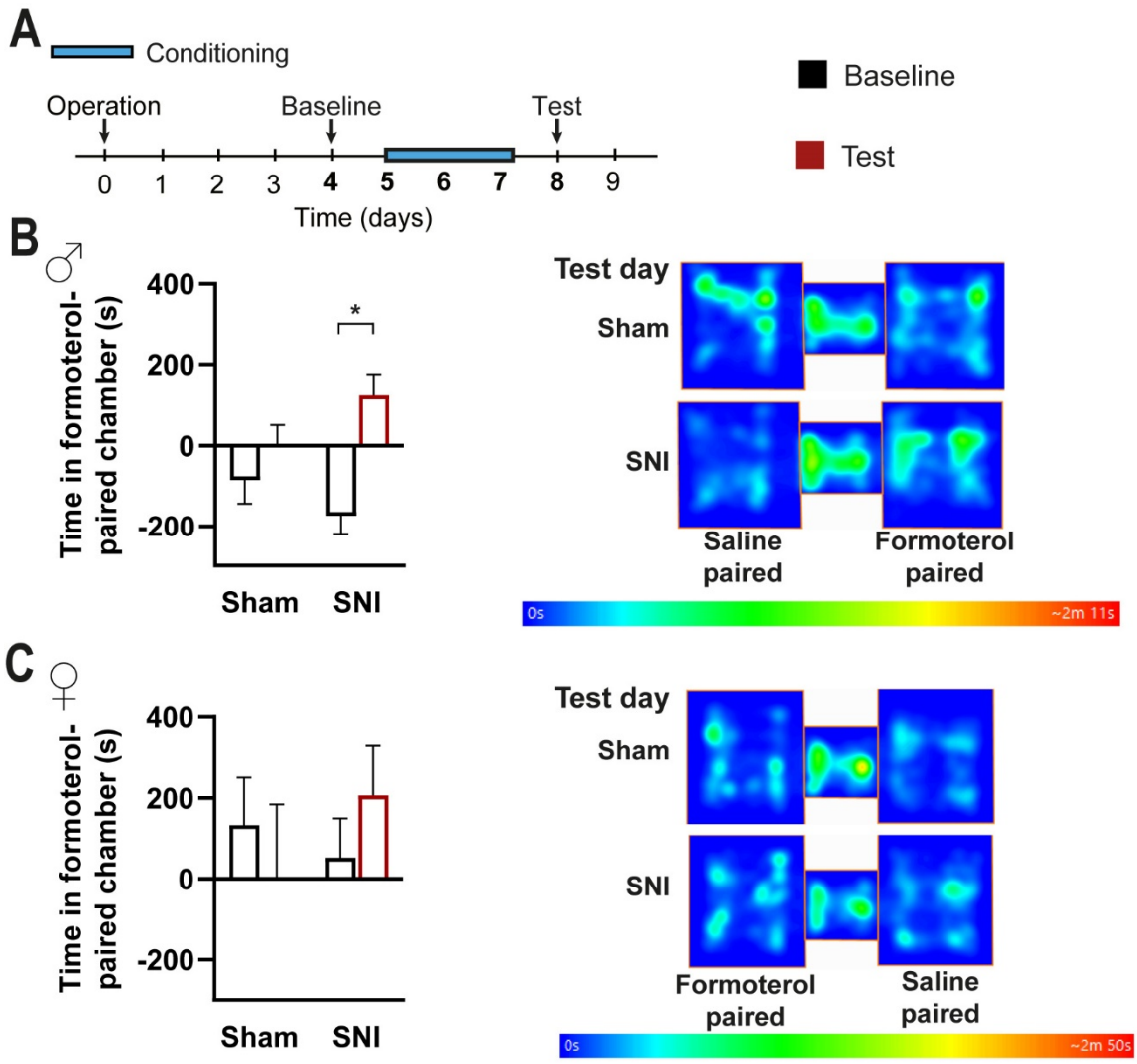

Figure 10. β2-AR agonist reduced ongoing pain in SNI in the initial phase post-SNI.

(A) Experiment timeline for CPP when Formoterol was tested at early stages post-SNI or sham surgery. (B) Post-conditioned male SNI mice exhibited a significant CPP to the chamber associated with Formoterol (left), shown as heat plots on the baseline and test day (right). (C) CPP analysis for female-operated mice was depicted as cumulative time (left) and heat maps (right). n = 6–7/sham group; n = 8/SNI group; Mann-Whitney test was conducted; * $p < 0.05$ as compared baseline to test day. Data are represented as mean ± SEM.

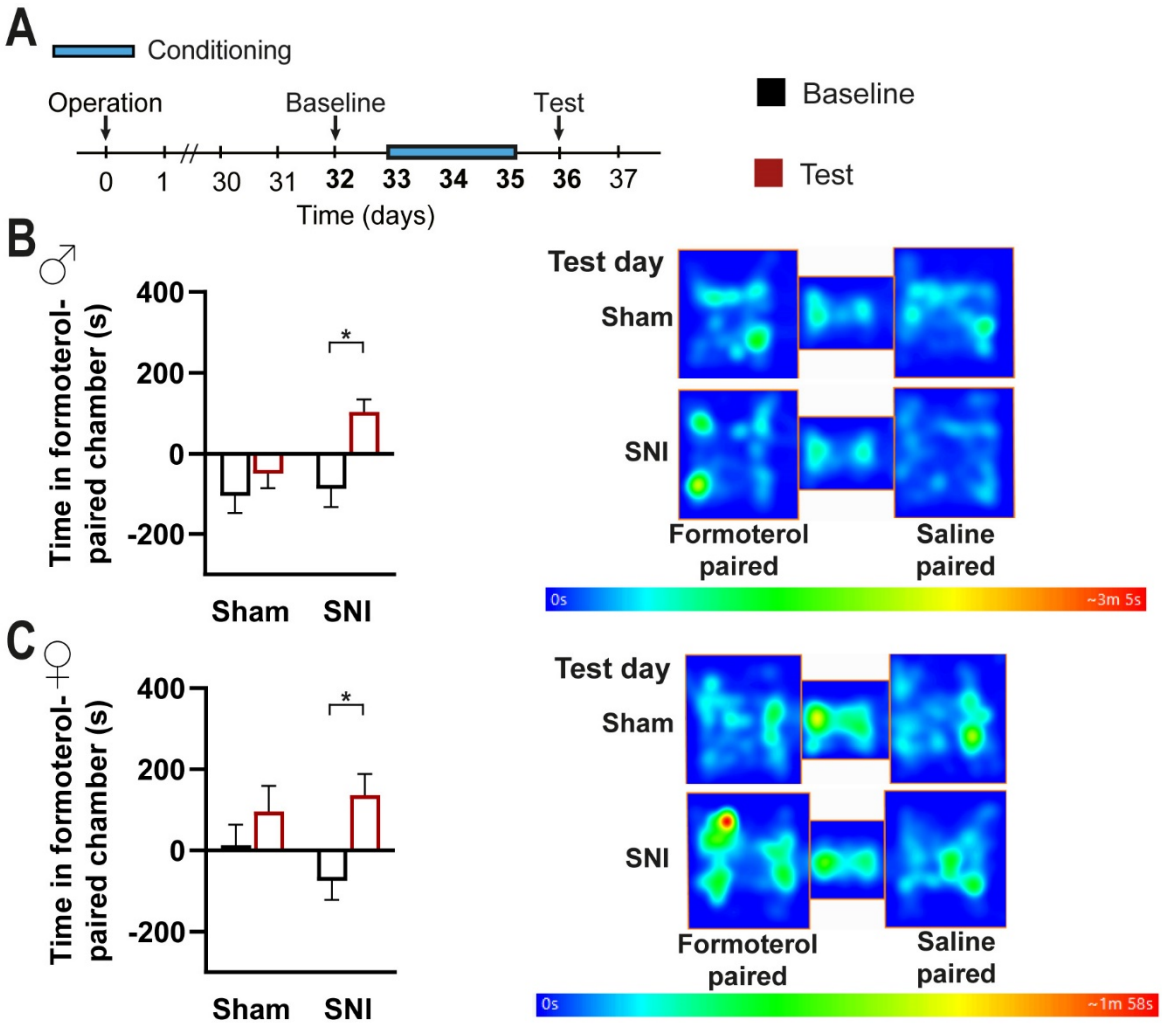

Figure 11. Conditioned place preference showed that the β2-AR agonist administration decreased ongoing pain at a late stage post-SNI.

(A) CPP schematic for Formoterol application at late stages after surgery. (B) Post-conditioned male neuropathic mice exhibited a significant CPP to the chamber associated with Formoterol (left), demonstrated as heat plots on the baseline and test day (right). (C) CPP analysis for female-operated mice was depicted as cumulative time (left) and heat maps (right). n = 6–7/sham group; n = 8/SNI group; Mann-Whitney test was conducted; * $p < 0.05$ as compared baseline to test day. Data are represented as mean ± SEM.

4.4 Investigation of the effects of Formoterol in astrocytes and microglia

4.4.1 Formoterol systemic application reduces microgliosis in early days post-nerve injury

Given their function as resident immune cells in the CNS, microglia promptly respond to inflammatory circumstances. Animal models of neuropathic pain have suggested that diverse cell types release pro-inflammatory mediators that can trigger microglia to adopt a reactive phenotype (Masuda et al., 2020). Nerve injury induces microgliosis and β2-AR agonist administration may dampen this phenomenon. Microgliosis can be evaluated by changes in cell density and morphology. Three days post-SNI, spinal microglia density and morphology were evaluated post-Formoterol systemic delivery. Studies have reported that the contribution of microglia in neuropathic pain can differ depending on sexual dimorphism (Tansley et al., 2022). Therefore, the data were analyzed according to the sex of the mice. Microglial accumulation was determined by measuring the density of Iba1-positive cells in the ipsilateral and contralateral lamina I-III of the SDH (Figure 12A, B). Three days post-surgery, microglia significantly accumulated in the SDH of SNI compared to sham mice, as demonstrated in Figure 12. However single i.p. Formoterol injection significantly decreased Iba1-positive cell density in the ipsilateral SDH of SNI mice of both sexes (Figure 12A, B). Furthermore, microglia morphology was evaluated by analyzing the perimeter of the soma and the length of the processes (Figure 12C). SNI surgery induced a shift from ramified homeostatic microglia to an amoeboid phenotype compared to sham mice, with an expansion of the soma and a shortening of the length of the microglial processes. Those morphological parameters were significantly reversed by Formoterol administration in mice of both sexes (Figure 12C, E). Formoterol treatment did not change significantly microglia accumulation or morphological structure in sham mice (Figure 12B, D, E).

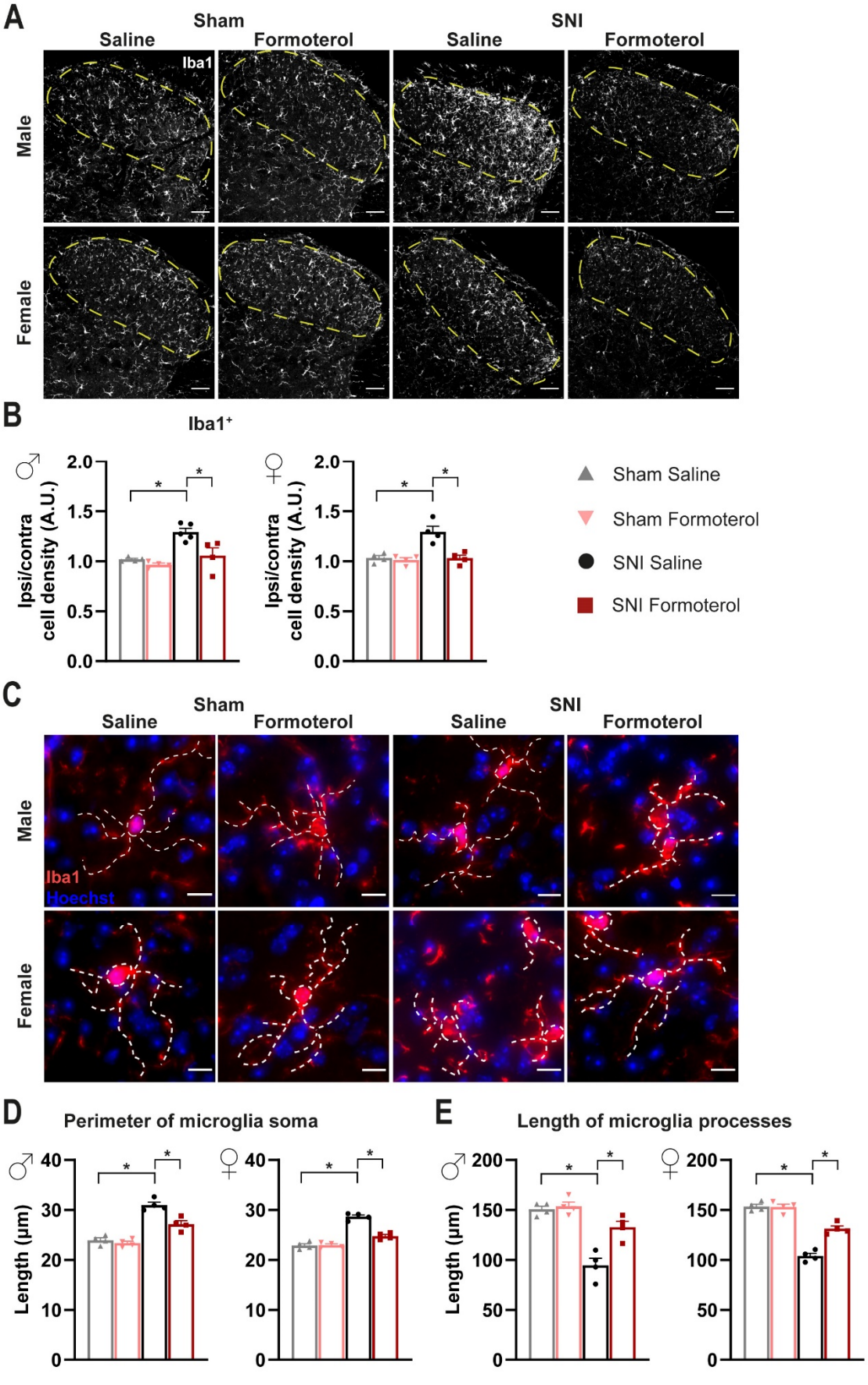
A
Sham
SNI
Saline
Formoterol
Saline
Formoterol
Iba1
Male
Female
B
Iba1+
♂
♀
Ipsi/contra cell density (A.U.)
2.0
1.5
1.0
0.5
0.0
*
*
Sham Saline
Sham Formoterol
SNI Saline
SNI Formoterol
C
Sham
SNI
Saline
Formoterol
Saline
Formoterol
Male
Female
Iba1
Hoechst
D
Perimeter of microglia soma
Length (µm)
40
30
20
10
0
E
Length of microglia processes
200
150
100
50
0

Figure 12. β2-AR agonist administration significantly diminished microgliosis in the ipsilateral spinal dorsal horn (SDH) of SNI mice on day three post-nerve injury.

(A, B) Representative images (A) and quantitative assessment (B) of Iba1-positive microglia density in the ipsilateral SDH of mice (male, left; female, right) injected with Formoterol or vehicle on day 3 post-surgery. The density of Iba1-positive microglia was significantly reduced post-Formoterol injection in male and female mice. Scale bar = 60 µm. Ipsi/contra = density value ratio between the ipsi and contralateral dorsal horn. A.U. = arbitrary unit. (C) Illustrative pictures of microglia (Iba1-positive and Hoechst counterstaining for cell nuclei), with soma and processes outlined by white, dashed lines. Scale bar = 10 µm. (D, E) Quantification of the perimeter of microglia soma (D) and the length of microglial processes (E) in the ipsilateral SDH of mice (male, left; female, right) post-Formoterol or vehicle injection on day 3 post-surgery. n = 4/group; two-way ANOVA test was conducted followed by post-hoc Tukey's test; * $p < 0.05$. Data are represented as mean ± SEM.

Another independent indication of the responsive state of microglia is the expression of activation markers, including p38 and JNK MAPKs in their activated (i.e. phosphorylated) forms. Microglia are known to be the major cells expressing p38 in the spinal cord, an important player in nociceptive hypersensitivity through the stimulation of inflammatory cytokines (Tsuda, 2016), while JNK signaling is involved in apoptosis and pro-inflammatory mediators modulation (Caraci et al., 2019). Colocalization quantifications were conducted to study the impact of Formoterol systemic delivery on microglial activation markers p38 and JNK in nerve-injured mice.

As depicted in Figure 13A, B, the number of double-positive cells for Iba1 and phosphorylated p38 (p-p38) signal was significantly augmented in SNI compared to sham mice of both sexes on day 3 post-surgery, and Formoterol treatment significantly reduced this phenomenon (Figure 13A, B). Similarly, phosphorylated JNK (p-JNK) signals were increased in spinal Iba1-positive microglia, of SNI mice of both sexes and were significantly diminished by Formoterol treatment (Figure 13C, D). No significant alterations were observed in microglia activity markers in sham mice following Formoterol treatment (Figure 13B, D).

Overall, the analysis of microglia reactivity following the β2-AR agonist treatment in neuropathic mice indicates that Formoterol administration significantly restores homeostatic microglial phenotype three days after neuropathic pain development in both male and female mice.

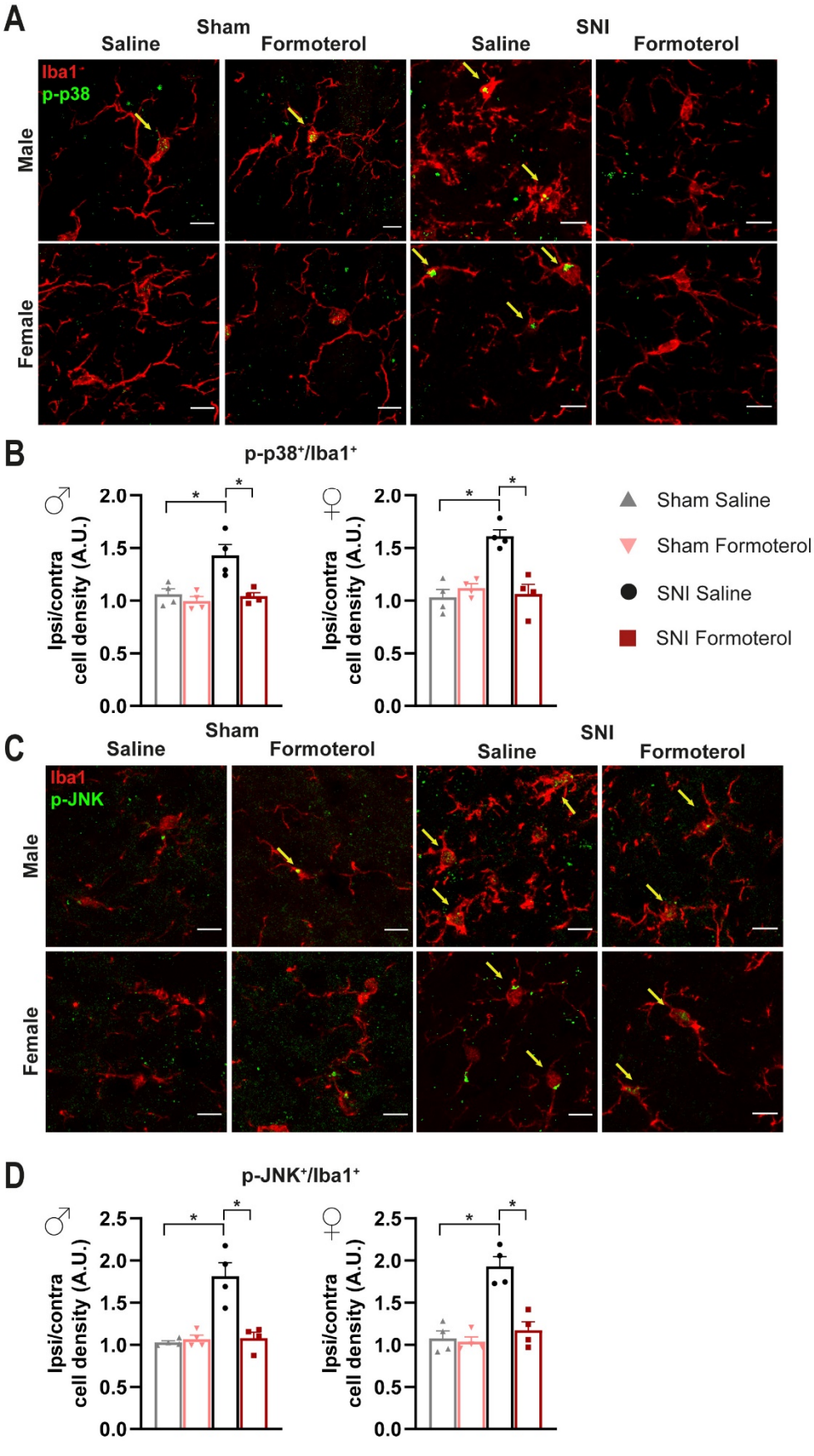
A
Sham
SNI
Saline
Formoterol
Saline
Formoterol
Iba1
p-p38
Male
Female
B
p-p38+/Iba1+
♂
♀
Ipsi/contra cell density (A.U.)
2.0
1.5
1.0
0.5
0.0
*
*
Sham Saline
Sham Formoterol
SNI Saline
SNI Formoterol
C
Sham
SNI
Saline
Formoterol
Saline
Formoterol
Iba1
p-JNK
Male
Female
D
p-JNK+/Iba1+
♂
♀
Ipsi/contra cell density (A.U.)
2.5
2.0
1.5
1.0
0.5
0.0
*
*

Figure 13. Formoterol reduced p-p38 and p-JNK colocalization in microglia in the spinal dorsal horn (SDH) of SNI mice on day three post-nerve injury.

(A, B) Representative images (A) and quantitative assessment (B) of Iba1-positive microglia and p-p38 co-immunohistochemistry in the ipsilateral SDH of mice (male, left; female, right) injected with Formoterol or vehicle on day 3 post-surgery. Arrows indicate double-positive cells. Ipsi/contra = density value ratio between the ipsi and contralateral dorsal horn. A.U. = arbitrary unit. Scale bar = 10 μm. (C, D) Illustrative images (C) and colocalization analysis (D) of Iba1 and p-JNK positive signals in the ipsilateral SDH of mice (male, left; female, right) injected with Formoterol or vehicle on day 3 post-surgery. n = 4/group; two-way ANOVA test was conducted followed by post-hoc Tukey's test; * $p < 0.05$. Data are represented as mean ± SEM.

4.4.2 Analysis of SNI surgery and Formoterol administration on astrocytes three days post-nerve injury

Astrocyte hypertrophy takes place three days following peripheral nerve injury and persists for several months (Li et al., 2020). I investigated whether this phenomenon followed a similar pattern in the SNI model. Additionally, since astrocytes express β2-ARs, Formoterol might exert an analgesic effect by activating these receptors on astrocytes. Using the same experimental protocol utilized in section 4.4.1, the effect of β2-AR stimulation on astrocytes was examined by identifying them with the GFAP and/or in combination with the classic activation marker, p-JNK. Notably, a significant intensification in GFAP fluorescence intensity was shown in female SNI mice compared to sham mice, but not in male SNI mice (Figure 14A, B). There were no statistically significant changes observed in GFAP intensity in sham mice treated with Formoterol compared to the saline-treated group (Figure 14B). P-JNK expression in astrocytes did not show any difference when comparing sham and SNI mice or among the Formoterol-injected groups matched to the saline-injected mice (Figure 14C, D).

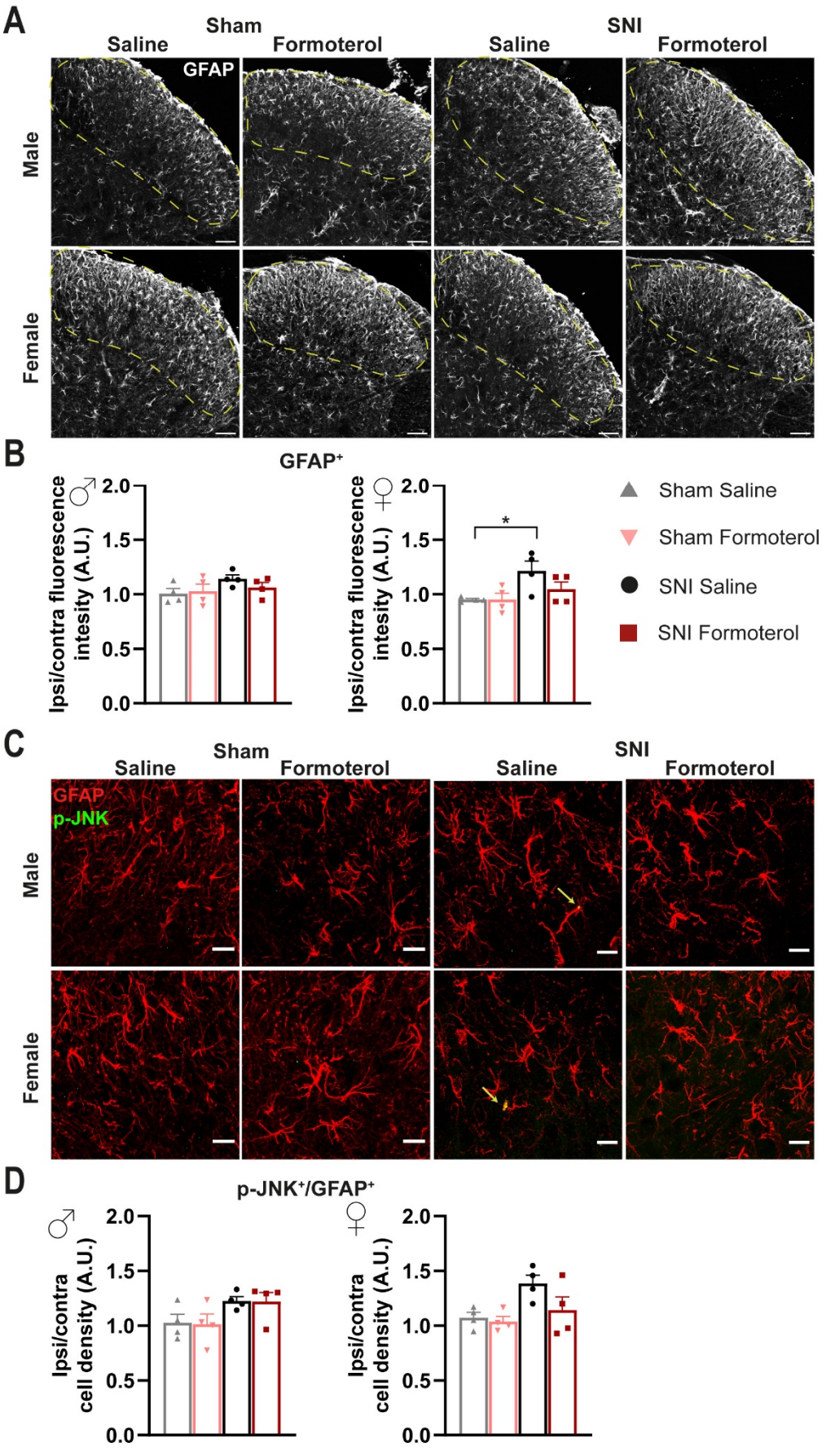
A
Sham
SNI
Saline
Formoterol
Saline
Formoterol
GFAP
Male
Female
B
GFAP+
♂
♀
Ipsi/contra fluorescence intesity (A.U.)
2.0
1.5
1.0
0.5
0.0
*
Sham Saline
Sham Formoterol
SNI Saline
SNI Formoterol
C
Sham
SNI
Saline
Formoterol
Saline
Formoterol
GFAP
p-JNK
Male
Female
D
p-JNK+/GFAP+
♂
♀
Ipsi/contra cell density (A.U.)
2.0
1.5
1.0
0.5
0.0

Figure 14. Spinal astrocytes reaction to neuropathic pain and Formoterol administration on day three post-surgery.

(A, B) Representative images (A) and quantitative assessment (B) of GFAP fluorescence intensity in the ipsilateral SDH of mice (male, left; female, right) injected with Formoterol or vehicle on day 3 post-surgery. Ipsi/contra = fluorescent intensity density value between the ipsi and contralateral dorsal horn. A.U. = arbitrary unit. Scale bar = 60 μm. (C, D) Illustrative images (C) and colocalization analysis (D) of GFAP and p-JNK positive signals in the ipsilateral SDH of mice (male, left; female, right) injected with Formoterol or vehicle on day 3 post-nerve injury. Arrows indicate double-positive cells. Ipsi/contra = density value ratio between the ipsi and contralateral dorsal horn. Scale bar = 10 μm. n = 4/group; two-way ANOVA test was conducted followed by post-hoc Tukey's test; * $p < 0.05$. Data are represented as mean ± SEM.

4.4.3 Systemic administration of Formoterol diminished microgliosis on days 6 and 21 after nerve injury

Microglial and astrocytic modulation during neuropathic pain and after Formoterol administration were evaluated on days 6 and 21 post-surgery in agreement with the behavioral experiments described in section 4.3.3 (Figure 8A).

As displayed in Figure 15, microglia density in the superficial laminae of the ipsilateral SDH in SNI male mice augmented significantly compared to male sham mice, on days 6 or 21 post-surgery. Female SNI mice showed a significant upregulation on day 6 post-SNI compared to sham mice, but not on day 21 post-surgery (Figure 15). Formoterol treatment fully reversed the SNI-induced augmentation of microglial density in the SDH (Figure 15). In terms of spinal microglia structural remodeling changes, neuropathic pain induced in microglia significant enlargement of the somata and the reduction of the processes, equally in both time points studied and sexes (Figure 16). β2-AR agonist application did not affect microglia density or morphology in sham mice (Figure 15, Figure 16). Notably, Formoterol application significantly diminished SNI-induced structural changes in males on days 6 and 21 post-surgery, whereas in female mice microglial changes were reversed only on day 6 post-surgery (Figure 16).

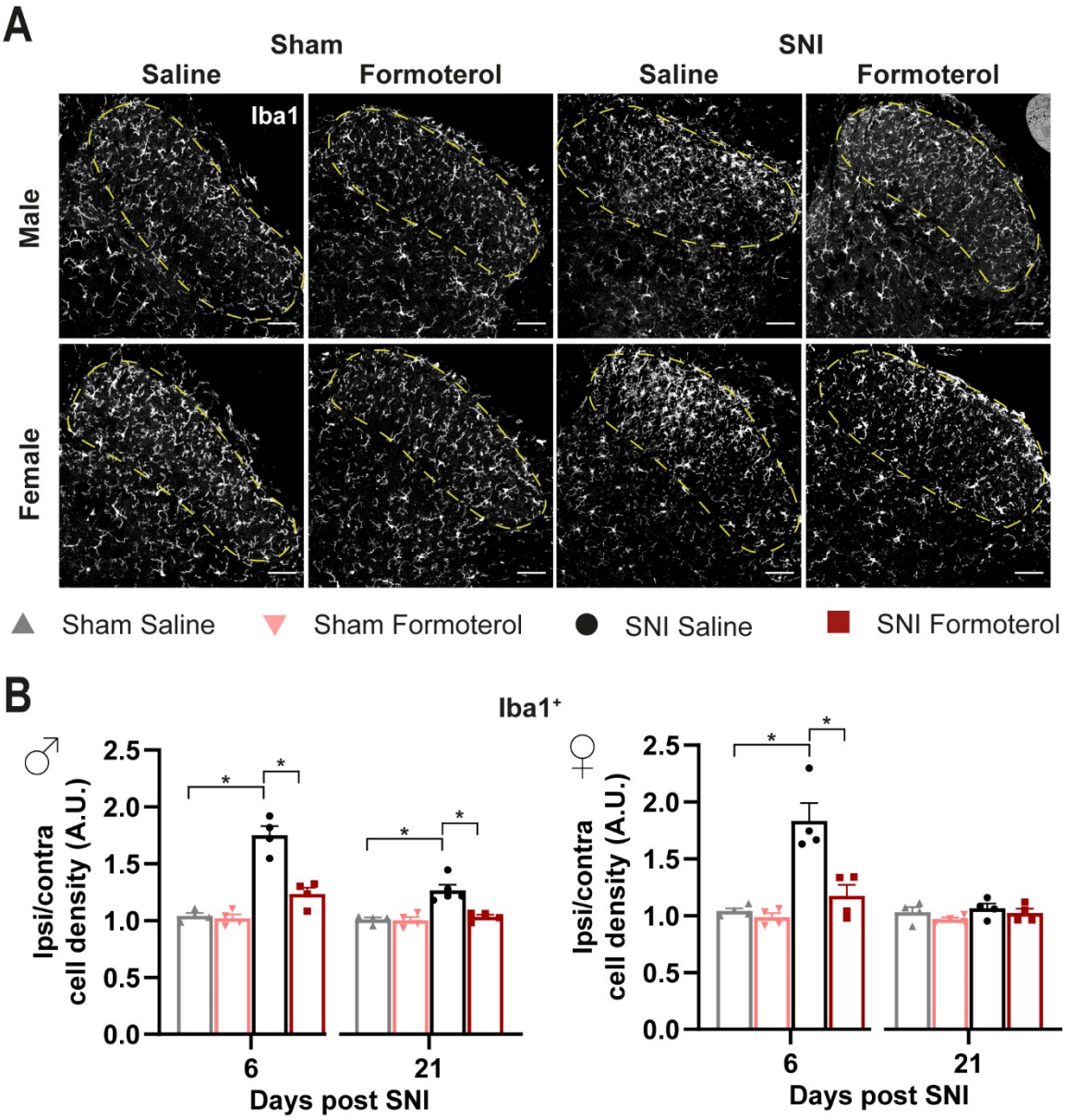

Figure 15. Formoterol systemic delivery reduced microglia density in the ipsilateral spinal dorsal horn (SDH) of SNI mice on days 6 and 21 post-surgery.

(A, B) Representative images of day 6 post-surgery (A) and quantitative assessment (B) of Iba1-positive microglia density in the ipsilateral SDH of mice (male, left; female, right) injected with Formoterol or vehicle on days 6 and 21 post-surgery. Scale bar = 60 μm. Ipsi/contra = density value ratio between the ipsi and contralateral dorsal horn. A.U. = arbitrary unit. n = 4/group; two-way ANOVA test was conducted followed by post-hoc Tukey's test; * $p < 0.05$. Data are represented as mean ± SEM.

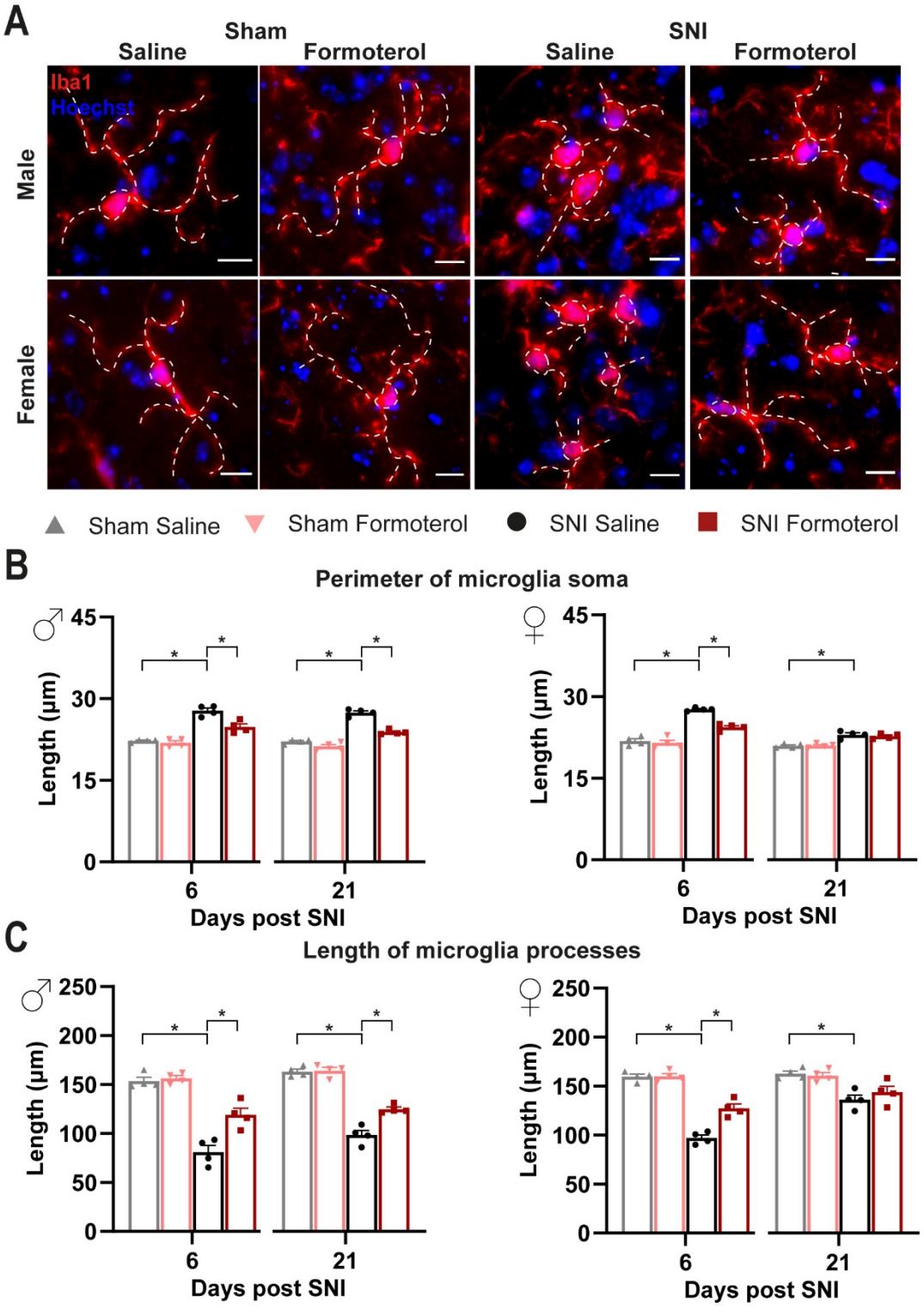

Figure 16. Effect of Formoterol treated on microglia morphology in the ipsilateral spinal dorsal horn (SDH) of SNI mice on days 6 and 21 post-surgery.

(A) Illustrative images of microglia (Iba1-positive and Hoechst counterstaining for cell nuclei), with soma and processes outlined by white, dashed lines. Scale bar = 10 µm. (B, C) Quantification of the perimeter of microglia soma (B) and the length of microglial processes (C) in the ipsilateral SDH of mice (male, left; female, right) injected with Formoterol or vehicle on days 6 and 21 post-surgery. n = 4/group; two-

way ANOVA test was conducted followed by post-hoc Tukey's test; * $p < 0.05$. Data are represented as mean ± SEM.

Furthermore, immunoreactivity for p-p38 and p-JNK in microglia was also evaluated on days 6 and 21 post-surgery. The double-positive signal of p-p38 in Iba1-positive microglia was significantly increased in mice of both sexes at early (6 days post-surgery) and late (21 days post-surgery) time points compared to sham mice and Formoterol treatment significantly reduced this phenomenon (Figure 17A, B). Formoterol application to sham mice did not result in any significant alterations in terms of microglia activity markers (Figure 17). SNI surgery augmented the upregulation of p-JNK in microglia on days 6 and 21 post-SNI in both sexes and was significantly diminished by β2-AR agonist administration, excluding female mice for the latest time point studied (Figure 17C, D).

Collectively, reactive microgliosis assessment in neuropathic mice after Formoterol treatment indicates that such treatment largely reinstates normal microglial phenotype during neuropathic pain progression in both sexes.

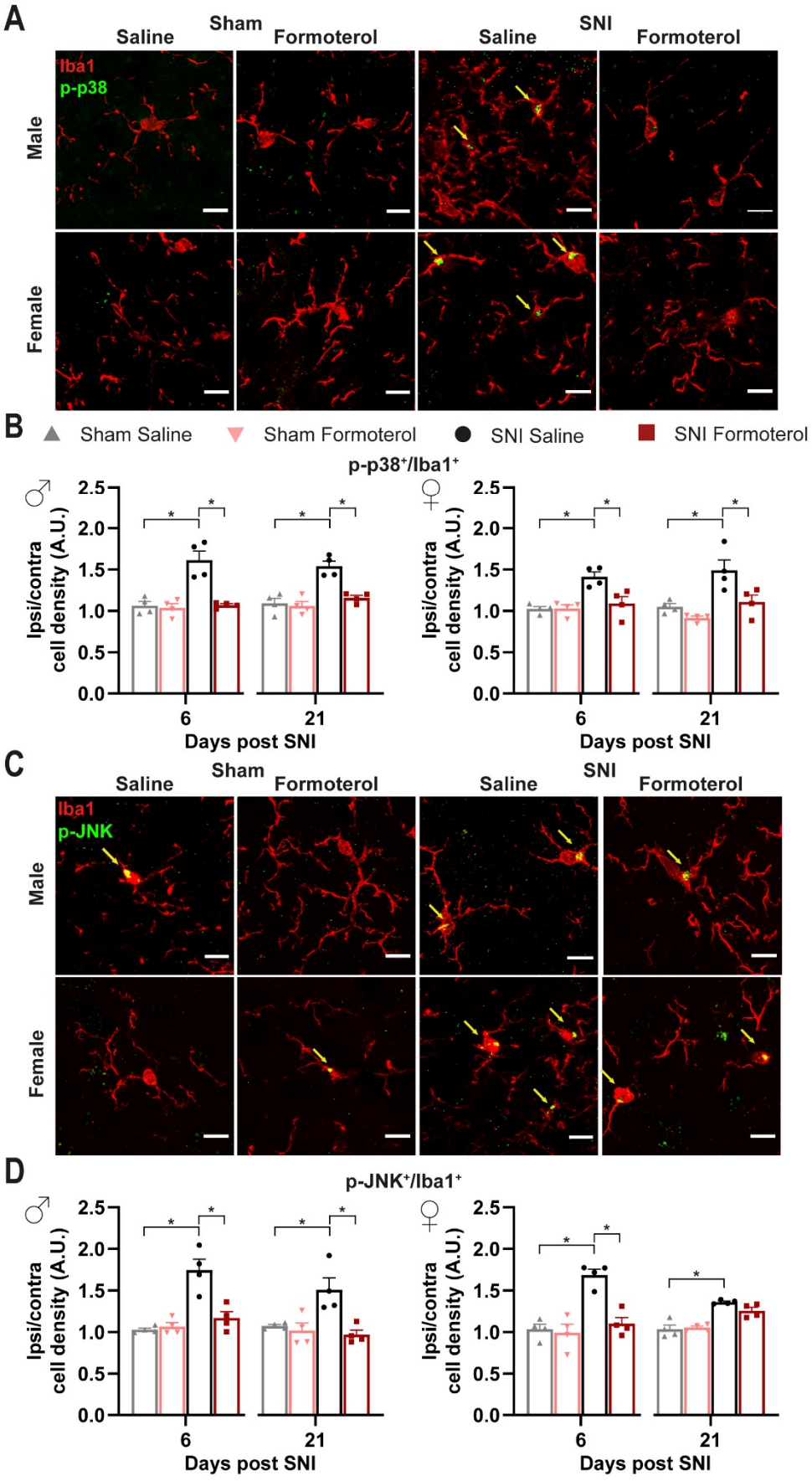
A
Sham
SNI
Saline
Formoterol
Saline
Formoterol
Iba1
p-p38
Male
Female
B
Sham Saline
Sham Formoterol
SNI Saline
SNI Formoterol
p-p38+/Iba1+
Ipsi/contra cell density (A.U.)
Days post SNI
C
Iba1
p-JNK
D
p-JNK+/Iba1+

Figure 17. Formoterol treatment reduced p-p38 and p-JNK localization in microglia in the ipsilateral spinal dorsal horn (SDH) of SNI mice on days 6 and 21 post-surgery.

(A, B) Representative images of day 6 post-surgery (A) and quantitative assessment (B) of Iba1-positive microglia and p-p38 co-immunohistochemistry in the ipsilateral SDH of mice (male, left; female, right) injected with Formoterol or vehicle on days 6 and 21 post-surgery. Arrows indicate double-positive cells. Ipsi/contra = density value ratio between the ipsi and contralateral dorsal horn. A.U. = arbitrary unit. Scale bar = 10 μm. (C, D) Illustrative images of day 6 post-surgery (C) and colocalization analysis (D) of Iba1 and p-JNK positive signals in the ipsilateral SDH of mice (male, left; female, right) injected with Formoterol or vehicle on days 6 and 21 post-surgery. n = 4/group; two-way ANOVA test was conducted followed by post-hoc Tukey's test; * $p < 0.05$. Data are represented as mean ± SEM.

4.4.4 Formoterol intraperitoneal administration reduced astrocytic activation on days 6 and 21 post-surgery

At late time points post-nerve injury (day 21 post-surgery), when neuropathic pain was fully developed, a significant increase in GFAP signal intensity was observed in mice of both sexes, but not over the early time points (Figure 18A, B). Formoterol application to sham mice did not result in any significant alterations in GFAP fluorescence intensity (Figure 18). Notably, Formoterol administration significantly inhibited SNI-triggered astrogliosis in male and female SNI compared to sham mice (Figure 18A, B). Nerve injury prompted an increase of p-JNK in GFAP-positive astrocytes in SNI mice compared to sham mice on days 6 and 21 post-surgery. Formoterol i.p. administration attenuated the upregulation of the activation marker prompted by nerve injury (Figure 18C, D), except for the 21-day time point for male SNI mice (Figure 18D).

The results of the increased GFAP signals in ipsilateral SDH of SNI mice on day 21 post-surgery are in agreement with previous studies reporting that spinal cord astrocytes sustain and maintain chronic pain (Chen et al., 2019; Lu & Gao, 2022).

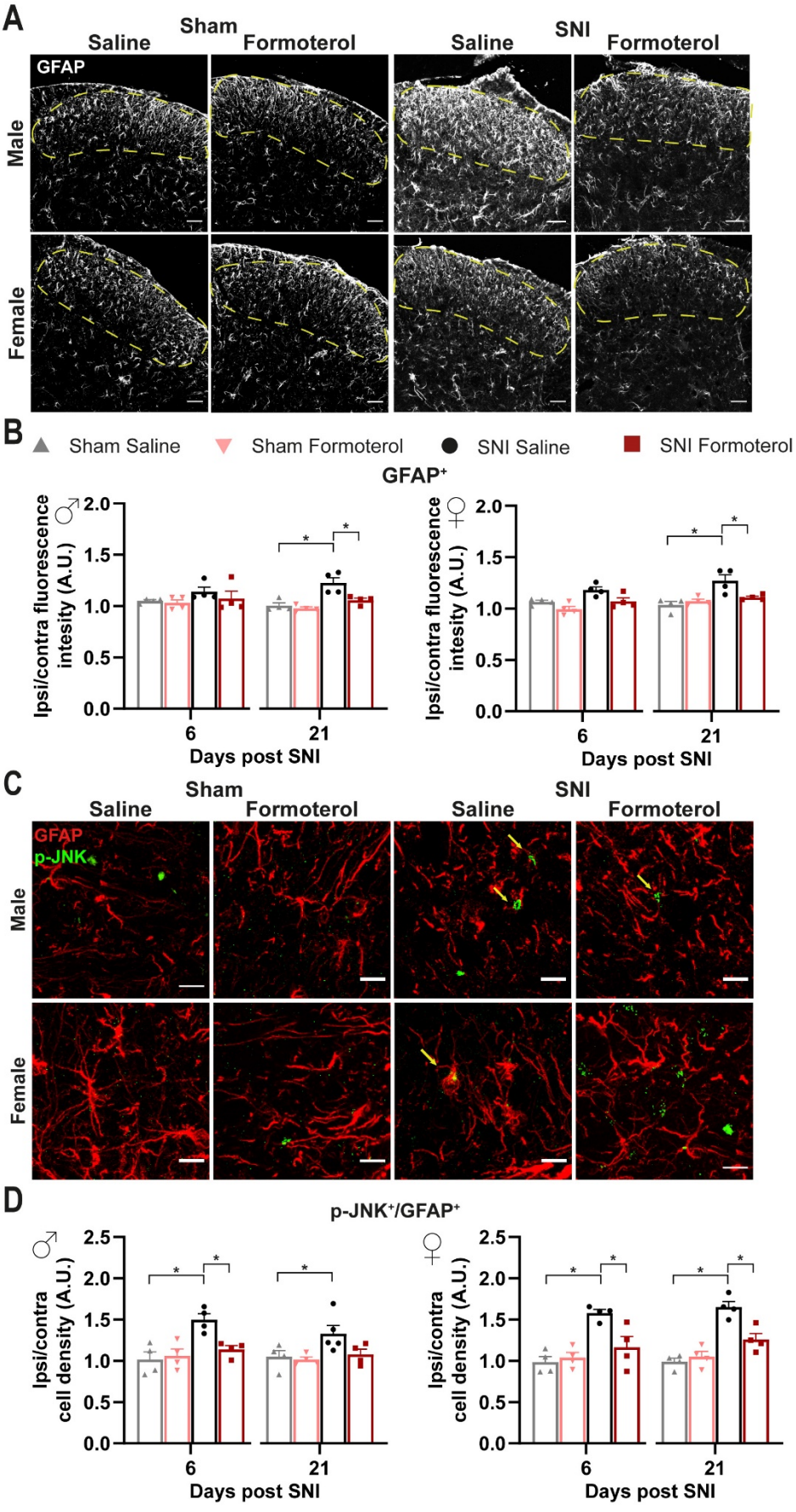
A
Sham
SNI
Saline
Formoterol
Saline
Formoterol
GFAP
Male
Female
B
Sham Saline
Sham Formoterol
SNI Saline
SNI Formoterol
GFAP+
♂
♀
Ipsi/contra fluorescence intesity (A.U.)
2.0
1.5
1.0
0.5
0.0
6
21
Days post SNI
C
Sham
SNI
Saline
Formoterol
Saline
Formoterol
GFAP
p-JNK
Male
Female
D
p-JNK+/GFAP+
♂
♀
Ipsi/contra cell density (A.U.)
2.5
2.0
1.5
1.0
0.5
0.0
6
21
Days post SNI

Figure 18. Spinal astrocytes reaction to neuropathic pain and β2-AR agonist systemic delivery on days 6 and 21 post-surgery.

(A, B) Representative images of day 21 post-surgery (A) and quantitative assessment (B) of GFAP fluorescence intensity in the ipsilateral SDH of mice (male, left; female, right) injected with Formoterol or vehicle on days 6 and 21 post-surgery. Ipsi/contra = fluorescent intensity density value between the ipsi and contralateral dorsal horn. A.U. = arbitrary unit. Scale bar = 60 µm. (C, D) Illustrative images of day 21 post-surgery (C) and colocalization analysis (D) of GFAP and p-JNK positive signals in the ipsilateral SDH of mice (male, left; female, right) injected with Formoterol or vehicle on days 6 and 21 post-surgery. Arrows indicate double-positive cells. Ipsi/contra = density value ratio between the ipsi and contralateral dorsal horn. Scale bar = 10 µm. n = 4/group; two-way ANOVA test was conducted followed by post-hoc Tukey's test; * $p < 0.05$. Data are represented as mean ± SEM.

4.4.5 Effect of a single Formoterol administration 21 days post-nerve injury on spinal microglia and astrocytes

Several studies have proposed that microglia reactivity following nerve injury in early stages is associated with subsequent astrocytic activation (McGinnis & Ji, 2023). In this study, the effect of Formoterol on astrocytes on day 21 could be influenced by its prior administration on day 6, which reduced the microglial reactivity and the release of pro-inflammatory mediators. To distinguish between these effects, a supplementary test was carried out, in which Formoterol was administered solely on day 21 post-surgery, as described in section 4.3.4 (Figure 9). Remarkably, this administration paradigm of Formoterol did not reduce microglial density in the SDH of male and female SNI mice (Figure 19A, B), but it was successful in decreasing astrogliosis (Figure 19C, D). The non-accumulation of microglia in the ipsilateral SDH in female SNI mice on day 21 post-surgery was expected from the previous results obtained (Figure 12B). For male SNI mice, the effects of Formoterol on microglia at later time points were influenced by the early administration of the β2-AR agonist. However, astrocyte responses were independent of its early administration. Thus, these findings suggest that microglial and astrocytic responses are not linked by β2-AR modulation.

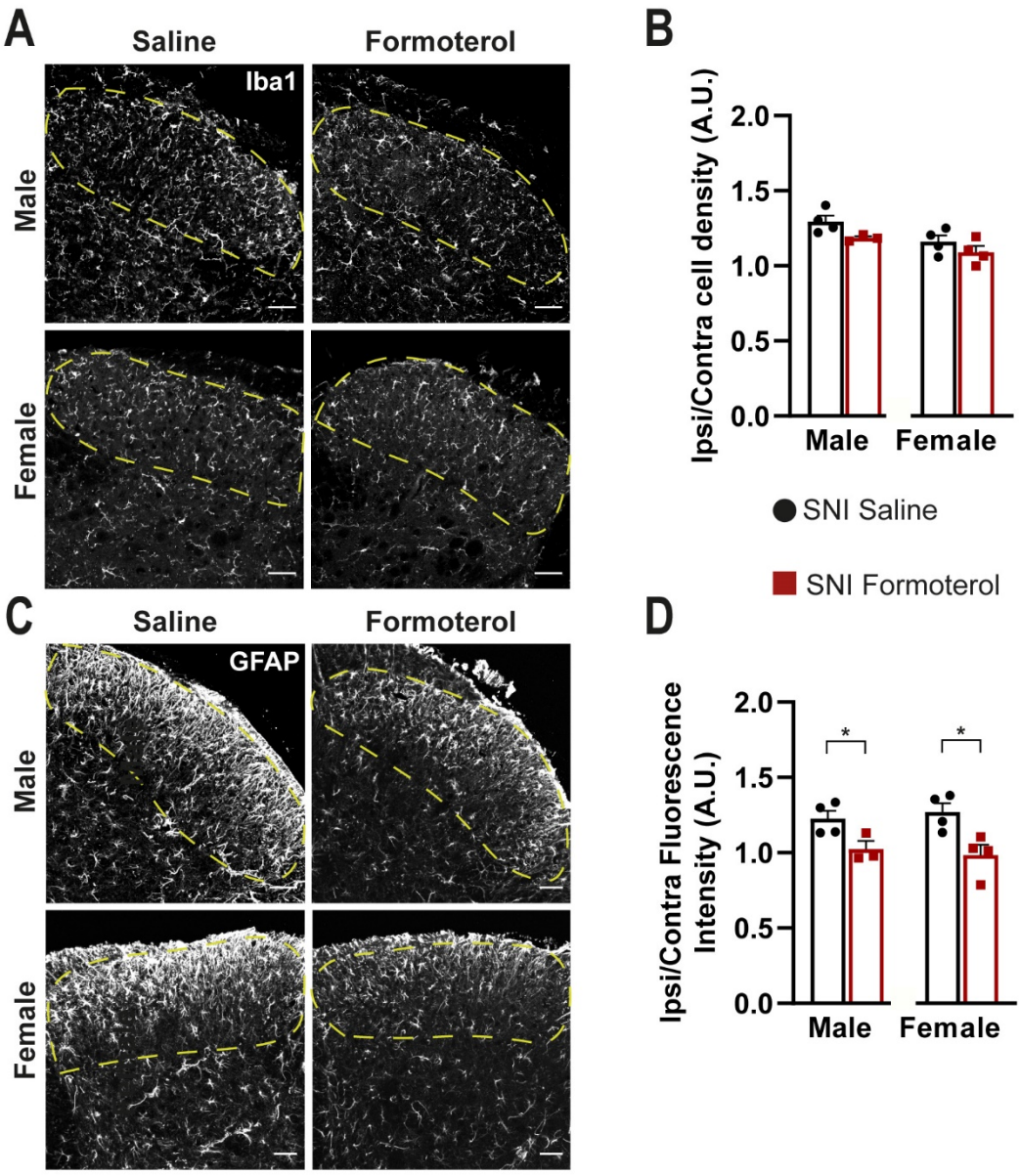

Figure 19. Microglial and astrocytic responses to a single Formoterol injection on day 21 post-nerve injury.

(A, B) Representative images of day 21 post-surgery (A) and quantitative assessment (B) of Iba1-positive microglia density in the ipsilateral SDH of mice injected with Formoterol or vehicle on day 21 post-surgery. Ipsi/contra = density value ratio between the ipsi and contralateral dorsal horn. A.U. = arbitrary unit. (C, D) Representative images of day 21 post-surgery (C) and quantitative assessment (D) of GFAP fluorescence intensity in the ipsilateral SDH of mice injected with Formoterol or vehicle on day 21 post-surgery. Ipsi/contra = fluorescent intensity density value between the ipsi and contralateral dorsal horn. Scale bar = 60 μm. n = 3–4/group; Mann-Whitney test was conducted; * $p < 0.05$ as compared baseline to test day. Data are represented as mean ± SEM.

4.5 Delineation of the role of β2-AR in microglia in neuropathic hypersensitivity

4.5.1 Generation of *Cx3Cr1*-specific knockout for β2-ARs

The previous experiments conducted in this study reveal that Formoterol system delivery can attenuate microglia reactivity in conditions of neuropathic pain. Since β2-ARs are broadly present in diverse cell populations, the subsequent objective was to investigate the role of microglial β2-AR in Formoterol-induced analgesia. Therefore, the generation of a conditional knockout mouse line was required by specifically deleting the *Adrb2* gene from microglia. This was achieved by crossbreeding *Cx3cr1-CreERT2* with *Adrb2*$^{fl/fl}$ mice, resulting in *Cx3cr1-Adrb2*$^{fl/f}$ mice (Figure 20A). Tamoxifen was administered to *Cx3cr1-Adrb2*$^{fl/fl}$ and control (*Adrb2*$^{fl/fl}$) mice at five weeks of age, and qPCR analyses were conducted on MACS-sorted microglial cells after four weeks. The outcomes verified that *Cx3cr1-Adrb2*$^{-/-}$ mice exhibited more than 80% reduction in *Adrb2* mRNA expression in microglia compared to control or *Cx3cr1-Adrb2*$^{fl/fl}$ mice that did not receive tamoxifen (Figure 20B).

Furthermore, CX3CR1 has been reported to be expressed in induced astrocytes following severe seizures (Yeo et al., 2011), but studies on the *Cx3cr1*-GFP mouse line have not shown any GFP reporter leakage into astrocytes under excitatory conditions (Kim et al., 2015). Nevertheless, astrocytes express functional β2-AR on their membranes. Therefore, I examined whether the recombination occurred in astrocytes in the mouse line utilized in this study. *Adrb2* mRNA expression in astrocytes did not differ between *Cx3cr1-Adrb2*$^{-/-}$ and *Adrb2*$^{fl/fl}$ mice post-tamoxifen administration (Figure 20C).

CX3CR1 is also expressed by macrophages; however, fate mapping studies have indicated that the *Cx3cr1-CreERT* mouse line exhibited the induction of gene rearrangements in resident macrophages and peripheral myeloid cells, including blood-circulating CCR2^{+} monocytes, followed by their gradual loss over time (Goldmann et al., 2013; Wolf et al., 2013). β2-AR is also expressed by macrophages; therefore, to ascertain the specificity of the mouse line utilized in this study, macrophages from the peritoneal cavity (blood-circulating monocyte-derived cells), and from the DRGs were isolated for *Adrb2* mRNA testing (Figure 20D, E; Figure 21). It was verified the purity of the cell isolation through F4/80^{+} and CD11b^{+} beads for macrophages derived from the peritoneal cavity and DRGs, respectively (Figure 21). The qPCR analysis demonstrated that *Adrb2* mRNA was not recombined in macrophages derived from the peritoneal cavity or in macrophages isolated from the DRGs when waiting for four weeks after tamoxifen injection before experiments in the *Cx3cr1-Adrb2*$^{fl/fl}$ mouse line (Figure 20).

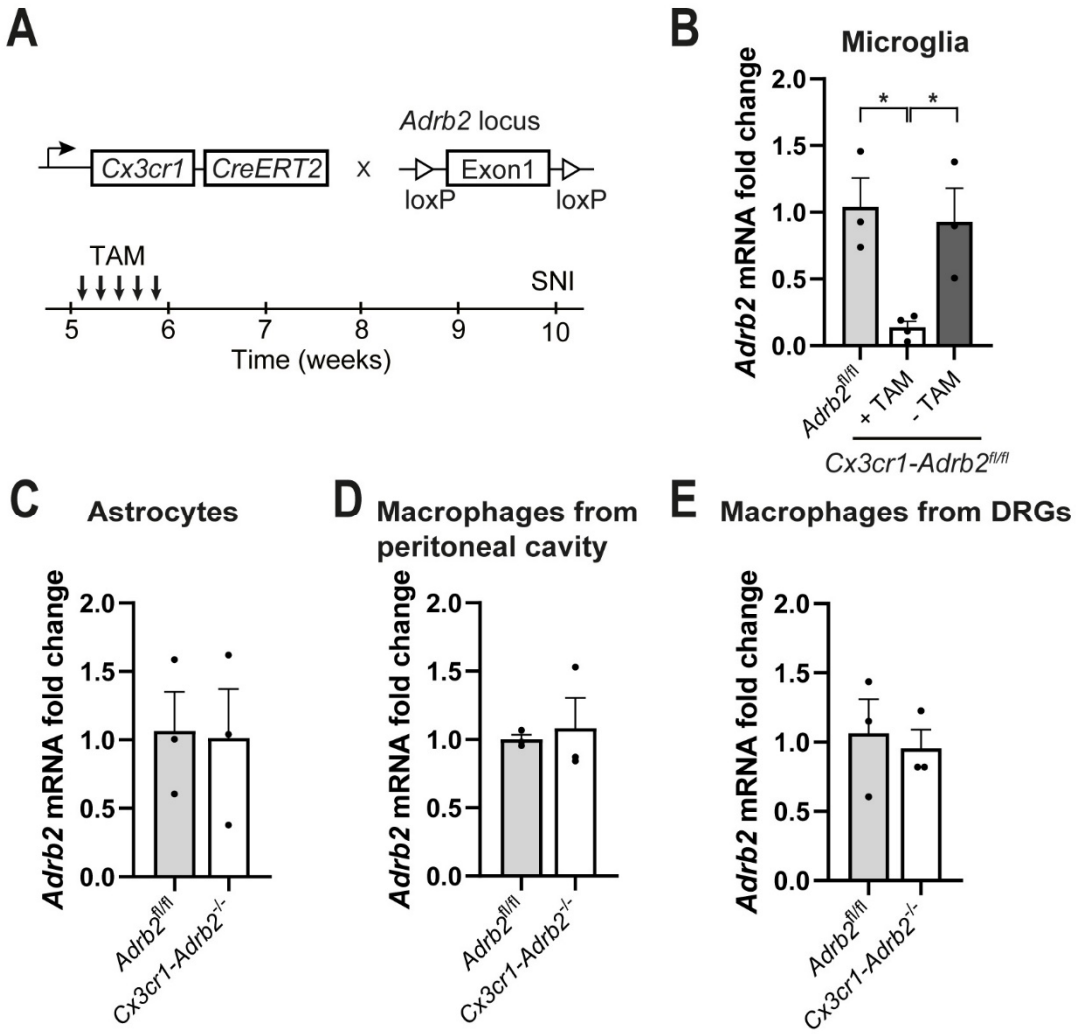

Figure 20. Generation of *Cx3cr1-Adrb2*$^{-/-}$ mouse line and gene rearrangement controls.

(A) Strategy used to generate mice that lacked the *Adrb2* gene specifically in microglia in a tamoxifen-inducible manner. TAM = Tamoxifen. (B) Analysis of *Adrb2* mRNA depletion in microglia four weeks after TAM administration. n = 3–4/group; two-way ANOVA test was conducted followed by post-hoc Tukey's test; * $p < 0.05$. (C–E) Spinal astrocytes (C), macrophages from the peritoneal cavity (D), and macrophages resident in the DRGs (E) from C*x3cr1-Adrb2*$^{-/-}$ mice exhibited no statistical reduction in *Adrb2* mRNA expression compared to *Adrb2*$^{fl/fl}$ mice four weeks post TAM injection. n = 3/group. Data are represented as mean ± SEM.

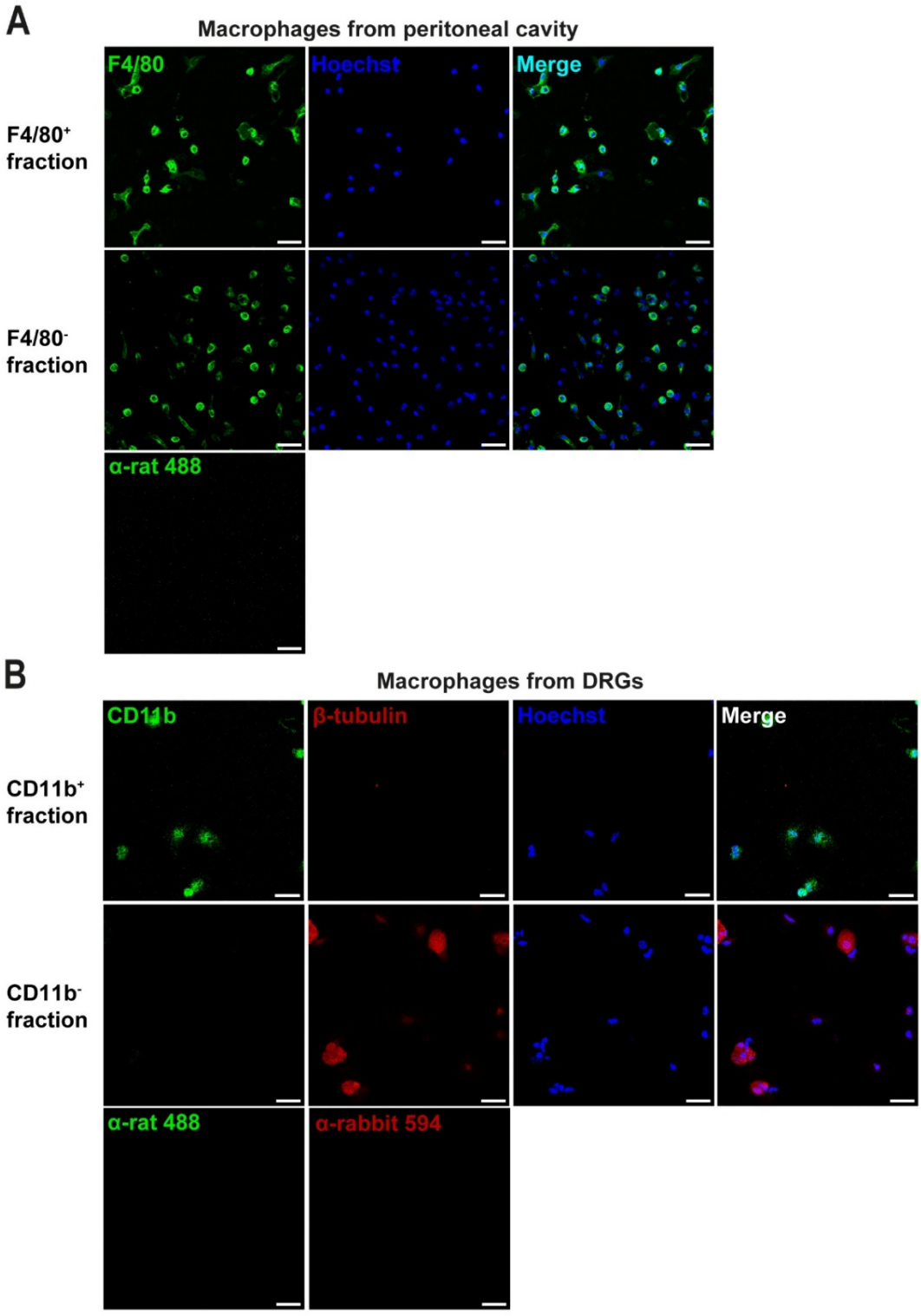

Figure 21. Macrophages isolated from the peritoneal cavity and DRGs.

(A) Representative examples from cultured macrophages isolated from the peritoneal cavity ($F4/80^+$). (B) Typical images from cultured macrophages ($CD11b^+$) and DRG neurons (β-tubulin III^+) isolated from the DRGs. Scale bar = 5 µm.

4.5.2 β2-AR deletion did not affect baseline nociception and hypersensitivity development following nerve injury

β2-ARs deletion, specifically in microglia, could potentially affect baseline nociceptive sensitivity or progression of allodynia/hyperalgesia following SNI. To investigate this, male and female *Cx3cr1-Adrb2*$^{-/-}$ mice were tested for baseline nociception and development of hypersensitivity using the same experimental scheme as described in section 4.3.3 (Figure 8A). Male and female *Cx3cr1-Adrb2*$^{-/-}$ mice showed similar baseline sensitivity levels pre-SNI or sham surgery (Figure 22B, Figure 23A) and developed hypersensitivity post-surgery comparable to the magnitude observed in *Adrb2*$^{fl/fl}$ controls (Figure 22B, Figure 23A). *Cx3cr1-Adrb2*$^{-/-}$ and *Adrb2*$^{fl/fl}$ SNI mice displayed an increased response rate to the 0.07 g filament on days 6 and 21 post-nerve injury compared to the respective sham-operated groups of mice (Figure 22B, Figure 23A). Additionally, mechanical hypersensitivity investigated as a cumulative response to all filaments applied was significantly higher in SNI mice compared to sham animals in both mouse lines and sexes post-surgery (Figure 22B, Figure 23A). Cold allodynia was tested for the same condition. Baseline and sensitivity development for cold allodynia were not impaired in *Cx3cr1-Adrb2*$^{-/-}$ SNI or sham compared to control *Adrb2*$^{fl/fl}$ mice (Figure 24A).

4.6 Involvement of β2-AR deletion in microglia to the anti-nociceptive effect of Formoterol

4.6.1 Effect of Formoterol administration on mechanical hypersensitivity and cold allodynia in neuropathic *Cx3cr1-Adrb2*$^{-/-}$ mice

The genetic modification did not compromise the lack of the effect of Formoterol in sham-operated mice when male and female mice were tested for mechanical hypersensitivity and cold allodynia on days 6 and 21 post-sham surgery (Figure 22C, Figure 23B, Figure 24B). In control *Adrb2*$^{fl/fl}$ SNI mice of both sexes, Formoterol systemic delivery significantly decreased mechanical hypersensitivity compared to the saline-treated group on days 6 and 21 post-surgery. Conversely, this phenomenon was not replicated in *Cx3cr1-Adrb2*$^{-/-}$ mice of both sexes (Figure 22D, Figure 23C). However, as demonstrated in Figure 22D (0.07 g filament), Formoterol-injected control male *Adrb2*$^{fl/fl}$ mice showed a tendency towards reduction compared to saline-injected SNI mice on day 21 post-surgery. There was no evident sexual dimorphism, as both male and female *Cx3cr1-Adrb2*$^{-/-}$ SNI mice exhibited a similar lack of analgesia in response to Formoterol injection (Figure 22D, Figure 23C).

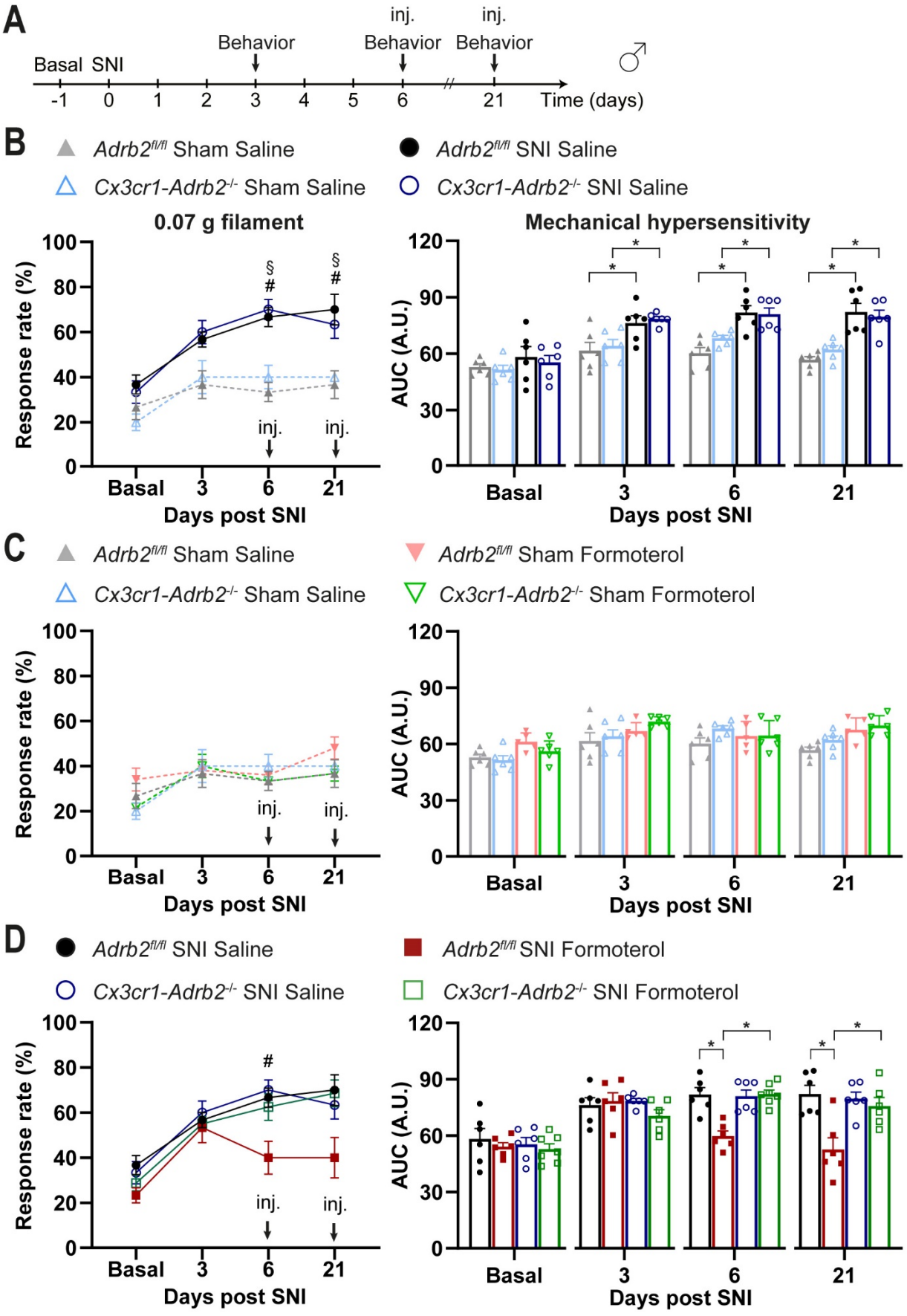
A
Basal SNI
Behavior
inj.
Behavior
inj.
Behavior
-1 0 1 2 3 4 5 6 21 Time (days)
♂
B
Adrb2fl/fl Sham Saline
Adrb2fl/fl SNI Saline
Cx3cr1-Adrb2-/- Sham Saline
Cx3cr1-Adrb2-/- SNI Saline
0.07 g filament
Response rate (%)
Days post SNI
Mechanical hypersensitivity
AUC (A.U.)
Basal 3 6 21
C
Adrb2fl/fl Sham Saline
Adrb2fl/fl Sham Formoterol
Cx3cr1-Adrb2-/- Sham Saline
Cx3cr1-Adrb2-/- Sham Formoterol
D
Adrb2fl/fl SNI Saline
Adrb2fl/fl SNI Formoterol
Cx3cr1-Adrb2-/- SNI Saline
Cx3cr1-Adrb2-/- SNI Formoterol

Figure 22. Analysis of mechanical hypersensitivity in *Cx3cr1-Adrb2*$^{-/-}$ male mice post-SNI and Formoterol administration.

(A) Strategy utilized for mechanical and cold nociception tests. Inj. = injection. (B) Mechanical sensitivity developed in male *Cx3cr1-Adrb2*$^{-/-}$ SNI or sham mice in a comparable manner as control mice, displayed as response rate to the 0.07 g filament (left) pre-surgery (basal), and on days 3, 6, and 21 post-surgery, and cumulative response to all the sets of filaments applied from 0.008 to 1.0 g (AUC, right). A.U. = arbitrary unit. n = 6/group; repeated measures two-way ANOVA was conducted followed by post-hoc Tukey's test; # $p < 0.05$, as compared to *Adrb2*$^{fl/fl}$ Sham Saline vs *Adrb2*$^{fl/fl}$ SNI Saline for the same time point; § $p < 0.05$, as compared to *Cx3cr1-Adrb2*$^{-/-}$ Sham Saline and *Cx3cr1-Adrb2*$^{-/-}$ SNI Saline for the same time point. Two-way ANOVA test was conducted followed by post-hoc Tukey's test; * $p < 0.05$. (C) Male *Adrb2*$^{fl/fl}$ and *Cx3cr1-Adrb2*$^{-/-}$ Sham mice did not exhibit any difference following Formoterol or saline injection in response to one von Frey filament (left), or to the full set of them (right). *Adrb2*$^{fl/fl}$ Sham Saline and *Cx3cr1-Adrb2*$^{-/-}$ Sham Saline groups are the same used in panel B. (D) The β2-AR agonist administration on days 6 and 21 post-nerve injury, alleviated mechanical hypersensitivity in *Adrb2*$^{fl/fl}$ but not in *Cx3cr1-Adrb2*$^{-/-}$ SNI mice. *Adrb2*$^{fl/fl}$ SNI Saline and *Cx3cr1-Adrb2*$^{-/-}$ SNI Saline groups are the same used in panel B. n = 6–7/group; repeated measures two-way ANOVA was conducted followed by post-hoc Tukey's test; # $p < 0.05$, as compared to *Adrb2*$^{fl/fl}$ SNI Saline and *Adrb2*$^{fl/fl}$ SNI Formoterol for the same time point. Two-way ANOVA test was conducted followed by post-hoc Tukey's test; * $p < 0.05$. Data are represented as mean ± SEM.

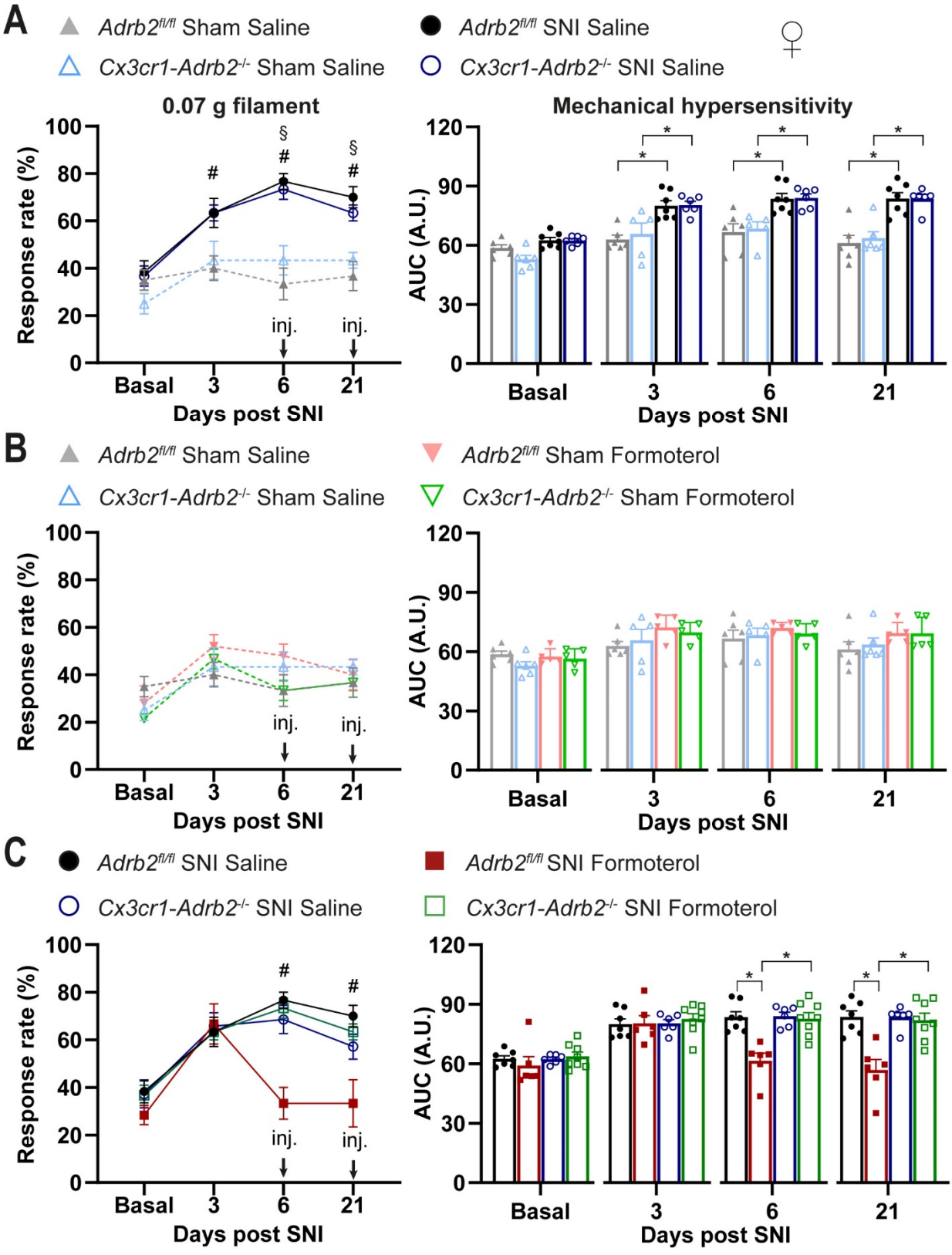

Figure 23. *Cx3cr1-Adrb2*$^{-/-}$ female mice were tested for mechanical hypersensitivity post-SNI and Formoterol administration.

(A) Mechanical sensitivity development was not impinged due to the *Adrb2* genetic deletion in female *Cx3cr1-Adrb2*$^{-/-}$ SNI or sham mice, displayed as response rate to the 0.07 g filament (left) pre-surgery

(basal), and on days 3, 6, and 21 post-surgery, and cumulative response to all the sets of filaments applied from 0.008 to 1.0 g (right). A.U. = arbitrary unit. n = 5–7/group; repeated measures two-way ANOVA was conducted followed by post-hoc Tukey's test; # $p < 0.05$, as compared to *Adrb2*$^{fl/fl}$ Sham Saline vs *Adrb2*$^{fl/fl}$ SNI Saline for the same time point; § $p < 0.05$, as compared to *Cx3cr1-Adrb2*$^{-/-}$ Sham Saline and *Cx3cr1-Adrb2*$^{-/-}$ SNI Saline for the same time point. Two-way ANOVA was conducted followed by post-hoc Tukey's test; * $p < 0.05$. (B) Female *Adrb2*$^{fl/fl}$ and *Cx3cr1-Adrb2*$^{-/-}$ Sham mice did not show any difference following Formoterol or saline injection in response to one filament (left), or to the full set of them (right). *Adrb2*$^{fl/fl}$ Sham Saline and *Cx3cr1-Adrb2*$^{-/-}$ Sham Saline groups are the same used in panel A. (C) The β2-AR agonist administration on days 6 and 21 post-nerve injury, alleviated mechanical hypersensitivity in *Adrb2*$^{fl/fl}$ but not in *Cx3cr1-Adrb2*$^{-/-}$ SNI mice. *Adrb2*$^{fl/fl}$ SNI Saline and *Cx3cr1-Adrb2*$^{-/-}$ SNI Saline groups are the same used in panel A. n = 6–8/group, repeated measures two-way ANOVA was conducted followed by post-hoc Tukey's test; # $p < 0.05$, as compared *Adrb2*$^{fl/fl}$ SNI Saline and *Adrb2*$^{fl/fl}$ SNI Formoterol for the same time point. Two-way ANOVA was conducted followed by post-hoc Tukey's test; * $p < 0.05$. Data are represented as mean ± SEM.

Moreover, Formoterol administration increased the paw withdrawal latency for control SNI-operated male and female mice both on days 6 and 21 post-surgery (Figure 24C). Conversely, Formoterol failed to ameliorate cold allodynia in male and female *Cx3cr1-Adrb2*$^{-/-}$ SNI animals at early stages. Notably, on day 21 post-surgery, the β2-AR agonist significantly alleviated cold allodynia in male *Cx3cr1-Adrb2*$^{-/-}$ compared to *Cx3cr1-Adrb2*$^{-/-}$ saline-injected mice and there was a tendency of thermal relief in female *Cx3cr1-Adrb2*$^{-/-}$ mice, but not with the same extent of Formoterol-injected control mice (Figure 24C).

These findings highlight that the microglial β2-AR is not directly implicated in baseline nociception or hyperalgesia development following nerve injury. Microglial β2-AR exerted a pivotal role in mediating the analgesic effects of Formoterol for mechanical hypersensitivity at early and late stages of neuropathic pain. For neuropathic cold allodynia, microglial β2-AR is important at early stages, but this effect is not prominent during the later phase following nerve injury.

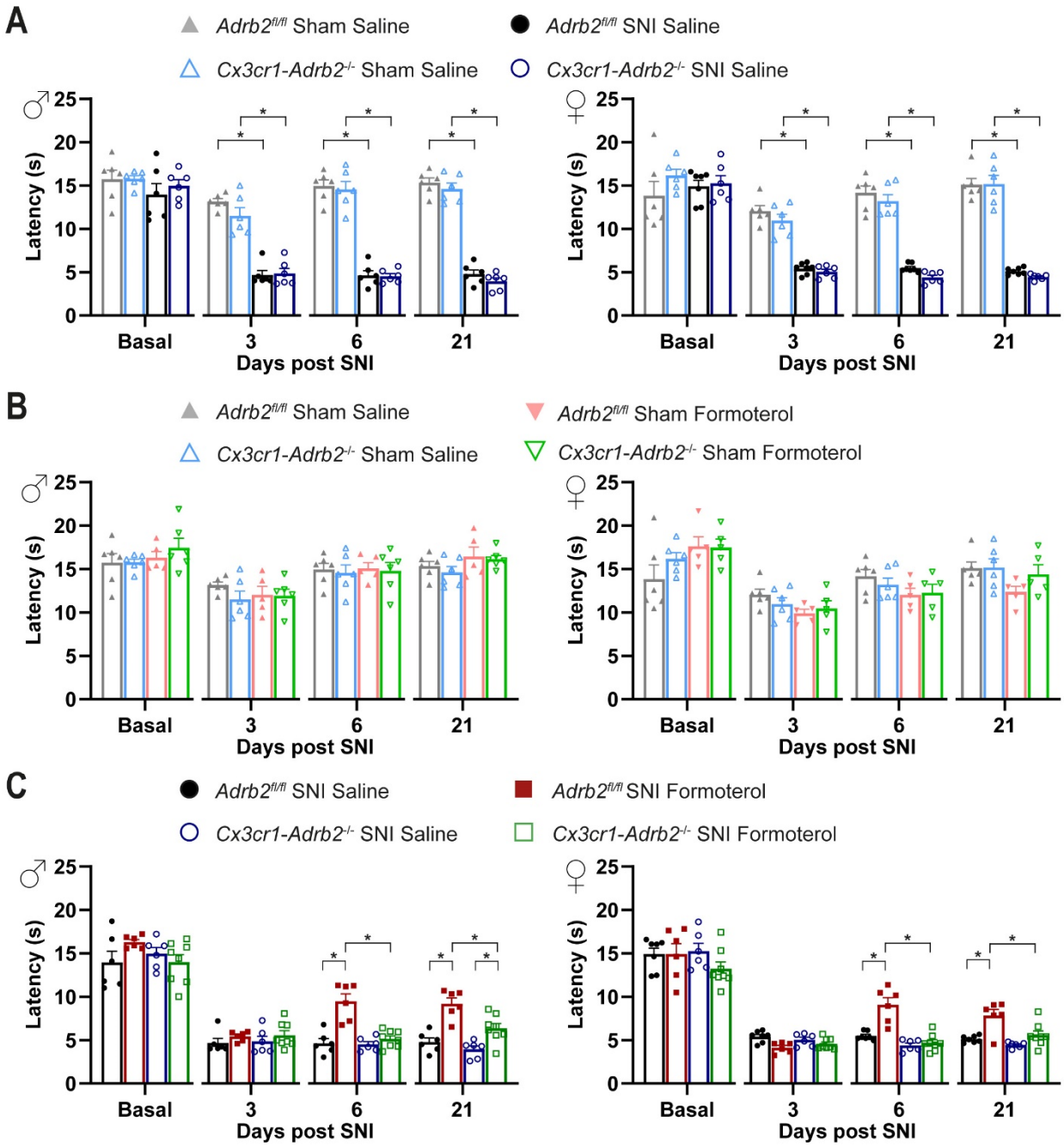

Figure 24. Cold sensitivity was investigated in *Cx3cr1-Adrb2*$^{-/-}$ mice in SNI and sham mice, after saline or Formoterol administration.

(A) No differences in cold sensitivity development were seen among the *Cx3cr1-Adrb2*$^{-/-}$ and *Adrb2*$^{fl/fl}$ mice on days 6 and 21 post-surgery. (B) *Cx3cr1-Adrb2*$^{-/-}$ and *Adrb2*$^{fl/fl}$ Sham mice did not show any difference due to the genetic deletion of the *Adrb2* genetic sequence. *Adrb2*$^{fl/fl}$ Sham Saline and *Cx3cr1-Adrb2*$^{-/-}$ Sham Saline groups are the same used in panel A. (C) Formoterol injection in *Cx3cr1-Adrb2*$^{-/-}$ mice did not alleviate cold allodynia, except in male *Cx3cr1-Adrb2*$^{-/-}$ mice on day 21 post-SNI. *Adrb2*$^{fl/fl}$ SNI Saline and *Cx3cr1-Adrb2*$^{-/-}$ SNI Saline groups are the same used in panel A. n = 6–8/group; two-way ANOVA was conducted followed by post-hoc Tukey's test; * $p < 0.05$. Data are represented as mean ± SEM.

4.6.2. Role of microglial β2-ARs in the suppressive effects of Formoterol on SNI-induced gliosis

Microglial-specific genetic deletion of *Adrb2* could potentially alter the gliosis response without the external intervention of a drug. Therefore, I investigated whether the deletion of microglial β2-AR had an impact on microgliosis in the SDH. Furthermore, the results from the WT mice suggested that Formoterol exerted an analgesic effect and attenuated gliosis in the ipsilateral SDH of nerve-injured mice. To test whether these effects on gliosis were mediated by the microglial β2-AR, further experiments were conducted following the same experimental timeline described in section 4.4.3.

β2-AR deletion in microglia did not change the increased density of microglia in the ipsilateral SDH induced by nerve injury (Figure 25, Figure 26), and the structural changes (Figure 27, Figure 28) compared to control *Adrb2*$^{fl/fl}$ mice. Additionally, Formoterol administration in sham *Cx3cr1-Adrb2*$^{-/-}$ and *Adrb2*$^{fl/fl}$ littermates did not change the microglial phenotype (Figure 26**,** Figure 28). Formoterol application in male and female *Cx3cr1-Adrb2*$^{-/-}$ SNI mice failed to diminish the accumulation of microglia in the ipsilateral SDH compared to control mice on day 6 post-surgery (Figure 26A) and in male *Cx3cr1-Adrb2*$^{-/-}$ mice on day 21 post-surgery as well (Figure 26B). Notably, female control and *Cx3cr1-Adrb2*$^{-/-}$ mice exhibited the same phenotype on day 21 post-SNI independently of Formoterol injection, revealing that microglia did not accumulate in the ipsilateral SDH (Figure 26B). Furthermore, the deletion of β2-AR in microglia abrogated Formoterol-induced morphological changes in *Cx3cr1-Adrb2*$^{-/-}$ mice (Figure 27, Figure 28), except for the length of microglia processes 21 days after SNI surgery in female mice, underlining the crucial role of microglial β2-AR for the anti-microgliosis effect of Formoterol. This further supports the involvement of microglial β2-AR in the anti-inflammatory action of Formoterol in neuropathic pain.

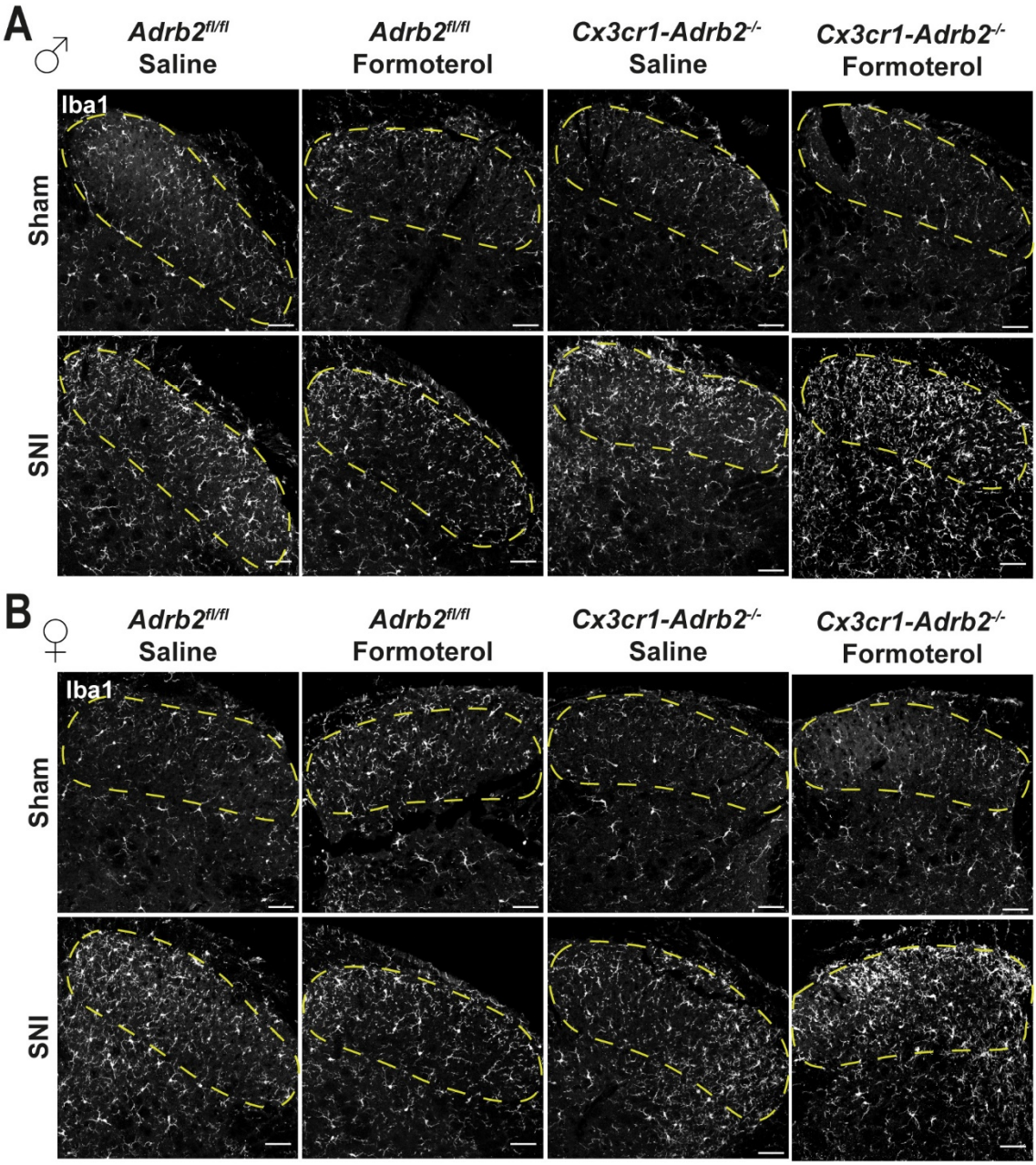

Figure 25. Microglia Iba1-positive staining in the ipsilateral spinal dorsal horn (SDH) of control and transgenic mice on day 6 post-surgery.

(A, B) Representative images of Iba1-positive staining in the ipsilateral SDH of male (A) and female (B) *Adrb2*$^{fl/fl}$ and *Cx3cr1-Adrb2*$^{-/-}$ mice injected with saline or Formoterol on day 6 post-surgery. Scale bar = 60 μm.

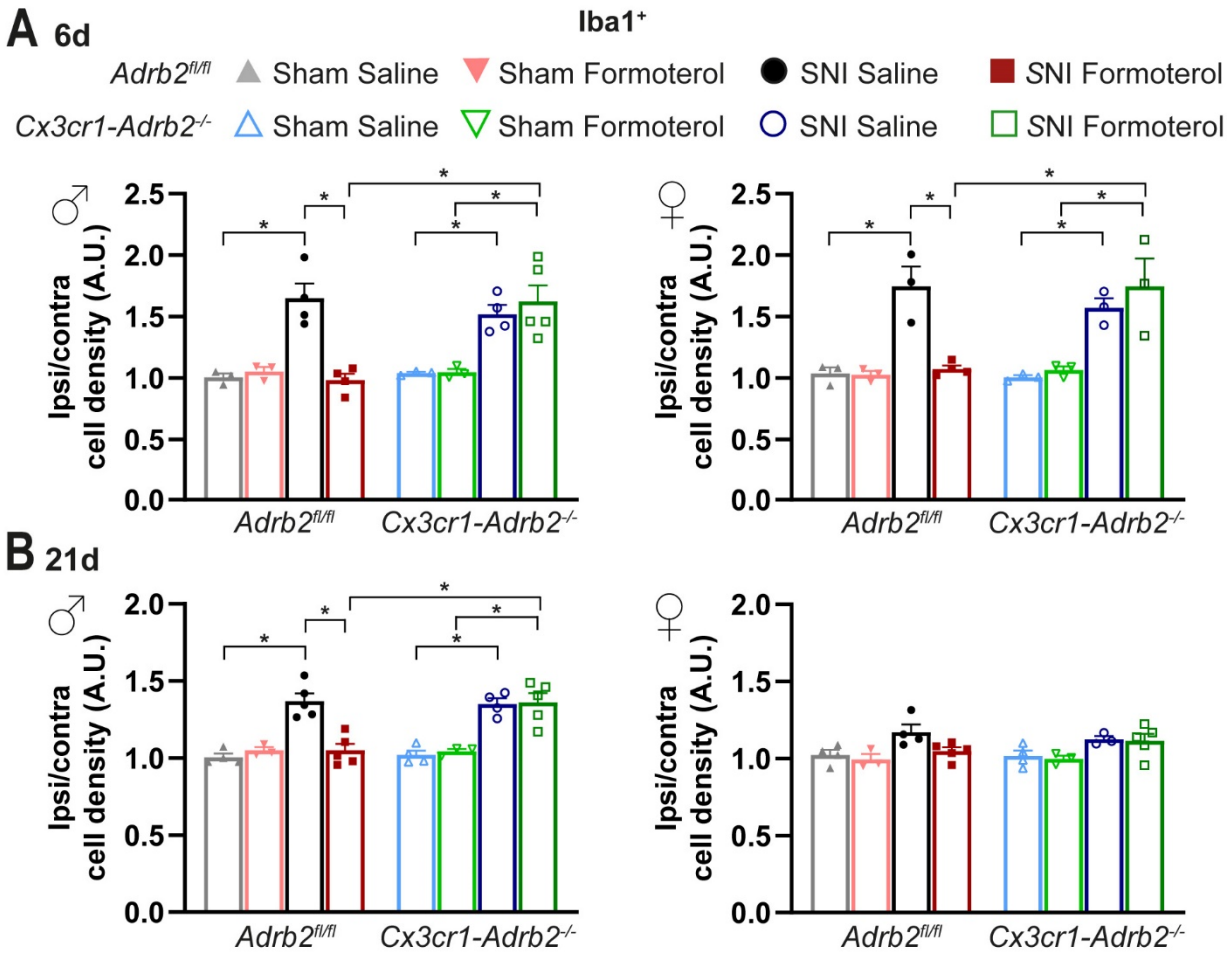

Figure 26. Analysis of microglial density in the ipsilateral spinal dorsal horn (SDH) of *Adrb2*$^{fl/fl}$ *and Cx3cr1-Adrb2*$^{-/-}$ in response to Formoterol on days 6 and 21 post-surgery.

(A, B) Quantitative analysis of Iba1-positive microglia density of male (left) and female (right) *Adrb2*$^{fl/fl}$ and *Cx3cr1-Adrb2*$^{-/-}$ mice injected with Formoterol or vehicle on days 6 (A) and 21 (B) post-surgery. Ipsi/contra = density value ratio between the ipsi and contralateral dorsal horn. A.U. = arbitrary unit. n = 3–5/group; three-way ANOVA was conducted followed by post-hoc Bonferroni´s test; * $p < 0.05$. Data are represented as mean ± SEM.

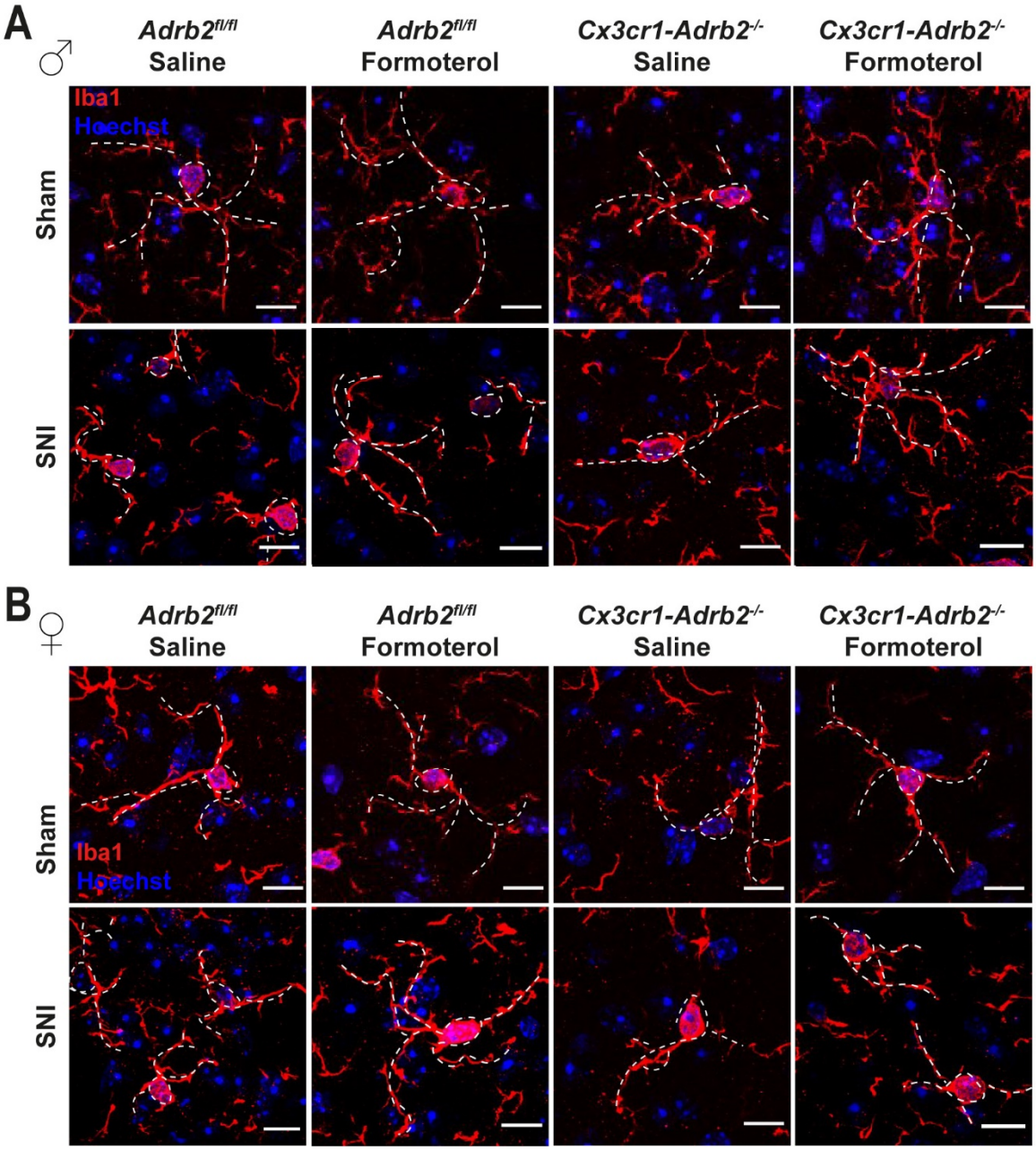

Figure 27. Effect of the β2-AR agonist on microglial morphology in the ipsilateral spinal dorsal horn (SDH) of control and transgenic mice on day 6 post-surgery.

(A, B) Representative images of microglia in the ipsilateral SDH in male (A) and female (B) *Adrb2*$^{fl/fl}$ and *Cx3cr1-Adrb2*$^{-/-}$ mice injected with saline or Formoterol on day 6 post-surgery. Microglial soma and processes were depicted by white, dashed lines. Scale bar = 10 µm.

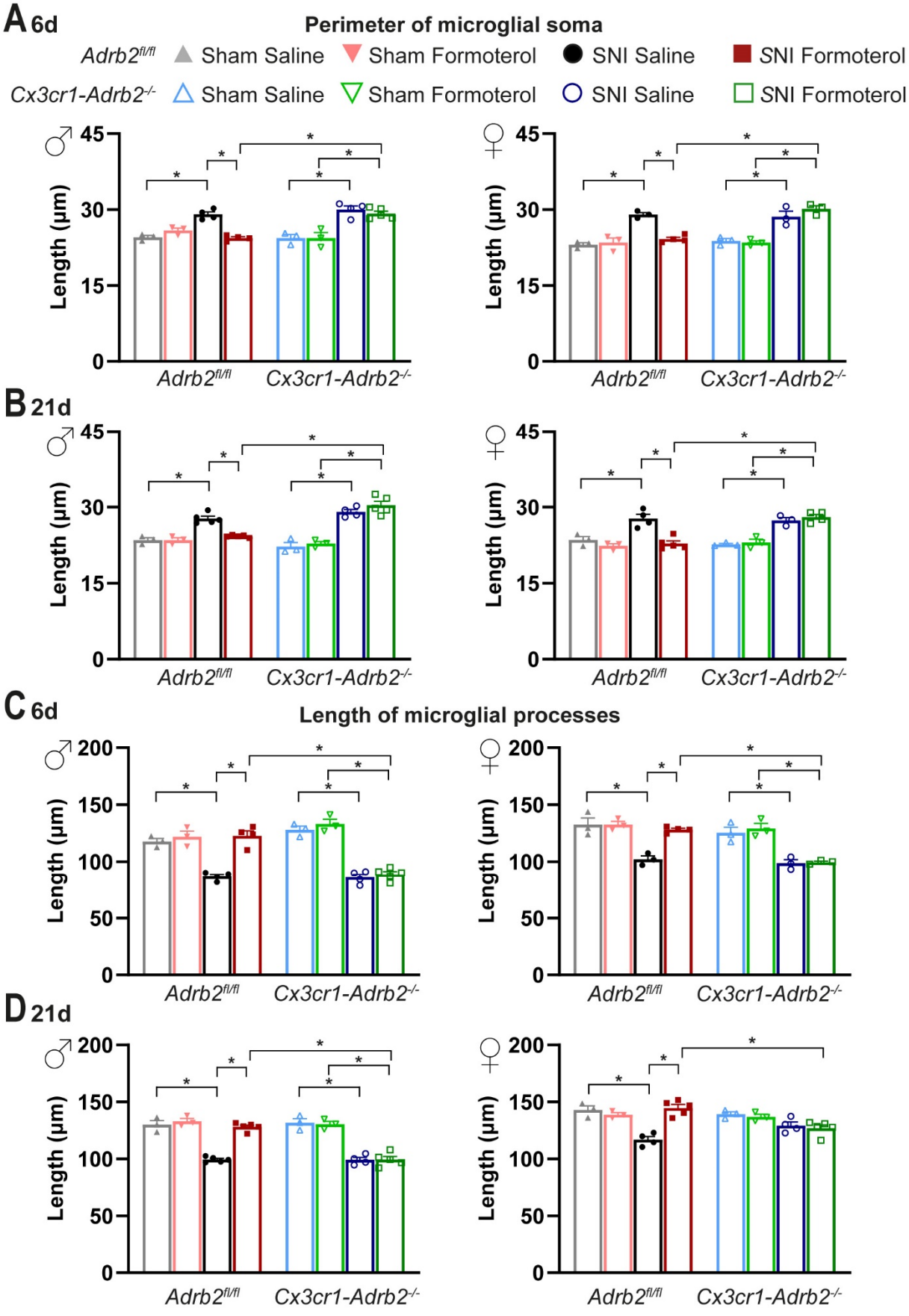
A 6d
Perimeter of microglial soma
Adrb2fl/fl Sham Saline
Sham Formoterol
SNI Saline
SNI Formoterol
Cx3cr1-Adrb2-/- Sham Saline
Sham Formoterol
SNI Saline
SNI Formoterol
Length (µm)
0
15
30
45
Adrb2fl/fl
Cx3cr1-Adrb2-/-
B 21d
C 6d
Length of microglial processes
0
50
100
150
200
D 21d

Figure 28. Analysis of microglial morphology of ipsilateral spinal dorsal horn (SDH) of *Adrb2*$^{fl/fl}$ *and Cx3cr1-Adrb2*$^{-/-}$ after Formoterol or saline treatment on days 6 and 21 post-surgery.
(A, B) Formoterol and saline application to male (left) and female (right) control and transgenic mice, 6 (A) or 21 (B) days post-SNI influenced the microglial perimeter of the soma. (C, D) Quantification of the length of microglial processes in male (left) and female (right) control and transgenic mice, 6 (C) or 21 (D) days post-SNI. n = 3–5/group; three-way ANOVA was conducted followed by post-hoc Bonferroni´s test; * $p < 0.05$. Data are represented as mean ± SEM.

To endorse the hypothesis of microglial β2-AR-mediated Formoterol-induced suppression of microgliosis, analyses of the co-immunohistochemistry of the activity markers p-p38 and p-JNK in microglia were conducted in control and transgenic mice (Figure 29, Figure 31). The absence of the *Adrb2* gene did not impact the upregulation of the microglial activity markers during the onset and sustenance of neuropathic pain nor Formoterol administration in *Cx3cr1-Adrb2*$^{-/-}$ mice subjected to sham surgery (Figure 30, Figure 32). Notably, Formoterol injection in *Cx3cr1-Adrb2*$^{-/-}$ mice of both sexes failed to reduce p-38 and p-JNK signals upregulation in microglia compared to control mice on day 6 and 21 post-SNI in control mice (Figure 30, Figure 32).

In summary, microglia-specific β2-AR deletion impaired the beneficial impact of Formoterol on microgliosis markers.

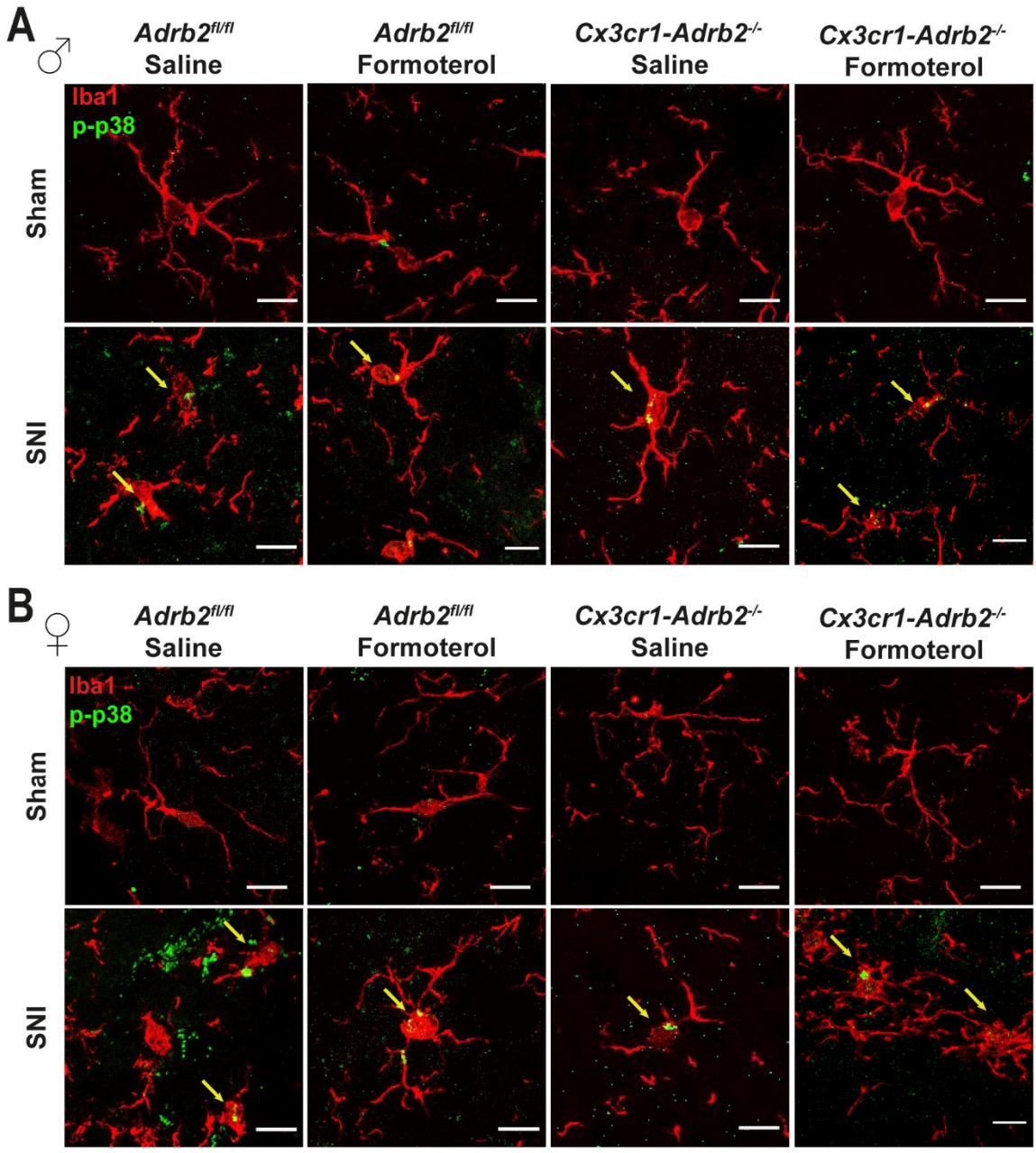

Figure 29. P-p38 activation markers in microglia in the ipsilateral spinal dorsal horn (SDH) of control and transgenic mice on day 6 post-surgery.

(A, B) Representative images of p-p38 and Iba1-positive colocalization staining in the ipsilateral SDH of male (A) and female (B) *Adrb2*$^{fl/fl}$ and *Cx3cr1-Adrb2*$^{-/-}$ mice injected with saline or Formoterol on day 6 post-surgery. Yellow arrows indicate double-positive cells. Scale bar = 10 μm.

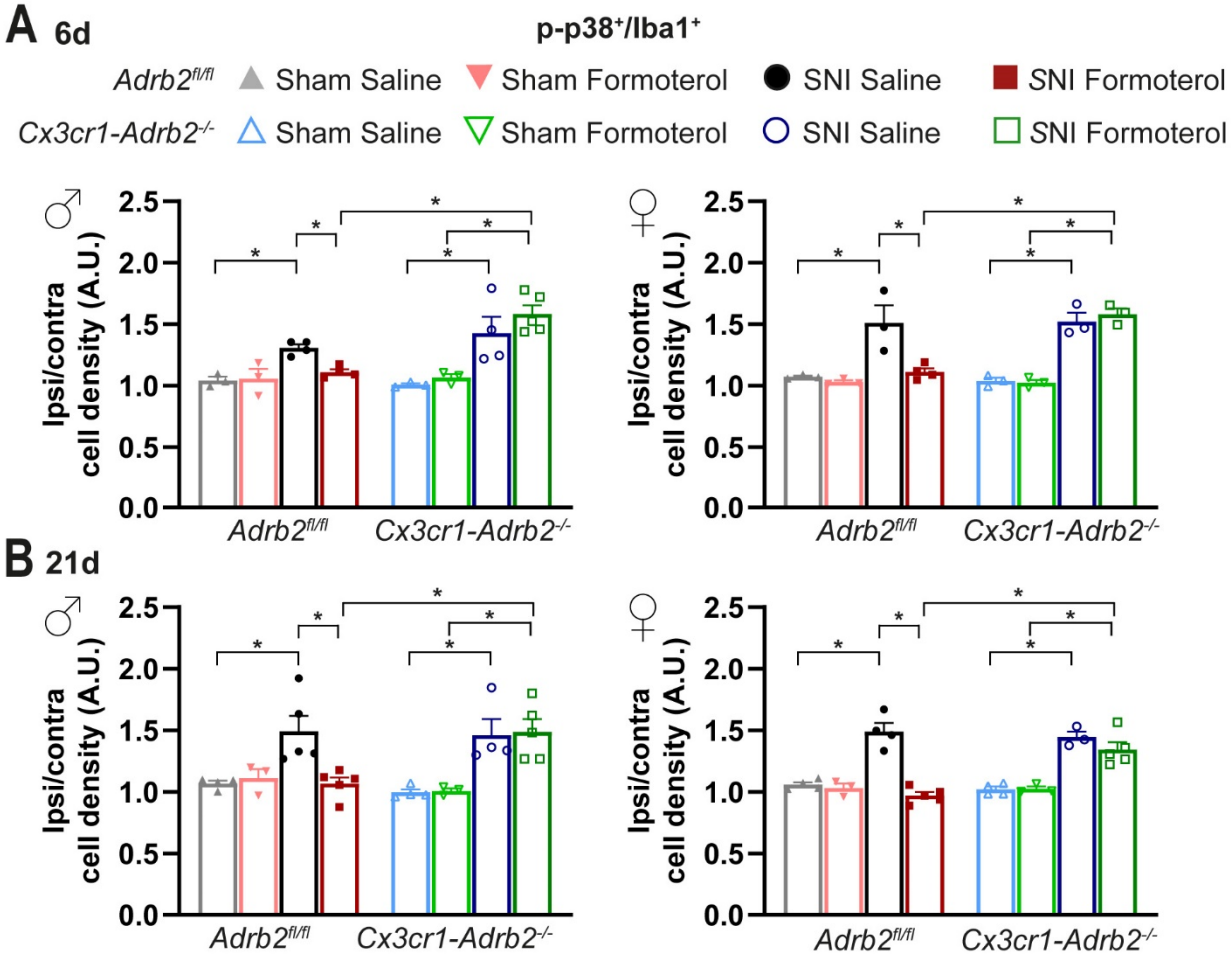

Figure 30. Microglial β2-AR deletion impaired the effect of Formoterol in lowering microglial p-p38 level in the ipsilateral spinal dorsal horn (SDH) of SNI mice on days 6 and 21 post-surgery. (A, B) Quantitative analysis of the double-positive Iba1 and p-p38-positive cells of male (left) and female (right) *Adrb2*$^{fl/fl}$ and *Cx3cr1-Adrb2*$^{-/-}$ mice injected with Formoterol or vehicle on days 6 (A) and 21 (B) post-surgery. Ipsi/contra = density value ratio between the ipsi and contralateral dorsal horn. A.U. = arbitrary unit. n = 3–5/group; three-way ANOVA was conducted followed by post-hoc Bonferroni´s test; * $p < 0.05$. Data are represented as mean ± SEM.

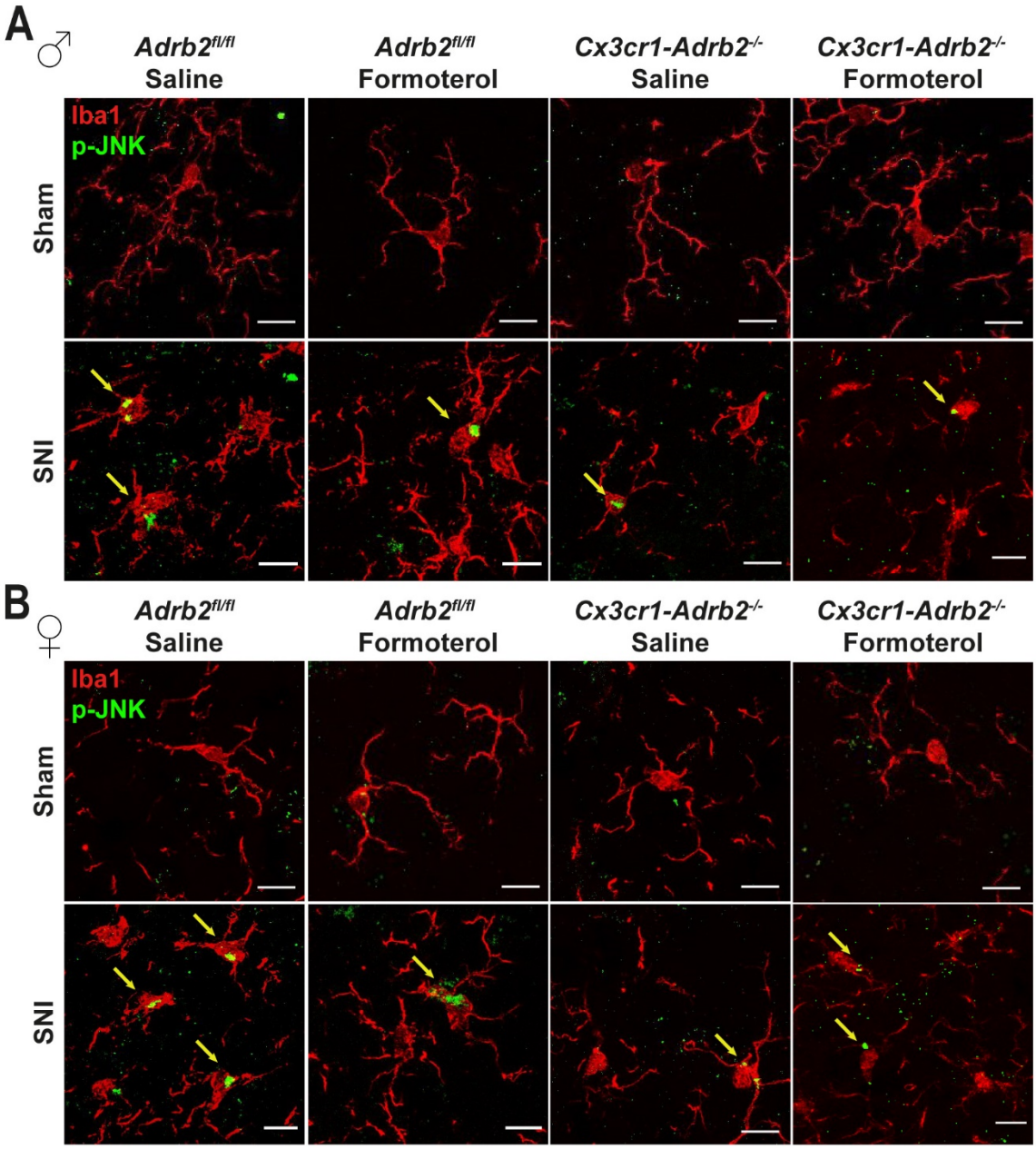

Figure 31. P-JNK activation marker in microglia in the ipsilateral spinal dorsal horn (SDH) of control and transgenic mice on day 6 post-surgery.

(A, B) Representative images of p-JNK and Iba1-positive co-immunohistochemistry staining in the ipsilateral SDH of male (A) and female (B) *Adrb2*$^{fl/fl}$ and *Cx3cr1-Adrb2*$^{-/-}$ mice injected with saline or Formoterol on day 6 post-surgery. Yellow arrows indicated double-positive cells. Scale bar = 10 μm.

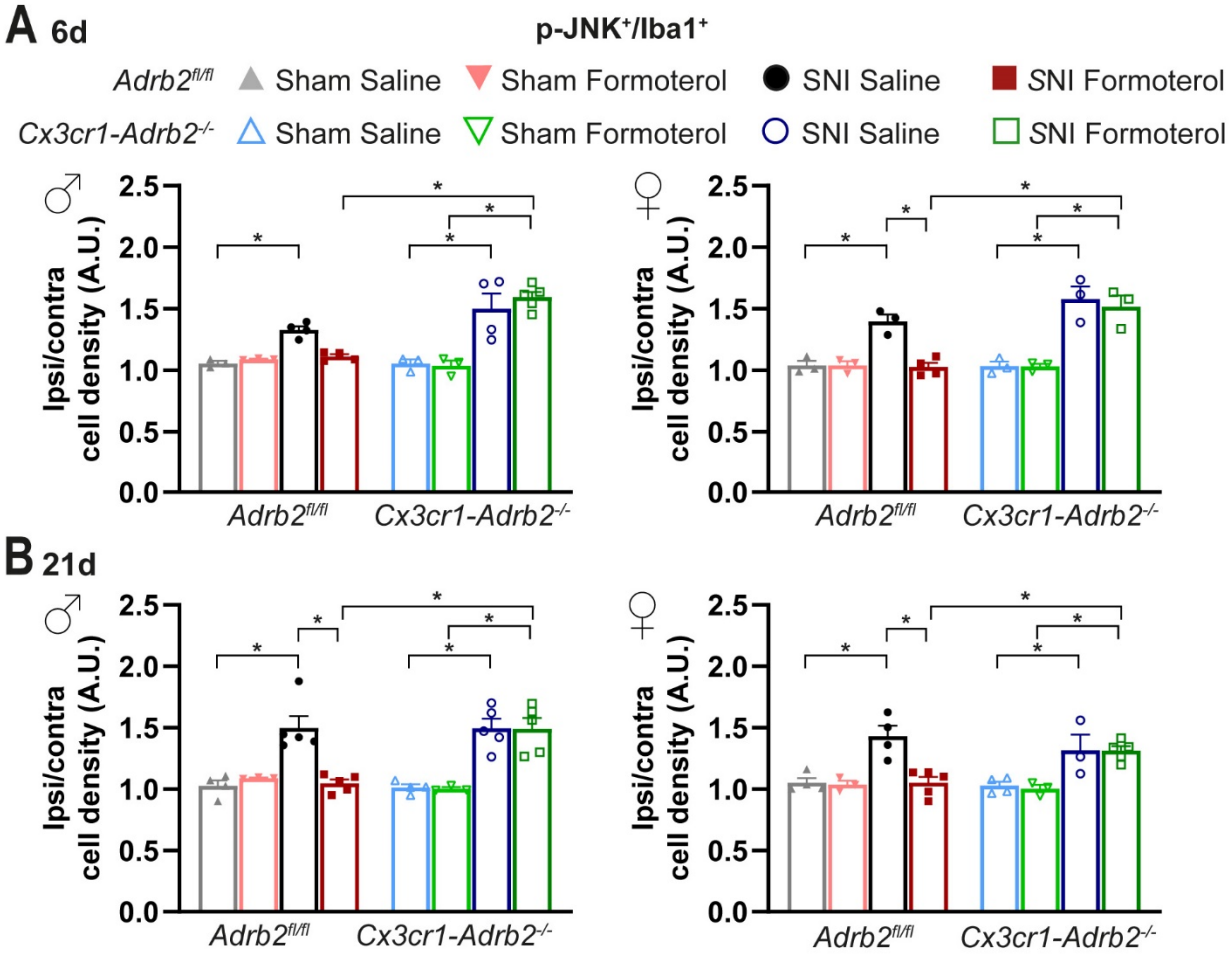

Figure 32. Microglial β2-AR deletion weakened the effect of Formoterol in reducing microglial p-JNK level in the ipsilateral spinal dorsal horn (SDH) of SNI mice on days 6 and 21 post-surgery. (A, B) Quantitative analysis of the double-positive Iba1 and p-JNK-positive cells of male (left) and female (right) *Adrb2*$^{fl/fl}$ and *Cx3cr1-Adrb2*$^{-/-}$ mice injected with Formoterol or vehicle on days 6 (A) and 21 (B) post-surgery. Ipsi/contra = density value ratio between the ipsi and contralateral dorsal horn. A.U. = arbitrary unit. n = 3–5/group; three-way ANOVA was conducted followed by post-hoc Bonferroni´s test; * $p < 0.05$. Data are represented as mean ± SEM.

β2-AR is also expressed by astrocytes and here it was investigated if Formoterol reduced astrocytes reactivity directly by binding the receptor on astrocytes, or if it needed the microglial β2-AR involvement, via GFAP fluorescence intensity and p-JNK/GFAP density analysis (Figure 33, Figure 35). In both male and female *Cx3cr1-Adrb2*$^{-/-}$ SNI mice, nerve injury induced a significant upregulation of GFAP fluorescence intensity on day 21 but not on day 6 post-surgery compared to *Cx3cr1-Adrb2*$^{-/-}$ sham mice when neuropathic pain is not completely established. Formoterol injection did not alter GFAP signal or p-JNK density in GFAP-positive astrocytes in *Cx3cr1-Adrb2*$^{-/-}$ and *Adrb2*$^{fl/fl}$ sham mice (Figure 34, Figure 36). and it significantly impeded the GFAP signal increment in control mice of both sexes (Figure 34). Notably, this was reported for female *Cx3cr1-Adrb2*$^{-/-}$ mice as well, whereas it could not be ruled out for male *Cx3cr1-Adrb2*$^{-/-}$ mice due to the data variability. Nerve injury increased p-JNK signal in astrocytes at both time points studies, but the effect of the β2-AR agonist was not observed in *Cx3cr1-Adrb2*$^{-/-}$ mice of both sexes, except a tendency in female *Cx3cr1-Adrb2*$^{-/-}$ SNI mice on day 21 post-SNI (Figure 36A, B).

The results suggest that after three weeks following neuropathic pain, the involvement of microglial β2-ARs in the effects of Formoterol on astrocytes is marginal.

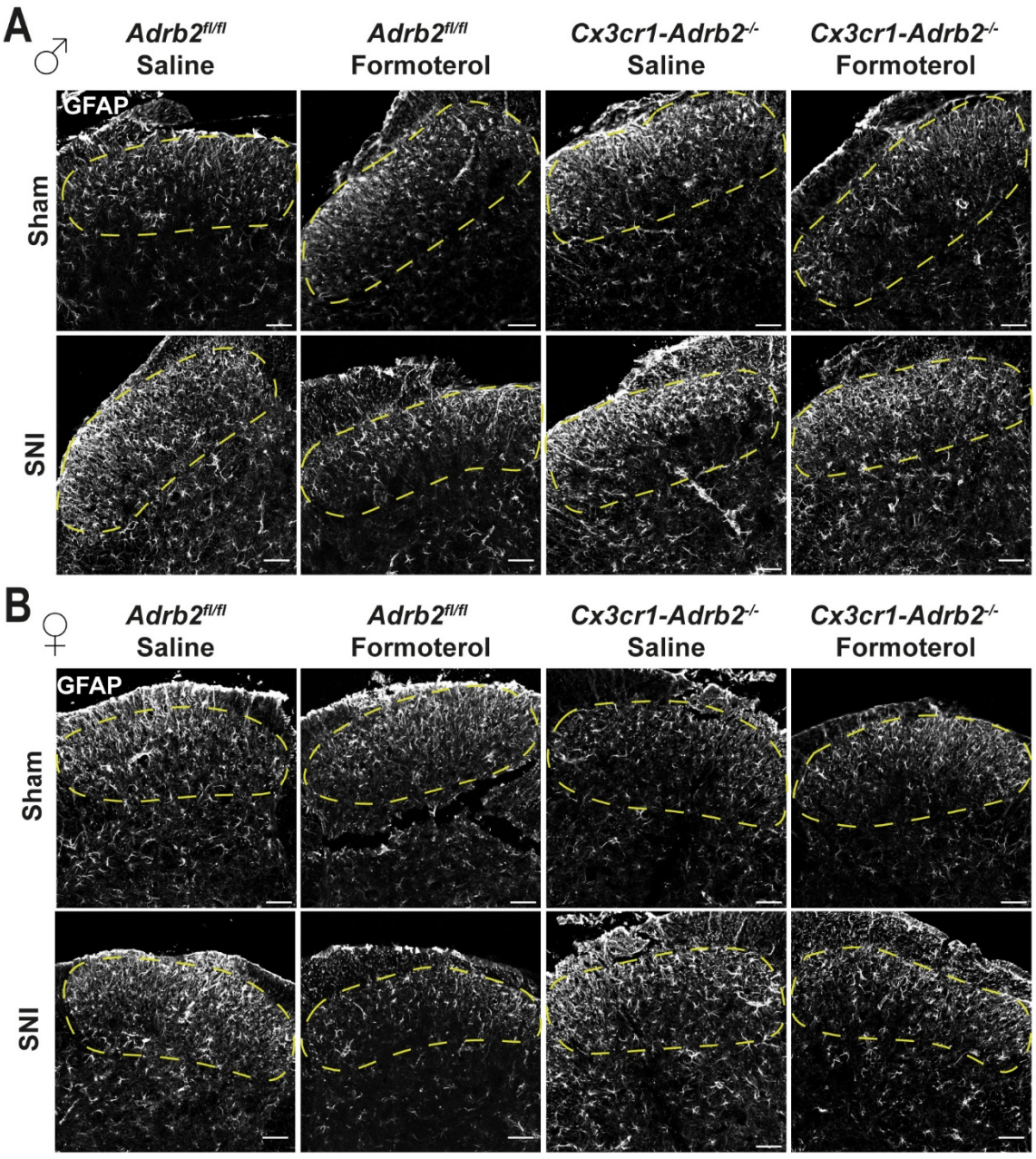

Figure 33. GFAP fluorescence signals in the ipsilateral spinal dorsal horn (SDH) of control and transgenic mice on day 21 post-surgery.

(A, B) Representative images of GFAP immune reactivity in the ipsilateral SDH of mice (male, A; female, B) injected with Formoterol or vehicle on day 21 post-surgery. Scale bar = 60 µm.

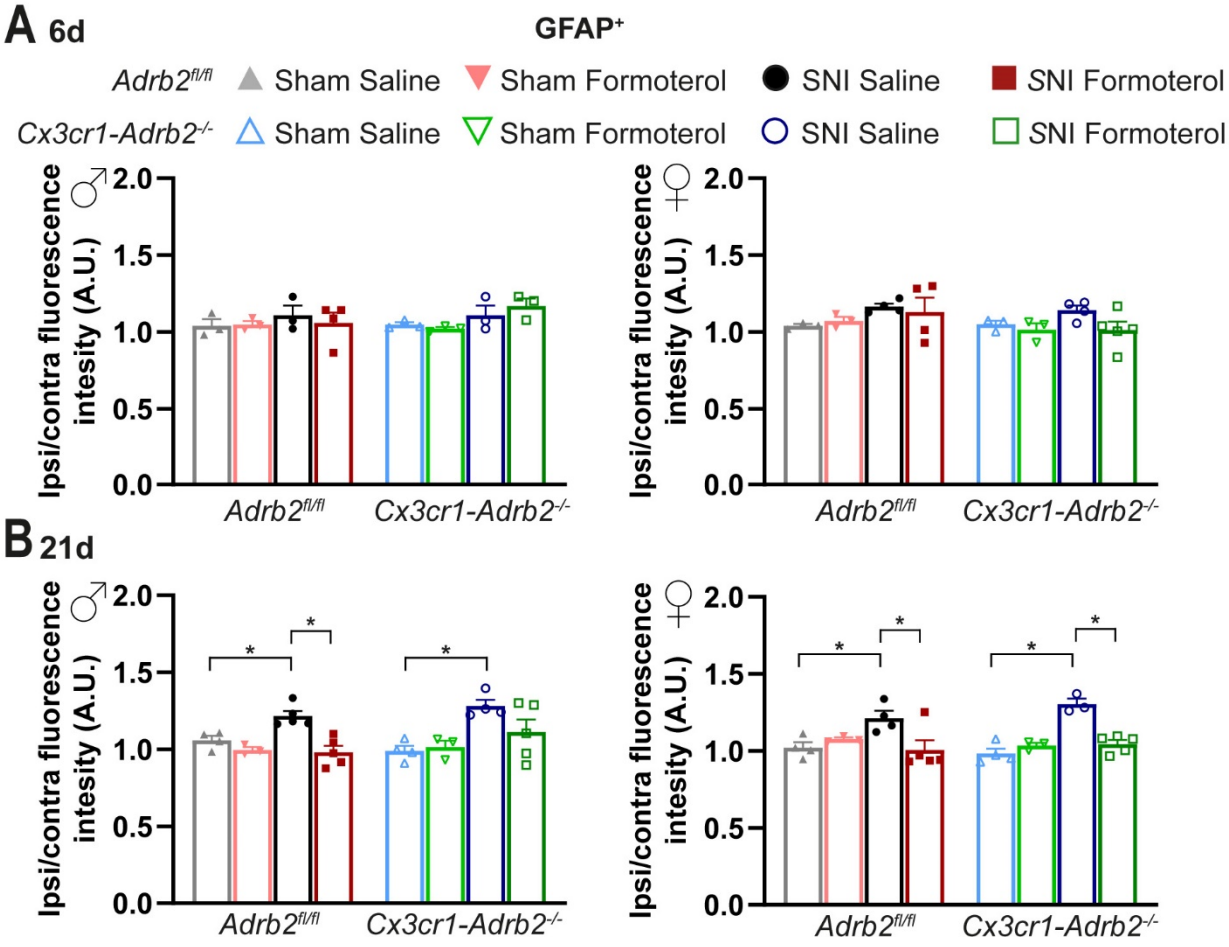

Figure 34. Microglial β2-AR deletion did not modulate astroglial response to Formoterol.

(A, B) Quantitative assessment of GFAP fluorescent intensity of male (left) and female (right) *Adrb2*$^{fl/fl}$ and *Cx3cr1-Adrb2*$^{-/-}$ mice injected with Formoterol or vehicle on days 6 (A) and 21 (B) post-surgery. Ipsi/contra fluorescent intensity = fluorescent intensity density value between the ipsi and contralateral dorsal horn. A.U. = arbitrary unit. n = 3–5/group; three-way ANOVA was conducted followed by post-hoc Bonferroni´s test; * $p < 0.05$. Data are represented as mean ± SEM.

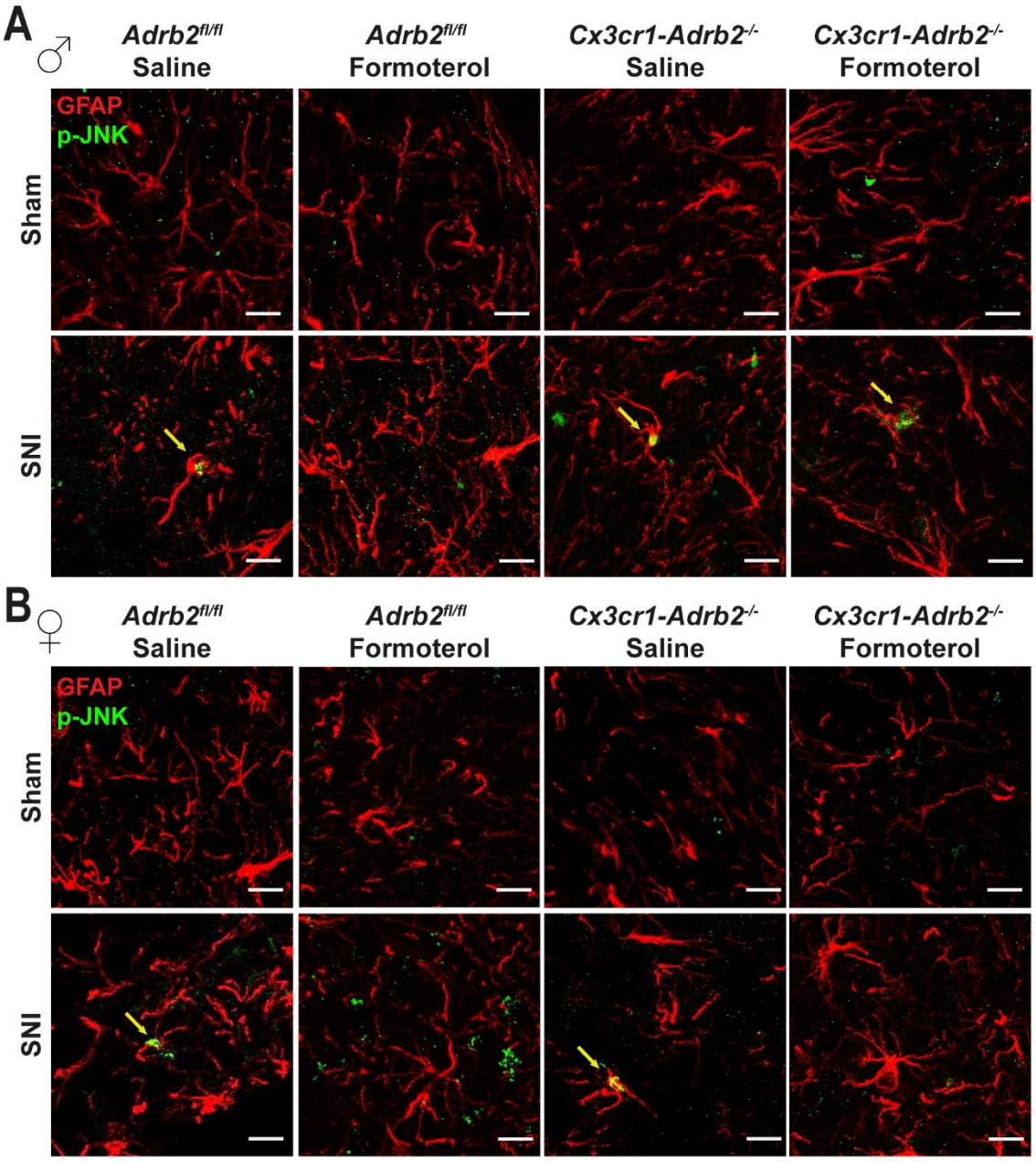

Figure 35. Images of GFAP astrocytic marker and p-JNK in the ipsilateral spinal dorsal horn (SDH) of control and transgenic mice on day 21 post-surgery.

(A, B) Representative examples of colocalization of GFAP and p-JNK in the ipsilateral SDH of mice (male, A; female, B) injected with Formoterol or vehicle on day 21 post-surgery. Scale bar = 10 μm.

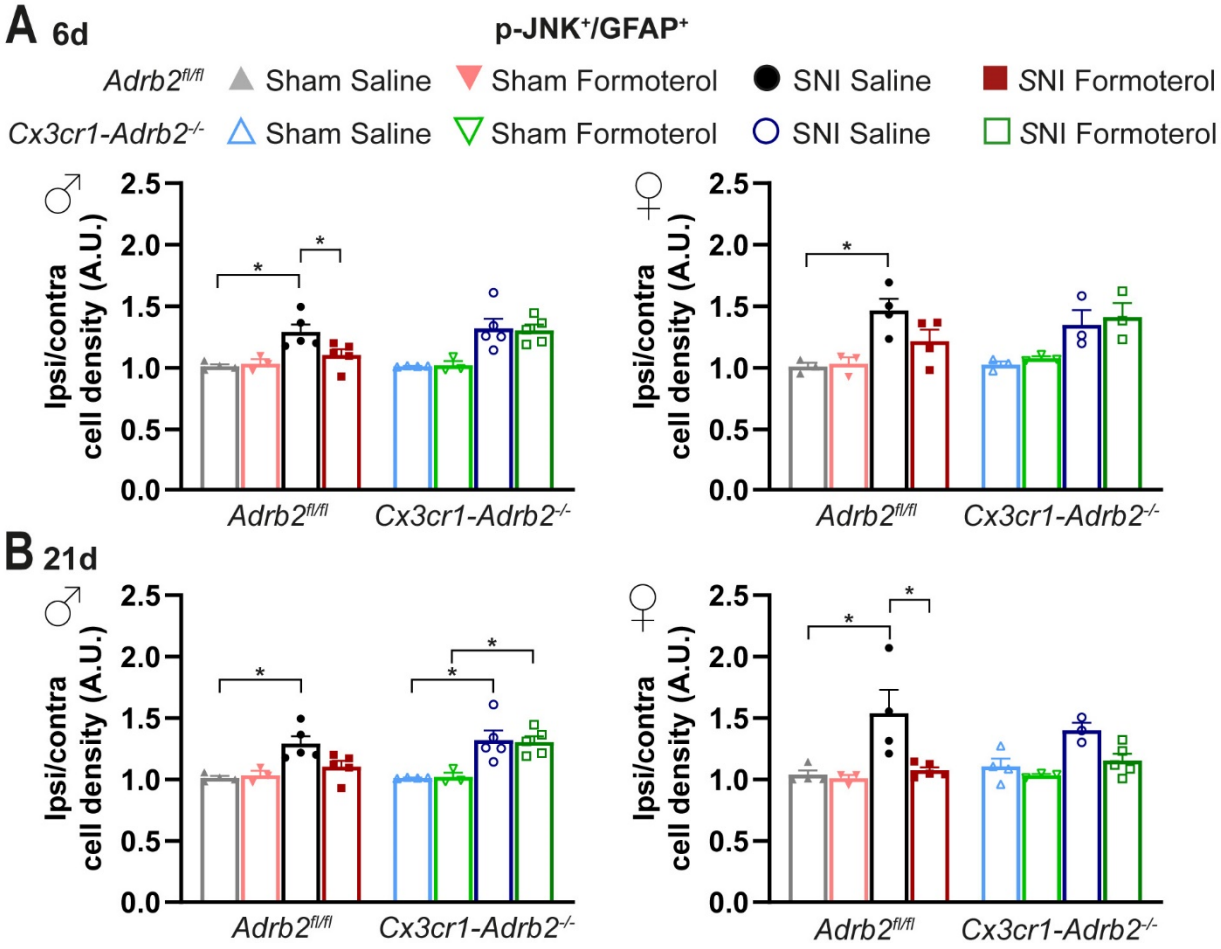

Figure 36. Effect of the microglial β2-AR deletion on p-JNK levels in GFAP-positive astrocytes in the ipsilateral spinal dorsal horn (SDH) of control and transgenic mice on days 6 and 21 post-surgery.

(A, B) Quantitative assessment of the colocalization of GFAP and p-JNK in the SDH of male (left) and female (right) mice treated with saline or Formoterol, 6 (A) and 21 (B) days post-surgery. Ipsi/contra = ratio between the ipsilateral and contralateral SDH. A.U. = arbitrary unit. n = 3–5/group; three-way ANOVA was conducted followed by post-hoc Bonferroni´s test; * $p < 0.05$. Data are represented as mean ± SEM.

5. Discussion

The involvement of noradrenergic signaling in the development of chronic pain has been extensively documented (Kuner & Kuner, 2021; Suarez-Pereira et al., 2022), and drugs targeting inhibitory α2-ARs have been studied both in preclinical and clinical settings (Finnerup et al., 2021; Kuner & Flor, 2016). Despite these efforts, there is still a need for more effective and targeted treatments for neuropathic pain management.

The primary focus of the present study was to highlight the noradrenergic glial involvement in response to neuropathic pain and the effect of Formoterol administration, a β2-AR agonist, in this condition. The study investigated the impact of Formoterol in neuropathic mice and the contribution of the microglial β2-AR. To explore this hypothesis, a conditional knock-out mouse line lacking the β2-AR specifically in microglia was generated. The genetic deletion outcome was investigated using behavioral readouts and immunofluorescence staining. Additionally, to study the impact of β2-AR stimulation on microglia, glial cell isolation, primary microglia culture, and *ex vivo* spinal cord slices were utilized. The results revealed that microglial β2-AR is crucial for the analgesic actions of Formoterol, providing valuable insights into potential new targets for the development of effective neuropathic pain treatments.

5.1 Effect of systemic delivery of Formoterol in wild type and *Cx3cr1-creERT2; Adrb2$^{fl/fl}$* mice

Preclinical studies report anti-nociceptive effects of β2-AR agonists in different neuropathic pain models, including sciatic nerve cuffing (Ceredig et al., 2019; Choucair-Jaafar et al., 2009; Kremer et al., 2020; Yalcin et al., 2010), surgical incision pain (Arora et al., 2021), paclitaxel-induced neuropathic pain (PINP) (Chen et al., 2021), DPN (Baraka et al., 2015; Choucair-Jaafar et al., 2014), and SNL model (Zhang et al., 2016),

This study investigated the effect of pharmacological stimulation of β2-ARs on microglial and astrocytic cells over neuropathic pain development and maintenance in the SNI model. This work not only confirms earlier reports but also uncovers new insights, including (i) stage-specific modulation effect of β2-AR activation on diverse neuropathic pain-associated behaviors; (ii) β2-AR activation-mediated suppression of the sensory component together with the reduction of negative aspects of neuropathic pain in chronic stages, and (iii) the requirement of microglia-specific expression of β2-AR for the anti-allodynic effect of β2-ARs agonist.

5.1.1 Investigation of the effects of Formoterol systemic application in wild type mice

The results of this study suggest that i.p. administration of Formoterol can effectively alleviate neuropathic pain both in early and chronic stages following SNI surgery. This is consistent with previous data showing that acute systemic injection of Clenbuterol, a β2-AR agonist, improved mechanical hypersensitivity in the plantar incision surgery model (Arora et al., 2021), and acute intrathecal injection of Terbutaline, another β2-AR agonist, and Formoterol ameliorated the mechanical hypersensitivity induced by PSNL and PINP, respectively (Chen et al., 2021; Zhang et al., 2016). However, other studies report that chronic, rather than acute, intraperitoneal or oral treatment with β2-AR agonists is necessary to reduce neuropathic pain (Ceredig et al., 2019; Choucair-Jaafar et al., 2009; Kremer et al., 2020; Yalcin et al., 2010). The discrepancy could be attributed to differences in the dosages and methodologies of β2-AR agonists administration, as well as the distinct nature of the peripheral nerve injury. For example, the sciatic nerve cuffing model used in C57BL/6J mice presents hyperalgesia to a hot thermal stimulus for only three weeks while the mechanical allodynia remains stable over two months (Benbouzid et al., 2008). Heat hyperalgesia is usually present in inflammatory pain, but it is neither a clinical feature of neuropathic pain nor a component of the SNI model in rodents.

The effect of Formoterol on cold allodynia has not been studied by other groups, which focus only on mechanical hypersensitivity. In the present study, the optimal concentration and timing of Formoterol administration for both mechanical hypersensitivity and cold allodynia in the SNI model were determined. Previous reports suggest that once effective, the dose of systemic injections of β-mimetics has only a minor influence on the length of the analgesic effect (Choucair-Jaafar et al., 2009; Yalcin et al., 2010). Here, two doses of Formoterol, 50 and 500 µg/kg, are effective in relieving both mechanical and cold allodynia, with a similar duration of analgesic effect. For this reason and to avoid side effects due to unspecific activation of other receptors, the lower dose of 50 µg/kg is used throughout the thesis. Different regimens of Formoterol were tested and they all led to a significant reduction of mechanical hypersensitivity and alleviation of cold allodynia.

Additionally, I investigated whether the aversive component of neuropathic pain was alleviated after Formoterol administration. In CPP experiments, male mice exhibit a preference toward the Formoterol-conditioned chamber, both early and one month after SNI surgery, whereas female mice show relief of the affective aspect of pain only at the later time point, despite showing a trend of preference in the early day after SNI. This may underline a sex-specific difference in the ability of the β2-AR agonist to alleviate ongoing pain during the first week of neuropathic pain establishment. It is plausible that this discrepancy is due to distinct

mechanisms and pharmacological sensitivities of allodynia and spontaneous pain (King et al., 2009).

Overall, these findings suggest that the β2-AR agonist Formoterol reverses both sensory and affective components of chronically established neuropathic pain and thus pave the way for clinical testing of Formoterol as a potential medication for neuropathic pain management.

5.1.2 Study of Formoterol administration in *Cx3cr1-CreERT2; Adrb2$^{fl/fl}$* mice

To delve deeper into the mechanisms underlying the analgesic impact of the β2-AR agonist, the *Cx3cr1-CreERT2; Adrb2$^{fl/fl}$* mouse line was generated wherein the *Adrb2* gene is conditionally deleted only in microglia. This approach allowed us to examine the dependence of the effect of systemically administered Formoterol on microglial β2-AR and the behavioral consequences of the receptor elimination.

Here, the deletion of the microglial β2-AR altered neither basal nociception nor the development and maintenance of mechanical and cold hypersensitivity. This further clarified concordant studies showing that depletion of noradrenergic axons in various regions of the brainstem and spinal cord or the selective destruction of sympathetic fibers through guanethidine did not affect basal mechanical withdrawal threshold or nerve injury-induced allodynia (Bohren et al., 2013; Hayashida et al., 2012). Hence, the noradrenergic system may have little effect in baseline conditions or the development of neuropathic pain, but it mediates a pivotal function via noradrenergic inhibition feedback in sustained pain conditions.

The observations acquired endorse the hypothesis that the analgesic effect of β2-AR agonist in neuropathic pain is mainly mediated by modulation of microglia, particularly during the initial phase of neuropathic hypersensitivity. Notably, mice of both sexes with microglia-specific deletion of β2-AR, do not respond to the analgesic effect of Formoterol on nociceptive behaviors when administrate on day 6 post-SNI. Similarly, Formoterol exhibits a lack of effect on mechanical sensitivity on day 21 after surgery, whereas the effect of Formoterol on cold allodynia was preserved in *Cx3cr1-CreERT2; Adrb2$^{-/-}$* mice, but not with the same magnitude as in control mice. Taken together, the analgesic effects of Formoterol are carried through different modalities for the two sensory characteristics of neuropathic pain. Mechanical and thermal hypersensitivity are distinct pain modalities mediated by different mechanisms, and their stimuli recruit distinct nociceptors to convey the nociceptive information (Abrahamsen et al., 2008; Cobos et al., 2018; Jensen & Finnerup, 2014). Thus, it is commonly reported that the same drug has different effects on mechanical or thermal responses (Montilla-Garcia et al., 2018; Olesen et al., 2010; Tsagareli et al., 2013). Regarding cold allodynia, the β2-AR agonist may exert beneficial effects through β2-ARs expressed by other cell types besides microglia.

Longitudinal studies represent a promising approach for investigating the potential effects of Formoterol on microglia involvement and pain resolution. This approach involves the repeated assessment of mechanical hyperalgesia and cold allodynia over a prolonged period. It is possible to observe and quantify changes in these variables over time and determine whether treatment with the β2-AR agonist leads to a sustained reversal of pain-associated behaviors and subsequent pain resolution. Additionally, longitudinal studies may provide insights into potential inter-individual differences in response to Formoterol treatment (Sadler et al., 2022). These differences can reflect genetic or other factors that influence treatment effectiveness.

5.2 Beneficial effect of selective activation of β2-ARs by Formoterol in reactive glia

One of the remarkable developments in the field of pain over the early 21st century is the emergence of the concept that the central immune system plays a pivotal role in the onset and maintenance of chronic neuropathic pain (Hashizume et al., 2000). Noradrenergic descending pathways stimulation has been recognized to modulate neuroinflammation processes. Therefore, the effects of β2-ARs pharmacological activation on primary microglia culture and glial cells during different stages of neuropathic pain onset and maintenance were investigated in the SNI model.

The current research presents several novel underpinnings on β2-ARs, including: (i) β2-AR stimulation in primary microglia culture reduced their reactive phenotype; (ii) neuropathic pain augments β2-AR expression on spinal microglia; (iii) microglia and astrocytes are involved differentially in β2-AR-mediated analgesic effect at different time frames of neuropathic pain; (iv) β2-AR activation reduces astrocytic activation when neuropathic pain is chronically established, and (v) the contribution of the microglial β2-ARs in the anti-astrogliosis effects of Formoterol is minimal.

5.2.1 The stimulation of β2-AR in primary microglia culture attenuates microglial reactivity

Previous studies demonstrated that NE and β2-AR agonists have anti-inflammatory effects whereas blocking β2-AR receptors with β-blockers can promote neuroinflammation in several pathological models, including Alzheimer's disease and Parkinson's disease (Evans et al., 2020). In cultured macrophages, the stimulation of β2-AR results in increased cAMP levels, which activate the cAMP-PKA pathway, promoting the release of anti-inflammatory substances (Keranen et al., 2016), and leading to the inhibition of the release of proinflammatory cytokines (IL-1β, IL-6, TNF-α, and free radicals) (Izeboud et al., 1999; Keranen et al., 2017). Additionally,

β2-AR agonists stimulate the shift of LPS-activated microglia from a reactive to a resting-like phenotype through multiple signaling pathways, including the cAMP-PKA response element-binding protein (CREB) pathway, phosphoinositide 3-kinase (PI3K), and p38 MAPK signaling (Sharma et al., 2019). (Evans et al., 2020). Despite LPS is not a model of neuropathic pain, β2-AR agonists modulate pathways linked to microglial activation, migration, and phagocytic activity, all important aspects for the resolution of neuropathic pain.

To explore further these findings, cultured primary microglial cells from the spinal cord of adult mice were activated using a condition mimicking nerve injury and then incubated with β2-AR agonist. This resulted in a downregulation of the release of pro-inflammatory cytokines and an upregulation of the secretion of anti-inflammatory mediators. This is noteworthy as cytokines can increase spinal cord neuron activity, exacerbating pain generation (Xanthos & Sandkuhler, 2014). For example, in activated microglia culture, Formoterol reduced IL-17 and TNF-α levels, both of which induce neuronal sensitization and hyperalgesia through various pathways (Pinho-Ribeiro et al., 2017; Steeland et al., 2018). Recent studies have indicated that modulating resident spinal cord microglia can inhibit the pronociceptive phenotype of glial cells and neuronal hyperexcitability, suppressing central sensitization (Fiore et al., 2023; Kohno et al., 2022). Therefore, modulating microglia may play a protective role in the resolution of neuropathic pain.

5.2.2 Adrenergic receptors are modulated in neuropathic pain

The expression of β2-AR on astrocytes has been a topic of debate due to diverging reports. In Chen et al., β2-AR has been reported to be colocalized in neurons, and to a lesser extent also in GFAP- and Iba1-positive cells in the SDH (Chen et al., 2021), while in Arora et al., no clear localization of β2-AR in astrocytes has been observe (Arora et al., 2021). This discrepancy may be attributed to the employment of different animal models or diverse anti-β2-AR antibodies. Moreover, the modulation of ARs in response to neuropathic pain has been investigated. In this work, changes in spinal microglial and astrocytic *Adrb2* were examined three days after surgery. In SNI and sham mice, astrocytes expressed *Adrb2* mRNA but it was not modulated. However, astrocytes are not fully activated at this time point after nerve injury, so it is not possible to exclude a late up or downregulation. Whereas nerve injury significantly increased microglial expression of *Adrb2* mRNA. This newly discovered molecular change complements previously identified increases in spinal α2C-AR following SNL (Stone et al., 1999). The noradrenergic analgesic system plays an important role in contrast to the maladaptive changes that occur following nerve injury (Caraci et al., 2019). In preclinical research, it has been revealed that descending noradrenergic pathways effectively inhibit mechanical and thermal hypersensitivity by augmenting BDNF levels (Hayashida & Eisenach, 2010; Hayashida et al., 2008) and that these pathways attenuate glutamatergic transmission

in the SDH via pre-and postsynaptic α2-ARs increased activity (Chen et al., 2011). Therefore, the rise of microglia *Adrb2* mRNA expression may be an analgesic response of the endogenous noradrenergic system at the onset of neuropathic pain. When neuropathic pain is established, the glutamatergic system that controls NE release from LC noradrenergic neurons is impaired, thereby these neurons are less responsive to noxious stimuli (Kimura et al., 2015). Notably, studies with patients suffering from neuropathic pain indicate a diminished capability to activate descending inhibition (Lewis et al., 2012). Additionally, nerve injury upregulates noradrenaline transporter (NET) at the spinal cord level in the SNL rat model (Rojo et al., 2012). In this work, the *Adrb2* mRNA was upregulated a few days after induction of neuropathic pain. Overall, these findings underline the significance of descending noradrenergic pathways in endogenous analgesia and indicate that targeting β2-ARs in the early phase could decelerate the progression of the condition.

5.2.3 Microglia are implicated in the β2-AR-mediated anti-inflammatory effect during diverse time frames of neuropathic pain

The expression of the microglial marker Iba1 is widely utilized to assess microglial reactivity and accumulation. It is known that Iba1 expression markedly increases in the spinal cord following nerve injury (Inoue & Tsuda, 2018). Additionally, previous studies indicate that MAPKs intracellular signaling pathways control the production and release of inflammatory mediators, including cytokines, chemokines, and innate immunity mediators (Ji et al., 2013) and microglial p38 may be essential in modulating pain transmission under neuropathic conditions, as intrathecal treatment with p38 inhibitors ameliorates neuropathic pain (Tsuda et al., 2004).

In this study, a significant accumulation of microglia in the segments L3–L4 of the SDH is observed in both male and female WT mice shortly after surgery, whereas at late time point occurs only in male mice. Furthermore, there was an upregulation of the activated, e.g., phosphorylated form of p38 and JNK after nerve injury, and no sex dissimilarities were detected at any of the time points analyzed. Notably, a single administration of Formoterol rapidly reversed the microglial accumulation and lowered the level of microglial-activated p38 and JNK MAPK in the ipsilateral SDH of SNI mice. Significant molecular alterations are found in pure populations of microglia in response to Formoterol, promoting an anti-inflammatory phenotype.

Furthermore, Formoterol fully reverses nerve injury-induced changes in microglial populations in the SDH *in vivo*. In general, microglia are characterized by their remarkable morphological plasticity, which allows them to adopt a range of shapes stretching from hyper-ramified to amoeboid in response to various pathophysiological conditions (Hansen et al., 2022). The amoeboid phenotype of microglia was already present after three days post-surgery,

suggesting a shift from resting to reactive microglia. Both *in vivo* and *ex vivo* data suggested that Formoterol alters the morphologic phenotype of active microglia. Stimulation with the β2-AR agonist successfully increased the overall ramification of microglia. Notably, the effects of Formoterol on microglia in *ex vivo* spinal cord slices were not limited to the duration of Formoterol incubation but rather persist during the washout phase, when the β2-AR agonist is no longer present, leading to sustained modifications in microglial activity even after the washout phase.

The results obtained in this thesis and other lines of evidence support the idea that anti-inflammatory proprieties of β2-AR agonists primarily act on microglia to alleviate neuropathic hypersensitivity, particularly during the early stage of hypersensitivity (Arora et al., 2021; Zhang et al., 2016). Chemogenetic activation of LC-noradrenergic neurons with the subsequent release of NE dissipated the reactive state and microglial accumulation in the ipsilateral SDH of CCI mice (Li et al., 2022), thus microglial β2-AR may convey the anti-microgliosis effect of NE.

With the employment of the *Cx3cr1-CreERT2; Adrb2*$^{fl/fl}$ mouse line it was shown that the anti-inflammatory effect of Formoterol was the result of the direct activation of β2-ARs on microglia and not paracrine signals from adjacent cells expressing the β2-AR. Formoterol application not only failed to suppress microgliosis in both male and female *Cx3cr1-Adrb2*$^{-/-}$ mice but also did not show any analgesic effects. Thus, Formoterol reduces nociception through its anti-microgliosis effects.

These findings suggest that therapeutic use of β2-AR agonists can hinder pro-inflammatory spinal cord microglial signaling during the initial phase post-injury, which possibly can prevent the full manifestation of neuropathic pain.

5.2.4 Effect of β2-AR agonist at different temporal phases of neuropathic pain in spinal astrocytes

Previous studies indicate that astrocytic α1A-ARs mediate mechanical pain hypersensitivity upon intrathecal administration of NE, and chemogenetic stimulation of SDH astrocytes alone can induce hypersensitivity (Kohro et al., 2020). However, chemogenetic activation of LC noradrenergic neurons projection to the SDH leads to NE-mediated inhibition of pain transmission and astrocytic activation (Li et al., 2022). Furthermore, modulation of astrocytic β2-AR tone can alter NF-κB-dependent effects and the immune cell content of the SDH in inflammatory states (Laureys et al., 2010). It is possible that Formoterol binds to astrocytic receptors and modulates the inflammatory response to nerve injury. However, data showed that astrocytes reactivity is evident only at later time points studied. In nerve-injured mice, Formoterol inhibition of astrocyte activation was observed when neuropathic pain is chronically

established. This is in agreement with previous research indicating that the activated form of JNK, e.g. phosphorylated JNK, is upregulated in astrocytes two weeks after nerve injury, and Formoterol administration can reverse this phenomenon (Zhang et al., 2016; Zhuang et al., 2006).

β2-ARs are expressed in astrocytes; therefore, Formoterol has some effect on spinal astrocytes. Three weeks after injury, microglia do not accumulate in the ipsilateral SDH of female *Cx3cr1-Adrb2*$^{-/-}$ mice. Formoterol administration failed to reduce microglial p-p38 and p-JNK MAPK levels compare to sham mice after but succeed to decrease astrocytic activation. Conversely, in male *Cx3cr1-Adrb2*$^{-/-}$ mice, microglia accumulated in the ipsilateral SDH, and Formoterol application did not disengage microgliosis. Due to the high variability of the data, it is not possible to conclude whether Formoterol deactivated astrocytes in male mice. Therefore, the inflammatory response of microglia may have a dominant effect on the spinal environment. Nevertheless, sex factors can regulate the diverse effect of Formoterol on astrocytes. To investigate this hypothesis further studies involving the astrocyte-specific deletion of *Adbr2* will clarify this mechanism.

5.2.5 Crosstalk between microglia and astrocytes involving noradrenergic signaling

Evidence suggests that microglia are sequentially activated early after injury, followed by astrocytes (Nam et al., 2016; Raghavendra et al., 2003), and there is compelling evidence of crosstalk between these different cell types (Matejuk & Ransohoff, 2020). The interaction between astrocytes and microglia is mediated, in part, by various secreted mediators including neurotransmitters, cytokines, chemokines, NO, ROS, innate-immunity mediators, tissue damage molecules, mitogenic factors, growth factors, and metabolic mediators. Both types of cells have storage sites for many chemokines, of which receptors are expressed by the other cell type (Zhang et al., 2023). These mediators play important roles in both cellular metabolism and tissue modifications, highlighting the strong association between microglia and astrocytes (Matejuk & Ransohoff, 2020).

The current study suggests that β2-AR-mediated noradrenergic signaling in microglia and astrocytes occurs independently of each other at late time points after nerve injury. The results indicated that the analgesic effect of Formoterol following nerve injury can be mediated by at least two distinct temporal modes of action: one by microglia and another by astrocytes at the early and late phases of nerve injury, respectively. Thus, even in cases of established neuropathic pain, Formoterol may still be effective via the astrocytic β2-ARs, which is promising for patients seeking therapy at late stages post-nerve injury. Nevertheless, as already mentioned in section 5.2.4, this thesis focused on microglial manipulations and the

generation of a mouse line with the loss of *Adbr2* in astrocytes will be necessary to fully elucidate the role of astrocytes on the NE-mediated analgesia in models of neuropathic pain. In addition, reactive astrocytes are not always correlated with reactive microglia. Studies conducted on rats have revealed that chemotherapy-induced peripheral neuropathy (CIPN) is linked to pronounced spinal astrogliosis, but limited microgliosis (Robinson et al., 2014; Zhang et al., 2012). Notably, CIPNs are mechanistically different from those generated by nerve trauma (G. Fumagalli et al., 2020; Zhang et al., 2012).

These findings and previous data suggest that the analgesic effects of β2-ARs in pain management arise from their capacity to inhibit inflammatory signaling among spinal neurons and glial cells post-nerve injury. Nonetheless, to gain a better understanding of the possible therapeutic applications of noradrenergic receptor modulators in neuropathic pain conditions, studies need to explore the dynamic relationship between the expression and function of these receptors in such conditions.

5.3 Sex dimorphism in microglia in pain

Chronic pain has a higher occurrence in women than men, and this is mirrored in pain responses even in the absence of a pathological pain state (Ghazisaeidi et al., 2023). Both animals and human studies show suggests that microglial and astrocytes play a critical role in chronic pain (Del Valle et al., 2009; Loggia et al., 2015).

In recent years, there has been growing interest in investigating sex differences in microglia-mediated hypersensitivity to better understand the underlying mechanisms and improve pain management in both sexes (Midavaine et al., 2021; Mogil, 2020). Studies targeting the activation of p38 MAPK and P2X4-BDNF-TrkB pathway in female mice show an unsuccessful reduction in pain hypersensitivity, indicating a male-specific microglial response that depends on testosterone (Sorge et al., 2015; Taves et al., 2016). Single-cell RNA-sequencing studies showed that peripheral nerve injury induces a more robust microglial inflammatory response in male mice than in female mice. However, the increased proliferation of microglia in males is similar to that in females 7 days after SNI (Sorge et al., 2015; Tansley et al., 2022). Furthermore, many studies report no apparent sexual dimorphism in the analgesic effect of microglial inhibitors, deletion of microglia, or genetic knockout of microglial-selective molecules in different neuropathic pain models (Batti et al., 2016; Gu, Eyo, et al., 2016; Peng et al., 2016).

This study showed that microgliosis is equally present in both sexes on days 3 and 6 post-SNI, and the β2-AR agonist reversed this phenomenon. Conversely, female microglia do not show a reactive phenotype in the late phase of neuropathic pain. Additionally, Formoterol is less successful in diminishing ongoing pain in female than in male mice soon after nerve injury. These differences support the importance of considering sex differences in the course,

severity, and management of neuropathic pain. Furthermore, here spinal astrocyte activation is not affected by sex following nerve injury or systemic delivery of Formoterol, consistent with previous studies (Chen, Luo, et al., 2018; Ghazisaeidi et al., 2023).

Overall, the functioning of microglia on day 21 following nerve injury, and the impact of Formoterol on spontaneous pain, indicate the presence of sexual dimorphism. Therefore, these findings may have implications for the selection of drugs and regimens for neuropathic pain management. Clinical trials using glial inhibitors have shown mixed results. For example, minocycline has been described to induce an analgesic action in radicular pain patients after two weeks of treatment (Vanelderen et al., 2015), but it fails when administered before the surgery as a prophylactic treatment to lumbar discectomy or hand surgery (Curtin et al., 2017; Martinez et al., 2013). These unconvincing results may be due to the lack of selectivity or unfavorable pharmacodynamic properties of these compounds, or the need to target specific signaling pathways within glial cells rather than inhibiting their entire physiological function. Sex differences in glial cell activation kinetics and response to drugs have been reported (Gensel et al., 2019; Inyang et al., 2019; Sorge et al., 2015), highlighting the importance of considering both sexes in the study design when recruiting participants and to integrate the sex factor into the data analysis in chronic pain clinical studies.

5.4 Confounding factors and future directions

5.4.1 Different routes of drug administration

Systemic administration of Formoterol does not aid in elucidating the regional specificity of receptor activity. While the transgenic mouse line offers cellular-level specificity, it does not provide specificity at the regional level, such as supraspinal, spinal, or peripheral regions. Intrathecal delivery can narrow the possible location of beneficial effects on the CNS and its associated nerves and exclude peripheral regions.

When Formoterol and Terbutaline are injected intrathecally, they reduce mechanical hypersensitivity in murine neuropathic pain models and mediate changes in glial populations of the spinal cord (Chen et al., 2021; Zhang et al., 2016). However intrathecal injection also affects the DRGs, and chronic administration of β2-AR agonists suppresses mechanical hypersensitivity in nerve-injured mice partially by suppressing the peripheral release of TNF-α from DRG satellite cells (Bohren et al., 2013).

Other studies have tested the location of β2-ARs analgesic effect. During chronic i.p. administration of Salbutamol, a β2-AR agonist, intrathecal and i.p., but not intracerebroventricular or intraplantar blockade of β2-ARs suppressed the anti-allodynic effect of the Salbutamol (Choucair-Jaafar et al., 2009). Furthermore, Terbutaline i.p. application in

sympathectomized mice receive i.p. is still operative in the deficiency of sympathetic fibers in the DRGs (Bohren et al., 2013). This suggests that the β2-ARs responsible for the anti-allodynic action are not situated in supraspinal regions or at the level of peripheral terminals, but rather have a downstream, postsynaptic location.

To target a specific region of the CNS, viral constructs such as rAAV6-CD68 (Rosario et al., 2016) or rAAV9-CD68 (Grace et al., 2018) can be used to express Cre recombinase under the CD68 promoter in *Adrb2*$^{fl/fl}$ mice. This approach would facilitate the study of the microglial β2-AR involvement specifically in the injection region in the analgesic effect of Formoterol.

In addition, poly lactic-co-glycolic acid (PLGA) nanoparticles can be used as a carrier for drugs or siRNA delivery (Kim et al., 2021; Lee et al., 2021). PLGA nanoparticles have shown potential for specific targeting of microglia (Kim et al., 2021). In Pan et al., it has been shown that suppression of NF-κB diminished microglia reactivity and correlates with the elimination of neuropathic symptoms (Pan et al., 2010). Generally, the NF-κB dimers are found within the cytoplasm in their inactive state in complexes with the inhibitor of κB (IκB) family members. Phosphorylation of IκB by IκB kinase (IKBKB) prompts complex disassembling, releasing NF-κB and promoting its nuclear translocation to modulate gene expression (Hayden & Ghosh, 2012). In SNL rats, the use of PLGA nanoparticles to deliver IKBKB siRNA results in analgesia and decreased secretion of pro-inflammatory mediators due to NF-κB blockade (Lee et al., 2021). Encapsulating Formoterol in nanoparticles allows drug relocation with the potential of a prolonged analgesic effect and reduced side effects.

5.4.2 β2-ARs are expressed in SGCs and peripheral immune cells

The peripheral anti-allodynic effects of β2-AR activation should be considered when administering Formoterol i.p. in WT mice, as β2-ARs are expressed in SGCs and peripheral immune cells (Bohren et al., 2013; Sharma & Farrar, 2020). β2-AR signaling suppresses inflammatory cytokine secretion and modulates various innate immune cell activities, affecting macrophages and dendritic cells in response to LPS (Agac et al., 2018; Donnelly et al., 2010; Grailer et al., 2014), but also B and T cell responses (Kim & Jones, 2010; Mizuno et al., 2005; Takenaka et al., 2016).

In this study, the *Adrb2* gene is specifically deleted in *Cx3cr1-CreERT2*-expressing cells. SGCs do not express the Cx3cr1 gene (Avraham et al., 2021), whereas the majority of peripheral immune cells present CX3CR1 and exhibit Cre-dependent rearrangement. However, due to their lifespan, they are continuously replenished by bone marrow-derived cells (Goldmann et al., 2013; Yona et al., 2013). Thereby, the analysis of genetic rearrangement in *Cx3cr1-CreERT2; Adrb2*$^{fl/fl}$ mice four weeks after tamoxifen administration, resulted in the deletion of the *Adrb2* gene in spinal microglia, but not in peripheral macrophages, in agreement

with fate mapping studies (Goldmann et al., 2013; Wolf et al., 2013; Yona et al., 2013). Moreover, microglial proliferation in the spinal cord after nerve injury arises from resident microglia rather than infiltrating monocytes (Gu, Peng, et al., 2016; Guimaraes et al., 2019; Yao et al., 2016) and no ectopic recombination was found in astrocytes, confirming previous studies (Goldmann et al., 2013; Zhao et al., 2019). Thus, microglia are the only cells in the CNS lacking β2-ARs deleted in the transgenic mice employed in this study.

Taken together, the use of the conditional mouse line *Cx3cr1*-CreERT2*; Adrb2*$^{fl/fl}$ is an effective method to target microglia *in vivo*. To endure specific deletion of the *Adrb2* gene in microglia, it is necessary to wait four weeks after tamoxifen injection before inducing neuropathic pain. This allows sufficient time for the Cre recombinase to be activated and for the *Adrb2* gene to be deleted in microglia while minimizing the potential off-target effects and ensuring the specificity of the genetic manipulation.

5.4.3 Interaction between β2-ARs and opioids receptors

The study by Kremer et al. provides evidence for the contribution of δ opioid receptors (DOP), but not μ (MOP) or κ (KOP) opioid receptors, in the anti-allodynic effect of β2-mimetics, specifically Terbutaline and Formoterol, in the cuff model of neuropathic pain (Kremer et al., 2020). Formoterol alleviation of mechanical allodynia requires DOPs expressed in Nav1.8+ neuronal cells (Ceredig et al., 2019). Furthermore, DOP antagonist naltrindole blocks the analgesic effect of β2-AR agonists when chronically administrated (Choucair-Jaafar et al., 2014; Yalcin et al., 2010). However, the precise mechanism underlying the link between DOPs and β2-ARs remains unclear. Although there are some controversies regarding the expression of opioid receptors in microglia and astrocytes (Corder et al., 2017; Machelska & Celik, 2020; Sypek et al., 2021), microglia do not present DOP on their membrane, which precludes direct molecular interactions (Mika et al., 2014; Sypek et al., 2021). However, it is standard knowledge that NE in the spinal cord promotes the release of enkephalins from spinal interneurons independently from microglia, which block spinal transmission of nociceptive information via both presynaptic and postsynaptic receptors (i.e. on primary afferent terminals and spinal neurons).

The pleiotropic cytokine TNF-α mediates pro-inflammatory signaling and it is upregulated in maladaptive conditions, including chronic pain (Maguire et al., 2021), and Formoterol exerts its anti-inflammatory action also reducing TNF-α increased expression in neuropathic pain states (Bohren et al., 2013). However, another class of drugs used in neuropathic pain treatment, gabapentinoids, decreases the levels of TNF-α without the involvement of opioid receptors in their anti-neuroinflammatory and analgesic effects (Kremer, Yalcin, et al., 2016). Therefore, the anti-neuroinflammatory effect and the requirement of DOP activity may be

independent. Testing the efficacy of DOP agonist on the *Cx3cr1-CreERT2*; *Adrb2*$^{fl/fl}$ mouse line can reveal the independence of the microglia β2-AR from the DOP receptor, and possibly offer a safer approach to alleviate neuropathic pain with fewer side effects than general β2-AR agonists (including headache and palpitations).

5.5 From bench to bedside: challenges in translation to the clinic

5.5.1 β2-ARs as therapeutic targets in patients suffering from neuropathic pain

β2-AR agonists including Formoterol, are FDA-approved for the management of respiratory diseases such as asthma and COPD, including chronic bronchitis and emphysema, and they have also been investigated as potential analgesics in preclinical studies (Baker et al., 2015; Bravo et al., 2019). However, none of these drugs have been specifically developed for the treatment of neuropathic pain.

In prior studies, Terbutaline was used at doses typically prescribed clinically for asthmatic patients, and in mice, the chronic treatment of Terbutaline had no significant impact on various cardiac parameters (Choucair-Jaafar et al., 2011). In this work, Formoterol acted through the microglial β2-AR and it was administered at a dose of 0.05 mg/kg. Nonetheless, the β2-AR agonist relieved mechanical and thermal hypersensitivity soon after neuropathic pain was induced. The therapeutic effect observed at these low doses suggests that β2-mimetics may offer an alternative to the current drugs for the relief of neuropathic pain and give an indication for the dosing regimen in patients. This potential is supported by a case study reporting relief of pain symptoms with β2-AR agonist Salbutamol used for 1 month at a dose usually prescribed against asthma in 6 patients with pharmaco-resistant neuropathic pain (Cok et al., 2010). Further confirmation in randomized, controlled, and blind studies are required. Another clinical trial evaluating the analgesic effect of Terbutaline in post-thoracotomy neuropathic pain (Betapain) is terminated without available results due to the difficulty of recruitment (NCT01582646; https://clinicaltrials.gov). Besides, the same β2-agonist does not have a pain-relieving effect in patients with painful polyneuropathy (Gillving et al., 2021). The discrepancy between the two clinical studies might reflect on the procedure of evaluating mechanical nociception. Animal studies typically evaluate the effect of drugs using limb withdrawal measures (Rice et al., 2018), which only reflect the evoked pain component, and may not be suitable for patients with polyneuropathy characterized by sensory loss. Additional studies testing emotional components of pain are therefore required.

Together with pre-clinical findings and case reports, these data support the interest in clinically testing β2-agonists as an alternative to treat neuropathic pain.

β-blockers are commonly used to treat conditions like hypertension, chest pain (angina), and arrhythmias (Grandi & Ripplinger, 2019; Nedoshivin et al., 2022; Weir, 2009). Different drugs from this class have been shown to suppress experimental nociception, including inhibition of the nociceptive response induced by formalin (Davidson et al., 2001; Favaro-Moreira et al., 2012) or acute mechanical stimulus in rats (Chen et al., 2012). Moreover, β-blockers can be effective in treating certain pain states, such as migraine headaches (C. Fumagalli et al., 2020), but their use is often limited by their partial, non-specific blocking of both β1-ARs (found mainly in the heart) and β2-ARs (found in the lungs and blood vessels), which can lead to unwanted side effects, such as bradycardia, bronchoconstriction, and hypotension. Therefore, β-blockers are usually reserved for patients who do not respond to other pain medications.

Furthermore, non-synonymous single nucleotide polymorphisms (nsSNPs) in the *Adrb2* gene can alter the function and signaling pathway of the receptor in a cell type-specific manner and may predispose to chronic pain development at a population level (Hocking et al., 2010). For instance, particular *Adrb2* haplotypes are crucial for certain chronic pain conditions, including sickle cell disease (Jhun et al., 2019), temporomandibular disorder (Diatchenko et al., 2006), and fibromyalgia as seen in a small case-control study of Mexican and Spanish patients (Vargas-Alarcon et al., 2009). Understanding the cell-specific signaling and impact of nsSNPs in β2-AR regulation may have implications for personalized medicine and the development of therapeutic strategies regarding the β2-AR.

Taken together, β2-AR agonists and antagonists may have potential as novel treatments for neuropathic pain, either alone, in combination or associated with existing therapies. However, further research is needed to better understand the mechanisms underlying the analgesic effects of β2-AR modulators on neuropathic pain, to identify the patient populations that may benefit the most from these treatments, and to confirm their efficacy and safety. Given the high burden of neuropathic pain and the limited number of effective treatments, further investigation into the use of β2-AR modulators is warranted.

5.5.2 β2-AR involvement in the currently prescribed treatment of neuropathic pain

Table 1 summarizes the current pharmacological interventions for the treatment of neuropathic pain. Amitriptyline and Duloxetine efficacy likely involve the descending noradrenergic inhibitory system increasing the concentration of NE in the spinal cord (Ito et al., 2018; Wright & Rizzolo, 2017) and preclinical studies highlight the contribution of ARs in their analgesic effect. In conditions of neuropathic pain, the analgesic effect of Amitriptyline is lost in mice lacking α2-ARs (Ozdogan et al., 2004), and the beneficial impact of Duloxetine is reversed by

intrathecal injection of Yohimbine, an α2-AR antagonist (Ito et al., 2018). Additionally, these antidepressants-mediated mechanical hyperalgesia alleviation is abrogated in mice lacking β2-ARs (Kremer et al., 2018).

Reboxetine, a selective noradrenaline reuptake inhibitor (sNRI), has been indicated as a potential treatment for fibromyalgia and whereas its efficacy is based mostly on case reports (Krell et al., 2005), Esreboxetine, its enantiomer, reduces pain in a randomized, double-blind, placebo-controlled trial (Arnold et al., 2012). In preclinical studies using the cuff model of neuropathic pain, chronic treatment with Reboxetine failed to produce analgesia in mice lacking β2-ARs or during co-administration with the β2-AR antagonist ICI 118,551, but not with Yohimbine (Yalcin et al., 2009). However, in another animal model, the tibial nerve transection, the anti-allodynic effect of intrathecal Reboxetine was inhibited by prior administration of Yohimbine, but not by Propranolol (β-AR antagonist) or Prazosin (α1-AR antagonist) application (Hughes et al., 2015). Furthermore, Reboxetine chronic treatment improved the hyperalgesic and allodynic responses secondary to diabetes mellitus via β2-ARs, D1-, D2/D3-dopaminergic receptors, and DOPs pharmacological mechanisms (Turan Yucel et al., 2020). The β2-ARs are also involved in the beneficial mechanism of other treatments as β-AR antagonists modulate the ability of opioids and NSAIDs to alleviate nociception in neuropathic pain models (Bravo et al., 2019).

Thus, considering that β2-ARs are implicated in the efficacy of current treatments for pain management, it would be valuable to explore the extent to which microglial β2-AR are involved in these processes.

5.5.3 Future directions

The work of this thesis leads to several intriguing findings and hypotheses for the exploration of the anti-allodynic effects of β2-AR agonist Formoterol. The involvement of microglial β2-AR in the analgesic and anti-inflammatory effects of Formoterol has been shown through the use of the *Cx3cr1-CreERT2; Adrb2*$^{-/-}$ mouse line. Additionally, the study has determined the optimal timeframe for the β2-AR agonist application. Further studies are needed to understand the possible interactions of microglial β2-AR with other receptors and the microglial β2-AR-dependency of drugs that are already employed for neuropathic pain treatment. Previous studies targeting microglia in neuropathic pain brought ambivalent results, likely due to the lack of specificity and possible sex dimorphism. Here, the microglial β2-AR is proposed as a specific target for the development of more specific drugs with fewer aversive effects in future preclinical studies and clinical trials.

6. Conclusion

The study of β2-ARs contribution in alleviating neuropathic pain in mice reveals that the analgesic benefits of Formoterol were mainly attributed to microglia, modulating nerve injury-induced morphological changes and functional activation.

In conclusion,

1. Neuropathic pain modulates the expression of spinal microglial β2-ARs.
2. Formoterol inhibits the stimulus-evoked and spontaneous pain-associated behaviors both in early times and when neuropathic pain is established.
3. Formoterol suppresses the release of pro-inflammatory mediators from primary microglia and reactive-microglia phenotype *in vivo*, with sexual dimorphism in the late phase of neuropathic pain.
4. Formoterol acts on astrocytes, reducing their reactivity three weeks after SNI surgery, unrelated to β2-AR signaling in microglia.
5. The analgesic effect of Formoterol on stimulus-evoked behaviors shows no apparent sex dependency, whereas on ongoing pain it indicates the presence of sexual dimorphism.
6. The specific deletion of β2-ARs on microglia impacts the analgesic and microglial anti-inflammatory outcomes of Formoterol.

Overall, this study sheds new light on the potential use of β2-AR agonists for the management of neuropathic pain by elucidating the role of microglia in this process.

7. References

Abbott, N. J., Ronnback, L., & Hansson, E. (2006). Astrocyte-endothelial interactions at the blood-brain barrier. *Nat Rev Neurosci*, *7*(1), 41-53. https://doi.org/10.1038/nrn1824

Abdelmotilib, H., & West, A. B. (2017). Breathing new life into an old target: pulmonary disease drugs for Parkinson's disease therapy. *Genome Med*, *9*(1), 88. https://doi.org/10.1186/s13073-017-0483-4

Abosamak, N. R., & Shahin, M. H. (2022). Beta 2 Receptor Agonists/Antagonists. In *StatPearls*. https://www.ncbi.nlm.nih.gov/pubmed/32644495

Abrahamsen, B., Zhao, J., Asante, C. O., Cendan, C. M., Marsh, S., Martinez-Barbera, J. P., Nassar, M. A., Dickenson, A. H., & Wood, J. N. (2008). The cell and molecular basis of mechanical, cold, and inflammatory pain. *Science*, *321*(5889), 702-705. https://doi.org/10.1126/science.1156916

Aby, F., Lorenzo, L. E., Grivet, Z., Bouali-Benazzouz, R., Martin, H., Valerio, S., Whitestone, S., Isabel, D., Idi, W., Bouchatta, O., De Deurwaerdere, P., Godin, A. G., Herry, C., Fioramonti, X., Landry, M., De Koninck, Y., & Fossat, P. (2022). Switch of serotonergic descending inhibition into facilitation by a spinal chloride imbalance in neuropathic pain. *Sci Adv*, *8*(30), eabo0689. https://doi.org/10.1126/sciadv.abo0689

Agac, D., Estrada, L. D., Maples, R., Hooper, L. V., & Farrar, J. D. (2018). The beta2-adrenergic receptor controls inflammation by driving rapid IL-10 secretion. *Brain Behav Immun*, *74*, 176-185. https://doi.org/10.1016/j.bbi.2018.09.004

Ahlquist, R. P. (1948). A study of the adrenotropic receptors. *Am J Physiol*, *153*(3), 586-600. https://doi.org/10.1152/ajplegacy.1948.153.3.586

Alba-Delgado, C., Mountadem, S., Mermet-Joret, N., Monconduit, L., Dallel, R., Artola, A., & Antri, M. (2018). 5-HT(2A) Receptor-Induced Morphological Reorganization of PKCgamma-Expressing Interneurons Gates Inflammatory Mechanical Allodynia in Rat. *J Neurosci*, *38*(49), 10489-10504. https://doi.org/10.1523/JNEUROSCI.1294-18.2018

Allahyari, R. V., Heinsinger, N. M., Hwang, D., Jaffe, D. A., Rasouli, J., Shiers, S., Thomas, S. J., Price, T. J., Rostami, A., & Lepore, A. C. (2022). Response of Astrocyte Subpopulations Following Spinal Cord Injury. *Cells*, *11*(4). https://doi.org/10.3390/cells11040721

Alvarez, J. I., Katayama, T., & Prat, A. (2013). Glial influence on the blood brain barrier. *Glia*, *61*(12), 1939-1958. https://doi.org/10.1002/glia.22575

Anand, P., & Bley, K. (2011). Topical capsaicin for pain management: therapeutic potential and mechanisms of action of the new high-concentration capsaicin 8% patch. *Br J Anaesth*, *107*(4), 490-502. https://doi.org/10.1093/bja/aer260

Anand, P., Privitera, R., Donatien, P., Fadavi, H., Tesfaye, S., Bravis, V., & Misra, V. P. (2022). Reversing painful and non-painful diabetic neuropathy with the capsaicin 8% patch: Clinical evidence for pain relief and restoration of function via nerve fiber regeneration. *Front Neurol*, *13*, 998904. https://doi.org/10.3389/fneur.2022.998904

Andrew, D. (2009). Sensitization of lamina I spinoparabrachial neurons parallels heat hyperalgesia in the chronic constriction injury model of neuropathic pain. *J Physiol*, *587*(Pt 9), 2005-2017. https://doi.org/10.1113/jphysiol.2009.170290

Antal, M., Petko, M., Polgar, E., Heizmann, C. W., & Storm-Mathisen, J. (1996). Direct evidence of an extensive GABAergic innervation of the spinal dorsal horn by fibres descending from the rostral ventromedial medulla. *Neuroscience*, *73*(2), 509-518. https://doi.org/10.1016/0306-4522(96)00063-2

Arcourt, A., & Lechner, S. G. (2015). Peripheral and spinal circuits involved in mechanical allodynia. *Pain*, *156*(2), 220-221. https://doi.org/10.1097/01.j.pain.0000460818.62406.38

Arnold, L. M., Hirsch, I., Sanders, P., Ellis, A., & Hughes, B. (2012). Safety and efficacy of esreboxetine in patients with fibromyalgia: a fourteen-week, randomized, double-blind, placebo-controlled, multicenter clinical trial. *Arthritis Rheum*, *64*(7), 2387-2397. https://doi.org/10.1002/art.34390

Arora, V., Morado-Urbina, C. E., Gwak, Y. S., Parker, R. A., Kittel, C. A., Munoz-Islas, E., Miguel Jimenez-Andrade, J., Romero-Sandoval, E. A., Eisenach, J. C., & Peters, C. M. (2021). Systemic administration of a beta2-adrenergic receptor agonist reduces mechanical allodynia and suppresses the immune response to surgery in a rat model of persistent post-incisional hypersensitivity. *Mol Pain*, *17*, 1744806921997206. https://doi.org/10.1177/1744806921997206

Auffray, C., Fogg, D., Garfa, M., Elain, G., Join-Lambert, O., Kayal, S., Sarnacki, S., Cumano, A., Lauvau, G., & Geissmann, F. (2007). Monitoring of blood vessels and tissues by a population of monocytes with patrolling behavior. *Science*, *317*(5838), 666-670. https://doi.org/10.1126/science.1142883

Avraham, O., Feng, R., Ewan, E. E., Rustenhoven, J., Zhao, G., & Cavalli, V. (2021). Profiling sensory neuron microenvironment after peripheral and central axon injury reveals key pathways for neural repair. *Elife*, *10*. https://doi.org/10.7554/eLife.68457

Azzi, M., Charest, P. G., Angers, S., Rousseau, G., Kohout, T., Bouvier, M., & Pineyro, G. (2003). Beta-arrestin-mediated activation of MAPK by inverse agonists reveals distinct active conformations for G protein-coupled receptors. *Proc Natl Acad Sci U S A*, *100*(20), 11406-11411. https://doi.org/10.1073/pnas.1936664100

Bacou, E., Haurogne, K., Allard, M., Mignot, G., Bach, J. M., Herve, J., & Lieubeau, B. (2017). beta2-adrenoreceptor stimulation dampens the LPS-induced M1 polarization in pig macrophages. *Dev Comp Immunol*, *76*, 169-176. https://doi.org/10.1016/j.dci.2017.06.007

Bahari, Z., & Meftahi, G. H. (2019). Spinal alpha2 -adrenoceptors and neuropathic pain modulation; therapeutic target. *Br J Pharmacol*, *176*(14), 2366-2381. https://doi.org/10.1111/bph.14580

Baker, J. G., Proudman, R. G., & Hill, S. J. (2015). Salmeterol's extreme beta2 selectivity is due to residues in both extracellular loops and transmembrane domains. *Mol Pharmacol*, *87*(1), 103-120. https://doi.org/10.1124/mol.114.095364

Baliki, M. N., Petre, B., Torbey, S., Herrmann, K. M., Huang, L., Schnitzer, T. J., Fields, H. L., & Apkarian, A. V. (2012). Corticostriatal functional connectivity predicts transition to chronic back pain. *Nat Neurosci*, *15*(8), 1117-1119. https://doi.org/10.1038/nn.3153

Bantel, C., Eisenach, J. C., Duflo, F., Tobin, J. R., & Childers, S. R. (2005). Spinal nerve ligation increases alpha2-adrenergic receptor G-protein coupling in the spinal cord. *Brain Res*, *1038*(1), 76-82. https://doi.org/10.1016/j.brainres.2005.01.016

Baraka, A. M., Darwish, I. E., Ghoneim, M. T., & Korayem, H. K. (2015). beta2-Adrenoceptor agonists as potential therapeutic drugs in diabetic peripheral neuropathy. *Eur J Pharmacol*, *746*, 89-95. https://doi.org/10.1016/j.ejphar.2014.11.004

Barisione, G., Baroffio, M., Crimi, E., & Brusasco, V. (2010). Beta-Adrenergic Agonists. *Pharmaceuticals (Basel)*, *3*(4), 1016-1044. https://doi.org/10.3390/ph3041016

Barnes, P. J. (1993). Beta-adrenoceptors on smooth muscle, nerves and inflammatory cells. *Life Sci*, *52*(26), 2101-2109. https://doi.org/10.1016/0024-3205(93)90725-i

Baron, R., Binder, A., & Wasner, G. (2010). Neuropathic pain: diagnosis, pathophysiological mechanisms, and treatment. *Lancet Neurol*, *9*(8), 807-819. https://doi.org/10.1016/S1474-4422(10)70143-5

Basbaum, A. I., Bautista, D. M., Scherrer, G., & Julius, D. (2009). Cellular and molecular mechanisms of pain. *Cell*, *139*(2), 267-284. https://doi.org/10.1016/j.cell.2009.09.028

Batti, L., Sundukova, M., Murana, E., Pimpinella, S., De Castro Reis, F., Pagani, F., Wang, H., Pellegrino, E., Perlas, E., Di Angelantonio, S., Ragozzino, D., & Heppenstall, P. A. (2016). TMEM16F Regulates Spinal Microglial Function in Neuropathic Pain States. *Cell Rep*, *15*(12), 2608-2615. https://doi.org/10.1016/j.celrep.2016.05.039

Benbouzid, M., Pallage, V., Rajalu, M., Waltisperger, E., Doridot, S., Poisbeau, P., Freund-Mercier, M. J., & Barrot, M. (2008). Sciatic nerve cuffing in mice: a model of sustained neuropathic pain. *Eur J Pain*, *12*(5), 591-599. https://doi.org/10.1016/j.ejpain.2007.10.002

Benfante, A., Basile, M., Battaglia, S., Spatafora, M., & Scichilone, N. (2016). Use of ICS/LABA (extra-fine and non-extra-fine) in elderly asthmatics. *Ther Clin Risk Manag*, *12*, 1553-1562. https://doi.org/10.2147/TCRM.S103709

Bennett, G. J., & Xie, Y. K. (1988). A peripheral mononeuropathy in rat that produces disorders of pain sensation like those seen in man. *Pain*, *33*(1), 87-107. https://doi.org/10.1016/0304-3959(88)90209-6

Bohlen, C. J., Bennett, F. C., Tucker, A. F., Collins, H. Y., Mulinyawe, S. B., & Barres, B. A. (2017). Diverse Requirements for Microglial Survival, Specification, and Function Revealed by Defined-Medium Cultures. *Neuron*, *94*(4), 759-773.e758. https://doi.org/10.1016/j.neuron.2017.04.043

Bohn, L. M., Xu, F., Gainetdinov, R. R., & Caron, M. G. (2000). Potentiated opioid analgesia in norepinephrine transporter knock-out mice. *J Neurosci*, *20*(24), 9040-9045. https://doi.org/10.1523/JNEUROSCI.20-24-09040.2000

Bohren, Y., Tessier, L. H., Megat, S., Petitjean, H., Hugel, S., Daniel, D., Kremer, M., Fournel, S., Hein, L., Schlichter, R., Freund-Mercier, M. J., Yalcin, I., & Barrot, M. (2013). Antidepressants

suppress neuropathic pain by a peripheral beta2-adrenoceptor mediated anti-TNFalpha mechanism. *Neurobiol Dis*, *60*, 39-50. https://doi.org/10.1016/j.nbd.2013.08.012
Bourquin, A. F., Suveges, M., Pertin, M., Gilliard, N., Sardy, S., Davison, A. C., Spahn, D. R., & Decosterd, I. (2006). Assessment and analysis of mechanical allodynia-like behavior induced by spared nerve injury (SNI) in the mouse. *Pain*, *122*(1-2), 14 e11-14. https://doi.org/10.1016/j.pain.2005.10.036
Braga, M. F., Aroniadou-Anderjaska, V., Manion, S. T., Hough, C. J., & Li, H. (2004). Stress impairs alpha(1A) adrenoceptor-mediated noradrenergic facilitation of GABAergic transmission in the basolateral amygdala. *Neuropsychopharmacology*, *29*(1), 45-58. https://doi.org/10.1038/sj.npp.1300297
Bravo, L., Llorca-Torralba, M., Berrocoso, E., & Micó, J. A. (2019). Monoamines as Drug Targets in Chronic Pain: Focusing on Neuropathic Pain. *Front Neurosci*, *13*, 1268. https://doi.org/10.3389/fnins.2019.01268
Brodin, E., Ernberg, M., Olgart, L. (2016). Neurobiology: General considerations - from acute to chronic pain. *Nor Tannlegeforen Tid*, *126*, 28-33. https://doi.org/10.56373/2016-1-6
Bylund, D. B., Eikenberg, D. C., Hieble, J. P., Langer, S. Z., Lefkowitz, R. J., Minneman, K. P., Molinoff, P. B., Ruffolo, R. R., Jr., & Trendelenburg, U. (1994). International Union of Pharmacology nomenclature of adrenoceptors. *Pharmacol Rev*, *46*(2), 121-136. https://www.ncbi.nlm.nih.gov/pubmed/7938162
Caraci, F., Merlo, S., Drago, F., Caruso, G., Parenti, C., & Sortino, M. A. (2019). Rescue of Noradrenergic System as a Novel Pharmacological Strategy in the Treatment of Chronic Pain: Focus on Microglia Activation. *Front Pharmacol*, *10*, 1024. https://doi.org/10.3389/fphar.2019.01024
Cavalli, E., Mammana, S., Nicoletti, F., Bramanti, P., & Mazzon, E. (2019). The neuropathic pain: An overview of the current treatment and future therapeutic approaches. *Int J Immunopathol Pharmacol*, *33*, 2058738419838383. https://doi.org/10.1177/2058738419838383
Cazzola, M., Imperatore, F., Salzillo, A., Di Perna, F., Calderaro, F., Imperatore, A., & Matera, M. G. (1998). Cardiac effects of formoterol and salmeterol in patients suffering from COPD with preexisting cardiac arrhythmias and hypoxemia. *Chest*, *114*(2), 411-415. https://doi.org/10.1378/chest.114.2.411
Ceredig, R. A., Pierre, F., Doridot, S., Alduntzin, U., Hener, P., Salvat, E., Yalcin, I., Gaveriaux-Ruff, C., Barrot, M., & Massotte, D. (2019). Peripheral Delta Opioid Receptors Mediate Formoterol Anti-allodynic Effect in a Mouse Model of Neuropathic Pain. *Front Mol Neurosci*, *12*, 324. https://doi.org/10.3389/fnmol.2019.00324
Chai, G. S., Wang, Y. Y., Yasheng, A., & Zhao, P. (2016). Beta 2-adrenergic receptor activation enhances neurogenesis in Alzheimer's disease mice. *Neural Regen Res*, *11*(10), 1617-1624. https://doi.org/10.4103/1673-5374.193241
Chen, G., Luo, X., Qadri, M. Y., Berta, T., & Ji, R. R. (2018). Sex-Dependent Glial Signaling in Pathological Pain: Distinct Roles of Spinal Microglia and Astrocytes. *Neurosci Bull*, *34*(1), 98-108. https://doi.org/10.1007/s12264-017-0145-y
Chen, G., Park, C. K., Xie, R. G., Berta, T., Nedergaard, M., & Ji, R. R. (2014). Connexin-43 induces chemokine release from spinal cord astrocytes to maintain late-phase neuropathic pain in mice. *Brain*, *137*(Pt 8), 2193-2209. https://doi.org/10.1093/brain/awu140
Chen, G., Zhang, Y. Q., Qadri, Y. J., Serhan, C. N., & Ji, R. R. (2018). Microglia in Pain: Detrimental and Protective Roles in Pathogenesis and Resolution of Pain. *Neuron*, *100*(6), 1292-1311. https://doi.org/10.1016/j.neuron.2018.11.009
Chen, N., Ge, M. M., Li, D. Y., Wang, X. M., Liu, D. Q., Ye, D. W., Tian, Y. K., Zhou, Y. Q., & Chen, J. P. (2021). beta2-adrenoreceptor agonist ameliorates mechanical allodynia in paclitaxel-induced neuropathic pain via induction of mitochondrial biogenesis. *Biomed Pharmacother*, *144*, 112331. https://doi.org/10.1016/j.biopha.2021.112331
Chen, S. R., Chen, H., Yuan, W. X., & Pan, H. L. (2011). Increased presynaptic and postsynaptic alpha2-adrenoceptor activity in the spinal dorsal horn in painful diabetic neuropathy. *J Pharmacol Exp Ther*, *337*(1), 285-292. https://doi.org/10.1124/jpet.110.176586
Chen, Y. W., Chu, C. C., Chen, Y. C., Hung, C. H., & Wang, J. J. (2012). Propranolol elicits cutaneous analgesia against skin nociceptive stimuli in rats. *Neurosci Lett*, *524*(2), 129-132. https://doi.org/10.1016/j.neulet.2012.07.036
Chen, Z., Doyle, T. M., Luongo, L., Largent-Milnes, T. M., Giancotti, L. A., Kolar, G., Squillace, S., Boccella, S., Walker, J. K., Pendleton, A., Spiegel, S., Neumann, W. L., Vanderah, T. W., & Salvemini, D. (2019). Sphingosine-1-phosphate receptor 1 activation in astrocytes contributes

to neuropathic pain. *Proc Natl Acad Sci U S A*, *116*(21), 10557-10562. https://doi.org/10.1073/pnas.1820466116

Cherezov, V., Rosenbaum, D. M., Hanson, M. A., Rasmussen, S. G., Thian, F. S., Kobilka, T. S., Choi, H. J., Kuhn, P., Weis, W. I., Kobilka, B. K., & Stevens, R. C. (2007). High-resolution crystal structure of an engineered human beta2-adrenergic G protein-coupled receptor. *Science*, *318*(5854), 1258-1265. https://doi.org/10.1126/science.1150577

Choucair-Jaafar, N., Beetz, N., Gilsbach, R., Yalcin, I., Waltisperger, E., Freund-Mercier, M. J., Monassier, L., Hein, L., & Barrot, M. (2011). Cardiovascular effects of chronic treatment with a beta2-adrenoceptor agonist relieving neuropathic pain in mice. *Neuropharmacology*, *61*(1-2), 51-60. https://doi.org/10.1016/j.neuropharm.2011.02.015

Choucair-Jaafar, N., Salvat, E., Freund-Mercier, M. J., & Barrot, M. (2014). The antiallodynic action of nortriptyline and terbutaline is mediated by beta(2) adrenoceptors and delta opioid receptors in the ob/ob model of diabetic polyneuropathy. *Brain Res*, *1546*, 18-26. https://doi.org/10.1016/j.brainres.2013.12.016

Choucair-Jaafar, N., Yalcin, I., Rodeau, J. L., Waltisperger, E., Freund-Mercier, M. J., & Barrot, M. (2009). Beta2-adrenoceptor agonists alleviate neuropathic allodynia in mice after chronic treatment. *Br J Pharmacol*, *158*(7), 1683-1694. https://doi.org/10.1111/j.1476-5381.2009.00510.x

Cichon, J., Sun, L., & Yang, G. (2018). Spared Nerve Injury Model of Neuropathic Pain in Mice. *Bio Protoc*, *8*(6). https://doi.org/10.21769/bioprotoc.2777

Cobos, E. J., Nickerson, C. A., Gao, F., Chandran, V., Bravo-Caparros, I., Gonzalez-Cano, R., Riva, P., Andrews, N. A., Latremoliere, A., Seehus, C. R., Perazzoli, G., Nieto, F. R., Joller, N., Painter, M. W., Ma, C. H. E., Omura, T., Chesler, E. J., Geschwind, D. H., Coppola, G., . . . Costigan, M. (2018). Mechanistic Differences in Neuropathic Pain Modalities Revealed by Correlating Behavior with Global Expression Profiling. *Cell Rep*, *22*(5), 1301-1312. https://doi.org/10.1016/j.celrep.2018.01.006

Cok, O. Y., Eker, H. E., Yalcin, I., Barrot, M., & Aribogan, A. (2010). Is there a place for beta-mimetics in clinical management of neuropathic pain? Salbutamol therapy in six cases. *Anesthesiology*, *112*(5), 1276-1279. https://doi.org/10.1097/ALN.0b013e3181d40399

Colloca, L., Ludman, T., Bouhassira, D., Baron, R., Dickenson, A. H., Yarnitsky, D., Freeman, R., Truini, A., Attal, N., Finnerup, N. B., Eccleston, C., Kalso, E., Bennett, D. L., Dworkin, R. H., & Raja, S. N. (2017). Neuropathic pain. *Nat Rev Dis Primers*, *3*, 17002. https://doi.org/10.1038/nrdp.2017.2

Corder, G., Tawfik, V. L., Wang, D., Sypek, E. I., Low, S. A., Dickinson, J. R., Sotoudeh, C., Clark, J. D., Barres, B. A., Bohlen, C. J., & Scherrer, G. (2017). Loss of mu opioid receptor signaling in nociceptors, but not microglia, abrogates morphine tolerance without disrupting analgesia. *Nat Med*, *23*(2), 164-173. https://doi.org/10.1038/nm.4262

Costigan, M., Scholz, J., & Woolf, C. J. (2009). Neuropathic pain: a maladaptive response of the nervous system to damage. *Annu Rev Neurosci*, *32*, 1-32. https://doi.org/10.1146/annurev.neuro.051508.135531

Coull, J. A., Beggs, S., Boudreau, D., Boivin, D., Tsuda, M., Inoue, K., Gravel, C., Salter, M. W., & De Koninck, Y. (2005). BDNF from microglia causes the shift in neuronal anion gradient underlying neuropathic pain. *Nature*, *438*(7070), 1017-1021. https://doi.org/10.1038/nature04223

Courteix, C., Eschalier, A., & Lavarenne, J. (1993). Streptozocin-induced diabetic rats: behavioural evidence for a model of chronic pain. *Pain*, *53*(1), 81-88. https://doi.org/10.1016/0304-3959(93)90059-X

Cruccu, G., Aziz, T. Z., Garcia-Larrea, L., Hansson, P., Jensen, T. S., Lefaucheur, J. P., Simpson, B. A., & Taylor, R. S. (2007). EFNS guidelines on neurostimulation therapy for neuropathic pain. *Eur J Neurol*, *14*(9), 952-970. https://doi.org/10.1111/j.1468-1331.2007.01916.x

Curtin, C. M., Kenney, D., Suarez, P., Hentz, V. R., Hernandez-Boussard, T., Mackey, S., & Carroll, I. R. (2017). A Double-Blind Placebo Randomized Controlled Trial of Minocycline to Reduce Pain After Carpal Tunnel and Trigger Finger Release. *J Hand Surg Am*, *42*(3), 166-174. https://doi.org/10.1016/j.jhsa.2016.12.011

Damo, E. (2022). Glial cells as target for antidepressants in neuropathic pain. *Neuroforum*, *28*(2), 85-94. https://doi.org/10.1515/nf-2021-0036

Damo, E., Agarwal, A., & Simonetti, M. (2023). Activation of beta2-Adrenergic Receptors in Microglia Alleviates Neuropathic Hypersensitivity in Mice. *Cells*, *12*(2). https://doi.org/10.3390/cells12020284

Dang, V., Medina, B., Das, D., Moghadam, S., Martin, K. J., Lin, B., Naik, P., Patel, D., Nosheny, R., Wesson Ashford, J., & Salehi, A. (2014). Formoterol, a long-acting beta2 adrenergic agonist, improves cognitive function and promotes dendritic complexity in a mouse model of Down syndrome. *Biol Psychiatry*, *75*(3), 179-188. https://doi.org/10.1016/j.biopsych.2013.05.024

Davidson, E. M., Doursout, M. F., Szmuk, P., & Chelly, J. E. (2001). Antinociceptive and cardiovascular properties of esmolol following formalin injection in rats. *Can J Anaesth*, *48*(1), 59-64. https://doi.org/10.1007/BF03019816

de Geus, T. J., Franken, G., & Joosten, E. A. J. (2023). Spinal Cord Stimulation Paradigms and Pain Relief: A Preclinical Systematic Review on Modulation of the Central Inflammatory Response in Neuropathic Pain. *Neuromodulation*, *26*(1), 25-34. https://doi.org/10.1016/j.neurom.2022.04.049

De Luca, C., Virtuoso, A., Korai, S. A., Cirillo, R., Gargano, F., Papa, M., & Cirillo, G. (2022). Altered Spinal Homeostasis and Maladaptive Plasticity in GFAP Null Mice Following Peripheral Nerve Injury. *Cells*, *11*(7). https://doi.org/10.3390/cells11071224

de Quervain, D., Schwabe, L., & Roozendaal, B. (2017). Stress, glucocorticoids and memory: implications for treating fear-related disorders. *Nat Rev Neurosci*, *18*(1), 7-19. https://doi.org/10.1038/nrn.2016.155

Decosterd, I., & Woolf, C. J. (2000). Spared nerve injury: an animal model of persistent peripheral neuropathic pain. *Pain*, *87*(2), 149-158. https://doi.org/10.1016/S0304-3959(00)00276-1

Del Valle, L., Schwartzman, R. J., & Alexander, G. (2009). Spinal cord histopathological alterations in a patient with longstanding complex regional pain syndrome. *Brain Behav Immun*, *23*(1), 85-91. https://doi.org/10.1016/j.bbi.2008.08.004

Dello Russo, C., Boullerne, A. I., Gavrilyuk, V., & Feinstein, D. L. (2004). Inhibition of microglial inflammatory responses by norepinephrine: effects on nitric oxide and interleukin-1beta production. *J Neuroinflammation*, *1*(1), 9. https://doi.org/10.1186/1742-2094-1-9

Devor, M., Wall, P. D., & Catalan, N. (1992). Systemic lidocaine silences ectopic neuroma and DRG discharge without blocking nerve conduction. *Pain*, *48*(2), 261-268. https://doi.org/10.1016/0304-3959(92)90067-L

Diatchenko, L., Anderson, A. D., Slade, G. D., Fillingim, R. B., Shabalina, S. A., Higgins, T. J., Sama, S., Belfer, I., Goldman, D., Max, M. B., Weir, B. S., & Maixner, W. (2006). Three major haplotypes of the beta2 adrenergic receptor define psychological profile, blood pressure, and the risk for development of a common musculoskeletal pain disorder. *Am J Med Genet B Neuropsychiatr Genet*, *141B*(5), 449-462. https://doi.org/10.1002/ajmg.b.30324

Ding, F., O'Donnell, J., Thrane, A. S., Zeppenfeld, D., Kang, H., Xie, L., Wang, F., & Nedergaard, M. (2013). alpha1-Adrenergic receptors mediate coordinated Ca2+ signaling of cortical astrocytes in awake, behaving mice. *Cell Calcium*, *54*(6), 387-394. https://doi.org/10.1016/j.ceca.2013.09.001

Dixon, R. A., Kobilka, B. K., Strader, D. J., Benovic, J. L., Dohlman, H. G., Frielle, T., Bolanowski, M. A., Bennett, C. D., Rands, E., Diehl, R. E., Mumford, R. A., Slater, E. E., Sigal, I. S., Caron, M. G., Lefkowitz, R. J., & Strader, C. D. (1986). Cloning of the gene and cDNA for mammalian beta-adrenergic receptor and homology with rhodopsin. *Nature*, *321*(6065), 75-79. https://doi.org/10.1038/321075a0

Dixon, W. J. (1980). Efficient analysis of experimental observations. *Annu Rev Pharmacol Toxicol*, *20*, 441-462. https://doi.org/10.1146/annurev.pa.20.040180.002301

Dogrul, A., Ossipov, M. H., & Porreca, F. (2009). Differential mediation of descending pain facilitation and inhibition by spinal 5HT-3 and 5HT-7 receptors. *Brain Res*, *1280*, 52-59. https://doi.org/10.1016/j.brainres.2009.05.001

Doly, S., Fischer, J., Brisorgueil, M. J., Verge, D., & Conrath, M. (2005). Pre- and postsynaptic localization of the 5-HT7 receptor in rat dorsal spinal cord: immunocytochemical evidence. *J Comp Neurol*, *490*(3), 256-269. https://doi.org/10.1002/cne.20667

Donello, J. E., Guan, Y., Tian, M., Cheevers, C. V., Alcantara, M., Cabrera, S., Raja, S. N., & Gil, D. W. (2011). A peripheral adrenoceptor-mediated sympathetic mechanism can transform stress-induced analgesia into hyperalgesia. *Anesthesiology*, *114*(6), 1403-1416. https://doi.org/10.1097/ALN.0b013e31821c3878

Dong, J. H., Chen, X., Cui, M., Yu, X., Pang, Q., & Sun, J. P. (2012). beta2-adrenergic receptor and astrocyte glucose metabolism. *J Mol Neurosci*, *48*(2), 456-463. https://doi.org/10.1007/s12031-012-9742-4

Dong, J. H., Wang, Y. J., Cui, M., Wang, X. J., Zheng, W. S., Ma, M. L., Yang, F., He, D. F., Hu, Q. X., Zhang, D. L., Ning, S. L., Liu, C. H., Wang, C., Wang, Y., Li, X. Y., Yi, F., Lin, A., Kahsai, A. W., Cahill, T. J., 3rd, . . . Sun, J. P. (2017). Adaptive Activation of a Stress Response Pathway

Improves Learning and Memory Through Gs and beta-Arrestin-1-Regulated Lactate Metabolism. *Biol Psychiatry*, *81*(8), 654-670. https://doi.org/10.1016/j.biopsych.2016.09.025
Donnelly, C. R., Andriessen, A. S., Chen, G., Wang, K., Jiang, C., Maixner, W., & Ji, R. R. (2020). Central Nervous System Targets: Glial Cell Mechanisms in Chronic Pain. *Neurotherapeutics*, *17*(3), 846-860. https://doi.org/10.1007/s13311-020-00905-7
Donnelly, L. E., Tudhope, S. J., Fenwick, P. S., & Barnes, P. J. (2010). Effects of formoterol and salmeterol on cytokine release from monocyte-derived macrophages. *Eur Respir J*, *36*(1), 178-186. https://doi.org/10.1183/09031936.00158008
Eliav, E., Herzberg, U., Ruda, M. A., & Bennett, G. J. (1999). Neuropathic pain from an experimental neuritis of the rat sciatic nerve. *Pain*, *83*(2), 169-182. https://doi.org/10.1016/s0304-3959(99)00102-5
Estrada, L. D., Agac, D., & Farrar, J. D. (2016). Sympathetic neural signaling via the beta2-adrenergic receptor suppresses T-cell receptor-mediated human and mouse CD8(+) T-cell effector function. *Eur J Immunol*, *46*(8), 1948-1958. https://doi.org/10.1002/eji.201646395
Evans, A. K., Ardestani, P. M., Yi, B., Park, H. H., Lam, R. K., & Shamloo, M. (2020). Beta-adrenergic receptor antagonism is proinflammatory and exacerbates neuroinflammation in a mouse model of Alzheimer's Disease. *Neurobiol Dis*, *146*, 105089. https://doi.org/10.1016/j.nbd.2020.105089
Faulkner, J. R., Herrmann, J. E., Woo, M. J., Tansey, K. E., Doan, N. B., & Sofroniew, M. V. (2004). Reactive astrocytes protect tissue and preserve function after spinal cord injury. *J Neurosci*, *24*(9), 2143-2155. https://doi.org/10.1523/JNEUROSCI.3547-03.2004
Favaro-Moreira, N. C., Parada, C. A., & Tambeli, C. H. (2012). Blockade of beta(1)-, beta(2)- and beta(3)-adrenoceptors in the temporomandibular joint induces antinociception especially in female rats. *Eur J Pain*, *16*(9), 1302-1310. https://doi.org/10.1002/j.1532-2149.2012.00132.x
Feinstein, D. L., Kalinin, S., & Braun, D. (2016). Causes, consequences, and cures for neuroinflammation mediated via the locus coeruleus: noradrenergic signaling system. *J Neurochem*, *139 Suppl 2*, 154-178. https://doi.org/10.1111/jnc.13447
Ferreira, N. R., Junqueira, Y. N., Correa, N. B., Fonseca, E. O., Brito, N. B. M., Menezes, T. A., Magini, M., Fidalgo, T. K. S., Ferreira, D., de Lima, R. L., Carvalho, A. C., & DosSantos, M. F. (2019). The efficacy of transcranial direct current stimulation and transcranial magnetic stimulation for chronic orofacial pain: A systematic review. *PLoS One*, *14*(8), e0221110. https://doi.org/10.1371/journal.pone.0221110
Fields, H. L., Bry, J., Hentall, I., & Zorman, G. (1983). The activity of neurons in the rostral medulla of the rat during withdrawal from noxious heat. *J Neurosci*, *3*(12), 2545-2552. https://doi.org/10.1523/JNEUROSCI.03-12-02545.1983
Finnerup, N. B. (2019). Nonnarcotic Methods of Pain Management. *N Engl J Med*, *380*(25), 2440-2448. https://doi.org/10.1056/NEJMra1807061
Finnerup, N. B., Attal, N., Haroutounian, S., McNicol, E., Baron, R., Dworkin, R. H., Gilron, I., Haanpää, M., Hansson, P., Jensen, T. S., Kamerman, P. R., Lund, K., Moore, A., Raja, S. N., Rice, A. S., Rowbotham, M., Sena, E., Siddall, P., Smith, B. H., & Wallace, M. (2015). Pharmacotherapy for neuropathic pain in adults: a systematic review and meta-analysis. *Lancet Neurol*, *14*(2), 162-173. https://doi.org/10.1016/S1474-4422(14)70251-0
Finnerup, N. B., Kuner, R., & Jensen, T. S. (2021). Neuropathic Pain: From Mechanisms to Treatment. *Physiol Rev*, *101*(1), 259-301. https://doi.org/10.1152/physrev.00045.2019
Finnerup, N. B., Sindrup, S. H., & Jensen, T. S. (2010). The evidence for pharmacological treatment of neuropathic pain. *Pain*, *150*(3), 573-581. https://doi.org/10.1016/j.pain.2010.06.019
Fiore, N. T., Debs, S. R., Hayes, J. P., Duffy, S. S., & Moalem-Taylor, G. (2023). Pain-resolving immune mechanisms in neuropathic pain. *Nat Rev Neurol*. https://doi.org/10.1038/s41582-023-00777-3
Fornasari, D. (2017). Pharmacotherapy for Neuropathic Pain: A Review. *Pain Ther*, *6*(Suppl 1), 25-33. https://doi.org/10.1007/s40122-017-0091-4
Freeman, M. R. (2010). Specification and morphogenesis of astrocytes. *Science*, *330*(6005), 774-778. https://doi.org/10.1126/science.1190928
Frieden, T. R. (2016). Foreword. *MMWR Suppl*, *65*(3), 1-3. https://doi.org/10.15585/mmwr.su6503a1
Fumagalli, C., Maurizi, N., Marchionni, N., & Fornasari, D. (2020). beta-blockers: Their new life from hypertension to cancer and migraine. *Pharmacol Res*, *151*, 104587. https://doi.org/10.1016/j.phrs.2019.104587
Fumagalli, G., Monza, L., Cavaletti, G., Rigolio, R., & Meregalli, C. (2020). Neuroinflammatory Process Involved in Different Preclinical Models of Chemotherapy-Induced Peripheral Neuropathy. *Front Immunol*, *11*, 626687. https://doi.org/10.3389/fimmu.2020.626687

Gao, V., Suzuki, A., Magistretti, P. J., Lengacher, S., Pollonini, G., Steinman, M. Q., & Alberini, C. M. (2016). Astrocytic beta2-adrenergic receptors mediate hippocampal long-term memory consolidation. *Proc Natl Acad Sci U S A*, *113*(30), 8526-8531. https://doi.org/10.1073/pnas.1605063113

Garcia, J. J., del Carmen Saez, M., De la Fuente, M., & Ortega, E. (2003a). Noradrenaline and its end metabolite 3-methoxy-4-hydroxyphenylglycol inhibit lymphocyte chemotaxis: role of alpha- and beta-adrenoreceptors. *Mol Cell Biochem*, *254*(1-2), 305-309. https://doi.org/10.1023/a:1027349904589

Garcia, J. J., del Carmen Saez, M., De la Fuente, M., & Ortega, E. (2003b). Regulation of phagocytic process of macrophages by noradrenaline and its end metabolite 4-hydroxy-3-metoxyphenyl-glycol. Role of alpha- and beta-adrenoreceptors. *Mol Cell Biochem*, *254*(1-2), 299-304. https://doi.org/10.1023/a:1027345820519

Garrison, C. J., Dougherty, P. M., Kajander, K. C., & Carlton, S. M. (1991). Staining of glial fibrillary acidic protein (GFAP) in lumbar spinal cord increases following a sciatic nerve constriction injury. *Brain research*, *565*(1), 1-7. https://doi.org/10.1016/0006-8993(91)91729-K

Geissmann, F., Jung, S., & Littman, D. R. (2003). Blood monocytes consist of two principal subsets with distinct migratory properties. *Immunity*, *19*(1), 71-82. https://doi.org/10.1016/s1074-7613(03)00174-2

Gensel, J. C., Donahue, R. R., Bailey, W. M., & Taylor, B. K. (2019). Sexual Dimorphism of Pain Control: Analgesic Effects of Pioglitazone and Azithromycin in Chronic Spinal Cord Injury. *J Neurotrauma*, *36*(15), 2372-2376. https://doi.org/10.1089/neu.2018.6207

Ghazisaeidi, S., Muley, M. M., & Salter, M. W. (2023). Neuropathic Pain: Mechanisms, Sex Differences, and Potential Therapies for a Global Problem. *Annu Rev Pharmacol Toxicol*, *63*, 565-583. https://doi.org/10.1146/annurev-pharmtox-051421-112259

Gillving, M., Demant, D., Holbech, J. V., Gylfadottir, S. S., Bach, F. W., Jensen, T. S., Finnerup, N. B., & Sindrup, S. H. (2021). A randomized, controlled trial of a beta2-agonist in painful polyneuropathy. *Pain*, *162*(5), 1364-1373. https://doi.org/10.1097/j.pain.0000000000002140

Goldmann, T., Wieghofer, P., Muller, P. F., Wolf, Y., Varol, D., Yona, S., Brendecke, S. M., Kierdorf, K., Staszewski, O., Datta, M., Luedde, T., Heikenwalder, M., Jung, S., & Prinz, M. (2013). A new type of microglia gene targeting shows TAK1 to be pivotal in CNS autoimmune inflammation. *Nat Neurosci*, *16*(11), 1618-1626. https://doi.org/10.1038/nn.3531

Grace, P. M., Wang, X., Strand, K. A., Baratta, M. V., Zhang, Y., Galer, E. L., Yin, H., Maier, S. F., & Watkins, L. R. (2018). DREADDed microglia in pain: Implications for spinal inflammatory signaling in male rats. *Exp Neurol*, *304*, 125-131. https://doi.org/10.1016/j.expneurol.2018.03.005

Graham, R. M. (1990). Adrenergic receptors: structure and function. *Cleve Clin J Med*, *57*(5), 481-491. https://doi.org/10.3949/ccjm.57.5.481

Grailer, J. J., Haggadone, M. D., Sarma, J. V., Zetoune, F. S., & Ward, P. A. (2014). Induction of M2 regulatory macrophages through the beta2-adrenergic receptor with protection during endotoxemia and acute lung injury. *J Innate Immun*, *6*(5), 607-618. https://doi.org/10.1159/000358524

Grandi, E., & Ripplinger, C. M. (2019). Antiarrhythmic mechanisms of beta blocker therapy. *Pharmacol Res*, *146*, 104274. https://doi.org/10.1016/j.phrs.2019.104274

Gu, N., Eyo, U. B., Murugan, M., Peng, J., Matta, S., Dong, H., & Wu, L. J. (2016). Microglial P2Y12 receptors regulate microglial activation and surveillance during neuropathic pain. *Brain Behav Immun*, *55*, 82-92. https://doi.org/10.1016/j.bbi.2015.11.007

Gu, N., Peng, J., Murugan, M., Wang, X., Eyo, U. B., Sun, D., Ren, Y., DiCicco-Bloom, E., Young, W., Dong, H., & Wu, L. J. (2016). Spinal Microgliosis Due to Resident Microglial Proliferation Is Required for Pain Hypersensitivity after Peripheral Nerve Injury. *Cell Rep*, *16*(3), 605-614. https://doi.org/10.1016/j.celrep.2016.06.018

Guan, Z., Kuhn, J. A., Wang, X., Colquitt, B., Solorzano, C., Vaman, S., Guan, A. K., Evans-Reinsch, Z., Braz, J., Devor, M., Abboud-Werner, S. L., Lanier, L. L., Lomvardas, S., & Basbaum, A. I. (2016). Injured sensory neuron-derived CSF1 induces microglial proliferation and DAP12-dependent pain. *Nat Neurosci*, *19*(1), 94-101. https://doi.org/10.1038/nn.4189

Guida, F., De Gregorio, D., Palazzo, E., Ricciardi, F., Boccella, S., Belardo, C., Iannotta, M., Infantino, R., Formato, F., Marabese, I., Luongo, L., de Novellis, V., & Maione, S. (2020). Behavioral, Biochemical and Electrophysiological Changes in Spared Nerve Injury Model of Neuropathic Pain. *Int J Mol Sci*, *21*(9). https://doi.org/10.3390/ijms21093396

Guimaraes, R. M., Davoli-Ferreira, M., Fonseca, M. M., Damasceno, L. E. A., Santa-Cecilia, F. V., Kusuda, R., Menezes, G. B., Cunha, F. Q., Alves-Filho, J. C., & Cunha, T. M. (2019). Frontline

Science: Blood-circulating leukocytes fail to infiltrate the spinal cord parenchyma after spared nerve injury. *J Leukoc Biol*, *106*(3), 541-551. https://doi.org/10.1002/JLB.HI1118-458R
Guo, S., Song, Z., He, J., Yin, G., Zhu, J., Liu, H., Yang, L., Ji, X., Xu, X., Liu, Z., & Liu, J. (2022). Akt/Aquaporin-4 Signaling Aggravates Neuropathic Pain by Activating Astrocytes after Spinal Nerve Ligation in Rats. *Neuroscience*, *482*, 116-131. https://doi.org/10.1016/j.neuroscience.2021.12.015
Gyoneva, S., & Traynelis, S. F. (2013). Norepinephrine modulates the motility of resting and activated microglia via different adrenergic receptors. *J Biol Chem*, *288*(21), 15291-15302. https://doi.org/10.1074/jbc.M113.458901
Hansen, J. N., Bruckner, M., Pietrowski, M. J., Jikeli, J. F., Plescher, M., Beckert, H., Schnaars, M., Fulle, L., Reitmeier, K., Langmann, T., Forster, I., Boche, D., Petzold, G. C., & Halle, A. (2022). MotiQ: an open-source toolbox to quantify the cell motility and morphology of microglia. *Mol Biol Cell*, *33*(11), ar99. https://doi.org/10.1091/mbc.E21-11-0585
Hao, J. X., Blakeman, K. H., Yu, W., Hultenby, K., Xu, X. J., & Wiesenfeld-Hallin, Z. (2000). Development of a mouse model of neuropathic pain following photochemically induced ischemia in the sciatic nerve. *Exp Neurol*, *163*(1), 231-238. https://doi.org/10.1006/exnr.2000.7373
Harris, R. E., Napadow, V., Huggins, J. P., Pauer, L., Kim, J., Hampson, J., Sundgren, P. C., Foerster, B., Petrou, M., Schmidt-Wilcke, T., & Clauw, D. J. (2013). Pregabalin rectifies aberrant brain chemistry, connectivity, and functional response in chronic pain patients. *Anesthesiology*, *119*(6), 1453-1464. https://doi.org/10.1097/ALN.0000000000000017
Hashizume, H., Rutkowski, M. D., Weinstein, J. N., & DeLeo, J. A. (2000). Central administration of methotrexate reduces mechanical allodynia in an animal model of radiculopathy/sciatica. *Pain*, *87*(2), 159-169. https://doi.org/10.1016/S0304-3959(00)00281-5
Hathway, G. J., Vega-Avelaira, D., Moss, A., Ingram, R., & Fitzgerald, M. (2009). Brief, low frequency stimulation of rat peripheral C-fibres evokes prolonged microglial-induced central sensitization in adults but not in neonates. *Pain*, *144*(1-2), 110-118. https://doi.org/10.1016/j.pain.2009.03.022
Hayashida, K., & Eisenach, J. C. (2010). Spinal alpha 2-adrenoceptor-mediated analgesia in neuropathic pain reflects brain-derived nerve growth factor and changes in spinal cholinergic neuronal function. *Anesthesiology*, *113*(2), 406-412. https://doi.org/10.1097/ALN.0b013e3181de6d2c
Hayashida, K., Peters, C. M., Gutierrez, S., & Eisenach, J. C. (2012). Depletion of endogenous noradrenaline does not prevent spinal cord plasticity following peripheral nerve injury. *J Pain*, *13*(1), 49-57. https://doi.org/10.1016/j.jpain.2011.09.009
Hayashida, K. I., Clayton, B. A., Johnson, J. E., & Eisenach, J. C. (2008). Brain derived nerve growth factor induces spinal noradrenergic fiber sprouting and enhances clonidine analgesia following nerve injury in rats. *Pain*, *136*(3), 348-355. https://doi.org/10.1016/j.pain.2007.07.014
Hayden, M. S., & Ghosh, S. (2012). NF-kappaB, the first quarter-century: remarkable progress and outstanding questions. *Genes Dev*, *26*(3), 203-234. https://doi.org/10.1101/gad.183434.111
Hebert, H. L., Veluchamy, A., Baskozos, G., Fardo, F., Van Ryckeghem, D. M. L., Pascal, M. M. V., Jones, C., Milburn, K., Pearson, E. R., Crombez, G., Bennett, D. L. H., Meng, W., Palmer, C. N. A., & Smith, B. H. (2021). Cohort profile: DOLORisk Dundee: a longitudinal study of chronic neuropathic pain. *BMJ Open*, *11*(5), e042887. https://doi.org/10.1136/bmjopen-2020-042887
Heinricher, M. M., Tavares, I., Leith, J. L., & Lumb, B. M. (2009). Descending control of nociception: Specificity, recruitment and plasticity. *Brain Res Rev*, *60*(1), 214-225. https://doi.org/10.1016/j.brainresrev.2008.12.009
Heneka, M. T., Nadrigny, F., Regen, T., Martinez-Hernandez, A., Dumitrescu-Ozimek, L., Terwel, D., Jardanhazi-Kurutz, D., Walter, J., Kirchhoff, F., Hanisch, U. K., & Kummer, M. P. (2010). Locus ceruleus controls Alzheimer's disease pathology by modulating microglial functions through norepinephrine. *Proc Natl Acad Sci U S A*, *107*(13), 6058-6063. https://doi.org/10.1073/pnas.0909586107
Hertz, L., Lovatt, D., Goldman, S. A., & Nedergaard, M. (2010). Adrenoceptors in brain: cellular gene expression and effects on astrocytic metabolism and [Ca(2+)]i. *Neurochem Int*, *57*(4), 411-420. https://doi.org/10.1016/j.neuint.2010.03.019
Hirschberg, S., Li, Y., Randall, A., Kremer, E. J., & Pickering, A. E. (2017). Functional dichotomy in spinal- vs prefrontal-projecting locus coeruleus modules splits descending noradrenergic analgesia from ascending aversion and anxiety in rats. *Elife*, *6*. https://doi.org/10.7554/eLife.29808

Hocking, L. J., Smith, B. H., Jones, G. T., Reid, D. M., Strachan, D. P., & Macfarlane, G. J. (2010). Genetic variation in the beta2-adrenergic receptor but not catecholamine-O-methyltransferase predisposes to chronic pain: results from the 1958 British Birth Cohort Study. *Pain*, *149*(1), 143-151. https://doi.org/10.1016/j.pain.2010.01.023

Howorth, P. W., Teschemacher, A. G., & Pickering, A. E. (2009). Retrograde adenoviral vector targeting of nociresponsive pontospinal noradrenergic neurons in the rat in vivo. *J Comp Neurol*, *512*(2), 141-157. https://doi.org/10.1002/cne.21879

Huang, E. Y., Liu, T. C., & Tao, P. L. (2003). Co-administration of dextromethorphan with morphine attenuates morphine rewarding effect and related dopamine releases at the nucleus accumbens. *Naunyn Schmiedebergs Arch Pharmacol*, *368*(5), 386-392. https://doi.org/10.1007/s00210-003-0803-7

Hughes, S., Hickey, L., Donaldson, L. F., Lumb, B. M., & Pickering, A. E. (2015). Intrathecal reboxetine suppresses evoked and ongoing neuropathic pain behaviours by restoring spinal noradrenergic inhibitory tone. *Pain*, *156*(2), 328-334. https://doi.org/10.1097/01.j.pain.0000460313.73358.31

Iadecola, C., & Nedergaard, M. (2007). Glial regulation of the cerebral microvasculature. *Nat Neurosci*, *10*(11), 1369-1376. https://doi.org/10.1038/nn2003

Inoue, K., & Tsuda, M. (2018). Microglia in neuropathic pain: cellular and molecular mechanisms and therapeutic potential. *Nat Rev Neurosci*, *19*(3), 138-152. https://doi.org/10.1038/nrn.2018.2

Inyang, K. E., Szabo-Pardi, T., Wentworth, E., McDougal, T. A., Dussor, G., Burton, M. D., & Price, T. J. (2019). The antidiabetic drug metformin prevents and reverses neuropathic pain and spinal cord microglial activation in male but not female mice. *Pharmacol Res*, *139*, 1-16. https://doi.org/10.1016/j.phrs.2018.10.027

Iqbal, Z., Lei, Z., Ramkrishnan, A. S., Liu, S., Hasan, M., Akter, M., Lam, Y. Y., & Li, Y. (2023). Adrenergic signalling to astrocytes in anterior cingulate cortex contributes to pain-related aversive memory in rats. *Commun Biol*, *6*(1), 10. https://doi.org/10.1038/s42003-022-04405-6

Ishii, Y., Yamaizumi, A., Kawakami, A., Islam, A., Choudhury, M. E., Takahashi, H., Yano, H., & Tanaka, J. (2015). Anti-inflammatory effects of noradrenaline on LPS-treated microglial cells: Suppression of NFκB nuclear translocation and subsequent STAT1 phosphorylation. *Neurochem Int*, *90*, 56-66. https://doi.org/10.1016/j.neuint.2015.07.010

Ito, S., Suto, T., Saito, S., & Obata, H. (2018). Repeated Administration of Duloxetine Suppresses Neuropathic Pain by Accumulating Effects of Noradrenaline in the Spinal Cord. *Anesth Analg*, *126*(1), 298-307. https://doi.org/10.1213/ANE.0000000000002380

Izeboud, C. A., Monshouwer, M., van Miert, A. S., & Witkamp, R. F. (1999). The beta-adrenoceptor agonist clenbuterol is a potent inhibitor of the LPS-induced production of TNF-alpha and IL-6 in vitro and in vivo. *Inflamm Res*, *48*(9), 497-502. https://doi.org/10.1007/s000110050493

Jensen, C. J., Demol, F., Bauwens, R., Kooijman, R., Massie, A., Villers, A., Ris, L., & De Keyser, J. (2016). Astrocytic beta2 Adrenergic Receptor Gene Deletion Affects Memory in Aged Mice. *PLoS One*, *11*(10), e0164721. https://doi.org/10.1371/journal.pone.0164721

Jensen, T. S., & Finnerup, N. B. (2014). Allodynia and hyperalgesia in neuropathic pain: clinical manifestations and mechanisms. *Lancet Neurol*, *13*(9), 924-935. https://doi.org/10.1016/S1474-4422(14)70102-4

Jensen, T. S., Gottrup, H., Sindrup, S. H., & Bach, F. W. (2001). The clinical picture of neuropathic pain. *Eur J Pharmacol*, *429*(1-3), 1-11. https://doi.org/10.1016/s0014-2999(01)01302-4

Jhun, E. H., Sadhu, N., Hu, X., Yao, Y., He, Y., Wilkie, D. J., Molokie, R. E., & Wang, Z. J. (2019). Beta2-Adrenergic Receptor Polymorphisms and Haplotypes Associate With Chronic Pain in Sickle Cell Disease. *Front Pharmacol*, *10*, 84. https://doi.org/10.3389/fphar.2019.00084

Ji, R. R., Berta, T., & Nedergaard, M. (2013). Glia and pain: is chronic pain a gliopathy? *Pain*, *154 Suppl 1*, S10-S28. https://doi.org/10.1016/j.pain.2013.06.022

Ji, R. R., Chamessian, A., & Zhang, Y. Q. (2016). Pain regulation by non-neuronal cells and inflammation. *Science*, *354*(6312), 572-577. https://doi.org/10.1126/science.aaf8924

Ji, R. R., Donnelly, C. R., & Nedergaard, M. (2019). Astrocytes in chronic pain and itch. *Nat Rev Neurosci*, *20*(11), 667-685. https://doi.org/10.1038/s41583-019-0218-1

Kato, G., Yasaka, T., Katafuchi, T., Furue, H., Mizuno, M., Iwamoto, Y., & Yoshimura, M. (2006). Direct GABAergic and glycinergic inhibition of the substantia gelatinosa from the rostral ventromedial medulla revealed by in vivo patch-clamp analysis in rats. *J Neurosci*, *26*(6), 1787-1794. https://doi.org/10.1523/JNEUROSCI.4856-05.2006

Keranen, T., Hommo, T., Hamalainen, M., Moilanen, E., & Korhonen, R. (2016). Anti-Inflammatory Effects of beta2-Receptor Agonists Salbutamol and Terbutaline Are Mediated by MKP-1. *PLoS One*, *11*(2), e0148144. https://doi.org/10.1371/journal.pone.0148144

Keranen, T., Hommo, T., Moilanen, E., & Korhonen, R. (2017). beta2-receptor agonists salbutamol and terbutaline attenuated cytokine production by suppressing ERK pathway through cAMP in macrophages. *Cytokine*, *94*, 1-7. https://doi.org/10.1016/j.cyto.2016.07.016

Khasar, S. G., McCarter, G., & Levine, J. D. (1999). Epinephrine produces a beta-adrenergic receptor-mediated mechanical hyperalgesia and in vitro sensitization of rat nociceptors. *J Neurophysiol*, *81*(3), 1104-1112. https://doi.org/10.1152/jn.1999.81.3.1104

Khoury, S. J., Healy, B. C., Kivisakk, P., Viglietta, V., Egorova, S., Guttmann, C. R., Wedgwood, J. F., Hafler, D. A., Weiner, H. L., Buckle, G., Cook, S., & Reddy, S. (2010). A randomized controlled double-masked trial of albuterol add-on therapy in patients with multiple sclerosis. *Arch Neurol*, *67*(9), 1055-1061. https://doi.org/10.1001/archneurol.2010.222

Kim, B. J., & Jones, H. P. (2010). Epinephrine-primed murine bone marrow-derived dendritic cells facilitate production of IL-17A and IL-4 but not IFN-gamma by CD4+ T cells. *Brain Behav Immun*, *24*(7), 1126-1136. https://doi.org/10.1016/j.bbi.2010.05.003

Kim, I., Mlsna, L. M., Yoon, S., Le, B., Yu, S., Xu, D., & Koh, S. (2015). A postnatal peak in microglial development in the mouse hippocampus is correlated with heightened sensitivity to seizure triggers. *Brain Behav*, *5*(12), e00403. https://doi.org/10.1002/brb3.403

Kim, S. I., Shin, J., Tran, Q., Park, H., Kwon, H. H., Shin, N., Hwang, J. A., Shin, H. J., Lee, J., Lee, W. H., Lee, S. Y., & Kim, D. W. (2021). Application of PLGA nanoparticles to enhance the action of duloxetine on microglia in neuropathic pain. *Biomater Sci*, *9*(18), 6295-6307. https://doi.org/10.1039/d1bm00486g

Kimura, M., Suto, T., Morado-Urbina, C. E., Peters, C. M., Eisenach, J. C., & Hayashida, K. (2015). Impaired Pain-evoked Analgesia after Nerve Injury in Rats Reflects Altered Glutamate Regulation in the Locus Coeruleus. *Anesthesiology*, *123*(4), 899-908. https://doi.org/10.1097/ALN.0000000000000796

Kinali, M., Mercuri, E., Main, M., De Biasia, F., Karatza, A., Higgins, R., Banks, L. M., Manzur, A. Y., & Muntoni, F. (2002). Pilot trial of albuterol in spinal muscular atrophy. *Neurology*, *59*(4), 609-610. https://doi.org/10.1212/wnl.59.4.609

King, T., Vera-Portocarrero, L., Gutierrez, T., Vanderah, T. W., Dussor, G., Lai, J., Fields, H. L., & Porreca, F. (2009). Unmasking the tonic-aversive state in neuropathic pain. *Nat Neurosci*, *12*(11), 1364-1366. https://doi.org/10.1038/nn.2407

Kobayashi, K., Yamanaka, H., Fukuoka, T., Dai, Y., Obata, K., & Noguchi, K. (2008). P2Y12 receptor upregulation in activated microglia is a gateway of p38 signaling and neuropathic pain. *J Neurosci*, *28*(11), 2892-2902. https://doi.org/10.1523/JNEUROSCI.5589-07.2008

Kobilka, B. K., MacGregor, C., Daniel, K., Kobilka, T. S., Caron, M. G., & Lefkowitz, R. J. (1987). Functional activity and regulation of human beta 2-adrenergic receptors expressed in Xenopus oocytes. *J Biol Chem*, *262*(32), 15796-15802. https://www.ncbi.nlm.nih.gov/pubmed/2824467

Kohno, K., Shirasaka, R., Yoshihara, K., Mikuriya, S., Tanaka, K., Takanami, K., Inoue, K., Sakamoto, H., Ohkawa, Y., Masuda, T., & Tsuda, M. (2022). A spinal microglia population involved in remitting and relapsing neuropathic pain. *Science*, *376*(6588), 86-90. https://doi.org/10.1126/science.abf6805

Kohro, Y., Matsuda, T., Yoshihara, K., Kohno, K., Koga, K., Katsuragi, R., Oka, T., Tashima, R., Muneta, S., Yamane, T., Okada, S., Momokino, K., Furusho, A., Hamase, K., Oti, T., Sakamoto, H., Hayashida, K., Kobayashi, R., Horii, T., . . . Tsuda, M. (2020). Spinal astrocytes in superficial laminae gate brainstem descending control of mechanosensory hypersensitivity. *Nature neuroscience*, *23*(11), 1376-1387. https://doi.org/10.1038/S41593-020-00713-4

Koplovitch, P., Minert, A., & Devor, M. (2012). Spontaneous pain in partial nerve injury models of neuropathy and the role of nociceptive sensory cover. *Exp Neurol*, *236*(1), 103-111. https://doi.org/10.1016/j.expneurol.2012.04.005

Krell, H. V., Leuchter, A. F., Cook, I. A., & Abrams, M. (2005). Evaluation of reboxetine, a noradrenergic antidepressant, for the treatment of fibromyalgia and chronic low back pain. *Psychosomatics*, *46*(5), 379-384. https://doi.org/10.1176/appi.psy.46.5.379

Kremer, M., Megat, S., Bohren, Y., Wurtz, X., Nexon, L., Ceredig, R. A., Doridot, S., Massotte, D., Salvat, E., Yalcin, I., & Barrot, M. (2020). Delta opioid receptors are essential to the antiallodynic action of Beta2-mimetics in a model of neuropathic pain. *Mol Pain*, *16*, 1744806920912931. https://doi.org/10.1177/1744806920912931

Kremer, M., Salvat, E., Muller, A., Yalcin, I., & Barrot, M. (2016). Antidepressants and gabapentinoids in neuropathic pain: Mechanistic insights. *Neuroscience*, *338*, 183-206. https://doi.org/10.1016/j.neuroscience.2016.06.057

Kremer, M., Yalcin, I., Goumon, Y., Wurtz, X., Nexon, L., Daniel, D., Megat, S., Ceredig, R. A., Ernst, C., Turecki, G., Chavant, V., Theroux, J. F., Lacaud, A., Joganah, L. E., Lelievre, V., Massotte,

D., Lutz, P. E., Gilsbach, R., Salvat, E., & Barrot, M. (2018). A Dual Noradrenergic Mechanism for the Relief of Neuropathic Allodynia by the Antidepressant Drugs Duloxetine and Amitriptyline. *J Neurosci*, *38*(46), 9934-9954. https://doi.org/10.1523/JNEUROSCI.1004-18.2018

Kremer, M., Yalcin, I., Nexon, L., Wurtz, X., Ceredig, R. A., Daniel, D., Hawkes, R. A., Salvat, E., & Barrot, M. (2016). The antiallodynic action of pregabalin in neuropathic pain is independent from the opioid system. *Mol Pain*, *12*. https://doi.org/10.1177/1744806916633477

Kuner, R., & Flor, H. (2016). Structural plasticity and reorganisation in chronic pain. *Nat Rev Neurosci*, *18*(1), 20-30. https://doi.org/10.1038/nrn.2016.162

Kuner, R., & Kuner, T. (2021). Cellular Circuits in the Brain and Their Modulation in Acute and Chronic Pain. *Physiol Rev*, *101*(1), 213-258. https://doi.org/10.1152/physrev.00040.2019

Laureys, G., Clinckers, R., Gerlo, S., Spooren, A., Wilczak, N., Kooijman, R., Smolders, I., Michotte, Y., & De Keyser, J. (2010). Astrocytic beta(2)-adrenergic receptors: from physiology to pathology. *Prog Neurobiol*, *91*(3), 189-199. https://doi.org/10.1016/j.pneurobio.2010.01.011

Ledeboer, A., Sloane, E. M., Milligan, E. D., Frank, M. G., Mahony, J. H., Maier, S. F., & Watkins, L. R. (2005). Minocycline attenuates mechanical allodynia and proinflammatory cytokine expression in rat models of pain facilitation. *Pain*, *115*(1-2), 71-83. https://doi.org/10.1016/j.pain.2005.02.009

Lee, H. G., Wheeler, M. A., & Quintana, F. J. (2022). Function and therapeutic value of astrocytes in neurological diseases. *Nat Rev Drug Discov*, *21*(5), 339-358. https://doi.org/10.1038/s41573-022-00390-x

Lee, S., Shin, H. J., Noh, C., Kim, S. I., Ko, Y. K., Lee, S. Y., Lim, C., Hong, B., Yang, S. Y., Kim, D. W., Lee, W. H., & Kim, Y. H. (2021). IKBKB siRNA-Encapsulated Poly (Lactic-co-Glycolic Acid) Nanoparticles Diminish Neuropathic Pain by Inhibiting Microglial Activation. *Int J Mol Sci*, *22*(11). https://doi.org/10.3390/ijms22115657

Lefaucheur, J. P., Antal, A., Ahdab, R., Ciampi de Andrade, D., Fregni, F., Khedr, E. M., Nitsche, M., & Paulus, W. (2008). The use of repetitive transcranial magnetic stimulation (rTMS) and transcranial direct current stimulation (tDCS) to relieve pain. *Brain Stimul*, *1*(4), 337-344. https://doi.org/10.1016/j.brs.2008.07.003

Lewis, G. N., Rice, D. A., & McNair, P. J. (2012). Conditioned pain modulation in populations with chronic pain: a systematic review and meta-analysis. *J Pain*, *13*(10), 936-944. https://doi.org/10.1016/j.jpain.2012.07.005

Leyh, J., Paeschke, S., Mages, B., Michalski, D., Nowicki, M., Bechmann, I., & Winter, K. (2021). Classification of Microglial Morphological Phenotypes Using Machine Learning. *Front Cell Neurosci*, *15*, 701673. https://doi.org/10.3389/fncel.2021.701673

Li, J., Wei, Y., Zhou, J., Zou, H., Ma, L., Liu, C., Xiao, Z., Liu, X., Tan, X., Yu, T., & Cao, S. (2022). Activation of locus coeruleus-spinal cord noradrenergic neurons alleviates neuropathic pain in mice via reducing neuroinflammation from astrocytes and microglia in spinal dorsal horn. *J Neuroinflammation*, *19*(1), 123. https://doi.org/10.1186/s12974-022-02489-9

Li, J. N., & Sheets, P. L. (2018). The central amygdala to periaqueductal gray pathway comprises intrinsically distinct neurons differentially affected in a model of inflammatory pain. *J Physiol*, *596*(24), 6289-6305. https://doi.org/10.1113/JP276935

Li, W., Shi, X., Wang, L., Guo, T., Wei, T., Cheng, K., Rice, K. C., Kingery, W. S., & Clark, J. D. (2013). Epidermal adrenergic signaling contributes to inflammation and pain sensitization in a rat model of complex regional pain syndrome. *Pain*, *154*(8), 1224-1236. https://doi.org/10.1016/j.pain.2013.03.033

Li, X., Li, M., Tian, L., Chen, J., Liu, R., & Ning, B. (2020). Reactive Astrogliosis: Implications in Spinal Cord Injury Progression and Therapy. *Oxid Med Cell Longev*, *2020*, 9494352. https://doi.org/10.1155/2020/9494352

Liampas, A., Rekatsina, M., Vadalouca, A., Paladini, A., Varrassi, G., & Zis, P. (2020). Non-Pharmacological Management of Painful Peripheral Neuropathies: A Systematic Review. *Adv Ther*, *37*(10), 4096-4106. https://doi.org/10.1007/s12325-020-01462-3

Liedgens, H., Obradovic, M., De Courcy, J., Holbrook, T., & Jakubanis, R. (2016). A burden of illness study for neuropathic pain in Europe. *Clinicoecon Outcomes Res*, *8*, 113-126. https://doi.org/10.2147/CEOR.S81396

Linden, A., Rabe, K. F., & Lofdahl, C. G. (1996). Pharmacological basis for duration of effect: formoterol and salmeterol versus short-acting beta 2-adrenoceptor agonists. *Lung*, *174*(1), 1-22. https://doi.org/10.1007/BF00167947

Liu, L., Dai, L., Xu, D., Wang, Y., Bai, L., Chen, X., Li, M., Yang, S., & Tang, Y. (2022). Astrocyte secretes IL-6 to modulate PSD-95 palmitoylation in basolateral amygdala and depression-like

behaviors induced by peripheral nerve injury. *Brain Behav Immun*, *104*, 139-154. https://doi.org/10.1016/j.bbi.2022.05.014
Liu, X., He, J., Gao, J., & Xiao, Z. (2022). Fluorocitrate and neurotropin confer analgesic effects on neuropathic pain in diabetic rats via inhibition of astrocyte activation in the periaqueductal gray. *Neurosci Lett*, *768*, 136378. https://doi.org/10.1016/j.neulet.2021.136378
Loggia, M. L., Chonde, D. B., Akeju, O., Arabasz, G., Catana, C., Edwards, R. R., Hill, E., Hsu, S., Izquierdo-Garcia, D., Ji, R. R., Riley, M., Wasan, A. D., Zurcher, N. R., Albrecht, D. S., Vangel, M. G., Rosen, B. R., Napadow, V., & Hooker, J. M. (2015). Evidence for brain glial activation in chronic pain patients. *Brain*, *138*(Pt 3), 604-615. https://doi.org/10.1093/brain/awu377
Lopes, D. M., Malek, N., Edye, M., Jager, S. B., McMurray, S., McMahon, S. B., & Denk, F. (2017). Sex differences in peripheral not central immune responses to pain-inducing injury. *Sci Rep*, *7*(1), 16460. https://doi.org/10.1038/s41598-017-16664-z
Lorton, D., & Bellinger, D. L. (2015). Molecular mechanisms underlying beta-adrenergic receptor-mediated cross-talk between sympathetic neurons and immune cells. *Int J Mol Sci*, *16*(3), 5635-5665. https://doi.org/10.3390/ijms16035635
Loughlin, S. E., Foote, S. L., & Grzanna, R. (1986). Efferent projections of nucleus locus coeruleus: morphologic subpopulations have different efferent targets. *Neuroscience*, *18*(2), 307-319. https://doi.org/10.1016/0306-4522(86)90156-9
Lu, H. J., & Gao, Y. J. (2022). Astrocytes in Chronic Pain: Cellular and Molecular Mechanisms. *Neurosci Bull*. https://doi.org/10.1007/s12264-022-00961-3
Lu, Y., & Perl, E. R. (2007). Selective action of noradrenaline and serotonin on neurones of the spinal superficial dorsal horn in the rat. *J Physiol*, *582*(Pt 1), 127-136. https://doi.org/10.1113/jphysiol.2007.131565
Machelska, H., & Celik, M. O. (2020). Opioid Receptors in Immune and Glial Cells-Implications for Pain Control. *Front Immunol*, *11*, 300. https://doi.org/10.3389/fimmu.2020.00300
Maguire, A. D., Bethea, J. R., & Kerr, B. J. (2021). TNFalpha in MS and Its Animal Models: Implications for Chronic Pain in the Disease. *Front Neurol*, *12*, 780876. https://doi.org/10.3389/fneur.2021.780876
Mai, L., Jia, S., Liu, Q., Chu, Y., Liu, J., Yang, S., Huang, F., & Fan, W. (2022). Sympathectomy Ameliorates CFA-Induced Mechanical Allodynia via Modulating Phenotype of Macrophages in Sensory Ganglion in Mice. *J Inflamm Res*, *15*, 6263-6274. https://doi.org/10.2147/JIR.S388322
Martin, S. L., Reid, A. J., Verkhratsky, A., Magnaghi, V., & Faroni, A. (2019). Gene expression changes in dorsal root ganglia following peripheral nerve injury: roles in inflammation, cell death and nociception. *Neural Regen Res*, *14*(6), 939-947. https://doi.org/10.4103/1673-5374.250566
Martinez, V., Szekely, B., Lemarie, J., Martin, F., Gentili, M., Ben Ammar, S., Lepeintre, J. F., Garreau de Loubresse, C., Chauvin, M., Bouhassira, D., & Fletcher, D. (2013). The efficacy of a glial inhibitor, minocycline, for preventing persistent pain after lumbar discectomy: a randomized, double-blind, controlled study. *Pain*, *154*(8), 1197-1203. https://doi.org/10.1016/j.pain.2013.03.028
Martins, I., Carvalho, P., de Vries, M. G., Teixeira-Pinto, A., Wilson, S. P., Westerink, B. H., & Tavares, I. (2015). Increased noradrenergic neurotransmission to a pain facilitatory area of the brain is implicated in facilitation of chronic pain. *Anesthesiology*, *123*(3), 642-653. https://doi.org/10.1097/ALN.0000000000000749
Martins, I., & Tavares, I. (2017). Reticular Formation and Pain: The Past and the Future. *Front Neuroanat*, *11*, 51. https://doi.org/10.3389/fnana.2017.00051
Marty-Lombardi, S., Lu, S., Ambroziak, W., Wende, H., Schrenk-Siemens, K., DePaoli-Roach, A. A., Hagenston, A. M., Tappe-Theodor, A., Simonetti, M., Kuner, R., Fleming, T., & Siemens, J. (2022). Neuron-astrocyte metabolic coupling facilitates spinal plasticity and maintenance of persistent pain. *bioRxiv*, 2022.2012.2003.518519. https://doi.org/10.1101/2022.12.03.518519
Masuda, T., Sankowski, R., Staszewski, O., & Prinz, M. (2020). Microglia Heterogeneity in the Single-Cell Era. *Cell Rep*, *30*(5), 1271-1281. https://doi.org/10.1016/j.celrep.2020.01.010
Matejuk, A., & Ransohoff, R. M. (2020). Crosstalk Between Astrocytes and Microglia: An Overview. *Front Immunol*, *11*, 1416. https://doi.org/10.3389/fimmu.2020.01416
McGinnis, A., & Ji, R. R. (2023). The Similar and Distinct Roles of Satellite Glial Cells and Spinal Astrocytes in Neuropathic Pain. *Cells*, *12*(6). https://doi.org/10.3390/cells12060965
Midavaine, E., Cote, J., Marchand, S., & Sarret, P. (2021). Glial and neuroimmune cell choreography in sexually dimorphic pain signaling. *Neurosci Biobehav Rev*, *125*, 168-192. https://doi.org/10.1016/j.neubiorev.2021.01.023

Mika, J., Popiolek-Barczyk, K., Rojewska, E., Makuch, W., Starowicz, K., & Przewlocka, B. (2014). Delta-opioid receptor analgesia is independent of microglial activation in a rat model of neuropathic pain. *PLoS One*, *9*(8), e104420. https://doi.org/10.1371/journal.pone.0104420

Mizuno, K., Takahashi, H. K., Iwagaki, H., Katsuno, G., Kamurul, H. A., Ohtani, S., Mori, S., Yoshino, T., Nishibori, M., & Tanaka, N. (2005). Beta2-adrenergic receptor stimulation inhibits LPS-induced IL-18 and IL-12 production in monocytes. *Immunol Lett*, *101*(2), 168-172. https://doi.org/10.1016/j.imlet.2005.05.008

Moehring, F., Halder, P., Seal, R. P., & Stucky, C. L. (2018). Uncovering the Cells and Circuits of Touch in Normal and Pathological Settings. *Neuron*, *100*(2), 349-360. https://doi.org/10.1016/j.neuron.2018.10.019

Mogil, J. S. (2020). Qualitative sex differences in pain processing: emerging evidence of a biased literature. *Nat Rev Neurosci*, *21*(7), 353-365. https://doi.org/10.1038/s41583-020-0310-6

Montilla-Garcia, A., Perazzoli, G., Tejada, M. A., Gonzalez-Cano, R., Sanchez-Fernandez, C., Cobos, E. J., & Baeyens, J. M. (2018). Modality-specific peripheral antinociceptive effects of mu-opioid agonists on heat and mechanical stimuli: Contribution of sigma-1 receptors. *Neuropharmacology*, *135*, 328-342. https://doi.org/10.1016/j.neuropharm.2018.03.025

Morioka, N., Tanabe, H., Inoue, A., Dohi, T., & Nakata, Y. (2009). Noradrenaline reduces the ATP-stimulated phosphorylation of p38 MAP kinase via beta-adrenergic receptors-cAMP-protein kinase A-dependent mechanism in cultured rat spinal microglia. *Neurochem Int*, *55*(4), 226-234. https://doi.org/10.1016/j.neuint.2009.03.004

Muzio, L., Viotti, A., & Martino, G. (2021). Microglia in Neuroinflammation and Neurodegeneration: From Understanding to Therapy. *Front Neurosci*, *15*, 742065. https://doi.org/10.3389/fnins.2021.742065

Nam, Y., Kim, J. H., Kim, J. H., Jha, M. K., Jung, J. Y., Lee, M. G., Choi, I. S., Jang, I. S., Lim, D. G., Hwang, S. H., Cho, H. J., & Suk, K. (2016). Reversible Induction of Pain Hypersensitivity following Optogenetic Stimulation of Spinal Astrocytes. *Cell Reports*, *17*(11), 3049-3061. https://doi.org/10.1016/J.CELREP.2016.11.043

Nedoshivin, A., Petrova, P. T. S., & Karpov, Y. (2022). Efficacy and Safety of Ivabradine in Combination with Beta-Blockers in Patients with Stable Angina Pectoris: A Systematic Review and Meta-analysis. *Adv Ther*, *39*(9), 4189-4204. https://doi.org/10.1007/s12325-022-02222-1

Nees, T. A., Wang, N., Adamek, P., Zeitzschel, N., Verkest, C., La Porta, C., Schaefer, I., Virnich, J., Balkaya, S., Prato, V., Morelli, C., Begay, V., Lee, Y. J., Tappe-Theodor, A., Lewin, G. R., Heppenstall, P. A., Taberner, F. J., & Lechner, S. G. (2023). Role of TMEM100 in mechanically insensitive nociceptor un-silencing. *Nat Commun*, *14*(1), 1899. https://doi.org/10.1038/s41467-023-37602-w

Nguyen, J. P., Nizard, J., Keravel, Y., & Lefaucheur, J. P. (2011). Invasive brain stimulation for the treatment of neuropathic pain. *Nat Rev Neurol*, *7*(12), 699-709. https://doi.org/10.1038/nrneurol.2011.138

Ni, H., Wang, Y., An, K., Liu, Q., Xu, L., Zhu, C., Deng, H., He, Q., Wang, T., Xu, M., Zheng, Y., Huang, B., Fang, J., & Yao, M. (2019). Crosstalk between NFkappaB-dependent astrocytic CXCL1 and neuron CXCR2 plays a role in descending pain facilitation. *J Neuroinflammation*, *16*(1), 1. https://doi.org/10.1186/s12974-018-1391-2

Nimmerjahn, A., Kirchhoff, F., & Helmchen, F. (2005). Resting microglial cells are highly dynamic surveillants of brain parenchyma in vivo. *Science*, *308*(5726), 1314-1318. https://doi.org/10.1126/science.1110647

O'Donnell, J., Zeppenfeld, D., McConnell, E., Pena, S., & Nedergaard, M. (2012). Norepinephrine: a neuromodulator that boosts the function of multiple cell types to optimize CNS performance. *Neurochem Res*, *37*(11), 2496-2512. https://doi.org/10.1007/s11064-012-0818-x

Obata, K., & Noguchi, K. (2004). MAPK activation in nociceptive neurons and pain hypersensitivity. *Life Sci*, *74*(21), 2643-2653. https://doi.org/10.1016/j.lfs.2004.01.007

Oe, Y., Wang, X., Patriarchi, T., Konno, A., Ozawa, K., Yahagi, K., Hirai, H., Tsuboi, T., Kitaguchi, T., Tian, L., McHugh, T. J., & Hirase, H. (2020). Distinct temporal integration of noradrenaline signaling by astrocytic second messengers during vigilance. *Nat Commun*, *11*(1), 471. https://doi.org/10.1038/s41467-020-14378-x

Olave, M. J., & Maxwell, D. J. (2003). Neurokinin-1 projection cells in the rat dorsal horn receive synaptic contacts from axons that possess alpha2C-adrenergic receptors. *J Neurosci*, *23*(17), 6837-6846. https://doi.org/10.1523/JNEUROSCI.23-17-06837.2003

Old, E. A., Clark, A. K., & Malcangio, M. (2015). The role of glia in the spinal cord in neuropathic and inflammatory pain. *Handb Exp Pharmacol*, *227*, 145-170. https://doi.org/10.1007/978-3-662-46450-2_8

Olesen, A. E., Staahl, C., Arendt-Nielsen, L., & Drewes, A. M. (2010). Different effects of morphine and oxycodone in experimentally evoked hyperalgesia: a human translational study. *Br J Clin Pharmacol*, *70*(2), 189-200. https://doi.org/10.1111/j.1365-2125.2010.03700.x

Ono, T., Kohro, Y., Kohno, K., Tozaki-Saitoh, H., Nakashima, Y., & Tsuda, M. (2020). Mechanical pain of the lower extremity after compression of the upper spinal cord involves signal transducer and activator of transcription 3-dependent reactive astrocytes and interleukin-6. *Brain Behav Immun*, *89*, 389-399. https://doi.org/10.1016/j.bbi.2020.07.025

Orr, A. G., Orr, A. L., Li, X. J., Gross, R. E., & Traynelis, S. F. (2009). Adenosine A(2A) receptor mediates microglial process retraction. *Nat Neurosci*, *12*(7), 872-878. https://doi.org/10.1038/nn.2341

Ozdogan, U. K., Lahdesmaki, J., Mansikka, H., & Scheinin, M. (2004). Loss of amitriptyline analgesia in alpha 2A-adrenoceptor deficient mice. *Eur J Pharmacol*, *485*(1-3), 193-196. https://doi.org/10.1016/j.ejphar.2003.11.047

Pan, H. L., Wu, Z. Z., Zhou, H. Y., Chen, S. R., Zhang, H. M., & Li, D. P. (2008). Modulation of Pain Transmission by G Protein-Coupled Receptors. *Pharmacology & therapeutics*, *117*(1), 141-141. https://doi.org/10.1016/J.PHARMTHERA.2007.09.003

Pan, Y. D., Guo, Q. L., Wang, E., Ye, Z., He, Z. H., Zou, W. Y., Cheng, Z. G., & Wang, Y. J. (2010). Intrathecal infusion of pyrrolidine dithiocarbamate for the prevention and reversal of neuropathic pain in rats using a sciatic chronic constriction injury model. *Reg Anesth Pain Med*, *35*(3), 231-237. https://doi.org/10.1097/AAP.0b013e3181df245b

Paris, I., Savage, J. C., Escobar, L., Abiega, O., Gagnon, S., Hui, C. W., Tremblay, M. E., Sierra, A., & Valero, J. (2018). ProMoIJ: A new tool for automatic three-dimensional analysis of microglial process motility. *Glia*, *66*(4), 828-845. https://doi.org/10.1002/glia.23287

Patel, R., & Dickenson, A. H. (2016). Mechanisms of the gabapentinoids and alpha 2 delta-1 calcium channel subunit in neuropathic pain. *Pharmacol Res Perspect*, *4*(2), e00205. https://doi.org/10.1002/prp2.205

Peng, J., Gu, N., Zhou, L., U, B. E., Murugan, M., Gan, W. B., & Wu, L. J. (2016). Microglia and monocytes synergistically promote the transition from acute to chronic pain after nerve injury. *Nat Commun*, *7*, 12029. https://doi.org/10.1038/ncomms12029

Perez, D. M. (2020). alpha(1)-Adrenergic Receptors in Neurotransmission, Synaptic Plasticity, and Cognition. *Front Pharmacol*, *11*, 581098. https://doi.org/10.3389/fphar.2020.581098

Perrin, F. E., Gerber, Y. N., Teigell, M., Lonjon, N., Boniface, G., Bauchet, L., Rodriguez, J. J., Hugnot, J. P., & Privat, A. M. (2011). Anatomical study of serotonergic innervation and 5-HT(1A) receptor in the human spinal cord. *Cell Death Dis*, *2*(10), e218. https://doi.org/10.1038/cddis.2011.98

Pertovaara, A. (2006). Noradrenergic pain modulation. *Prog Neurobiol*, *80*(2), 53-83. https://doi.org/10.1016/j.pneurobio.2006.08.001

Phillips, C., Fahimi, A., Das, D., Mojabi, F. S., Ponnusamy, R., & Salehi, A. (2016). Noradrenergic System in Down Syndrome and Alzheimer's Disease A Target for Therapy. *Curr Alzheimer Res*, *13*(1), 68-83. https://doi.org/10.2174/1567205012666150921095924

Pinho-Ribeiro, F. A., Verri, W. A., Jr., & Chiu, I. M. (2017). Nociceptor Sensory Neuron-Immune Interactions in Pain and Inflammation. *Trends Immunol*, *38*(1), 5-19. https://doi.org/10.1016/j.it.2016.10.001

Pitzer, C., Kuner, R., & Tappe-Theodor, A. (2016). EXPRESS: Voluntary and evoked behavioral correlates in neuropathic pain states under different housing conditions. *Mol Pain*, *12*. https://doi.org/10.1177/1744806916656635

Plummer, N. W., Chandler, D. J., Powell, J. M., Scappini, E. L., Waterhouse, B. D., & Jensen, P. (2020). An Intersectional Viral-Genetic Method for Fluorescent Tracing of Axon Collaterals Reveals Details of Noradrenergic Locus Coeruleus Structure. *eNeuro*, *7*(3). https://doi.org/10.1523/ENEURO.0010-20.2020

Polomano, R. C., Mannes, A. J., Clark, U. S., & Bennett, G. J. (2001). A painful peripheral neuropathy in the rat produced by the chemotherapeutic drug, paclitaxel. *Pain*, *94*(3), 293-304. https://doi.org/10.1016/S0304-3959(01)00363-3

Porreca, F., Ossipov, M. H., & Gebhart, G. F. (2002). Chronic pain and medullary descending facilitation. *Trends Neurosci*, *25*(6), 319-325. https://doi.org/10.1016/s0166-2236(02)02157-4

Prinz, M., Jung, S., & Priller, J. (2019). Microglia Biology: One Century of Evolving Concepts. *Cell*, *179*(2), 292-311. https://doi.org/10.1016/j.cell.2019.08.053

Qian, C., Tan, D., Wang, X., Li, L., Wen, J., Pan, M., Li, Y., Wu, W., & Guo, J. (2018). Peripheral Nerve Injury-Induced Astrocyte Activation in Spinal Ventral Horn Contributes to Nerve Regeneration. *Neural Plast*, *2018*, 8561704. https://doi.org/10.1155/2018/8561704

Qian, L., Wu, H. M., Chen, S. H., Zhang, D., Ali, S. F., Peterson, L., Wilson, B., Lu, R. B., Hong, J. S., & Flood, P. M. (2011). beta2-adrenergic receptor activation prevents rodent dopaminergic neurotoxicity by inhibiting microglia via a novel signaling pathway. *J Immunol*, *186*(7), 4443-4454. https://doi.org/10.4049/jimmunol.1002449

Querin, G., D'Ascenzo, C., Peterle, E., Ermani, M., Bello, L., Melacini, P., Morandi, L., Mazzini, L., Silani, V., Raimondi, M., Mandrioli, J., Romito, S., Angelini, C., Pegoraro, E., & Soraru, G. (2013). Pilot trial of clenbuterol in spinal and bulbar muscular atrophy. *Neurology*, *80*(23), 2095-2098. https://doi.org/10.1212/WNL.0b013e318295d766

Raghavendra, V., Tanga, F., & DeLeo, J. A. (2003). Inhibition of microglial activation attenuates the development but not existing hypersensitivity in a rat model of neuropathy. *J Pharmacol Exp Ther*, *306*(2), 624-630. https://doi.org/10.1124/jpet.103.052407

Rahman, W., Bannister, K., Bee, L. A., & Dickenson, A. H. (2011). A pronociceptive role for the 5-HT2 receptor on spinal nociceptive transmission: an in vivo electrophysiological study in the rat. *Brain Res*, *1382*, 29-36. https://doi.org/10.1016/j.brainres.2011.01.057

Raja, S. N., Carr, D. B., Cohen, M., Finnerup, N. B., Flor, H., Gibson, S., Keefe, F. J., Mogil, J. S., Ringkamp, M., Sluka, K. A., Song, X. J., Stevens, B., Sullivan, M. D., Tutelman, P. R., Ushida, T., & Vader, K. (2020). The revised International Association for the Study of Pain definition of pain: concepts, challenges, and compromises. *Pain*, *161*(9), 1976-1982. https://doi.org/10.1097/j.pain.0000000000001939

Raja, S. N., Treede, R. D., Davis, K. D., & Campbell, J. N. (1991). Systemic alpha-adrenergic blockade with phentolamine: a diagnostic test for sympathetically maintained pain. *Anesthesiology*, *74*(4), 691-698. https://doi.org/10.1097/00000542-199104000-00012

Rexed, B. (1952). The cytoarchitectonic organization of the spinal cord in the cat. *J Comp Neurol*, *96*(3), 414-495. https://doi.org/10.1002/cne.900960303

Rice, A. S. C., Finnerup, N. B., Kemp, H. I., Currie, G. L., & Baron, R. (2018). Sensory profiling in animal models of neuropathic pain: a call for back-translation. *Pain*, *159*(5), 819-824. https://doi.org/10.1097/j.pain.0000000000001138

Rieder, P., Gobbo, D., Stopper, G., Welle, A., Damo, E., Kirchhoff, F., & Scheller, A. (2022). Astrocytes and Microglia Exhibit Cell-Specific Ca(2+) Signaling Dynamics in the Murine Spinal Cord. *Front Mol Neurosci*, *15*, 840948. https://doi.org/10.3389/fnmol.2022.840948

Robinson, C. R., Zhang, H., & Dougherty, P. M. (2014). Astrocytes, but not microglia, are activated in oxaliplatin and bortezomib-induced peripheral neuropathy in the rat. *Neuroscience*, *274*, 308-317. https://doi.org/10.1016/j.neuroscience.2014.05.051

Rojo, M. L., Rodriguez-Gaztelumendi, A., Pazos, A., & Diaz, A. (2012). Differential adaptive changes on serotonin and noradrenaline transporters in a rat model of peripheral neuropathic pain. *Neurosci Lett*, *515*(2), 181-186. https://doi.org/10.1016/j.neulet.2012.03.050

Rosario, A. M., Cruz, P. E., Ceballos-Diaz, C., Strickland, M. R., Siemienski, Z., Pardo, M., Schob, K. L., Li, A., Aslanidi, G. V., Srivastava, A., Golde, T. E., & Chakrabarty, P. (2016). Microglia-specific targeting by novel capsid-modified AAV6 vectors. *Mol Ther Methods Clin Dev*, *3*, 16026. https://doi.org/10.1038/mtm.2016.26

Sadler, K. E., Mogil, J. S., & Stucky, C. L. (2022). Innovations and advances in modelling and measuring pain in animals. *Nat Rev Neurosci*, *23*(2), 70-85. https://doi.org/10.1038/s41583-021-00536-7

Salvat, E., Schweitzer, B., Massard, G., Meyer, N., de Blay, F., Muller, A., & Barrot, M. (2015). Effects of beta2 agonists on post-thoracotomy pain incidence. *Eur J Pain*, *19*(10), 1428-1436. https://doi.org/10.1002/ejp.673

Sandkuhler, J. (2009). Models and mechanisms of hyperalgesia and allodynia. *Physiol Rev*, *89*(2), 707-758. https://doi.org/10.1152/physrev.00025.2008

Sara, S. J., & Bouret, S. (2012). Orienting and reorienting: the locus coeruleus mediates cognition through arousal. *Neuron*, *76*(1), 130-141. https://doi.org/10.1016/j.neuron.2012.09.011

Scanzano, A., & Cosentino, M. (2015). Adrenergic regulation of innate immunity: a review. *Front Pharmacol*, *6*, 171. https://doi.org/10.3389/fphar.2015.00171

Schilero, G. J., Hobson, J. C., Singh, K., Spungen, A. M., Bauman, W. A., & Radulovic, M. (2018). Bronchodilator effects of ipratropium bromide and albuterol sulfate among subjects with tetraplegia. *J Spinal Cord Med*, *41*(1), 42-47. https://doi.org/10.1080/10790268.2016.1235753

Seltzer, Z., Dubner, R., & Shir, Y. (1990). A novel behavioral model of neuropathic pain disorders produced in rats by partial sciatic nerve injury. *Pain*, *43*(2), 205-218. https://doi.org/10.1016/0304-3959(90)91074-S

Sharma, D., & Farrar, J. D. (2020). Adrenergic regulation of immune cell function and inflammation. *Semin Immunopathol*, *42*(6), 709-717. https://doi.org/10.1007/s00281-020-00829-6

Sharma, M., Arbabzada, N., & Flood, P. M. (2019). Mechanism underlying beta2-AR agonist-mediated phenotypic conversion of LPS-activated microglial cells. *J Neuroimmunol*, *332*, 37-48. https://doi.org/10.1016/j.jneuroim.2019.03.017

Sharma, M., & Flood, P. M. (2019). Adrenergic Receptors as Pharmacological Targets for Neuroinflammation and Neurodegeneration in Parkinson's Disease. In *Neuroprotection* IntechOpen. https://doi.org/10.5772/intechopen.81343

Shen, S., Tiwari, N., Madar, J., Mehta, P., & Qiao, L. Y. (2022). Beta 2-adrenergic receptor mediates noradrenergic action to induce cyclic adenosine monophosphate response element-binding protein phosphorylation in satellite glial cells of dorsal root ganglia to regulate visceral hypersensitivity. *Pain*, *163*(1), 180-192. https://doi.org/10.1097/j.pain.0000000000002330

Shenoy, S. K., Drake, M. T., Nelson, C. D., Houtz, D. A., Xiao, K., Madabushi, S., Reiter, E., Premont, R. T., Lichtarge, O., & Lefkowitz, R. J. (2006). beta-arrestin-dependent, G protein-independent ERK1/2 activation by the beta2 adrenergic receptor. *J Biol Chem*, *281*(2), 1261-1273. https://doi.org/10.1074/jbc.M506576200

Shukla, A. K., Xiao, K., & Lefkowitz, R. J. (2011). Emerging paradigms of beta-arrestin-dependent seven transmembrane receptor signaling. *Trends Biochem Sci*, *36*(9), 457-469. https://doi.org/10.1016/j.tibs.2011.06.003

Sideris-Lampretsas, G., & Malcangio, M. (2022). Pain-resolving microglia. *Science*, *376*(6588), 33-34. https://doi.org/10.1126/science.abo5592

Silva, R. L., Lopes, A. H., Guimaraes, R. M., & Cunha, T. M. (2017). CXCL1/CXCR2 signaling in pathological pain: Role in peripheral and central sensitization. *Neurobiol Dis*, *105*, 109-116. https://doi.org/10.1016/j.nbd.2017.06.001

Skelly, A., Chou, R., Dettori, J., Turner, J., Friedly, J., Rundell, S., Fu, R., Brodt, E., Wasson, N., Kantner, S., & Ferguson, A. (2022). Noninvasive Nonpharmacological Treatment for Chronic Pain: A Systematic Review Update. *Comparative Effectiveness Review*, *227*. https://doi.org/10.23970/AHRQEPCCER227

Sluka, K. A., & Westlund, K. N. (1992). Spinal projections of the locus coeruleus and the nucleus subcoeruleus in the Harlan and the Sasco Sprague-Dawley rat. *Brain Res*, *579*(1), 67-73. https://doi.org/10.1016/0006-8993(92)90742-r

Solorzano, C., Villafuerte, D., Meda, K., Cevikbas, F., Braz, J., Sharif-Naeini, R., Juarez-Salinas, D., Llewellyn-Smith, I. J., Guan, Z., & Basbaum, A. I. (2015). Primary afferent and spinal cord expression of gastrin-releasing peptide: message, protein, and antibody concerns. *J Neurosci*, *35*(2), 648-657. https://doi.org/10.1523/JNEUROSCI.2955-14.2015

Soraru, G., Pegoraro, E., Spinella, P., Turra, S., D'Ascenzo, C., Baggio, L., Mantovan, M. C., Vergani, L., & Angelini, C. (2006). A pilot trial with clenbuterol in amyotrophic lateral sclerosis. *Amyotroph Lateral Scler*, *7*(4), 246-248. https://doi.org/10.1080/14660820600600558

Sorge, R. E., Mapplebeck, J. C., Rosen, S., Beggs, S., Taves, S., Alexander, J. K., Martin, L. J., Austin, J. S., Sotocinal, S. G., Chen, D., Yang, M., Shi, X. Q., Huang, H., Pillon, N. J., Bilan, P. J., Tu, Y., Klip, A., Ji, R. R., Zhang, J., . . . Mogil, J. S. (2015). Different immune cells mediate mechanical pain hypersensitivity in male and female mice. *Nat Neurosci*, *18*(8), 1081-1083. https://doi.org/10.1038/nn.4053

Spengler, R. N., Chensue, S. W., Giacherio, D. A., Blenk, N., & Kunkel, S. L. (1994). Endogenous norepinephrine regulates tumor necrosis factor-alpha production from macrophages in vitro. *J Immunol*, *152*(6), 3024-3031. https://www.ncbi.nlm.nih.gov/pubmed/8144901

Staedtke, V., Bai, R. Y., Kim, K., Darvas, M., Davila, M. L., Riggins, G. J., Rothman, P. B., Papadopoulos, N., Kinzler, K. W., Vogelstein, B., & Zhou, S. (2018). Disruption of a self-amplifying catecholamine loop reduces cytokine release syndrome. *Nature*, *564*(7735), 273-277. https://doi.org/10.1038/s41586-018-0774-y

Steeland, S., Libert, C., & Vandenbroucke, R. E. (2018). A New Venue of TNF Targeting. *Int J Mol Sci*, *19*(5). https://doi.org/10.3390/ijms19051442

Steininger, T. S., Stutz, H., & Kerschbaum, H. H. (2011). Beta-adrenergic stimulation suppresses phagocytosis via Epac activation in murine microglial cells. *Brain Res*, *1407*, 1-12. https://doi.org/10.1016/j.brainres.2011.06.050

Stone, L. S., Vulchanova, L., Riedl, M. S., Wang, J., Williams, F. G., Wilcox, G. L., & Elde, R. (1999). Effects of peripheral nerve injury on alpha-2A and alpha-2C adrenergic receptor immunoreactivity in the rat spinal cord. *Neuroscience*, *93*(4), 1399-1407. https://doi.org/10.1016/s0306-4522(99)00209-2

Stremmel, C., Schuchert, R., Wagner, F., Thaler, R., Weinberger, T., Pick, R., Mass, E., Ishikawa-Ankerhold, H. C., Margraf, A., Hutter, S., Vagnozzi, R., Klapproth, S., Frampton, J., Yona, S., Scheiermann, C., Molkentin, J. D., Jeschke, U., Moser, M., Sperandio, M., . . . Schulz, C.

(2018). Yolk sac macrophage progenitors traffic to the embryo during defined stages of development. *Nat Commun*, *9*(1), 75. https://doi.org/10.1038/s41467-017-02492-2
Suarez-Pereira, I., Llorca-Torralba, M., Bravo, L., Camarena-Delgado, C., Soriano-Mas, C., & Berrocoso, E. (2022). The Role of the Locus Coeruleus in Pain and Associated Stress-Related Disorders. *Biol Psychiatry*, *91*(9), 786-797. https://doi.org/10.1016/j.biopsych.2021.11.023
Suter, M. R., Berta, T., Gao, Y. J., Decosterd, I., & Ji, R. R. (2009). Large A-fiber activity is required for microglial proliferation and p38 MAPK activation in the spinal cord: different effects of resiniferatoxin and bupivacaine on spinal microglial changes after spared nerve injury. *Mol Pain*, *5*, 53. https://doi.org/10.1186/1744-8069-5-53
Sypek, E. I., Collins, H. Y., McCallum, W. M., Bourdillon, A. T., Barres, B. A., Bohlen, C. J., & Scherrer, G. (2021). Diversity of microglial transcriptional responses during opioid exposure and neuropathic pain. *bioRxiv*, 2021.2012.2029.473853. https://doi.org/10.1101/2021.12.29.473853
Takenaka, M. C., Araujo, L. P., Maricato, J. T., Nascimento, V. M., Guereschi, M. G., Rezende, R. M., Quintana, F. J., & Basso, A. S. (2016). Norepinephrine Controls Effector T Cell Differentiation through beta2-Adrenergic Receptor-Mediated Inhibition of NF-kappaB and AP-1 in Dendritic Cells. *J Immunol*, *196*(2), 637-644. https://doi.org/10.4049/jimmunol.1501206
Tansley, S., Uttam, S., Urena Guzman, A., Yaqubi, M., Pacis, A., Parisien, M., Deamond, H., Wong, C., Rabau, O., Brown, N., Haglund, L., Ouellet, J., Santaguida, C., Ribeiro-da-Silva, A., Tahmasebi, S., Prager-Khoutorsky, M., Ragoussis, J., Zhang, J., Salter, M. W., . . . Khoutorsky, A. (2022). Single-cell RNA sequencing reveals time- and sex-specific responses of mouse spinal cord microglia to peripheral nerve injury and links ApoE to chronic pain. *Nat Commun*, *13*(1), 843. https://doi.org/10.1038/s41467-022-28473-8
Tappe-Theodor, A., & Kuner, R. (2014). Studying ongoing and spontaneous pain in rodents--challenges and opportunities. *Eur J Neurosci*, *39*(11), 1881-1890. https://doi.org/10.1111/ejn.12643
Tashkin, D. P., & Cooper, C. B. (2004). The role of long-acting bronchodilators in the management of stable COPD. *Chest*, *125*(1), 249-259. https://doi.org/10.1378/chest.125.1.249
Tavares, I., Costa-Pereira, J. T., & Martins, I. (2021). Monoaminergic and Opioidergic Modulation of Brainstem Circuits: New Insights Into the Clinical Challenges of Pain Treatment? In. Front. Pain Res. 2:696515. doi: 10.3389/fpain.2021.696515.
Taves, S., Berta, T., Chen, G., & Ji, R. R. (2013). Microglia and spinal cord synaptic plasticity in persistent pain. *Neural Plast*, *2013*, 753656. https://doi.org/10.1155/2013/753656
Taves, S., Berta, T., Liu, D. L., Gan, S., Chen, G., Kim, Y. H., Van de Ven, T., Laufer, S., & Ji, R. R. (2016). Spinal inhibition of p38 MAP kinase reduces inflammatory and neuropathic pain in male but not female mice: Sex-dependent microglial signaling in the spinal cord. *Brain Behav Immun*, *55*, 70-81. https://doi.org/10.1016/j.bbi.2015.10.006
Todd, A. J. (2010). Neuronal circuitry for pain processing in the dorsal horn. *Nat Rev Neurosci*, *11*(12), 823-836. https://doi.org/10.1038/nrn2947
Todd, A. J. (2017). Identifying functional populations among the interneurons in laminae I-III of the spinal dorsal horn. *Mol Pain*, *13*, 1744806917693003. https://doi.org/10.1177/1744806917693003
Todd, A. J. (2022). An Historical Perspective: The Second Order Neuron in the Pain Pathway. *Front Pain Res (Lausanne)*, *3*, 845211. https://doi.org/10.3389/fpain.2022.845211
Tsagareli, M. G., Nozadze, I. R., Gurtskaia, G. P., Carstens, M. I., Tsiklauri, N. J., & Carstens, E. E. (2013). Behavioral and Electrophysiological Study of Thermal and Mechanical Pain Modulation by TRP Channel Agonists. *Neurophysiology*, *45*(4), 329-339. https://doi.org/10.1007/s11062-013-9377-2
Tsuda, M. (2016). Microglia in the spinal cord and neuropathic pain. *J Diabetes Investig*, *7*(1), 17-26. https://doi.org/10.1111/jdi.12379
Tsuda, M., Mizokoshi, A., Shigemoto-Mogami, Y., Koizumi, S., & Inoue, K. (2004). Activation of p38 mitogen-activated protein kinase in spinal hyperactive microglia contributes to pain hypersensitivity following peripheral nerve injury. *Glia*, *45*(1), 89-95. https://doi.org/10.1002/glia.10308
Tsuda, M., Shigemoto-Mogami, Y., Koizumi, S., Mizokoshi, A., Kohsaka, S., Salter, M. W., & Inoue, K. (2003). P2X4 receptors induced in spinal microglia gate tactile allodynia after nerve injury. *Nature*, *424*(6950), 778-783. https://doi.org/10.1038/nature01786
Turan Yucel, N., Can, O. D., & Demir Ozkay, U. (2020). Catecholaminergic and opioidergic system mediated effects of reboxetine on diabetic neuropathic pain. *Psychopharmacology (Berl)*, *237*(4), 1131-1145. https://doi.org/10.1007/s00213-019-05443-5

Urban, R., Scherrer, G., Goulding, E. H., Tecott, L. H., & Basbaum, A. I. (2011). Behavioral indices of ongoing pain are largely unchanged in male mice with tissue or nerve injury-induced mechanical hypersensitivity. *Pain*, *152*(5), 990-1000. https://doi.org/10.1016/j.pain.2010.12.003

Vanelderen, P., Van Zundert, J., Kozicz, T., Puylaert, M., De Vooght, P., Mestrum, R., Heylen, R., Roubos, E., & Vissers, K. (2015). Effect of minocycline on lumbar radicular neuropathic pain: a randomized, placebo-controlled, double-blind clinical trial with amitriptyline as a comparator. *Anesthesiology*, *122*(2), 399-406. https://doi.org/10.1097/ALN.0000000000000508

Vargas-Alarcon, G., Fragoso, J. M., Cruz-Robles, D., Vargas, A., Martinez, A., Lao-Villadoniga, J. I., Garcia-Fructuoso, F., Vallejo, M., & Martinez-Lavin, M. (2009). Association of adrenergic receptor gene polymorphisms with different fibromyalgia syndrome domains. *Arthritis Rheum*, *60*(7), 2169-2173. https://doi.org/10.1002/art.24655

Verge, G. M., Milligan, E. D., Maier, S. F., Watkins, L. R., Naeve, G. S., & Foster, A. C. (2004). Fractalkine (CX3CL1) and fractalkine receptor (CX3CR1) distribution in spinal cord and dorsal root ganglia under basal and neuropathic pain conditions. *Eur J Neurosci*, *20*(5), 1150-1160. https://doi.org/10.1111/j.1460-9568.2004.03593.x

Viisanen, H., & Pertovaara, A. (2010). Roles of the rostroventromedial medulla and the spinal 5-HT(1A) receptor in descending antinociception induced by motor cortex stimulation in the neuropathic rat. *Neurosci Lett*, *476*(3), 133-137. https://doi.org/10.1016/j.neulet.2010.04.014

Volterra, A., & Meldolesi, J. (2005). Astrocytes, from brain glue to communication elements: the revolution continues. *Nat Rev Neurosci*, *6*(8), 626-640. https://doi.org/10.1038/nrn1722

Wang, D., Couture, R., & Hong, Y. (2014). Activated microglia in the spinal cord underlies diabetic neuropathic pain. *Eur J Pharmacol*, *728*, 59-66. https://doi.org/10.1016/j.ejphar.2014.01.057

Weir, M. R. (2009). Beta-blockers in the treatment of hypertension: are there clinically relevant differences? *Postgrad Med*, *121*(3), 90-98. https://doi.org/10.3810/pgm.2009.05.2007

Wilson, S. H., Hellman, K. M., James, D., Adler, A. C., & Chandrakantan, A. (2021). Mechanisms, diagnosis, prevention and management of perioperative opioid-induced hyperalgesia. *Pain Manag*, *11*(4), 405-417. https://doi.org/10.2217/pmt-2020-0105

Wolf, Y., Yona, S., Kim, K. W., & Jung, S. (2013). Microglia, seen from the CX3CR1 angle. *Front Cell Neurosci*, *7*, 26. https://doi.org/10.3389/fncel.2013.00026

Woolf, C. J., & Salter, M. W. (2000). Neuronal plasticity: increasing the gain in pain. *Science*, *288*(5472), 1765-1769. https://doi.org/10.1126/science.288.5472.1765

Wright, M. E., & Rizzolo, D. (2017). An update on the pharmacologic management and treatment of neuropathic pain. *JAAPA*, *30*(3), 13-17. https://doi.org/10.1097/01.JAA.0000512228.23432.f7

Xanthos, D. N., & Sandkuhler, J. (2014). Neurogenic neuroinflammation: inflammatory CNS reactions in response to neuronal activity. *Nat Rev Neurosci*, *15*(1), 43-53. https://doi.org/10.1038/nrn3617

Xu, Q., Ford, N. C., He, S., Huang, Q., Anderson, M., Chen, Z., Yang, F., Crawford, L. K., Caterina, M. J., Guan, Y., & Dong, X. (2021). Astrocytes contribute to pain gating in the spinal cord. *Sci Adv*, *7*(45), eabi6287. https://doi.org/10.1126/sciadv.abi6287

Xue, P., Chen, L., Lu, X., Zhang, J., Bao, G., Xu, G., Sun, Y., Guo, X., Jiang, J., Gu, H., & Cui, Z. (2017). Vimentin Promotes Astrocyte Activation After Chronic Constriction Injury. *J Mol Neurosci*, *63*(1), 91-99. https://doi.org/10.1007/s12031-017-0961-6

Yalcin, I., Tessier, L. H., Petit-Demouliere, N., Doridot, S., Hein, L., Freund-Mercier, M. J., & Barrot, M. (2009). Beta2-adrenoceptors are essential for desipramine, venlafaxine or reboxetine action in neuropathic pain. *Neurobiol Dis*, *33*(3), 386-394. https://doi.org/10.1016/j.nbd.2008.11.003

Yalcin, I., Tessier, L. H., Petit-Demoulière, N., Waltisperger, E., Hein, L., Freund-Mercier, M. J., & Barrot, M. (2010). Chronic treatment with agonists of beta(2)-adrenergic receptors in neuropathic pain. *Exp Neurol*, *221*(1), 115-121. https://doi.org/10.1016/j.expneurol.2009.10.008

Yao, Y., Echeverry, S., Shi, X. Q., Yang, M., Yang, Q. Z., Wang, G. Y., Chambon, J., Wu, Y. C., Fu, K. Y., De Koninck, Y., & Zhang, J. (2016). Dynamics of spinal microglia repopulation following an acute depletion. *Sci Rep*, *6*, 22839. https://doi.org/10.1038/srep22839

Yeo, S. I., Kim, J. E., Ryu, H. J., Seo, C. H., Lee, B. C., Choi, I. G., Kim, D. S., & Kang, T. C. (2011). The roles of fractalkine/CX3CR1 system in neuronal death following pilocarpine-induced status epilepticus. *J Neuroimmunol*, *234*(1-2), 93-102. https://doi.org/10.1016/j.jneuroim.2011.03.005

Yona, S., Kim, K. W., Wolf, Y., Mildner, A., Varol, D., Breker, M., Strauss-Ayali, D., Viukov, S., Guilliams, M., Misharin, A., Hume, D. A., Perlman, H., Malissen, B., Zelzer, E., & Jung, S.

(2013). Fate mapping reveals origins and dynamics of monocytes and tissue macrophages under homeostasis. *Immunity*, *38*(1), 79-91. https://doi.org/10.1016/j.immuni.2012.12.001

Zhang, F. F., Morioka, N., Abe, H., Fujii, S., Miyauchi, K., Nakamura, Y., Hisaoka-Nakashima, K., & Nakata, Y. (2016). Stimulation of spinal dorsal horn β2-adrenergic receptor ameliorates neuropathic mechanical hypersensitivity through a reduction of phosphorylation of microglial p38 MAP kinase and astrocytic c-jun N-terminal kinase. *Neurochem Int*, *101*, 144-155. https://doi.org/10.1016/j.neuint.2016.11.004

Zhang, H., Yoon, S. Y., Zhang, H., & Dougherty, P. M. (2012). Evidence that spinal astrocytes but not microglia contribute to the pathogenesis of Paclitaxel-induced painful neuropathy. *J Pain*, *13*(3), 293-303. https://doi.org/10.1016/j.jpain.2011.12.002

Zhang, T., Zhang, M., Cui, S., Liang, W., Jia, Z., Guo, F., Ou, W., Wu, Y., & Zhang, S. (2023). The core of maintaining neuropathic pain: Crosstalk between glial cells and neurons (neural cell crosstalk at spinal cord). *Brain Behav*, *13*(2), e2868. https://doi.org/10.1002/brb3.2868

Zhang, Y., Chen, K., Sloan, S. A., Bennett, M. L., Scholze, A. R., O'Keeffe, S., Phatnani, H. P., Guarnieri, P., Caneda, C., Ruderisch, N., Deng, S., Liddelow, S. A., Zhang, C., Daneman, R., Maniatis, T., Barres, B. A., & Wu, J. Q. (2014). An RNA-sequencing transcriptome and splicing database of glia, neurons, and vascular cells of the cerebral cortex. *J Neurosci*, *34*(36), 11929-11947. https://doi.org/10.1523/JNEUROSCI.1860-14.2014

Zhang, Z. J., Cao, D. L., Zhang, X., Ji, R. R., & Gao, Y. J. (2013). Chemokine contribution to neuropathic pain: respective induction of CXCL1 and CXCR2 in spinal cord astrocytes and neurons. *Pain*, *154*(10), 2185-2197. https://doi.org/10.1016/j.pain.2013.07.002

Zhao, X. F., Alam, M. M., Liao, Y., Huang, T., Mathur, R., Zhu, X., & Huang, Y. (2019). Targeting Microglia Using Cx3cr1-Cre Lines: Revisiting the Specificity. *eNeuro*, *6*(4). https://doi.org/10.1523/ENEURO.0114-19.2019

Zhuang, Z. Y., Kawasaki, Y., Tan, P. H., Wen, Y. R., Huang, J., & Ji, R. R. (2007). Role of the CX3CR1/p38 MAPK pathway in spinal microglia for the development of neuropathic pain following nerve injury-induced cleavage of fractalkine. *Brain Behav Immun*, *21*(5), 642-651. https://doi.org/10.1016/j.bbi.2006.11.003

Zhuang, Z. Y., Wen, Y. R., Zhang, D. R., Borsello, T., Bonny, C., Strichartz, G. R., Decosterd, I., & Ji, R. R. (2006). A peptide c-Jun N-terminal kinase (JNK) inhibitor blocks mechanical allodynia after spinal nerve ligation: respective roles of JNK activation in primary sensory neurons and spinal astrocytes for neuropathic pain development and maintenance. *J Neurosci*, *26*(13), 3551-3560. https://doi.org/10.1523/JNEUROSCI.5290-05.2006

Zhuo, M., & Gebhart, G. F. (1990). Characterization of descending inhibition and facilitation from the nuclei reticularis gigantocellularis and gigantocellularis pars alpha in the rat. *Pain*, *42*(3), 337-350. https://doi.org/10.1016/0304-3959(90)91147-B

Zoli, M., Jansson, A., Sykova, E., Agnati, L. F., & Fuxe, K. (1999). Volume transmission in the CNS and its relevance for neuropsychopharmacology. *Trends Pharmacol Sci*, *20*(4), 142-150. https://doi.org/10.1016/s0165-6147(99)01343-7

Zorec, R., Parpura, V., & Verkhratsky, A. (2018). Preventing neurodegeneration by adrenergic astroglial excitation. *FEBS J*, *285*(19), 3645-3656. https://doi.org/10.1111/febs.14456

8. Appendix

Exact p-values and interactions of each significant statistical result are listed in Table 14.

Table 14. Exact p-values and interactions.

Figure Number	Test	Exact p-value	F (interaction: treatment, operation)	p-value of F interaction
Figure 2C	Unpaired t-test	p = 0.0390		
Figure 3C	Unpaired t-test	INFγ p = 0.002519 IL-1α p = 0.007379 IL-9 p = 0.008750 IL-17 p = 0.004958 I-TAC p = 0.000281 MCP-1 p = 0.024476 MIG p = 0.007259 MIP-1γ p = 0.001475 SDF-1 p = 0.014283 TCA-3 p = 0.006518 TECK p = 0.026073 TNFα p = 0.039954		
Figure 4C	Unpaired t-test	p = 0.0115		
Figure 5B	Unpaired t-test	p = 0.0195		
Figure 6A (1h)	Repeated Two-way ANOVA	Saline vs 50 µg/kg Formoterol p = 0.0435 Saline vs 50 µg/kg Formoterol p = 0.0071	F (12, 72) = 1.365	p = 0.2029
Figure 6B (3h)	Repeated Two-way ANOVA	Saline vs 50 µg/kg Formoterol p = 0.0422 Saline vs 50 µg/kg Formoterol p = 0.0466	F (12, 68) = 1.452	p = 0.1646
Figure 7A (males)	Two-way ANOVA	Sham Saline vs SNI Saline p = 0.0039 SNI Saline vs SNI Formoterol p = 0.0106	F1, 18 = 3.35,	p = 0.0659
Figure 7A (females)	Two-way ANOVA	Sham Saline vs SNI Saline p = 0.0016 SNI Saline vs SNI Formoterol p = 0.0068	F1, 18 = 6.184	p = 0.0229
Figure 7B (males)	Two-way ANOVA	Sham Saline vs SNI Saline p = 0.0001 SNI Saline vs SNI Formoterol p = 0.0178	F1, 20 = 3.169;	p = 0.0903
Figure 7B (females)	Two-way ANOVA	Sham Saline vs SNI Saline p = 0.0003 SNI Saline vs SNI Formoterol p = 0.0299	F1, 18 = 5.561	p = 0.0299

Figure 7C (males)	Two-way ANOVA	Sham Saline vs SNI Saline p < 0.0001 SNI Saline vs SNI Formoterol p = 0.0005	F1, 20 = 8.808	p = 0.0076
Figure 7C (females)	Two-way ANOVA	Sham Saline vs SNI Saline p < 0.0001 SNI Saline vs SNI Formoterol p = 0.0052	F1, 18 = 4.913	p = 0.0398
Figure 8B (males)	Repeated two-way ANOVA	d6 - Sham Saline vs SNI Saline # p = 0.0091 SNI Saline vs SNI Formoterol *p = 0.0355 d21 - Sham Saline vs SNI Saline #p = 0.0242 SNI sal vs SNI Formoterol *p = 0.0033	F (9, 60) = 2.624	p = 0.8601
Figure 8B (females)	Repeated two-way ANOVA	d6 - Sham Saline vs SNI Saline #p = 0.0106 d21 - Sham Saline vs SNI Saline #p= 0.0221 SNI Saline vs SNI Formoterol *p = 0.050	F (9,63) = 3.337	p = 0.7632
Figure 8C (d6 - males)	Two-way ANOVA	Sham Saline vs SNI Saline p = 0.0002 SNI Saline vs SNI Formoterol p = 0.0143	F1, 22 = 3.338	p = 0.0813
Figure 8C (d6 - females)	Two-way ANOVA	Sham Saline vs SNI Saline p = 0.0021 SNI Saline vs SNI Formoterol p = 0.0104	F1, 21 = 9.356	p = 0.0060
Figure 8B (d21 - females)	Repeated two-way ANOVA	Sham Saline vs SNI Saline #p = 0.0221 SNI Saline vs SNI Formoterol *p = 0.050		
Figure 8D (d6 - females)	Two-way ANOVA	Sham Saline vs SNI Saline p < 0.0001 SNI Saline vs SNI Formoterol p = 0.0101	F1, 25 = 3.972	p = 0.0573
Figure 8D (d6 - females)	Two-way ANOVA	Sham Saline vs SNI Saline p < 0.0001 SNI Saline vs SNI Formoterol p = 0.0183	F1, 26 = 7.740	p = 0.0099
Figure 8C (d21 - males)	Two-way ANOVA	Sham Saline vs SNI Saline p < 0.0001 SNI Saline vs SNI Formoterol p = 0.0016	F1, 23 = 8.048	p = 0.0093
Figure 8C (d21 - males)	Two-way ANOVA	Sham Saline vs SNI Saline p = 0.0002 SNI Saline vs SNI Formoterol p = 0.0007	F1, 21 = 7.224	p = 0.0138
Figure 8D (d21 - males)	Two-way ANOVA	Sham Saline vs SNI Saline p < 0.0001	F1, 24 = 3.770	p = 0.0640

Figure 8D (d21 - females)	Two-way ANOVA	Sham Saline vs SNI Saline p < 0.0001	F1, 22 = 10.98	p = 0.0032
Figure 9B (males)	Unpaired t-test	p = 0.0480		
Figure 9B (females)	Unpaired t-test	p = 0.05		
Figure 9C (males)	Unpaired t-test	p = 0.033		
Figure 9C (females)	Unpaired t-test	p = 0.0120		
Figure 10B	Unpaired t-test	SNI Saline vs SNI Formoterol p = 0.0007		
Figure 11B	Unpaired t-test	SNI Saline vs SNI Formoterol p = 0.0091		
Figure 11C	Unpaired t-test	SNI Saline vs SNI Formoterol p = 0.0034		
Figure 12B (males)	Two-way ANOVA	Sham Saline vs SNI Saline p = 0.0026 SNI Saline vs SNI Formoterol p = 0.0084	F1, 13 = 4.350	p = 0.0573
Figure 12B (females)	Two-way ANOVA	Sham Saline vs SNI Saline p = 0.014 SNI Saline vs SNI Formoterol p = 0.0013	F1, 12 = 11.05	p = 0.0061
Figure 12D (males)	Two-way ANOVA	Sham Saline vs SNI Saline p < 0.0001 SNI Saline vs SNI Formoterol p = 0.0015	F1, 12 = 9.207	p = 0.0104
Figure 12D (females)	Two-way ANOVA	Sham Saline vs SNI Saline p < 0.0001 SNI Saline vs SNI Formoterol p < 0.0001	F1, 12 = 37.65	p < 0.0001
Figure 12E (males)	Two-way ANOVA	Sham Saline vs SNI Saline p < 0.0001 SNI Saline vs SNI Formoterol p = 0.0014	F1, 12 = 10.89	p = 0.0063
Figure 12E (females)	Two-way ANOVA	Sham Saline vs SNI Saline p < 0.0001 SNI Saline vs SNI Formoterol p < 0.0001	F1, 12 = 26.86	p = 0.0002
Figure 13B (males)	Two-way ANOVA	Sham Saline vs SNI Saline p = 0.0069 SNI Saline vs SNI Formoterol p = 0.0048	F1, 12 = 6.529	p = 0.0252
Figure 13B (females)	Two-way ANOVA	Sham Saline vs SNI Saline p = 0.0009 SNI Saline vs SNI Formoterol p = 0.0005	F1, 12 = 12.52	p = 0.0041
Figure 13D (males)	Two-way ANOVA	Sham Saline vs SNI Saline p = 0.0016 SNI Saline vs SNI Formoterol p = 0.0039	F1, 12 = 9.548	p = 0.0094

Figure 13D (females)	Two-way ANOVA	Sham Saline vs SNI Saline p = 0.0001 SNI Saline vs SNI Formoterol p = 0.0004	F1, 12 = 15.09	p = 0.0022
Figure 14 B (females)	Two-way ANOVA	Sham Saline vs SNI Saline p = 0.0494	F1, 12 = 1.835	p = 0.2005
Figure 15B (d6 - males)	Two-way ANOVA	Sham Saline vs SNI Saline p < 0.0001 SNI Saline vs SNI Formoterol p < 0.0001	F1, 12 = 22.62	p = 0.0005
Figure 15B (d6 - females)	Two-way ANOVA	Sham Saline vs SNI Saline p = 0.0003 SNI Saline vs SNI Formoterol p = 0.0016	F1, 12 = 10.28	p = 0.0075
Figure 16B (d6 - males)	Two-way ANOVA	Sham Saline vs SNI Saline p < 0.0001 SNI Saline vs SNI Formoterol p = 0.0014	F1, 12 = 9.737	p = 0.0088
Figure 16B (d6 - females)	Two-way ANOVA	Sham Saline vs SNI Saline p < 0.0001 SNI Saline vs SNI Formoterol p = 0.0002	F1, 12 = 16.83	p = 0.0015
Figure 16C (d6 - males)	Two-way ANOVA	Sham Saline vs SNI Saline p < 0.0001 SNI Saline vs SNI Formoterol p = 0.0014	F1, 12 = 10.78	p = 0.0065
Figure 16C (d6 - females)	Two-way ANOVA	Sham Saline vs SNI Saline p < 0.0001 SNI Saline vs SNI Formoterol p = 0.0001	F1, 12 = 20.92	p = 0.0006
Figure 17B (d6 - males)	Two-way ANOVA	Sham Saline vs SNI Saline p = 0.0004 SNI Saline vs SNI Formoterol p = 0.0004	F1, 12 = 15.50	p = 0.0020
Figure 17B (d6 - females)	Two-way ANOVA	Sham Saline vs SNI Saline p = 0.0021 SNI Saline vs SNI Formoterol p = 0.0081	F1, 12 = 8.325	p = 0.0137
Figure 17D (d6 - males)	Two-way ANOVA	Sham Saline vs SNI Saline p < 0.0002 SNI Saline vs SNI Formoterol p = 0.0009	F1, 12 = 15.84	p = 0.0018
Figure 17D (d6 - females)	Two-way ANOVA	Sham Saline vs SNI Saline p < 0.0003 SNI Saline vs SNI Formoterol p = 0.0009	F1, 12 = 12.27	p = 0.0044
Figure 18D (d6 - males)	Two-way ANOVA	Sham Saline vs SNI Saline p = 0.0035 SNI Saline vs SNI Formoterol p = 0.0259	F1, 12 = 7.089	p = 0.0207
Figure 18D (d6 - females)	Two-way ANOVA	Sham Saline vs SNI Saline p = 0.0013 SNI Saline vs SNI Formoterol p = 0.0178	F1, 12 = 8.117	p= 0.0146

Figure 15B (d21 - males)	Two-way ANOVA	Sham Saline vs SNI Saline p = 0.0005 SNI Saline vs SNI Formoterol p = 0.0013	F1, 13 = 10.86,	p = 0.0058
Figure 16B (d21 - males)	Two-way ANOVA	Sham Saline vs SNI Saline p < 0.0001 SNI Saline vs SNI Formoterol p < 0.0001	F1, 12 = 22.64	p = 0.0005
Figure 16B (d21 - females)	Two-way ANOVA	Sham Saline vs SNI Saline p = 0.0003	F1, 12 = 0.4001	p = 0.5389
Figure 16D (d21 - males)	Two-way ANOVA	Sham Saline vs SNI Saline p < 0.0001 SNI Saline vs SNI Formoterol p = 0.0006	F1, 12 = 14.27	p = 0.0026
Figure 16D (d21 - females)	Two-way ANOVA	Sham Saline vs SNI Saline p = 0.0051	F1, 12 = 1.159	p = 0.3028
Figure 17B (d21 - males)	Two-way ANOVA	Sham Saline vs SNI Saline p = 0.0003 SNI Saline vs SNI Formoterol p = 0.0013	F1, 12 = 11.09	p = 0.0060
Figure 17B (d21 - females)	Two-way ANOVA	Sham Saline vs SNI Saline p = 0.0011 SNI Saline vs SNI Formoterol p = 0.0215	F1, 12 = 11.01	p = 0.0061
Figure 17D (d21 - males)	Two-way ANOVA	Sham Saline vs SNI Saline p = 0.0233 SNI Saline vs SNI Formoterol p = 0.0056	F1, 12 = 7.225	p = 0.0197
Figure 17D (d21 - males)	Two-way ANOVA	Sham Saline vs SNI Saline p = 0.0001	F1, 12 = 3.269	p = 0.0957
Figure 17B (d21 - males)	Two-way ANOVA	Sham Saline vs SNI Saline sal p = 0.0016 SNI Saline vs SNI Formoterol p = 0.0124	F1, 12 = 5.003	p = 0.0451
Figure 17B (d21 - females)	Two-way ANOVA	Sham Saline vs SNI Saline p = 0.0023 SNI Saline vs SNI Formoterol p = 0.0284	F1, 12 = 8.059	p = 0.0149
Figure 18D (d21 - males)	Two-way ANOVA	Sham Saline vs SNI Saline p = 0.0394	F1, 13 = 2.850	p = 0.1152
Figure 18D (d21 - females)	Two-way ANOVA	Sham Saline vs SNI Saline p < 0.0001 SNI Saline vs SNI Formoterol p = 0.0041	F1, 12 = 12.89	p = 0.0037
Figure 19D (male)	Unpaired t-test	p = 0.0475		
Figure 19D (male)	Unpaired t-test	p =0.0198		
Figure 20B	Ordinary Two-way ANOVA	*Adrb2*$^{fl/fl}$ vs *Cx3cr1-Adrb2*$^{-/-}$ p = 0.0270	Tamoxifen = F (1, 7) = 11.03 Genotype = F (1, 7) = 0.1970	(Tamoxifen) p = 0.0127 (Genotype) p = 0.6705

		No tam *Cx3cr1-Adrb2$^{fl/fl}$* vs *Cx3cr1-Adrb2$^{-/-}$* p = 0.0493		
Figure 23A (d3)	Repeated Two-way ANOVA	*Adrb2$^{fl/fl}$* Sham Saline vs *Adrb2$^{fl/fl}$* SNI Saline p = 0.0198	F (9, 60) = 2.332	p = 0.0251
Figure 22B (d6)	Repeated Two-way ANOVA	*Adrb2$^{fl/fl}$* Sham Saline vs *Adrb2$^{fl/fl}$* SNI Saline p = 0.0026 *Cx3cr1-Adrb2$^{-/-}$* Sham Saline *vs Cx3cr1-Adrb2$^{-/-}$* SNI Saline p = 0.0065	F (9, 57) = 1.373	p = 0.2219
Figure 23A (d6)	Repeated Two-way ANOVA	*Adrb2$^{fl/fl}$* Sham Saline vs *Adrb2$^{fl/fl}$* SNI Saline p = 0.0024 *Cx3cr1-Adrb2$^{-/-}$* Sham Saline *vs Cx3cr1-Adrb2$^{-/-}$* SNI Saline p = 0.0135	F (9, 60) = 2.332	p = 0.0251
Figure 22D (d6)	Repeated Two-way ANOVA	*Adrb2$^{fl/fl}$* SNI Saline vs *Adrb2$^{fl/fl}$* SNI Formoterol p = 0.0489	F (9, 63) = 1.295	p = 0.2575
Figure 23C (d6)	Repeated Two-way ANOVA	*Adrb2$^{fl/fl}$* SNI Saline vs *Adrb2$^{fl/fl}$* SNI Formoterol p = 0.0024 *Adrb2$^{fl/fl}$* SNI Formoterol *vs Cx3cr1-Adrb2$^{-/-}$* SNI Formoterol p = 0.0113	F (9, 54) = 2.844	p = 0.0081
Figure 22B (d3)	Two-way ANOVA	*Adrb2$^{fl/fl}$* Sham Saline vs *Adrb2$^{fl/fl}$* SNI Saline p = 0.0287 *Cx3cr1-Adrb2$^{-/-}$* Sham Saline *vs Cx3cr1-Adrb2$^{-/-}$* SNI Saline p = 0.0335	F (1, 20) = 0.002664	p = 0.9594
Figure 23A (d3)	Two-way ANOVA	*Adrb2$^{fl/fl}$* Sham Saline vs *Adrb2$^{fl/fl}$* SNI Saline p = 0.0034 *Cx3cr1-Adrb2$^{-/-}$* Sham Saline *vs Cx3cr1-Adrb2$^{-/-}$* SNI Saline p = 0.0237	F (1, 20) = 0.1615	p = 0.6920
Figure 22B (d6)	Two-way ANOVA	*Adrb2$^{fl/fl}$* Sham Saline vs *Adrb2$^{fl/fl}$* SNI Saline p = 0.0003 *Cx3cr1-Adrb2$^{-/-}$* Sham Saline *vs Cx3cr1-Adrb2$^{-/-}$* SNI Saline p = 0.0331	F (1, 20) = 2.190	p = 0.1545
Figure 23A (d6)	Two-way ANOVA	*Adrb2$^{fl/fl}$* Sham Saline vs *Adrb2$^{fl/fl}$* SNI Saline p = 0.0052 *Cx3cr1-Adrb2$^{-/-}$* Sham Saline *vs Cx3cr1-Adrb2$^{-/-}$* SNI Saline p = 0.0183	F (1, 20) = 0.03553	p = 0.8524

Figure 22D (d6)	Two-way ANOVA	*Adrb2*$^{fl/fl}$ SNI Saline vs *Adrb2*$^{fl/fl}$ SNI Formoterol p = 0.0002 *Adrb2*$^{fl/fl}$ SNI Formoterol *vs* *Cx3cr1-Adrb2*$^{-/-}$ SNI Formoterol p = 0.0001	F (1, 21) = 15.40	p = 0.0008
Figure 23C (d6)	Two-way ANOVA	*Adrb2*$^{fl/fl}$ Sham Saline vs *Adrb2*$^{fl/fl}$ SNI Saline p = 0.0002 *Cx3cr1-Adrb2*$^{-/-}$ Sham Saline *vs Cx3cr1-Adrb2*$^{-/-}$ SNI Saline p = 0.0002	F (1, 23) = 11.87	p = 0.0022
Figure 24A (d3)	Two-way ANOVA	*Adrb2*$^{fl/fl}$ Sham Saline vs *Adrb2*$^{fl/fl}$ SNI Saline p < 0.0001 *Cx3cr1-Adrb2*$^{-/-}$ Sham Saline *vs Cx3cr1-Adrb2*$^{-/-}$ SNI Saline p < 0.0001	F (1, 20) = 2.025	p = 0.1701
Figure 24A (d3)	Two-way ANOVA	*Adrb2*$^{fl/fl}$ Sham Saline vs *Adrb2*$^{fl/fl}$ SNI Saline p < 0.0001 *Cx3cr1-Adrb2*$^{-/-}$ Sham Saline *vs Cx3cr1-Adrb2*$^{-/-}$ SNI Saline p < 0.0001	F (1, 21) = 0.5318	p = 0.4739
Figure 24A (d6)	Two-way ANOVA	*Adrb2*$^{fl/fl}$ Sham Saline vs *Adrb2*$^{fl/fl}$ SNI Saline p < 0.0001 *Cx3cr1-Adrb2*$^{-/-}$ Sham Saline *vs Cx3cr1-Adrb2*$^{-/-}$ SNI Saline p < 0.0001	F (1, 20) = 1.594	p = 0.2213
Figure 24A (d6)	Two-way ANOVA	*Adrb2*$^{fl/fl}$ Sham Saline vs *Adrb2*$^{fl/fl}$ SNI Saline p < 0.0001 *Cx3cr1-Adrb2*$^{-/-}$ Sham Saline *vs Cx3cr1-Adrb2*$^{-/-}$ SNI Saline p < 0.0001	F (1, 21) = 0.01587	p = 0.9010
Figure 24C (d6)	Two-way ANOVA	*Adrb2*$^{fl/fl}$ SNI Saline vs *Adrb2*$^{fl/fl}$ SNI Formoterol p < 0.0001 *Adrb2*$^{fl/fl}$ SNI Formoterol *vs* *Cx3cr1-Adrb2*$^{-/-}$ SNI Formoterol p < 0.0001	F (1, 22) = 15.79	p = 0.0006
Figure 24C (d6)	Two-way ANOVA	*Adrb2*$^{fl/fl}$ SNI Saline vs *Adrb2*$^{fl/fl}$ SNI Formoterol p < 0.0001 *Adrb2*$^{fl/fl}$ SNI Formoterol *vs* *Cx3cr1-Adrb2*$^{-/-}$ SNI Formoterol p < 0.0001	F (1, 23) = 13.89	p = 0.0011
Figure 22B (d21)	Repeated Two-way ANOVA	*Adrb2*$^{fl/fl}$ Sham Saline vs *Adrb2*$^{fl/fl}$ SNI Saline p = 0.05 *Cx3cr1-Adrb2*$^{-/-}$ Sham Saline *vs Cx3cr1-Adrb2*$^{-/-}$ SNI Saline p = 0.045	F (9, 57) = 1.373	p = 0.2219

Figure 23A (d21)	Repeated Two-way ANOVA	*Adrb2*$^{fl/fl}$ Sham Saline vs *Adrb2*$^{fl/fl}$ SNI Saline p = 0.0076 *Cx3cr1-Adrb2*$^{-/-}$ Sham Saline *vs Cx3cr1-Adrb2*$^{-/-}$ SNI Saline p = 0.078	F (9, 60) = 2.332	p = 0.0251
Figure 23C (d21)	Repeated Two-way ANOVA	*Adrb2*$^{fl/fl}$ SNI Saline vs *Adrb2*$^{fl/fl}$ SNI Formoterol p = 0.0461	F (9, 54) = 2.844	p = 0.0081
Figure 22A (d21)	Two-way ANOVA	*Adrb2*$^{fl/fl}$ Sham Saline vs *Adrb2*$^{fl/fl}$ SNI Saline p < 0.0001 *Cx3cr1-Adrb2*$^{-/-}$ Sham Saline *vs Cx3cr1-Adrb2*$^{-/-}$ SNI Saline p = 0.0045	F (1, 20) = 1.561	p = 0.2259
Figure 23A (d21)	Two-way ANOVA	*Adrb2*$^{fl/fl}$ Sham Saline vs *Adrb2*$^{fl/fl}$ SNI Saline p < 0.0003 *Cx3cr1-Adrb2*$^{-/-}$ Sham Saline *vs Cx3cr1-Adrb2*$^{-/-}$ SNI Saline p = 0.0016	F (1, 21) = 0.1580	p = 0.6950
Figure 22C (d21)	Two-way ANOVA	*Adrb2*$^{fl/fl}$ SNI Saline vs *Adrb2*$^{fl/fl}$ SNI Formoterol p = 0.0015 *Adrb2*$^{fl/fl}$ SNI Formoterol *vs Cx3cr1-Adrb2*$^{-/-}$ SNI Formoterol p = 0.128	F (1, 20) = 7.254	p = 0.0140
Figure 23C (d21)	Two-way ANOVA	*Adrb2*$^{fl/fl}$ SNI Saline vs *Adrb2*$^{fl/fl}$ SNI Formoterol p = 0.0002 *Adrb2*$^{fl/fl}$ SNI Formoterol *vs Cx3cr1-Adrb2*$^{-/-}$ SNI Formoterol p = 0.003	F (1, 23) = 11.86	p = 0.0022
Figure 24A (d21)	Two-way ANOVA	*Adrb2*$^{fl/fl}$ Sham Saline vs *Adrb2*$^{fl/fl}$ SNI Saline p < 0.0001 *Cx3cr1-Adrb2*$^{-/-}$ Sham Saline *vs Cx3cr1-Adrb2*$^{-/-}$ SNI Saline p < 0.0001	F (1, 20) = 2.163	p = 0.1569
Figure 24A (d21)	Two-way ANOVA	*Adrb2*$^{fl/fl}$ Sham Saline vs *Adrb2*$^{fl/fl}$ SNI Saline p < 0.0001 *Cx3cr1-Adrb2*$^{-/-}$ Sham Saline *vs Cx3cr1-Adrb2*$^{-/-}$ SNI Saline p < 0.0001	F (1, 21) = 0.4245	p = 0.5218
Figure 24C (d21)	Two-way ANOVA	*Adrb2*$^{fl/fl}$ SNI Saline vs *Adrb2*$^{fl/fl}$ SNI Formoterol p < 0.0001 *Adrb2*$^{fl/fl}$ SNI Formoterol *vs Cx3cr1-Adrb2*$^{-/-}$ SNI Formoterol p = 0.0041 *Cx3cr1-Adrb2*$^{-/-}$ SNI Saline vs *Cx3cr1-Adrb2*$^{-/-}$ SNI Formoterol p = 0.0232	F (1, 22) = 4.042	p = 0.0568

Figure 24C (d21)	Two-way ANOVA	*Adrb2*$^{fl/fl}$ SNI Saline vs *Adrb2*$^{fl/fl}$ SNI Formoterol p = 0.0011 *Adrb2*$^{fl/fl}$ SNI Formoterol *vs* *Cx3cr1-Adrb2*$^{-/-}$ SNI Formoterol p = 0.0056	F (1, 23) = 3.283	p = 0.0831
Figure Number	**Test**	**Exact p-value**	**F (interaction: genotype, treatment, operation)**	**p-value of F interaction**
Figure 26A (males)	Three-way ANOVA	*Adrb2*$^{fl/fl}$ SNI Formoterol vs. *Cx3cr1-Adrb2*$^{-/-}$ SNI Formoterol p =0.0002 *Adrb2*$^{fl/fl}$ SNI Saline vs. *Adrb2*$^{fl/fl}$ SNI Formoterol p = 0.0003 *Adrb2*$^{fl/fl}$ Sham Saline vs. *Adrb2*$^{fl/fl}$ SNI Saline p = 0.0011 *Cx3cr1-Adrb2*$^{-/-}$ Sham Saline vs. *Cx3cr1-Adrb2*$^{-/-}$ SNI Saline p = 0.0193 *Cx3cr1-Adrb2*$^{-/-}$ Sham Formoterol vs. *Cx3cr1-Adrb2*$^{-/-}$SNI Formoterol p = 0.0021	F (1, 21) = 9.435	p = 0.0058
Figure 26A (females)	Three-way ANOVA	*Adrb2*$^{fl/fl}$ SNI Formoterol vs. *Cx3cr1-Adrb2*$^{-/-}$ SNI Formoterol p =0.0015 *Adrb2*$^{fl/fl}$ SNI Saline vs. *Adrb2*$^{fl/fl}$ SNI Formoterol p = 0.0015 *Adrb2*$^{fl/fl}$ Sham Saline vs. *Adrb2*$^{fl/fl}$ SNI Saline p = 0.0017 *Cx3cr1-Adrb2*$^{-/-}$ Sham Saline vs. *Cx3cr1-Adrb2*$^{-/-}$ SNI Saline p = 0.0140 *Cx3cr1-Adrb2*$^{-/-}$ Sham Formoterol vs. *Cx3cr1-Adrb2*$^{-/-}$SNI Formoterol p = 0.0025	F (1, 17) = 7.441	p = 0.0143
Figure 26B (males)	Three-way ANOVA	*Adrb2*$^{fl/fl}$ SNI Formoterol vs. *Cx3cr1-Adrb2*$^{-/-}$ SNI Formoterol p < 0.0001 *Adrb2*$^{fl/fl}$ SNI Saline vs. *Adrb2*$^{fl/fl}$ SNI Formoterol p < 0.0001 *Adrb2*$^{fl/fl}$ Sham Saline vs. *Adrb2*$^{fl/fl}$ SNI Saline p = 0.0017 *Cx3cr1-Adrb2*$^{-/-}$ Sham Saline vs. *Cx3cr1-Adrb2*$^{-/-}$ SNI Saline p = 0.0002	F (1, 25) = 7.888	p = 0.0095

		Cx3cr1-Adrb2$^{-/-}$ Sham Formoterol vs. *Cx3cr1-Adrb2*$^{-/-}$ SNI Formoterol p = 0.0005		
Figure 28A (males)	Three-way ANOVA	*Adrb2*$^{fl/fl}$ SNI Formoterol vs. *Cx3cr1-Adrb2*$^{-/-}$ SNI Formoterol p < 0.0001 *Adrb2*$^{fl/fl}$ SNI Saline vs. *Adrb2*$^{fl/fl}$ SNI Formoterol p < 0.0001 *Adrb2*$^{fl/fl}$ Sham Saline vs. *Adrb2*$^{fl/fl}$ SNI Saline p = 0.0003 *Cx3cr1-Adrb2*$^{-/-}$ Sham Saline vs. *Cx3cr1-Adrb2*$^{-/-}$ SNI Saline p < 0.0001 *Cx3cr1-Adrb2*$^{-/-}$ Sham Formoterol vs. *Cx3cr1-Adrb2*$^{-/-}$ SNI Formoterol p < 0.0001	F (1, 21) = 9.832	p = 0.0050
Figure 28A (females)	Three-way ANOVA	*Adrb2*$^{fl/fl}$ SNI Formoterol vs. *Cx3cr1-Adrb2*$^{-/-}$ SNI Formoterol p < 0.0001 *Adrb2*$^{fl/fl}$ SNI Saline vs. *Adrb2*$^{fl/fl}$ SNI Formoterol p = 0.0002 *Adrb2*$^{fl/fl}$ Sham Saline vs. *Adrb2*$^{fl/fl}$ SNI Saline p < 0.0001 *Cx3cr1-Adrb2*$^{-/-}$ Sham Saline vs. *Cx3cr1-Adrb2*$^{-/-}$ SNI Saline p = 0.0005 *Cx3cr1-Adrb2*$^{-/-}$ Sham Formoterol vs. *Cx3cr1-Adrb2*$^{-/-}$ SNI Formoterol p < 0.0001	F (1, 17) = 16.99	p = 0.0007
Figure 28B (males)	Three-way ANOVA	*Adrb2*$^{fl/fl}$ SNI Formoterol vs. *Cx3cr1-Adrb2*$^{-/-}$ SNI Formoterol p < 0.0001 *Adrb2*$^{fl/fl}$ SNI Saline vs. *Adrb2*$^{fl/fl}$ SNI Formoterol p = 0.0004 *Adrb2*$^{fl/fl}$ Sham Saline vs. *Adrb2*$^{fl/fl}$ SNI Saline p = 0.0002 *Cx3cr1-Adrb2*$^{-/-}$ Sham Saline vs. *Cx3cr1-Adrb2*$^{-/-}$ SNI Saline p < 0.0001 *Cx3cr1-Adrb2*$^{-/-}$ Sham Formoterol vs. *Cx3cr1-Adrb2*$^{-/-}$ SNI Formoterol p < 0.0001	F (1, 23) = 7.050	p = 0.0141
Figure 28B (females)	Three-way ANOVA	*Adrb2*$^{fl/fl}$ SNI Formoterol vs. *Cx3cr1-Adrb2*$^{-/-}$ SNI Formoterol p < 0.0001	F (1, 20) = 5.365	p = 0.0313

		Adrb2$^{fl/fl}$ SNI Saline vs. *Adrb2*$^{fl/fl}$ SNI Formoterol p = 0.0002 *Adrb2*$^{fl/fl}$ Sham Saline vs. *Adrb2*$^{fl/fl}$ SNI Saline p = 0.0011 *Cx3cr1-Adrb2*$^{-/-}$ Sham Saline vs. *Cx3cr1-Adrb2*$^{-/-}$ SNI Saline p = 0.0007 *Cx3cr1-Adrb2*$^{-/-}$Sham Formoterol vs. *Cx3cr1-Adrb2*$^{-/-}$ SNI Formoterol p = 0.0001		
Figure 28A (males)	Three-way ANOVA	*Adrb2*$^{fl/fl}$ SNI Formoterol vs. *Cx3cr1-Adrb2*$^{-/-}$ SNI Formoterol p < 0.0001 *Adrb2*$^{fl/fl}$ SNI Saline vs. *Adrb2*$^{fl/fl}$ SNI Formoterol p < 0.0001 *Adrb2*$^{fl/fl}$ Sham Saline vs. *Adrb2*$^{fl/fl}$ SNI Saline p < 0.0001 *Cx3cr1-Adrb2*$^{-/-}$ Sham Saline vs. *Cx3cr1-Adrb2*$^{-/-}$ SNI Saline p < 0.0001 *Cx3cr1-Adrb2*$^{-/-}$ Sham Formoterol vs. *Cx3cr1-Adrb2*$^{-/-}$ SNI Formoterol p < 0.0001	F (1, 21) = 12.53	p = 0.0019
Figure 28A (females)	Three-way ANOVA	*Adrb2*$^{fl/fl}$ SNI Formoterol vs. *Cx3cr1-Adrb2*$^{-/-}$ SNI Formoterol p = 0.0002 *Adrb2*$^{fl/fl}$ SNI Saline vs. *Adrb2*$^{fl/fl}$ SNI Formoterol p = 0.0005 *Adrb2*$^{fl/fl}$ Sham Saline vs. *Adrb2*$^{fl/fl}$ SNI Saline p = 0.0002 *Cx3cr1-Adrb2*$^{-/-}$ Sham Saline vs. *Cx3cr1-Adrb2*$^{-/-}$ SNI Saline p = 0.0009 *Cx3cr1-Adrb2*$^{-/-}$ Sham Formoterol vs. *Cx3cr1-Adrb2*$^{-/-}$ SNI Formoterol p = 0.0003	F (1, 17) = 8.172	p = 0.0109
Figure 28B (males)	Three-way ANOVA	*Adrb2*$^{fl/fl}$ SNI Formoterol vs. *Cx3cr1-Adrb2*$^{-/-}$ SNI Formoterol p < 0.0001 *Adrb2*$^{fl/fl}$ SNI Saline vs. *Adrb2*$^{fl/fl}$ SNI Formoterol p < 0.0001 *Adrb2*$^{fl/fl}$ Sham Saline vs. *Adrb2*$^{fl/fl}$ SNI Saline p < 0.0001	F (1, 23) = 12.32	p = 0.0019

		Cx3cr1-Adrb2$^{-/-}$ Sham Saline vs. *Cx3cr1-Adrb2*$^{-/-}$ SNI Saline p < 0.0001 *Cx3cr1-Adrb2*$^{-/-}$ Sham Formoterol vs. *Cx3cr1-Adrb2*$^{-/-}$ SNI Formoterol p < 0.0001		
Figure 28B (males)	Three-way ANOVA	*Adrb2*$^{fl/fl}$ SNI Formoterol vs. *Cx3cr1-Adrb2*$^{-/-}$ SNI Formoterol p = 0.0006 *Adrb2*$^{fl/fl}$ SNI Saline vs. *Adrb2*$^{fl/fl}$ SNI Formoterol p < 0.0001 *Adrb2*$^{fl/fl}$ Sham Saline vs. *Adrb2*$^{fl/fl}$ SNI Saline p < 0.0001	F (1, 22) = 14.51	p = 0.0010
Figure 30A (males)	Three-way ANOVA	*Adrb2*$^{fl/fl}$ SNI Formoterol vs. *Cx3cr1-Adrb2*$^{-/-}$ SNI Formoterol p = 0.0004 *Cx3cr1-Adrb2*$^{-/-}$ Sham Saline vs. *Cx3cr1-Adrb2*$^{-/-}$ SNI Saline p = 0.0057 *Cx3cr1-Adrb2*$^{-/-}$ Sham Formoterol vs. *Cx3cr1-Adrb2*$^{-/-}$ SNI Formoterol p = 0.0003	F (1, 21) = 2.376	p = 0.1381
Figure 30A (females)	Three-way ANOVA	*Adrb2*$^{fl/fl}$ SNI Formoterol vs. *Cx3cr1-Adrb2*$^{-/-}$ SNI Formoterol p = 0.002 *Adrb2*$^{fl/fl}$ SNI Saline vs. *Adrb2*$^{fl/fl}$ SNI Formoterol p = 0.0013 *Adrb2*$^{fl/fl}$ Sham Saline vs. *Adrb2*$^{fl/fl}$ SNI Saline p = 0.001 *Cx3cr1-Adrb2*$^{-/-}$ Sham Saline vs. *Cx3cr1-Adrb2*$^{-/-}$ SNI Saline p = 0.0003 *Cx3cr1-Adrb2*$^{-/-}$ Sham Formoterol vs. *Cx3cr1-Adrb2*$^{-/-}$ SNI Formoterol p < 0.0001	F (1, 17) = 6.704	p = 0.0191
Figure 30B (males)	Three-way ANOVA	*Adrb2*$^{fl/fl}$ SNI Formoterol vs. *Cx3cr1-Adrb2*$^{-/-}$ SNI Formoterol p = 0.0141 *Adrb2*$^{fl/fl}$ SNI Saline vs. *Adrb2*$^{fl/fl}$ SNI Formoterol p = 0.0127 *Adrb2*$^{fl/fl}$ Sham Saline vs. *Adrb2*$^{fl/fl}$ SNI Saline p = 0.022 *Cx3cr1-Adrb2*$^{-/-}$ Sham Saline vs. *Cx3cr1-Adrb2*$^{-/-}$ SNI Saline p = 0.0158	F (1, 25) = 3.529	p = 0.0720

		Cx3cr1-Adrb2$^{-/-}$ Sham Formoterol vs. *Cx3cr1-Adrb2*$^{-/-}$ SNI Formoterol p = 0.0161		
Figure 30B (females)	Three-way ANOVA	*Adrb2*$^{fl/fl}$ SNI Formoterol vs. *Cx3cr1-Adrb2*$^{-/-}$ SNI Formoterol p < 0.0001 *Adrb2*$^{fl/fl}$ SNI Saline vs. *Adrb2*$^{fl/fl}$ SNI Formoterol p < 0.0001 *Adrb2*$^{fl/fl}$ Sham Saline vs. *Adrb2*$^{fl/fl}$ SNI Saline p < 0.0001*Cx3cr1-Adrb2*$^{-/-}$ Sham Saline vs. *Cx3cr1-Adrb2*$^{-/-}$ SNI Saline p < 0.0001 *Cx3cr1-Adrb2*$^{-/-}$ Sham Formoterol vs. *Cx3cr1-Adrb2*$^{-/-}$ SNI Formoterol p = 0.0006	F (1, 23) = 9.045	p = 0.0063
Figure 32A (males)	Three-way ANOVA	*Adrb2*$^{fl/fl}$ SNI Formoterol vs. *Cx3cr1-Adrb2*$^{-/-}$ SNI Formoterol p < 0.0001 *Adrb2*$^{fl/fl}$ Sham Saline vs. *Adrb2*$^{fl/fl}$ SNI Saline p = 0.0483 *Cx3cr1-Adrb2*$^{-/-}$ Sham Saline vs. *Cx3cr1-Adrb2*$^{-/-}$ SNI Saline p = 0.0004 *Cx3cr1-Adrb2*$^{-/-}$ Sham Formoterol vs. *Cx3cr1-Adrb2*$^{-/-}$ SNI Formoterol p < 0.0001	F (1, 21) = 4.678	p = 0.0422
Figure 32A (females)	Three-way ANOVA	*Adrb2*$^{fl/fl}$ SNI Formoterol vs. *Cx3cr1-Adrb2*$^{-/-}$ SNI Formoterol p < 0.0001 *Adrb2*$^{fl/fl}$ SNI Saline vs. *Adrb2*$^{fl/fl}$ SNI Formoterol p = 0.0019 *Adrb2*$^{fl/fl}$ Sham Saline vs. *Adrb2*$^{fl/fl}$ SNI Saline p = 0.0053 *Cx3cr1-Adrb2*$^{-/-}$ Sham Saline vs. *Cx3cr1-Adrb2*$^{-/-}$ SNI Saline p < 0.0001 *Cx3cr1-Adrb2*$^{-/-}$ Sham Formoterol vs. *Cx3cr1-Adrb2*$^{-/-}$SNI Formoterol p = 0.0004	F (1, 17) = 3.660	p = 0.0727
Figure 32B (males)	Three-way ANOVA	*Adrb2*$^{fl/fl}$ SNI Formoterol vs. *Cx3cr1-Adrb2*$^{-/-}$ SNI Formoterol p = 0.0004 *Adrb2*$^{fl/fl}$ SNI Saline vs. *Adrb2*$^{fl/fl}$ SNI Formoterol p = 0.0003	F (1, 26) = 7.075	p = 0.0132

		Adrb2$^{fl/fl}$ Sham Saline vs. *Adrb2*$^{fl/fl}$ SNI Saline p = 0.0004 *Cx3cr1-Adrb2*$^{-/-}$ Sham Saline vs. *Cx3cr1-Adrb2*$^{-/-}$ SNI Saline p = 0.0003 *Cx3cr1-Adrb2*$^{-/-}$ Sham Formoterol vs. *Cx3cr1-Adrb2*$^{-/-}$ SNI Formoterol p = 0.0004		
Figure 32B (females)	Three-way ANOVA	*Adrb2*$^{fl/fl}$ SNI Formoterol vs. *Cx3cr1-Adrb2*$^{-/-}$ SNI Formoterol p = 0.0178 *Adrb2*$^{fl/fl}$ SNI Saline vs. *Adrb2*$^{fl/fl}$ SNI Formoterol p = 0.0006 *Adrb2*$^{fl/fl}$ Sham Saline vs. *Adrb2*$^{fl/fl}$ SNI Saline p = 0.0012 *Cx3cr1-Adrb2*$^{-/-}$ Sham Saline vs. *Cx3cr1-Adrb2*$^{-/-}$ SNI Saline p = 0.03863 *Cx3cr1-Adrb2*$^{-/-}$:Sham Formoterol vs. *Cx3cr1-Adrb2*$^{-/-}$ SNI Formoterol p = 0.0134	F (1, 23) = 5.378	p = 0.0296
Figure 34B (males)	Three-way ANOVA	*Adrb2*$^{fl/fl}$ SNI Saline vs. *Adrb2*$^{fl/fl}$ SNI Formoterol p = 0.0103 *Cx3cr1-Adrb2*$^{-/-}$ Sham Formoterol vs. *Cx3cr1-Adrb2*$^{-/-}$ SNI Formoterol p = 0.0034	F (1, 25) = 0.02688	p = 0.8711
Figure 34B (females)	Three-way ANOVA	*Adrb2*$^{fl/fl}$ SNI Saline vs. *Adrb2*$^{fl/fl}$ SNI Formoterol p = 0.0116 *Cx3cr1-Adrb2*$^{-/-}$ SNI Saline vs *Cx3cr1-Adrb2*$^{-/-}$ SNI Formoterol p = 0.0026 *Adrb2*$^{fl/fl}$ Sham Saline vs. *Adrb2*$^{fl/fl}$ SNI Saline p = 0.0337 *Cx3cr1-Adrb2*$^{-/-}$ Sham Saline vs. *Cx3cr1-Adrb2*$^{-/-}$ SNI Saline p = 0.0003	F (1, 23) = 0.1867	p = 0.6697
Figure 36A (males)	Three-way ANOVA	*Adrb2*$^{fl/fl}$ SNI Saline vs. *Adrb2*$^{fl/fl}$ SNI Formoterol p = 0.0094 *Adrb2*$^{fl/fl}$ Sham Saline vs. *Adrb2*$^{fl/fl}$ SNI Saline p = 0.0004 *Cx3cr1-Adrb2*$^{-/-}$ Sham Saline vs. *Cx3cr1-Adrb2*$^{-/-}$ SNI Saline p = 0.0150	F (1, 21) = 6.226	p = 0.0210

Figure 36B (males)	Three-way ANOVA	*Adrb2*$^{fl/fl}$ Sham Saline vs. *Adrb2*$^{fl/fl}$ SNI Saline p = 0.0090 *Cx3cr1-Adrb2*$^{-/-}$ Sham Saline vs. *Cx3cr1-Adrb2*$^{-/-}$ SNI Saline p = 0.0031 *Cx3cr1-Adrb2*$^{-/-}$ Sham Formoterol vs. *Cx3cr1-Adrb2*$^{-/-}$ SNI Formoterol p = 0.0165	F (1, 26) = 1.452	p = 0.2391
Figure 36B (females)	Three-way ANOVA	*Adrb2*$^{fl/fl}$ SNI Saline vs. *Adrb2*$^{fl/fl}$ SNI Formoterol p = 0.0036 *Adrb2*$^{fl/fl}$ Sham Saline vs. *Adrb2*$^{fl/fl}$SNI Saline p = 0.0028	F (1, 23) = 1.174	p = 0.2897

9. Acknowledgements

First and foremost, I would like to express my gratitude to my dissertation advisor Prof. Dr. Rohini Kuner for her kind support, excellent mentoring, and for her insightful feedback. Her expertise and extensive knowledge have been instrumental in shaping this thesis, and her guidance has been invaluable in navigating the academic challenges of my Ph.D. journey.

I extend my heartfelt thanks to my supervisor Dr. Manuela Simonetti, who provided me with inestimable guidance and support throughout my Ph.D. research. Thank you for your patience and selfless help during my academic difficulties. Your effort in engaging in discussions with me and challenging my scientific thinking and views have trained me to be a better researcher.

I would like to thank Prof. Dr. Frank Kirchhoff, Dr. Amit Agarwal, and the researchers in their labs for their generous academic assistance. It was always a pleasure to discuss with them.

Likewise, I am grateful to the past and present members of the laboratory and the department of Pharmacology: Dr. Anke Tappe-Theodor, Dr. Katrin Schrenk-Siemens, Dr. Nitin Agarwal, Dr. Manfred Oswald, Dr. Carmen la Porta, Dr. Ylenia Capodanno, Dr. Sheng Liu, Dunja Baumgartl-Ahlert, Christl Gartner, Nadine Gehrig, Karin Meyer, Angela di Turi, Zheng Gan, Deepti Mittal, Amandine Prats, Juhyun Kang, Marzia Matejcek, Lea Grams, Theresa Roth, Alina Stegemann and Leah Zerlin, for providing me expertise, helpful advice and resources over the years; your friendliness makes our lab such a pleasant place to work. A special thanks to Nicolas Mandel, who was always there for me during the ups and downs of the Ph.D.

I am thankful to my friends, who have been a constant source of encouragement and cheer. They made me feel at home in Heidelberg.

Without Antonio´s unwavering support, I would have not been able to overcome the numerous challenges that came with pursuing a Ph.D. His firm belief in my abilities, even in times when I doubted myself, provided me with the motivation and inspiration I needed to keep pushing forward. Thank you for being my rock, my confidante, and my partner throughout this journey.

This would not have been possible without the sincere love of my family. I am highly grateful to my parents and my brother for always being there to comfort me and make me feel like I’m capable of anything.

10. Publications

- **Damo, Elisa,** Amit Agarwal, Simonetti, Manuela. (2023). Activation of beta2-Adrenergic Receptors in Microglia Alleviates Neuropathic Hypersensitivity in Mice. *Cells, 12(2)*, 284. doi: 10.3390/cells12020284

- **Damo, Elisa,** Simonetti, Manuela. (2022). Axon Guidance Molecules and Pain. *Cells*, 11(19), 3143. doi: 10.3390/cells11193143

- **Damo, Elisa**, Rieder, Phillip, Coban, Ilknur, Silva, Rangel Leal, Kirchhoff, Frank, Simonetti, Manuela, Agarwal, Amit. (2022). Glial cells as target for antidepressants in neuropathic pain. *Neuroforum*, 28(2), 85-94. doi: 10.1515/nf-2021-0036

    - **Chosen for cover: Damo, Elisa**, Rieder, Phillip. Cover Illustration for Neuroforum, 2022, 28(2). doi: 10.1515/nf-2022-frontmatter2

- Rieder, Phillip, Gobbo, Davide, Stopper, Gebhard, Welle, Anne, **Damo, Elisa,** Kirchhoff, Frank and Scheller, Anja. (2022). Astrocytes and Microglia Exhibit Cell-Specific Ca2+ Signaling Dynamics in the Murine Spinal Cord. *Front Mol Neurosci*, 15, 840948. doi: 10.3389/fnmol.2022.840948